ELECTROSPUN NANOFIBER SCAFFOLDS FOR TISSUE ENGINEERED SMALL-DIAMETER VASCULAR GRAFTS

HE WEI

NATIONAL UNIVERSITY OF SINGAPORE

2007

ELECTROSPUN NANOFIBER SCAFFOLDS FOR TISSUE ENGINEERED SMALL-DIAMETER VASCULAR GRAFTS

HE WEI

(M.Eng, SHANGHAI JIAOTONG UNIVERSITY, CHINA)

A THESIS SUBMITTED

FOR THE DEGREE OF PHD OF ENGINEERING

GRADUATE PROGRAM IN BIOENGINEERING

NATIONAL UNIVERSITY OF SINGAPORE

2007

Acknowledgements

I would like to give the sincere and heartfelt thanks to my supervisor, Prof. Seeram Ramakrishna, for his great encouragement and support during my Ph.D. study. His tenderness and kindness to students, his hardworking, his positive attitudes towards difficulties, and his wisdom and enthusiasm for science impressed me deeply and inspired my strong interest in the research work.

I also would like to thank Associate Prof. Wang Shu from the Department of Biological Science, Prof. Casey Chan from the Department of Orthopedic Surgery, and Prof. Peter Ashley Robless from the Department of Surgery for their collaboration and idea-sharing in this project. I must thank Dr. Shentil Kumar and Dr. Marcus Wong for their professional help in the microsurgery. I would like to thank Prof. Teoh Swee Hin, Associate Prof. Hanry Yu, and Associate Prof. Michael Raghunath, previous and current chairmen in Graduate Program in Bioengineering (GPBE), for their great effort in making GPBE an enriched, prosperous, and warm "family". My special appreciation to my friends in GPBE, especially the 2003 batch students, for all the unforgettable and sweet memories we spent together in NUS and in Singapore.

I must give my thanks to Nanobioengineering Labs, where I benefited a lot from the collaboration with our experienced colleagues with different backgrounds.

First, I must thank Dr. Thomas, an expert research fellow in cell & molecular biology, for his great help in teaching me the professional ways of carrying out the biological experiments. I learned RT-PCR, cDNA Microarray directly under his guidance. Second, I would like to thank Dr. Zuwei and Mr. Weeeong, our polymer chemistry research fellow and responsible lab officer, for their great help in materials-related part of my thesis. Third, I would like to thank Mr. Dong Yixiang for his creative design of the cell-seeding device. Fourth, I need to thank all our lab officers and professional officers such as Ms. Satinderpal Kaur, Mr. Ramakrishnan Ramaseshan, Mr. Zhang Yan Zhong, Ms. Yang Fang, and Miss. Karen Wang for their technical support in ATR-FTIR, SEM, tensile test, and cell culture *etc*. Especially, I must thank my junior, Miss. Ma Kun, and the NUSNNI administrator, Mr. Steffen, for their help in printing the thesis. Also I must thank Ms. Liao Susan for her kind help in revising the thesis. Finally, I would like to extend my thanks to all my friends in the lab: Ziyuan, Feng Yu, Karen Teo, Bojun, Yingjun, and Renugal *etc.* for their precious friendship and help during my Ph.D studies.

Especially I must thank NUS for proving students with outstanding facilities and research resources, attractive scholarship, and a pleasant studying environment. Also I would like to thank all of my friends in Worcester (USA) for their encouragement during the time I was writing the thesis.

I would like to give the highest thanks to my husband, my parents, and parents in law for their constant love, care, and support during my study. This thesis is especially dedicated to my dearest daughter, Esther.

Publications

Honors & Awards:

- **President Graduate Fellowship (PGF)**, National University of Singapore, 2005-2007.

- **Best Poster Award** for Symposium A (Advanced Biomaterials) in the 3rd International Conference on Materials for Advanced Technologies 2005 (ICMAT& IUMRS-ICAM 2005), July 2005, Singapore.

- **Joint Young Investigator Awards (YIA) in** the 12th International Conference on Biomedical Engineering (ICBME), December 2005, Singapore.

Journal Papers:

- **He W**, Ma ZW, Teo WE, Dong YX, Robless PA, Lim TC, Ramakrishna S. Tubular Nanofiber Scaffolds for Tissue Engineered Small-Diameter Vascular Grafts. ***Journal of Biomedical Materials Research: Part A***. 2008 (Articles online ahead of print)

- **He W**, Yong T, Ma ZW, Inai R, Teo WE, Ramakrishna S. Biodegradable Polymer Nanofiber Mesh to Maintain Functions of Endothelial Cells. ***Tissue Engineering*** 2006; 12:2457-2466.

- **He W**, Ma ZW, Yong T, Teo WE, Ramakrishna S. Fabrication of collagen-coated biodegradable copolymer nanofibers and their potential for endothelial cells growth. ***Biomaterials*** 2005; 26: 7606-7615.

- **He W**, Yong T, Teo WE, Ma ZW, Ramakrishna S. Fabrication and endothelialization of collagen-blended biodegradable polymer nanofiber: potential vascular grafts for the blood vessel tissue engineering. ***Tissue Engineering*** 2005; 11: 1574-1588**.**

- Teo WE, **He W**, Ramakrishna S. Electrospun scaffold tailored for tissue-specific extracellular matrix. **(Review)**.***Biotechnology Journal*** 2006; 1: 918-929.

- Liao S, Li BJ, Ma ZW, **He W**, Chan C, Ramakrishna S. Biomimetic electrospun nanofibers for tissue regeneration. **(Review)** ***Biomedical Materials***. 2006: 1: R45-R53.

- Ma ZW, **He W**, Yong T. Grafting of gelatin on electrospun poly (caprolactone) (PCL) nanofibers to improved endothelial cell's spreading and proliferation and to control cell orientation. ***Tissue Engineering*** 2005; 11: 1149-1158.

- Ma ZW, Kotaki M, Yong T, **He W**, Ramakrishna S. Surface engineering of electrospun polyethylene terephthalate (PET) nanofibers towards development of a new material for blood vessel engineering. ***Biomaterials*** 2005; 26**:** 2527-2536.

Book Chapters:

- **He W**, Feng Y, Ma ZW, and Ramakrishna S. "Polymers for Tissue Engineering", Polymers for Biomedical Applications, Edited by Anil Mahopatro and Ankur S Kulshrestha, American Chemical Society and Oxford University Press (2008) Chapter 19, 310-335.

- **He W**, Ma ZW, Ramakrishna S. "Surface modification of polymer nanofibers for tissue engineering applications", Surface Design and Modification of Biomaterials for Clinical Application, 2008, Edited by Junzo Tanaka, Soichiro Itoh, and Guoping Chen, Transworld Research Network (2008), Chapter 4, 95-114.

Conference Abstracts:

- **He W**, Yong T, Ma ZW, Inai R, Teo WE, Ramakrishna S. Biomimetic and bioactive polymer nanofiber mesh to maintain functions of endothelial cells. **The 12th International Conference on Biomedical Engineering (ICBME), December 2005, Singapore. (Oral presentation)**

- **He W**, Ma ZW, Yong T, Teo WE, Ramakrishna S. Fabrication of biomimetic collagen-coated P(LLA-CL) nanofiber mesh and its potential for vascular endothelial cell growth. **3rd International Conference on Materials for Advanced Technologies 2005** (**ICMAT& IUMRS-ICAM 2005), July 2005, Singapore. (Poster presentation)**

- Yong T, Ngiap CK, **He W**, Venugopal J, Xu CY, Yang F, Ramakrishna S. Molecular understanding of cell-synthetic nanofiber extra cellular matrix (ECM)

interactions. **Japan-Singapore Symposium on Nanoscience & Nanotechnology November 2004, Singapore, pp 76. (Poster Presentation)**

- Ma ZW, Teng XC, **He W**, Xu CY, Yong T, Ramakrishna S. ECM-mimic electrospun polymer nanofiber matrix as tissue engineering scaffold. **The First International SBE Conference on Bioengineering and Nanotechnology, September 2004, Singapore**, **pp 23. (Poster Presentation)**

- **He W**, Yong T, Ma ZW, Teo WE, Ramakrishna S. Collagen-polymeric nanofibers mimicking natural basement membrane for endothelial cell growth. **In Proc. 1st Nano-Engineering and Nano-Science Congress, July 2004, Singapore, pp72. (Oral presentation).**

Table of contents

Acknowledgements i

Publications iv

Table of Contents vii

Summary xiii

Abbreviations xvi

List of Tables xix

List of Figures xxi

Chapter 1 Introduction

1.1 Background 1

1.1.1 ECs-seeded tissue engineered vascular grafts 2

1.2 Thesis objectives 6

1.3 Thesis scope 9

1.4 Thesis values 10

Chapter 2 Literature Review

2.1 Challenges of small-diameter vascular grafts 12

2.2 Rationale of constructing tissue engineered vascular grafts 13

2.2.1 Natural vascular structure 13

2.2.2 Synthetic materials 18

2.2.3 Endothelialization 19

2.2.4 Mechanical properties 23

2.3 Current approaches 24

2.4 Potential of polymer nanofibers as tissue engineered scaffolds 29

2.4.1 Electrospinning 29

2.4.2 Nanofiber scaffolds 32

2.4.3 Surface modifications of polymer nanofibers 36

2.4.3.1 Physical methods 38

2.4.3.2 Chemical methods 43

2.4.4 Cells-nanofiber scaffolds interaction 48

2.4.5 Current research of polymer nanofibers as tissue engineered vascular grafts 50

Chapter 3 Collagen-Blended Nanofiber Meshes (NFM)

3.1 Materials and methods 55

3.1.1 Materials 54

3.1.2 Fabrication of collagen-blended P(LLA-CL) NFM 56

3.1.3 Material characterization 58

3.1.3.1 Physical properties 58

3.1.3.2 Surface chemistry 59

3.1.3.3 Mechanical properties 59

3.1.4 Characterization of cellular behaviors 59

3.1.4.1 *In vitro* cell culture 59

3.1.4.2 Cellular morphology 60

3.1.4.3 Cellular attachment and viability 61

3.1.4.4 RT-PCR analysis 62

3.1.5 Statistical analysis 65

3.2 Results and discussions 65

3.2.1 Material characterization 65

3.2.1.1 Physical properties 65

3.2.1.2 Surface chemistry 69

3.2.1.3 Mechanical properties 72

3.2.2 Cellular behaviors characterization 74

3.2.2.1 Cellular viability 74

3.2.2.2 Cellular morphology 77

3.2.2.3 Cellular attachment 80

3.2.2.4 Cellular phenotype 81

3.3 Conclusion 83

Chapter 4 Collagen-Coated Nanofiber Meshes (NFM)

4.1 Materials and methods 84

4.1.1 Materials 85

4.1.2 Fabrication of P(LLA-CL) NFM 85

4.1.3 P(LLA-CL) NFM modification by collagen coating 86

4.1.4 Materials characterization 87

4.1.4.1 Physical properties 87

4.1.4.2 Surface chemistry 88

4.1.4.3 Collagen distribution and quantification 88

4.1.5 Characterization of cellular behaviors 89

4.1.5.1 *In vitro* cell culture 89

4.1.5.2 Immunostaining 90

4.1.5.3 RT-PCR analysis 90

4.1.5.4 cDNA microarray analysis 91

4.1.6 Statistical analysis 92

4.2 Results and discussions 92

4.2.1 Materials characterization 92

4.2.1.1 Physical properties 92

4.2.1.2 Collagen coating 96

4.2.1.3 Surface chemistry 98

4.2.1.4 Mechanical properties 100

4.2.2 Characterization of cellular behaviors 102

4.2.2.1 Cellular morphology 102

4.2.2.2 Cellular viability and attachment 104

4.2.2.3 Cellular phenotype 106

4.2.2.4 Gene expression 109

4.3 Comparison between collagen-blended and collagen-coated NFM 112

4.4 Conclusion 113

Chapter 5 3-D Tubular Nanofiber Scaffolds

5.1 Materials and methods 115

5.1.1 Materials 115

5.1.2 Fabrication of P(LLA-CL) tubular nanofiber scaffolds 116

5.1.3 Mechanical properties 117

5.1.4 Cellular behaviors characterization 118

5.1.4.1 Rotational cell seeding 118

5.1.4.2 Hematoxylin & Eosin (H&E) staining 119

5.1.4.3 Immunostaining 120

5.2 Results and discussions 120

5.2.1 Materials characterization 120

5.2.1.1 Morphology 120

5.2.1.2 Surface chemistry 126

5.2.1.3 Mechanical properties 127

5.2.2 Characterization of cellular behaviors 129

5.2.2.1 Morphology and phenotype 129

5.3 Conclusion 133

Chapter 6 *In Vivo* Rabbit Model

6.1 Materials and methods 136

6.2 Results and discussions 138

6.3 Conclusion 142

Chapter 7 Conclusion and Recommendations

7.1 Main conclusions 144

7.2 Limitations 146

7.3 Recommendations 147

7.3.1 Advanced mechanical properties studies 147

7.3.2 Introducing growth factors into the nanofiber scaffolds 148

7.3.3 Constructing tubular nanofiber scaffolds with hierarchical structure 148

Reference 151

Appendix 164

Summary

Synthetic vascular grafts have rarely been proved successful in small-diameter (inner diameter < 6 mm) blood vessel replacements due to thrombosis and subsequent intimal hyperplasia, which could be alleviated by providing an anti-thrombogenic endothelial cells (ECs) monolayer onto the lumen surface of the grafts to mimic the situation in natural blood vessels. Electrospun nanofiber scaffolds, simulating extracellular matrix (ECM) below ECs, might well support ECs growth. This study was to construct nanofiber scaffolds with the objective of achieving effective endothelialization and final goal of constructing blood vessel-like tubular nanofiber scaffolds for tissue engineered small-diameter vascular grafts. The nanofiber scaffolds in this study were prepared from synthetic poly(L-lactic acid)-*co*-poly(ε-caprolactone) P(LLA-CL) and natural collagen type I by electrospinning. The diameters of nanofibers in the scaffolds ranged between 100 to 800 nm. Moreover, the nanofiber scaffolds were porous with the porosity around 70%.

Firstly, collagen-blended P(LLA-CL) nanofiber meshes (NFM) were constructed by electrospinning a mixture of collagen and P(LLA-CL) dissolved in 1,1,1,3,3,3-hexafluro-2-propanol (HFP). *In vitro* Human coronary artery endothelial cells (HCAECs) culture showed that the blended NFM has improved viability and attachment of HCAECs compared with the P(LLA-CL) NFM. HCAECs adopted a spreading polygonal shape on the blended NFM. Moreover, HCAECs maintained

phenotypic expression of cell adhesion molecules such as PECAM-1 (platelet endothelial cell ad adhesion molecule-1), ICAM-1 (intercellular adhesion molecule-1), VCAM-1 (vascular cell adhesion molecule-1), E-Selectin, and vWF by RT-PCR (reverse transcription-polymerase chain reaction) analysis.

P(LLA-CL) NFM were also modified by collagen coating method. P(LLA-CL) NFM were treated by inductive coupled radiofrequency glow discharge plasma, followed by collagen coating. Collagen was found to be evenly coated throughout the surface of nanofibers. Collagen coating improved the viability and attachment of HCAECs on P(LLA-CL) NFM. Immunostaining and RT-PCR analysis showed that HCAECs maintained the phenotypic expression of PECAM-1, fibronectin, and collagen IV. cDNA microarray analysis further indicated that HCAECs kept the expressions of 112 function-related genes. Particularly, aligned collagen-coated P(LLA-CL) NFM were constructed. The aligned NFM have higher mechanical strength and modulus than the random NFM. HCAECs grew along the direction of nanofiber alignment and showed elongated morphology.

Based on above studies, 3-D tubular P(LLA-CL) nanofiber scaffolds (inner diameter 3 mm) were fabricated by electrospinning onto a rotating metallic mandrel, followed by collagen coating in the above mentioned method. Expanded PTFE (Gore-Tex®) 3 mm vascular grafts were used as a control to study the mechanical properties and biocompatibility. Tensile properties of the tubular scaffold were closer to that of the natural human arteries compared with the Gore-Tex® grafts. HCAECs were

seeded onto the lumen of the scaffolds and rotated at the speed of 6 rpm for 4 hours, followed by a static culture. It was found that HCAECs spread evenly on the lumen of the scaffolds and reached sub-confluence immediately after seeding. After 10 day's culture, HCAECs possessed the phenotypic expression of PECAM-1 and existed as a thin layer covering the lumen of the scaffolds. On the Gore-Tex® grafts, there were few HCAECs present after seeding.

Finally, to prove the basic concept of using the tubular nanofiber scaffolds as vascular grafts, the tubular P(LLA-CL) nanofiber scaffolds without collagen coating and without ECs seeding were implanted *in vivo* into a rabbit model to replace the inferior superficial epigastric vein. Results showed the scaffolds could sustain the suturing during the implantation process and there was no blood leaking from the scaffolds. Further, the scaffolds kept the structure integrity and showed patency for up to 7 weeks.

Abbreviations

3-D: three-dimensional

ANF: aligned nanofiber meshes

ATR-FTIR: attenuated total reflectance Fourier transform infrared

BM: basement membrane

BNF: collagen-blended P(LLA-CL) nanofiber meshes

BSA: bovine serum albumin

CAMs: cell adhesion molecules

CMFDA: 5-chloromethyl fluorescein diacetate

DCM: Dichloromethane

DMF: *N*,*N*-dimethylformamide

ECs: endothelial cells

ECM: extracellular matrix

EPCs: endothelial progenitor cells

E-selectin: endothelial leucocyte adhesion molecules-1

FBS: fetal bovine serum

FITC: fluorescein isothiocyanate

GAGs: glycosaminoglycans

HCAECs: human coronary artery endothelial cells

HCASMCs: human coronary artery smooth muscle cells

List of Tables

Table 2.1. Synthetic material requirements for tissue engineered vascular grafts

Table 2.2. Comparison between the three methods of constructing tissue engineered vascular grafts (TEVG)

Table 2.3. Comparison between synthetic and natural polymers

Table 2.4. Summary of different combinations of biomolecules and polymers in blended nanofibers and their applications in tissue engineering

Table 2.5. Composite nanofibers fabricated through blended electrospinning

Table 2.6. Blended nanofibers containing heparin through blended electrospinning

Table 2.7. Summary of the three graft copolymerization methods applied to modify nanofiber surface

Table 2.8. Summary of constructing tubular tissue engineered vascular grafts through electrospinning

Table 3.1. PCR primers for RT-PCR analysis

Table 3.2. Diameter, thickness, apparent density, and porosity of collagen-blended P(LLA-CL) NFM with various weight ratios of P(LLA-CL) to collagen[a]

Table 3.3. Atomic ratios of carbon (C), nitrogen (N), and oxygen (O) on the surface of P(LLA-CL) NFM, collagen-blended P(LLA-CL) NFM with various

weight ratios of P(LLA-CL) to collagen, and collagen NFM as determined by XPS

Table 3.4. Tensile properties of collagen-blended P(LLA-CL) NFM, with the weight ratio of P(LLA-CL) to collagen 1:1, P(LLA-CL) NFM, and coronary artery[a]

Table 4.1. PCR primers for RT-PCR analysis

Table 4.2. Diameter, thickness, apparent density, porosity, and pore size of the random and aligned collagen-coated P(LLA-CL) NFM[a]

Table 4.3. Water contact angles of the P(LLA-CL) NFM and films before and after plasma treatment for various time[a]

Table 4.4. Atomic ratio of C, N, and O on the surface of the P(LLA-CL) NFM, the collagen-coated P(LLA-CL) NFM, and the pure collagen NFM determined by XPS

Table 4.5. Tensile properties of the random and aligned P(LLA-CL) NFM[a]

Table 4.6. Percentage (%) of genes with over-expressed, similar-expressed, and less-expressed levels between HCAECs grown on TCPS, random (RNF) and aligned (ANF) collagen-coated P(LLA-CL) NFM

Table 5.1. Comparison between the Gore-Tex® vascular grafts and the tubular nanofiber scaffolds in terms of inner diameter, wall thickness, pore size, and fabrication methods

Table 5.2. Tensile properties of the collagen-coated P(LLA-CL) tubular nanofiber scaffolds in both longitudinal and circumferential directions[a]

Table 5.3. Longitudinal and circumferential tensile strength of the tubular nanofiber scaffolds, Teflon® (TF-208), and natural abdominal aorta

H&E: Hematoxylin & Eosin

hEGF: human epidermal growth factor

hFGF-B: human fibroblast growth factor-B

HFP: 1,1,1,3,3,3-hexafluoro-2-propanol

ICAM-1: intercellular adhesion molecule-1

IGF-I: insulin-like growth factor type I

IH: intimal hyperplasia

LSCM: laser scanning confocal microscope

MSCs: mesenchymal stem cells

NF: nanofibers

NFM: nanofiber meshes

PBS: phosphate-buffered saline

PCL: polycaprolactone

PCR: Polymerase Chain Reaction

PECAM-1: platelet endothelial cell ad adhesion molecule-1

PEG: poly(ethylene glycol)

PEO: poly(ethylene oxide)

PES: polyethersulfone

PET: poly(ethylene terephthalate)

PGA: poly(glycolic acid)

PLA: poly(L-lactide)

PLGA: poly(lactide-*co*-glycolide)

P(LLA-CL): poly(L-lactic acid)-*co*-poly(ε-caprolactone)

PMMA: poly(methacrylic acid)

PTFE: polytetrafluoroethylene

ePTFE: expanded polytetrafluoroethylene

PU: polyurethane

PVA: poly(vinyl alcohol)

RBITC: rhodamine B isothiocyanate

RNF: random nanofiber meshes

RT-PCR: reverse transcription-polymerase chain reaction

SD: standard deviation

SEM: scanning electron microscope

SMCs: smooth muscle cells

TCPS: tissue culture polystyrene

TEM: transmission electron microscopy

TEVGs: tissue engineered vascular grafts

VCAM-1: vascular cell adhesion molecule-1

VEGF: vascular endothelial growth factor

vWF: von Willebrand Factor

XPS: x-ray photoelectron spectroscopy

List of Figures

Figure 1.1. Schematic outline for the study: step 1, fabrication of nanofiber meshes (NFM); step 2, evaluation of the *in vitro* endothelialization on the flat NFM; step 3, constructing the blood vessel-like 3-D tubular nanofiber scaffolds with the lumen seeded with ECs.

Figure 2.1. Schematic graph of the basic tri-lamellar structure of blood vessels.

Figure 2.2. Elastic fibers**.** These scanning electron micrographs show (A) a low-power view of a segment of a dog's aorta and (B) a high-power view of the dense network of longitudinally oriented elastic fibers in the outer layer of the same blood vessel. All the other components have been digested away with enzymes and formic acid. Reprint with permission from (Alberts *et al.*, 2002).

Figure 2.3. The basal lamina in the cornea of a chick embryo. In this scanning electron micrograph, some of the epithelial cells (E) have been removed to expose the upper surface of the matlike basal lamina (BL). A network of collagen fibrils (C) in the underlying connective tissue interacts with the lower face of the lamina. Reprint with permission from (Alberts *et al.*, 2002).

Figure 2.4. A model of the molecular structure of a basement membrane (basal lamina). Reprint with permission from (Alberts *et al.*, 2002).

Figure 2.5. Pathway of thrombus formation (A) and EC antithrombogenic signaling (B). Reprint with permission from (Mitchell and Niklason, 2003).

Figure 2.6. Schematic representations of a collagen-based construct. The most general configuration contains an adventitia-like layer, a media-like layer, a monolayer of ECs, and Dacron^{TM} sleeves for structural reinforcement. Reprint with permission from (Nerem and Seliktar, 2001).

Figure 2.7. Schematic representation of the cell self-assembly model. Vascular cells are cultured to form a continuous sheet of cells and extracellular matrix and then rolled over a central mandrel. The construct is matured over 10 weeks, allowing the cell to organize into a mechanically stable tubular construct. Reprint with permission from (Nerem and Seliktar, 2001).

Figure 2.8. Schematic representation of a cell-seeded polymeric scaffold. Vascular cells are cultured on a woven PGA mesh. The construct is matured over 8 weeks of dynamic culture, allowing the cells to proliferate and produce and organize extracellular matrix as the PGA degrades. Reprint with permission from (Nerem and Seliktar, 2001).

Figure 2.9. Electrospinning basic principles (Ramakrishna *et al.*, 2006).

Figure 2.10. Similarity between the native ECM protein structure and the electrospun polymer nanofiber scaffold. (a) Fibroblasts grown *in vivo* on collagen fibrils of rat cornea (Nishida *et al.*, 1988); (b) ECs cultured *in vitro* on the electrospun PCL nanofiber scaffold. Reprint with permission from (Ma *et al.*, 2005b).

Figure 2.11. Similarity between (a) the natural collagen bundles of the connective stroma of the small intestine (Ottani *et al.*, 2001) and (b) the electrospun collagen nanofibers. Reprint with permission from (Teo *et al.*, 2006).

Figure 2.12. General scheme of graft copolymerization on polymer surfaces.

Figure 2.13. Surface modification scheme for galactose conjugation to PCLEEP nanofibers. Reprint with permission from (Chua *et al.*, 2005).

Figure 2.14. Reaction scheme of the surface modification process for PCL nanofiber. RFGD, Radio-frequency glow discharge. Reprint with permission from (Ma *et al.*, 2005a).

Figure 2.15. Schematic representation of the surface modification process of PET nanofibers. Reprint with permission from (Ma *et al.*, 2005c).

Figure 3.1. Schematic setup and optimized operation parameters for fabrication of the collagen-blended P(LLA-CL) NFM.

Figure 3.2. SEM (A-D) and TEM (E and F) micrographs of collagen-blended P(LLA-CL) NFM with various weight ratios of P(LLA-CL) to collagen. Weight ratios of P(LLA-CL) to collagen: (A) 4:1; (B) 2:1; (C and E) 1:1; (D and F) 0:1 Total concentration of the electrospinning solution is 5 wt%.

Figure 3.3. Diameter distributions of the collagen-blended P(LLA-CL) NFM with various weight ratios of P(LLA-CL) to collagen.

Figure 3.4. ATR-FTIR spectra of (A) P(LLA-CL) NFM, (B) collagen NFM, and (C) collagen-blended P(LLA-CL) NFM with a 1:1 weight ratio of P(LLA-CL) to collagen.

Figure 3.5. Typical stress-strain curves of the P(LLA-PCL) NFM and collagen-blended P(LLA-CL) NFM with the weight ratio of P(LLA-CL) to collagen 1:1 under tensile loading.

Figure 3.6. Total viability of HCAECs cultured on TCPS, collagen NFM, collagen-blended P(LLA-CL) NFM (BNF) with various weight ratios of P(LLA-CL) to collagen(BNF 1:1, BNF 2:1, BNF 4:1), P(LLA-CL) NFM, and collagen-blended P(LLA-CL) film (Blended film).

Figure 3.7. Viability of HCAECs on day 3 and 7 shown in Figure 3.6 were summarized here for clearness.

Figure 3.8. LSCM [original magnification: (a): × 400; (b and c): × 200] and SEM [original magnification: (d-f): × 500] images of HCAECs cultured on (a and d) TCPS, (b and e) P(LLA-CL) NFM, and (c and f) collagen-blended P(LLA-CL) NFM.

Figure 3.9. Higher magnification of SEM micrographs (original magnification, × 3000), showing the detailed interactions between HCAECs and (a) the P(LLA-CL) NFM and (b) the collagen-blended P(LLA-CL) NFM at 5 days of culture.

Figure 3.10. Attachment of HCAECs on the TCPS, P(LLA-CL) NFM, and collagen-blended P(LLA-CL) NFM.

Figure 3.11. Expression of ECs-characteristic genes from HCAECs cultured on TCPS and collagen-blended P(LLA-CL) NFM (BNF) for 10 days. On day 10, total RNA was extracted and RT-PCR was performed with gene-specific primer pairs shown in Table 3.1, including E-Selectin (E-SEL, CD62E), VCAM-1 (CD106), ICAM-1 (CD54), won Willebrand factor (vWF), PECAM-1 (CD31), and β-actin as a housekeeping gene.

Figure 4.1. Experimental setups for fabricating the random and aligned P(LLA-CL) NFM, which were collected with a static plate (a) and rotating disk (b), respectively.

Figure 4.2. Schematic representation of the plasma treatment and collagen coating of the electrospun P(LLA-CL) nanofiber mesh.

Figure 4.3. SEM pictures of the cross section (a and d), 3-dimensional structure (b and e), and top view (c and f) of the random (a-c) and aligned (d-f) collagen-coated P(LLA-CL) NFM.

Figure 4.4. (a) Diameter distribution of the random and aligned collagen-coated P(LLA-CL) NFM. (b) Pore size distribution of the random collagen-coated P(LLA-CL) NFM.

Figure 4.5. 3-D laser scanning confocal microscopy (LSCM) (original magnification, × 600) of the collagen-coated random (a) and aligned (b) P(LLA-CL) NFM. Existence of rhodamine-labeled collagen was identified by its red fluorescence.

Figure 4.6. Stress-strain curves for the random and aligned P(LLA-PCL) NFM under tensile loading.

Figure 4.7. LSCM (original magnification, × 400) and SEM (original magnification, × 1000) images of HCAECs cultured on (a, d) TCPS, (b, e) P(LLA-CL) NFM, and (c, f) collagen-coated P(LLA-CL) NFM.

Figure 4.8. Immunofluorescent staining of PECAM-1 from HCAECs cultured on TCPS (a) and the collagen-coated P(LLA-CL) NFM (b). Existence of rhodamine-labeled collagen was identified by its red fluorescence in (b). White arrows indicate strong PECAM-1 expression at cell-cell interfaces.

Figure 4.9. Viability of HCAECs on the TCPS, P(LLA-CL) NFM, and collagen-coated P(LLA-CL) NFM. (* $p < 0.05$ compared with the P(LLA-CL) NFM).

Figure 4.10. Attachment of HCAECs on the TCPS, P(LLA-CL) NFM, and collagen-coated P(LLA-CL) NFM. (* $p < 0.05$ compared with the P(LLA-CL) NFM).

Figure 4.11. (A) Fluorescent microscopy (original magnification, × 600) and SEM (original magnification, × 1000) images from HCAECs on TCPS, random NFM (RNF) and aligned (ANF) collagen-coate P(LLA-CL) NFM. (B) LSCM images of fibronectin and collagen type IV expressions from HCAECs on the TCPS, RNF, and ANF. (C) RT-PCR analysis of expressions of PECAM-1, fibronectin, and collagen type IV from HCAECs on the TCPS, RNF, and ANF.

Figure 4.12. (A) Gene expression profiles of HCAECs on TCPS, random (RNF), and aligned (ANF) collagen-coated P(LLA-CL) NFM by cDNA microarray analysis. Expression of each gene is represented by the fluorescence of a tetra-spot. (B) Scatter plots showing the relative gene expression of (B1) RNT versus TCPS, (B2) ANF versus TCPS, and (B3) ANF versus RNF. (C). RT-PCR analysis of integrin α5 (ITGA5), αV (ITGAV), and β1 (ITGB1) expression from HCAECs cultured on TCPS, RNF, and ANF, which correlate to the genes in a red frame in (A).

Figure 5.1. (A) Setup and operation parameters for fabrication of the P(LLA-CL) tubular nanofiber scaffolds. (B) The electrospun tubular nanofiber scaffold collected on the mandrel.

Figure 5.2. Schematic illustration of HCAECs seeding onto the lumen of the collagen-coated P(LLA-CL) tubular nanofiber scaffold.

Figure 5.3. Macroscopic and microscopic structures of the collagen-coated P(LLA-CL) tubular nanofiber scaffolds . (a, b) optical images of macroscopic structures. (c, d, e, f) SEM photographs: (c) whole structure; (d) enlarged cross-section of wall; (e) inner layer; (f) out layer. Original magnification: × 50, × 2500, × 5000, × 5000 for c, d, e, f, respectively.

Figure 5.4. Macroscopic and microscopic structures of the Gore-Tex® vascular grafts. (a, b) optical images of macroscopic structures. (c, d, e, f) SEM photographs: (c) cross section; (d) enlarged cross-section of wall; (e) inner layer; (f) out layer.

Figure 5.5. (Left) 3-D LSCM (original magnification, × 600) image of the collagen-coated P(LLA-CL) tubular nanofiber scaffolds. (Right) Enlarged LSCM image of the frame in (A). Rhodamine-labeled collagen was identified by its red fluorescence.

Figure 5.6. Typical uniaxial stress-strain curves for the collagen-coated P(LLA-CL) tubular nanofiber scaffolds under tensile loading in longitudinal and circumferential directions.

Figure 5.7. HCAECs grew on the lumen of the tubular nanofiber scaffolds for 1 day (a and b), 5 days (c and d), and 7 days (e and f) after seeding at the density of 6×10^5 cells/cm^3. (b, d, and f): higher magnification images of (a, c, and e) respectively. Original magnification: a, × 200, c, × 42, e, × 80, b, d and f, × 1000.

Figure 5.8. HCAECs grew on the lumen of the tubular nanofiber scaffolds for 10 days after seeding. (a, b) SEM images showing the overall structure of the HCAECs-scaffold constructs: (a) cross-section of wall of the constructs; (b) enlarged quadrangle in (a). (c) H&E staining of the cross-section of the constructs. (d) Immunostaining of PECAM-1 from HCAECs on the lumen of the tubular nanofiber scaffolds. Original magnification: a, × 80, b, × 2000, c, × 200, d, × 630.

Figure 6.1. Image of the exposed inferior superficial epigastric vein in the rabbit model.

Figure 6.2. Image of the P(LLA-CL) tubular nanofiber scaffold (length: 1 cm, inner diameter: 1 mm).

Figure 6.3. Image of the replacement of the inferior superficial epigastric vein with the P(LLA-CL) tubular nanofiber scaffold.

Figure 6.4. SEM images showing morphology of the P(LLA-CL) NFM biodegraded in 1 × PBS at 37 ^{o}C for (a and b) 0 month, (c and d) 3 month, and (e and f) 8 month. (b, d, and f) are magnified images of (a, c, and e) respectively.

Figure 6.5. H&E staining image of the oblique-section of the explanted tubular nanofiber scaffold after 7 weeks' implantation in the rabbit model.

Figure 7.1. Experimental setup for electrospinning core-shell nanofibers (Zhang *et al.*, 2004).

Figure 7.2. Constructing tubular nanofiber scaffolds with hierarchical strructure: ECs-seeded NFM, SMC-contained aligned NFM, and fibroblasts-contained NFM can be used to construct the intima, media, and adventitia of blood vessels respectively.

Chapter 1

Introduction

1.1 Background

Cardiovascular diseases including blood vessel diseases such as coronary artery disease and peripheral vascular disease, and heart disease are the number one cause of death in USA and most European countries (Ross, 1993). Treatment of blood vessel diseases involves bypassing diseased blood vessels using various types of vascular grafts: autografts (grafts taken from a patient, *e.g.* saphenous veins or internal mammary arteries), allografts (grafts taken from other person, *e.g.* umbilical veins), xenografts (grafts taken from other species, *e.g.* bovine carotid arteries), and synthetic grafts (artificial grafts). Allografts and xenografts are rarely used now because of high failure rates resulting from immune rejections, aneurysms, and ruptures. With autografts, the problem is that as many as 30% of patients do not have suitable veins/arteries for grafting due to preexisting vascular diseases, vein stripping, or vein uses in prior procedures. Nowadays more than 600,000 vascular grafts bypass procedures are performed annually in USA. Thus there is a clear clinical need for synthetic grafts as alternatives to the use of autografts (Xue.L, 2000).

Although have being successfully used for large and medium blood vessel replacements, synthetic vascular grafts have rarely been proved successful in small-diameter blood vessel replacements (inner diameter < 6 mm, *e.g.* peripheral vessels below the knee and coronary arteries *etc*). Only 15-30% of small-diameter synthetic vascular grafts remain open (or patent) after 5 years (Seal *et al.*, 2001). The rate of thrombosis (static aggregation of blood factors) occurred in synthetic vascular grafts is greater than 40% in the early phase after 6 months followed by continuous intimal hyperplasia (excessive tissue ingrowth and plasma protein depositions) in the chronic phase (Sayers *et al.*, 1998). Thrombosis and intimal hyperplasia are caused by host-tissue foreign body responses, initiated first by plasma protein depositions, followed by leukocytes and platelets adhesion and migration of endothelial cells (ECs) and smooth muscle cells (SMCs) onto the lumen of vascular grafts. Effects of these factors will even be amplified in a low flow rate and high resistance small-diameter vascular graft, resulting in easier graft occlusion and subsequent failure. It is to this challenge that vascular tissue engineering is seeking to answer. One of the commonly accepted methods for developing tissue engineered small-diameter vascular grafts is to hybridize vascular grafts made from biodegradable materials with vascular cells (Ratcliffe, 2000;Thomas *et al.*, 2003;Kakisis *et al.*, 2005).

1.1.1 ECs-seeded tissue engineered vascular grafts

As mentioned above, thrombosis is one of the main reasons for occlusion of small-diameter vascular grafts. One approach to solve this problem is seeding

vascular ECs onto the lumen of vascular grafts to allow the formation of a monolayer of ECs prior to implantation. The rationale behind this approach is that thrombosis could be prevented by providing a anti-thrombogenic ECs monolayer to mimic the situation in natural blood vessels (Luscher and Barton, 1997). Although the lumen of vascular grafts implanted in animal models will ultimately be covered with confluent host ECs, such a process has not been demonstrated to occur in humen with any currently available vascular grafts (Tomizawa, 2003). The observation of this "incomplete endothelialization" in human is an important limitation to the patency of small-diameter vascular grafts, leading to great research interests in the development of "ECs-seeded" vascular grafts. The endothelialization approach is regarded as the beginning of the application of tissue engineering principle in the cardiovascular system (Nerem and Seliktar, 2001). Results from a 7-year clinical studies of peripheral implants have shown that autologous ECs-seeded ePTFE (expanded polytetrafluoroethylene) synthetic vascular grafts possessed improved patency when implanted into 136 patients (Meinhart *et al.*, 2001).

ECs seeding onto the lumen of vascular grafts have always been challenging because ECs show limited proliferation ability on synthetic graft materials (Sipehia *et al.*, 1996). Moreover, ECs can be detached from the lumen of vascular grafts upon exposure to shear force and cyclic strain due to blood circulation (Mitchell and Niklason, 2003). Thus optimizing ECs attachment and improving EC proliferation on the lumen of synthetic vascular grafts has received much attention in recent literature (Nerem and Seliktar, 2001). In clinical practice, endothelialization of vascular grafts

can be obtained using high ECs seeding densities, or by creating a ECs-compatible surface on which ECs can adhere and grow to confluent (Sipehia *et al.*, 1996). Extracellular matrix (ECM) proteins and peptides are commonly used biomolecules to modify the lumen surfaces of vascular grafts to promote EC adhesion and attachment *via* ligand-cell receptor interaction. For example, natural ECM proteins and their derivatives such as collagen (Lu and Sipehia, 2001), gelatin (Zhu *et al.*, 2004), and fibronectin (Unger *et al.*, 2005;Seeger and Klingman, 2006) have been immobilized onto surfaces of synthetic grafts to obtain improved EC attachment and spreading. Similarly, peptide sequences derived from ECM proteins such as RGD (Arg Gly Asp) from collagen/fibronectin, YIGSR (Tyr Ile Gly Ser Arg) from laminin 1, and REDV (Arg Glu Asp Val) from fibronectin have also been covalently bound onto surfaces of synthetic grafts. Mazzucotelli *et al*. reported coating of a recombinant adhesion factor containing the RGD peptide sequence onto the ePTFE graft surfaces. There was an increased adherence and survival of human saphenous vein endothelial cells on the coated surface for up to one week compared with the uncoated ePTFE surfaces (Mazzucotelli *et al.*, 1994). In addition to modifications using ECM proteins or bioactive peptides, other chemical surface modification methods have also been reported to improve biocompatibility of synthetic vascular grafts such as ammonia plasma treatment (Sipehia *et al.*, 1996) and hydroxylation (Mckeown *et al.*, 1991) *etc*.

Although ECM chemical cues (proteins and bioactive peptides) have been extensively studied, ECM physical cues such as 3-D geometry and porosity *etc*

should not be neglected. Since ECM plays an important role in cell development, organization, and function, it is important to emulate features of ECM as closely as possible in biomaterial design for optimized cell growth. Thus natural ECM around ECs can give hints on how to construct vascular grafts with good endothelialization. Natural ECM underlying ECs is called basement membrane (BM) which is mainly composed of EC-secreted collagen and laminin fibers embedded in heparin sulfate proteoglycan hydrogels. Further study of BM shows a nano- to submicron-scale topography of ECM macromolecules, including fiber mesh, pores, ridges, and grooves (Kwon *et al.*, 2005). The 3-D structure of BM has been shown to be as important as its chemistry in its influence on cellular processes (Schmeichel and Bissell, 2003;Schindler *et al.*, 2005).

Another important concern is cell function studies. It is not enough to characterize the normal status of ECs only in terms of cell morphology, proliferation, and attachment. It is quite possible that ECs may lose their phenotypic expression of anti-thrombogenic molecules, which is critical to the patency of ECs-seeded vascular grafts, and it can not be characterized only through cell morphology, proliferation, and attachment. Thus systematic investigations into ECs phenotype and gene expression level need to be carried out to understand the normal functional maintenance of ECs.

Finally, although flat sheet-like substrates have been extensively studied for endothelialization, tubular models which better represent the real environment where

ECs grow in the lumen of blood vessels should be paid more attention to. One big difference between EC growth on flat surfaces and tubular scaffolds is the seeding method. Seeding ECs onto the lumen of tubular scaffolds is more challenging since dynamically rotational seeding is required to achieve evenly distributed ECs. Thus, based on fundamental studies from ECs culture on flat sheet-like substrates, it would be helpful to go further into constructing tubular scaffolds and establishing the seeding technology in order to enable the development of ECs-seeded vascular grafts.

1.2 Thesis objectives

The purpose of this study was to construct biomimetic electrospun nanofiber scaffolds which mimic the extracellular matrix (ECM)/basemen membrane (BM) (step 1), with the objective of achieving effective endothelialization of the nanofiber scaffolds in terms of viability, attachment, as well as phenotypic and functional maintenance of ECs (step 2), and the final goal of constructing blood vessel-like 3-D tubular nanofiber scaffolds with the anti-thrombogenic lumen composed of ECs for tissue engineered small-diameter vascular grafts (step 3). The outline for this study is shown in Figure 1.1.

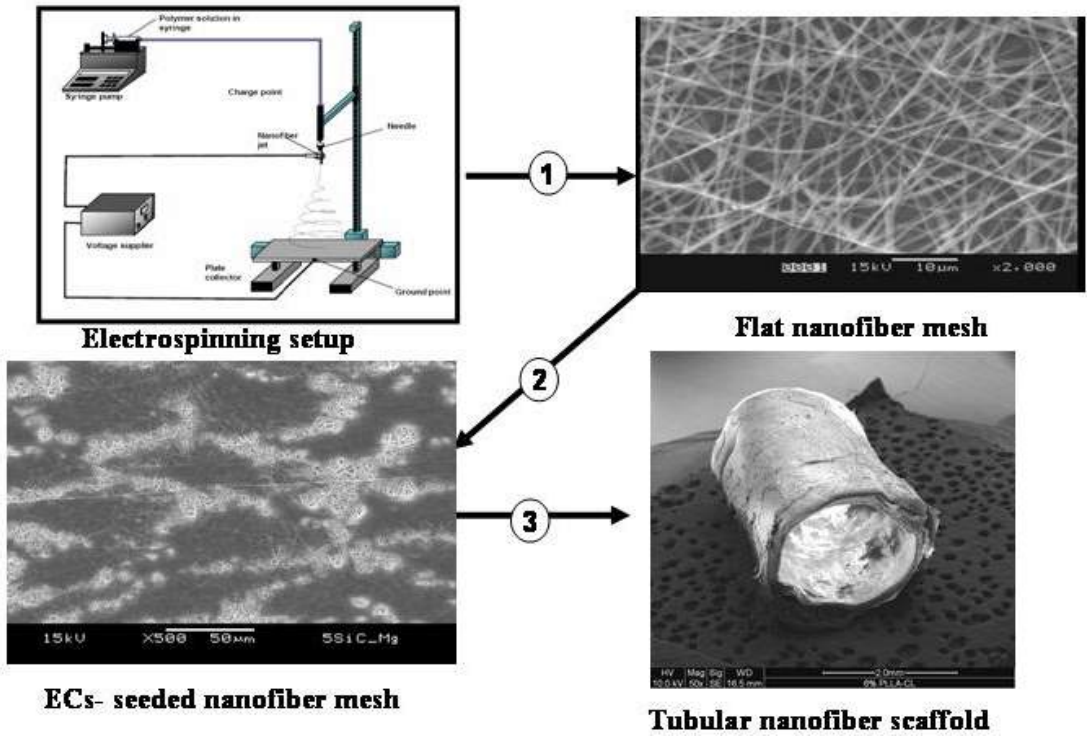

Figure 1.1. Schematic outline for the study: step 1, fabrication of nanofiber meshes (NFM); step 2, evaluation of the *in vitro* endothelialization on the flat NFM; step 3, constructing the blood vessel-like 3-D tubular nanofiber scaffolds with the lumen seeded with ECs.

Moreover we proposed to pursue the following specific aims in this study:

1. To fabricate collagen-modified nanofiber meshes (NFM) with high levels of controllability and reproducibility.

   Hypothesis: Bulk and surface modification of pure polymer NFM by blending or coating with collagen could promote ECs attachment *via* ligand-cell receptor interaction.

   a To include collagen into polymer NFM by physical blending or coating.

b To characterize the morphology, surface chemistry, and mechanical properties of the collagen-modified polymer NFM.

2. To evaluate *in vitro* endothelialization of the collagen-modified polymer NFM with respect to attachment, viability, as well as phenotypic and functional maintenance of ECs. Concurrently, NFM constructed from both random and aligned nanofiber will be studied.

Hypothesis: Electrospun collagen-modified polymer NFM could support *in vitro* endothelialization since the NFM mimic the natural basement membrane.

a To study ECs' morphology, attachment, viability as the basic biocompatibility evaluation of the collagen-modified polymer NFM.

b To analyze the phenotypic maintenance of ECs on the collagen-modified polymer NFM in terms of the expressions of cell adhesion molecules (CAMs) and EC-specific ECM proteins.

c To study the functional maintenance of ECs on the collagen-modified polymer NFM by cDNA microarray technology to analyze the expression profiles of the function-related genes.

3. To construct 3-D tubular collagen-modified polymer nanofiber scaffolds which facilitate quick, stable, and effective endothelialization in the lumen.

   Hypothesis: By rotational seeding ECs onto the lumen of the tubular nanofiber scaffolds, evenly distributed ECs would be achieved. Also similar endothelialization would occur onto the lumen of the 3-D tubular nanofiber scaffolds as that on the collagen-modified polymer NFM.

   a To construct 3-D tubular nanofiber scaffolds.

   b To rotationally seed ECs onto the lumen of the tubular nanofiber scaffolds.

   c To establish an animal model to prove the basic concept of using the tubular nanofiber scaffolds as vascular grafts.

1.3 Thesis scope

As one of the pioneer studies in the application of electrospun nanofiber scaffolds in tissue engineered small-diameter vascular grafts, we focused on scaffold fabrication and primary *in vitro* cell culture study. In order to mimic the physical cues of ECM such as porosity and 3-D fiber network, polymer nanofiber scaffolds were constructed by electrospinning. A copolymer from biodegradable aliphatic polyester family, the random poly(L-lactic acid)-*co*-poly(ε-caprolactone) P(LLA-CL 70:30),

was chosen. Such a kind of copolymer has a potential to enable its degradation rate and mechanical property to be controlled. PLLA is a semi-crystallized hard and brittle material, while PCL is a semi-crystalline material with rubbery properties, thus the copolymer of PLLA and PCL can achieve an adjustable mechanical property *via* adjusting the ratio of the two components. In order to add the chemical cue, we chose type I collagen, which is the main type of collagen in connective tissue and is present throughout the arterial wall, to be included into the P(LLA-CL) nanofiber scaffolds either through electrospining the mixture of P(LLA-CL) and collagen, or through collagen coating during postprocessing of the P(LLA-CL) nanofiber scaffolds. The ECs we chose was human coronary artery endothelial cells (HCAECs). *In vitro* EC growth on the nanofiber scaffolds was studied in terms of phenotypic maintenance through RT-PCR analysis for CAMs and ECM proteins, and functional maintenance through cDNA analysis for function-related 112 genes. A rabbit epigastric free flap model was established to prove the basic concept of using the 3-D tubular collagen-modified P(LLA-CL) nanofiber scaffolds as tissue engineered vascular grafts.

1.4 Thesis values

It is hope that this study would provide an approach to develop synthetic analogues of the natural ECM for improved ECs attachment and phenotype and functional maintenance, and ultimately approach the development of tissue engineered small-diameter vascular grafts for their clinical applications in the treatment of peripheral and cardiovascular disease. In addition to vascular graft

application, the nanofiber scaffold may also act as a new type of cell culture surface for different kinds of cell which can be incorporated into a variety of applications of tissue engineering and cell-based therapies.

Chapter 2

Literature Review

2.1 Challenges of small-diameter vascular grafts

The first synthetic vascular grafts used clinically were made of the woven fabric Vinyon N by Voorhees in 1952 (Voorhees *et al.*, 1952;Blakemore and Voorhees, 1954). From then on, a variety of materials including nylon, Orlon, PET (poly(ethylene terephthalate), Dacron®), ePTFE (expanded polytetrafluoroethylen, Teflon®), polyethylene, and polyurethane have been made into vascular grafts. For replacement of the abdominal aorta and iliac arteries, which have an inner diameter more than 6 mm, knitted Dacron® is the common choice, whilst for the femoropopliteal and femorotibial bypass, which have an inner diameter less than 6 mm, ePTFE is used together with knitted Dacron (Hastings, 1992). Although very inert, those materials do evoke host-tissue foreign body responses, initiated first by plasma protein deposition known as the Vroman effect (Vroman and Adams, 1969), followed by leukocytes and platelets adhesion and the migration of endothelial and smooth muscle cell. These lead to thrombosis (static aggregation of blood factors) in the early phase followed by a continuous and intimal hyperplasia (excessive SMC ingrowth and plasma protein deposits) in the chronic phase. Thrombosis phenomenon will be more severe in small-diameter vascular grafts (inner diameter < 6 mm)

(Niklason and Seruya, 2002). This is because in small-diameter vascular grafts, blood pressure, resistance of blood flow, shear stress, and surface-to-volume ratio are high, which result in increased contact time of blood components with grafts and increased activation of blood coagulation (thrombosis) (Matsuda, 2004). As a result, small-diameter synthetic vascular grafts suffer thrombosis rates greater than 40% after 6 months (Sayers *et al.*, 1998) and only 15-30% of them remain patent after 5 years (Seal *et al.*, 2001). The higher propensity of small-diameter vascular grafts to thrombosis has spurred the scientists to improve the standard materials and develop new materials. It is also to this challenge that tissue engineering approach is seeking to answer.

2.2 Rationale of constructing tissue engineered vascular grafts

2.2.1 Natural vascular structure

Current research on tissue engineered small-diameter vascular grafts focused more on the development of native blood vessel-like tubes (or conduits). The development of biomimetic vascular grafts relies on the understanding of the anatomical structure and the biological functions of blood vessels. Normal blood vessels (except capillaries) have tri-lamellar structures, with each layer having specific functional properties (Figure 2.1). The intima (tunica intima) contains the endothelium, which is a single layer of ECs functioning to prevent spontaneous blood coagulation. As an interface between dynamic blood flow and static blood vessel wall,

ECs are directly exposed to flow and the associated shear stress and blood pressure, which make ECs elongate in response to flow and orient their major axis with the direction of flow. Moreover ECs attach to a subendothelial layer which is a connective tissue bed, called the basement membrane (BM). This is adjacent to the internal elastic lamina which is a band of elastic fibers, found most prominently in larger arteries. The media layer (tunica media) is composed of smooth muscle cells (SMCs) and variable amount of connective tissues such as collagen, elastin, and proteoglycans. Specially, SMCs and collagen fibers have a marked circumferential orientation to withstand the higher pressures in the blood circulation, as well as their abilities to contract or relax in response to external stimulus. The adventitia layer (tunica adventitia) is composed primarily of fibroblasts and loose connective tissue fibers (Niklason and Seruya, 2002). In arteries with diameter greater than 1 mm, the innermost layer of the wall (intima) is nourished from blood flow in the lumen while the outer layers (the adventitia and part of the media) are supplied from small blood vessels called vasa vasorum (How, 1992).

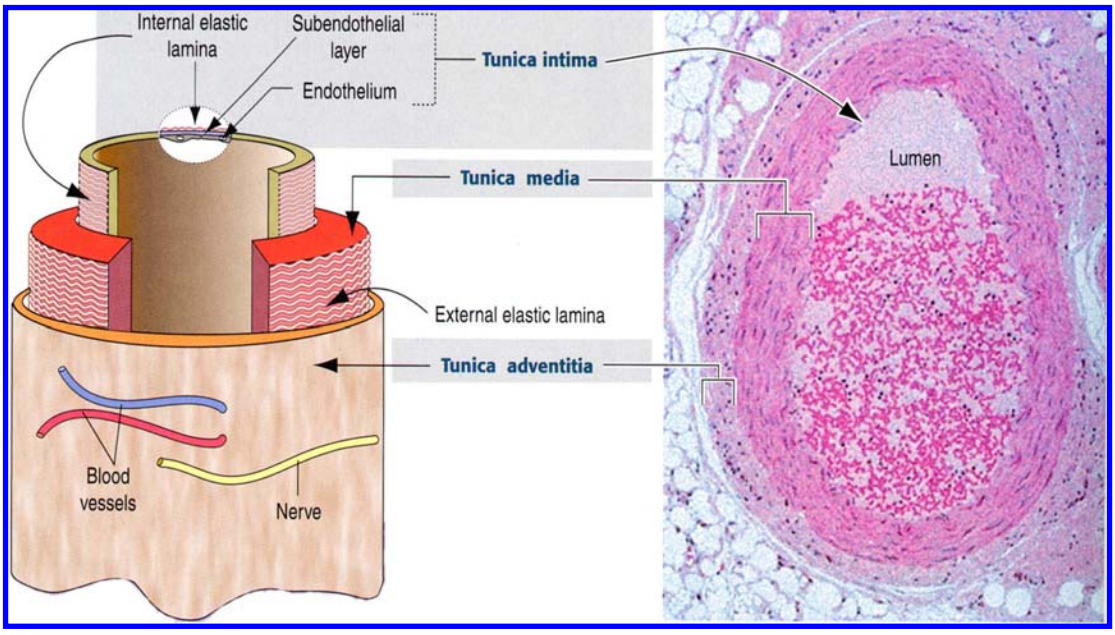

Figure 2.1. Schematic graph of the basic tri-lamellar structure of blood vessels.

The ECM in the vascular tissues forms a network composed primarily of collagen (mainly type I and III), elastin fibers (Figure 2.2), proteoglycans (including versican, decorin, biglycan, lumican, and perlecan), hyaluronan, and glycoproteins (mainly laminin, fibronectin, thrombospondin and tenascin). The mechanical properties critical to blood vessels' functions include tensile stiffness, compliance, elasticity and viscoelasticity. Collagen provides the tensile stiffness; elastin offer elastic properties; proteoglycans contribute to compressibility; the combination of all are responsible for the viscoelasticity property.

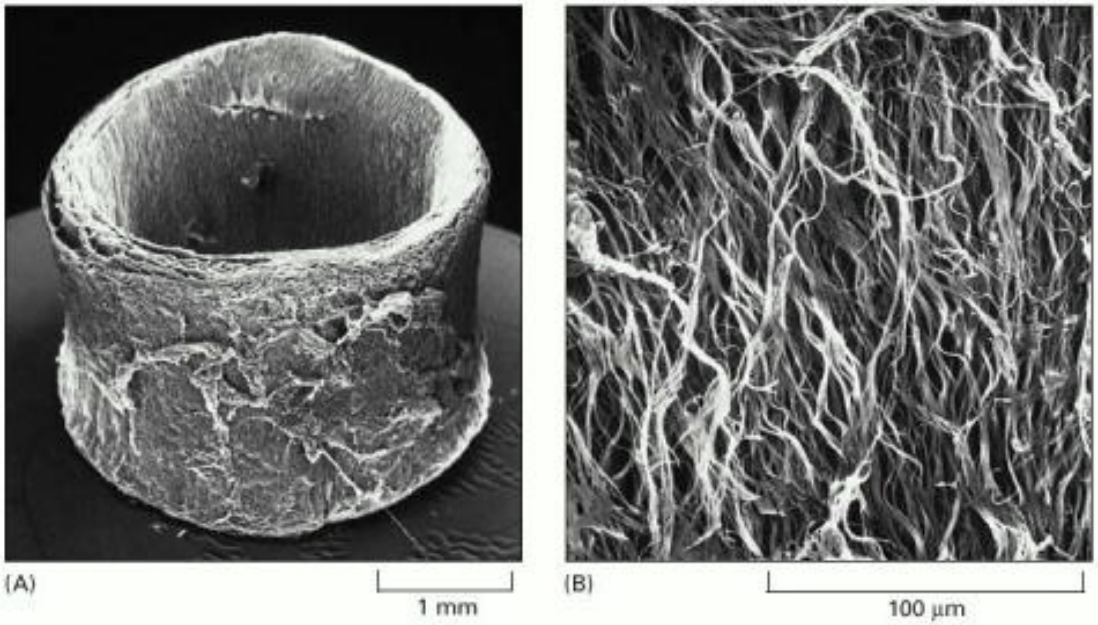

Figure 2.2. Elastic fibers**.** These scanning electron micrographs show (A) a low-power view of a segment of a dog's aorta and (B) a high-power view of the dense network of longitudinally oriented elastic fibers in the outer layer of the same blood vessel. All the other components have been digested away with enzymes and formic acid. Reprint with permission from (Alberts *et al.*, 2002).

One important ECM structure in human body is the basement membrane (also called basal lamina), which is a flexible thin (40-120 nm thick) mat that underlie all epithelial cells (Figure 2.3) or endothelial cell sheets to separate them from the underlying connective tissue. In blood vessels, the basement membrane under the EC layer is mainly composed of EC-secreted type IV collagen and laminin nanofibers embedded in heparin sulfate proteoglycan hydrogels. The basement membrane shows a nano- to submicron-scale topography of ECM macromolecules, including fiber mesh, pores, ridges, grooves, and peak valleys (Kwon *et al.*, 2005) (Figure 2.4), which are also the features of the nanofiber scaffold. Therefore it makes sense to use the non-woven polymer nanofiber scaffold to construct the inner surface of vascular graft capable of quick endothelialization.

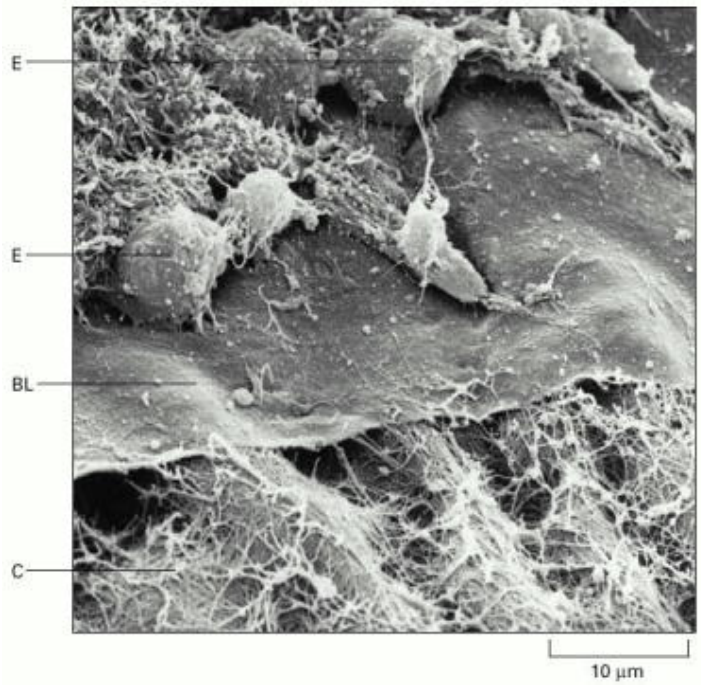

Figure 2.3. The basal lamina in the cornea of a chick embryo. In this scanning electron micrograph, some of the epithelial cells (E) have been removed to expose the upper surface of the matlike basal lamina (BL). A network of collagen fibrils (C) in the underlying connective tissue interacts with the lower face of the lamina. Reprint with permission from (Alberts *et al.*, 2002).

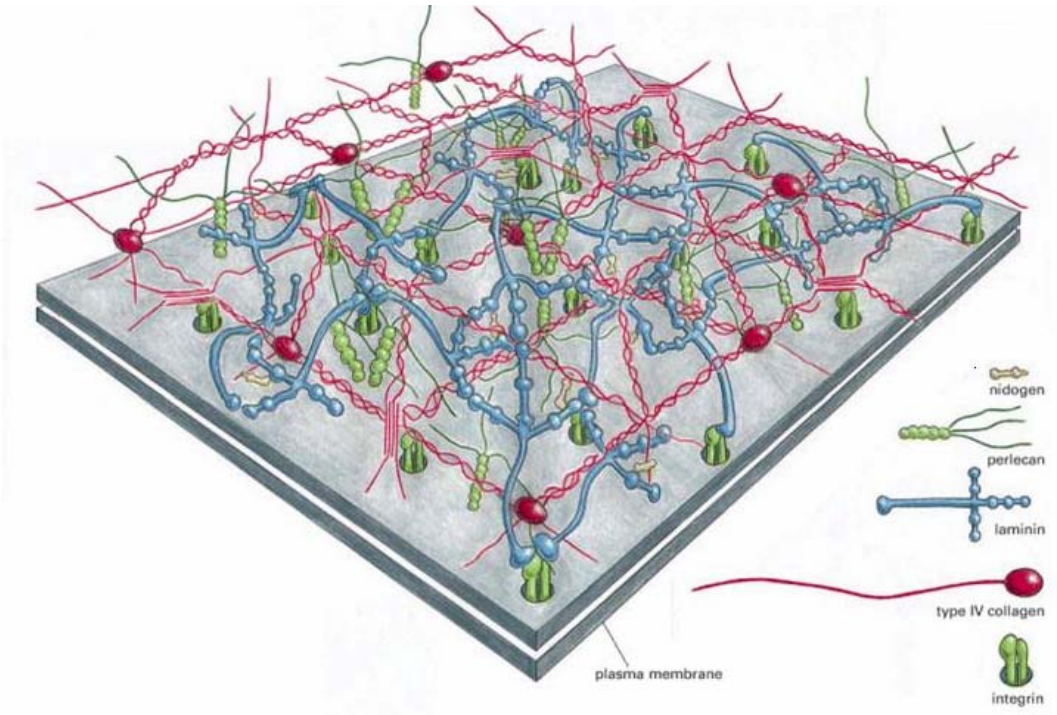

Figure 2.4. A model of the molecular structure of a basement membrane (basal lamina). Reprint with permission from (Alberts *et al.*, 2002).

Mimicing the three layer structure of native blood vessels has been the principle in tissue engineering approaches to design vascular grafts (Niklason and Seruya, 2002). Basically, three models have been used to construct the native-like tissue engineered vascular grafts using vascular cell types: 1) a mono-layer of EC-seeded collagen gel (Miwa and Matsuda, 1994); 2) a bi-layer of EC-monolayered intimal and SMC-inoculated medial layer (Matsuda and Miwa, 1995); 3) a three-layer of EC, SMC, and fibroblasts (Ishibashi and Matsuda, 1994). Results showed that three-layered vascular grafts had the highest potential of vascular wall regeneration, followed by the bi-layer vascular grafts (Matsuda, 2004). Robert Langer gave another criterion for the ideal tissue engineered vascular grafts: confluent endothelium, differentiated SMCs, sufficient mechanical integrity, and elastic modulus (Niklason *et al.*, 1999). It was found that the short-term patency of vascular grafts is highly dependent on the luminal surface properties while long-term patency depends on mechanical properties of the grafts (Dewey *et al.*, 1981).

2.2.2 Synthetic Materials

As mentioned before, tissue engineered vascular grafts have the potential to resolve the problem which limits application of synthetic vascular grafts in small-diameter blood vessel replacements. In order to do this, tissue engineered vascular grafts should have characteristics similar to those of healthy recipients' blood vessels, and allow complete integration into the biological environment with low host-tissue reactivity. Furthermore, an active anti-thrombogenic inner surface is necessary

(Tomizawa, 2003). Synthetic material's characteristics such as biocompatibility, biodegradability, porosity, mechanical properties, and surface chemistry *etc* affect independently or synergistically the patency of implanted vascular grafts (Table 2.1).

Table 2.1. Synthetic material requirements for tissue engineered vascular grafts

Requirements	**Explanation**
Biocompatibility	Haemocompatible; lack of thrombogenicity; low-inflammatory; nontoxic; non-carcinogenic; nonimmunogenic; resistant to infection
Biodegradability	By-products of polymer degradation are not toxic; degradation rate should match that of tissue regeneration
Porosity	Allowing cell infiltration from the adventitial; maintaining hemostasis; sufficient mass transfer of gases and nutrients
Mechanical property	Enough burst strength to withstand the physiological blood pressure and cyclic loading; compliant; elastic; good suturability, kink resistance
Surface chemistry	Bioactivity for cell attachment, spread, and proliferation
Others	Off the shelf availability in various diameters and lengths; uncomplicated storage or preparation requirements; ease of handling; ease of adequate sterilization; ease and low cost fabrication

2.2.3 Endothelialization

Seeding ECs onto the lumen of vascular grafts is a promising method to improve the anti-thrombogenic property of vascular grafts, which is regarded as the beginning of tissue engineering approach applied to the cardiovascular system (Nerem and Seliktar, 2001). Credit for this concept goes to Herring *et al* in 1978 (Herring *et al.*, 1978). The rationale behind ECs seeding is to provide a 'natural'

interface between the circulating blood and the underlying vascular grafts, which can improve resistance of vascular grafts to thrombosis and intimal hyperplasia. The invasion of vascular grafts by fibrous tissues and the deposition of ECs on the lumen were observed in animal models but not in humans, where the deposition of compacted fibrin was observed (Tomizawa, 2003). The "incomplete endothelialization" in humans is an important limitation to the patency of small-diameter vascular grafts, leading to great research interest in the development of "ECs-seeding" vascular grafts.

In addition to acting as natural interface between the blood and subendothelial tissues, an intact and quiescent endothelium proactively inhibits thrombosis (Maruyama, 1998;Pearson, 1999;Gross and Aird, 2000;Mitchell and Niklason, 2003). Figure 2.5 shows the pathway of EC anti-thrombogenic signaling. Thrombomodulin, a receptor expressed on the surface of ECs, catalyzes activation of protein C by binding thrombin. ECs also produce the anticoagulant protein S, a cofactor for protein C. Activated protein C proteolytically inactivates factors Va and VIIIa, thereby counteracting the coagulation cascade. ECs also synthesize heparan sulfate proteoglycans that bind antithrombin III, which neutralizes and inhibits thrombin. Platelet adhesion to a quiescent endothelium is suppressed by release of nitric oxide and prostacyclin, and by the presence of negatively charged proteoglycans on the EC surface. If coagulation occurs, ECs will secrete tissue-type plasminogen activator (t-PA), which lyses fibrin clots. Thus, in the development of tissue engineered vascular

grafts, an important goal should be to create a confluent and adherent ECs layer with many of these antithrombogenic properties.

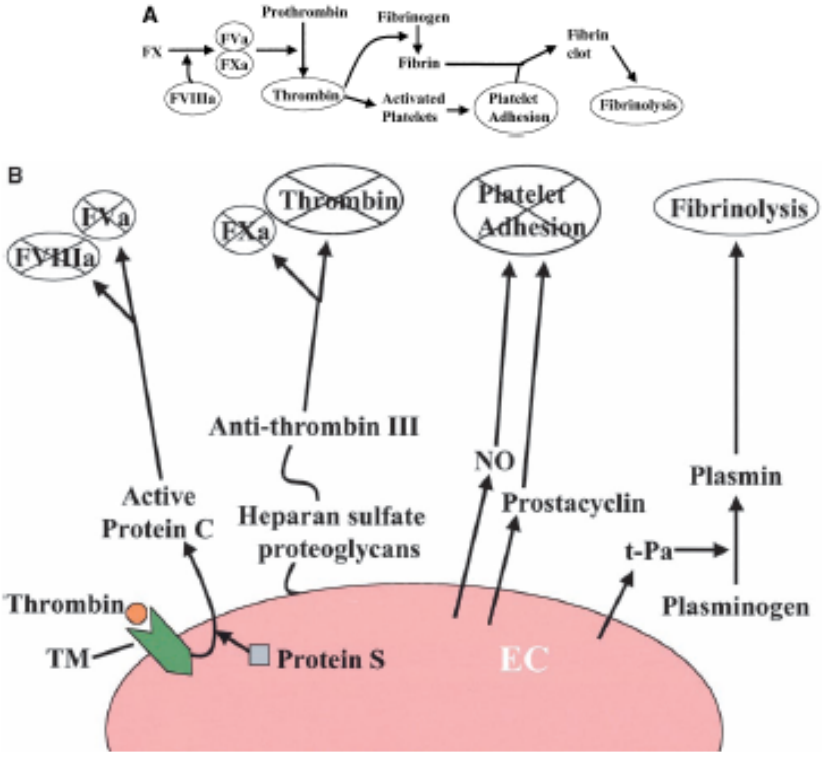

Figure 2.5. Pathway of thrombus formation (A) and EC antithrombogenic signaling (B). Reprint with permission from (Mitchell and Niklason, 2003).

Although ECs-seeding is effective to provide the anti-thrombogenic layer, however, endothelialization has always been limited because attached ECs can detach from the lumen of vascular grafts upon exposure to shear force and cyclic strain due to blood circulation (Xue.L, 2000). Other issues like source of ECs, seeding efficiency of ECs, and the functional maintenance of ECs are also challenging. For example, endothelial progenitor cells (EPCs) from the peripheral blood and genetically-modified fibroblasts were used as alternatives cell sources because of the

difficulty of harvesting ECs from patients and the lack of off-the-shelf availability, which is clinically important.

One of the approaches to enhance EC attachment is to immobilize either ECM proteins or bioactive peptides onto vascular graft's surface (Salacinski *et al.*, 2001b). For example, ePTFE was coated with fibronectin and RGD (Arg Gly Asp) containing peptides to improve EC attachment. The coated ePTFE was seeded with saphenous vein ECs for 30 min and exposed to shear stress in an artificial flow circuit. Both cell attachment and retention were significantly increased by coating with fibronectin as well as immobilization RGD containing peptides (Walluscheck *et al.*, 1996). However, some bioactive molecules and ECM proteins are not EC-specific, resulting in adhesions of other types of cells like activated platelets, which may lead to more thrombogenic surface. Thus it is critical to establish a confluence and stable ECs layer on the lumen of vascular grafts before implantation, which can completely cover vascular grafts' inner surfaces from contacting with blood cells (Shin *et al.*, 2003). Moreover, bioactive peptide like Arg-Glu-Asp-Val (REDV) sequence from III-CS domain of human plasma fibronectin was demonstrated to only interact with the receptor present in ECs. The surface modification with this peptide allowed EC attachment and spreading but limited adhesion of vascular SMCs and platelets (Hubbell *et al.*, 1991;Hubbell *et al.*, 1992).

2.2.4 Mechanical properties

Mechanical property is an important parameter to decide the long-term patency of vascular grafts (Dewey *et al.*, 1981). One of the main failure modes of vascular grafts is intimal hyperplasia especially at the anastomosis regions, which is believed to be associated with shear stress disturbances due to the compliance mismatch of the compliant artery and the rigid graft at the end-to-end anastomosis (Salacinski *et al.*, 2001a). Most of the commercialized vascular grafts made from PET (Dacron™) and PTFE (Teflon™) are much less compliant (or too stiff) compared with that of the native blood vessels. This is one of the reasons for their lack of patency when used as the small- diameter vascular grafts. Besides compliance, vascular grafts should have sufficient tensile stiffness to withstand forces from the initial wound contraction and later tissue remodeling (Hutmacher *et al.*, 2004), as well as the physiological blood pressure (120 mmHg for typical systolic pressure) (Niklason *et al.*, 1999). Although significant progress has been made, fabrication of vascular grafts with identical mechanical properties to those of native blood vessels remains an elusive goal. It should be highlighted, however, that a major advantage of tissue engineered vascular grafts is that they don't need to have mechanical properties identical to those of native blood vessels at implantation. Being composed of viable tissues with the potential to remodel, repair, and grow, tissue engineered vascular grafts should be theoretically able to completely adapt to local dynamic conditions and acquire the structure and mechanical features of the blood vessels, for which they replace.

2.3 Current approaches

Tissue engineering has been successfully used for repair of chronic wounds and burns, and at the experimental study level in repair of cartilage defects. It is believed that a biomimetic scaffold that degrades over time will allow natural tissue ingrowth and healing. Optimally, the breakdown of materials used will not create excessively toxic, allergenic, thrombogenic or carcinogenic by-products. Biodegradable scaffolds and vascular cells are vital constituents in the development of tissue engineered vascular grafts. The main approaches include collagen-based construct, cell self-assembly technologies (or cell-sheets), and biodegradable polymer vascular graft (Seal *et al.*, 2001).

One of the earliest methods was to construct collagen gel based vascular grafts. Weinberg *et al* reported in "*Science*" in 1986 the technique of fabricating a three layer vascular graft using vascular cells grown in a tubular collagen gel: an adventitia-like layer made from fibroblasts and collagen, a media-like layer made from SMC and collagen, and an intima-like EC monolayer constructed into a tubular configuration. The multilayered structure of the graft resembled that of an artery. However, in order to withstand physiological pressures, the graft required support sleeves made from non-biodegradable Dacron™ (Weinberg and Bell, 1986). Figure 2.6 illustrates the compositions and structure of this tubular construct. Improvements were mainly carried out to overcome the inherent mechanical weakness of the graft by enhancing the structure integrity (L'Heureux *et al.*, 1993) and circumferential tensile strength

(Tranquillo *et al.*, 1996). Dynamic culture was also used to improve its mechanical strength (Seliktar *et al.*, 2000). However, a collagen gel based vascular graft with mechanical properties comparable to that of a native blood vessel has not been shown with these approaches.

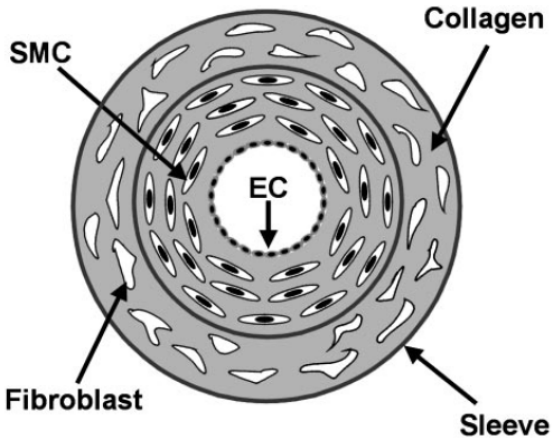

Figure 2.6. Schematic representations of a collagen-based construct. The most general configuration contains an adventitia-like layer, a media-like layer, a monolayer of ECs, and Dacron^{TM} sleeves for structural reinforcement. Reprint with permission from (Nerem and Seliktar, 2001).

The second approach used cell-assembly (cell-sheet) technology to construct vascular grafts, which was developed by Auger's group in 1998 (L'Heureux *et al.*, 1998). The cell self-assembly model is made with intact layers of human vascular cells grown to overconfluence to form viable sheets of cells and ECM (Figure 2.7). The monolayer cell sheets formed were rolled around a mandrel to form tissue layers within a tubular wall. After culture, ECs were seeded onto the inner surface. Therefore, a three layered vascular graft was formed which mimic the structure of a native blood vessel. The tubular structure made by this way could withstand 2000 mmHg pressure, similar to native arteries. When grafted *in vivo*, these vessels performed modestly, with a 50% patency rate at 1 week after implantation. The

advantage of this approach is that it can eliminate the immunological mismatch, provided autologous cells are used, which is unlike the collagen-gel based vascular grafts using reconstituted animal proteins. However, the main drawback of this technique is the very prolonged culture period to around 13 weeks (Nerem and Seliktar, 2001).

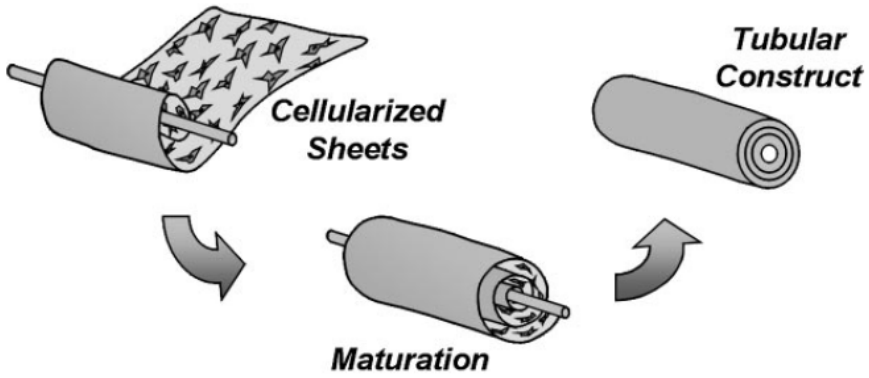

Figure 2.7. Schematic representation of the cell self-assembly model. Vascular cells are cultured to form a continuous sheet of cells and extracellular matrix and then rolled over a central mandrel. The construct is matured over 10 weeks, allowing the cell to organize into a mechanically stable tubular construct. Reprint with permission from (Nerem and Seliktar, 2001).

The third method, met with some success recently, was to hybridize biodegradable polymer materials with vascular cells. In one study, SMCs were seeded onto a porous poly(glycolic acid) (PGA) tubular scaffold and cultured for several weeks in a customized bioreactor applying pulsatile radial distention (Niklason *et al.*, 1999) (Figure 2.8). During this time, the cells produced large amounts of ECM proteins concurrently with the degradation of the PGA scaffold. The cells-PGA constructs were maintained in a culture medium that was supplemented with biochemicals to promote synthesis of ECM proteins. After 8 week's culture, the PGA scaffold had been replaced by a SMC medial layer. ECs were then seeded onto the

lumen of the construct to form a confluent monolayer. The initial findings demonstrated that the construct exhibited burst pressures greater than 2000 mmHg. When implanted into a swine, the construct was able to remain patent for up to 4 weeks. The use of a biocompatible and biodegradable scaffold to provide a structural support, as well as the dynamic bioreactor to provide mechanical stimulation, are particularly important in the tissue regeneration.

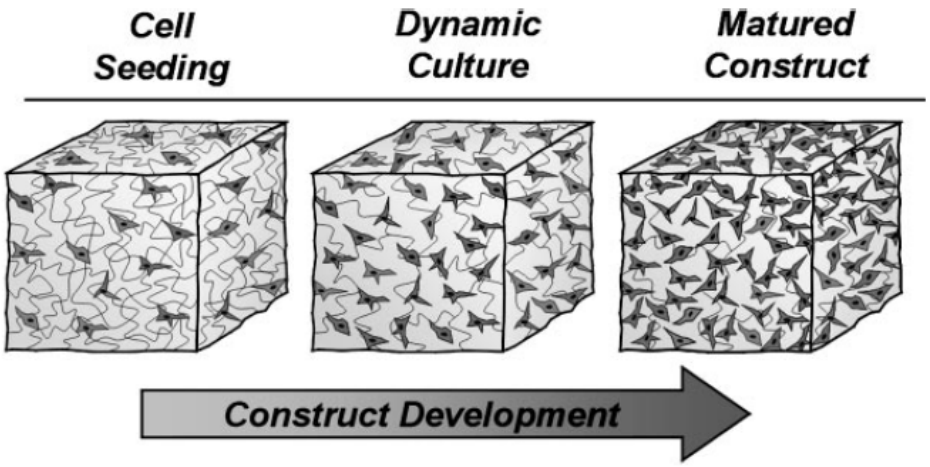

Figure 2.8. Schematic representation of a cell-seeded polymeric scaffold. Vascular cells are cultured on a woven PGA mesh. The construct is matured over 8 weeks of dynamic culture, allowing the cells to proliferate and produce and organize extracellular matrix as the PGA degrades. Reprint with permission from (Nerem and Seliktar, 2001).

The comparison between these three methods is summarized in Table 2.2.

Table 2.2. Comparison between the three methods of constructing tissue engineered vascular grafts (TEVG)

TEVG	Materials	Advantages	Disadvantages	Current Status
Collagen Gel	Collagen Type I, III	Good tissue remolding	Poor mechanical property; immunological mismatch	Bench study
Cell Sheet	None	Elimination of immunological mismatch	Minimum 3 months until implantable grafts were produced	Reported clinical application on human in 2006 (L'Heureux *et al.*, 2006)
Biodegradable Scaffolds	Polyester	Good mechanical property; good patency if combined with cell		First clinical application on human in 1999 using PCL-PLLA tube reinforced with woven PGA (Shin'oka *et al.*, 2001)

It can be seen from Table 2.2 that biodegradable polymer scaffolds approach went faster into the clinical practice than the other two methods. This may be due to that synthetic scaffolds enable better control over physical properties such as mechanical properties. Also varieties of surface modification methods like protein and peptide immobilization, plasma treatment can provide better biocompatibility to the original polymer materials (Waddell *et al.*, 1992;Chan *et al.*, 1996).

2.4 Potential of polymer nanofibers as tissue engineered scaffolds

2.4.1 Electrospinning

Methods to produce nanoscaled polymeric fibers include electrospinning, self-assembly, and phase separation, among which electrospinning is the most simple and efficient one. Electrospinning has been known for over seventy years. The patent of electrospinning was granted in 1902 in the USA (William, 1902). Special needs in biomedical and other applications have stimulated renewed interests and studies on electrospinning since 1990s. Since then over 200 universities and research institutes worldwide have investigated various aspects of electrospinning. The number of patents applied for process and applications based on electrospinning are also growing over the years. Startups such as eSpin Technologies, NanoTechnics, and KATO Tech are just some companies that sought to reap the unique advantages offered by electrospinning while companies such as Donaldson have been using electrospun fibers in their air filtration products for the last two decades (Ramakrishna *et al.*, 2006).

A key advantage of electrospinning to prepare ultra-fine polymer fibers is that almost any polymer with sufficiently high molecular weight that forms solution can be electrospun. Nanofibers made of natural polymers, polymer blends, nanoparticles or drug impregnated polymers and ceramic precursors have been successfully

electrospun. Different fiber morphologies such as beaded fibers, ribbon fibers, porous fibers and core-shell, have also been spun (Ramakrishna *et al.*, 2006).

The principle of electrospinning is to use an electric field to draw polymer solution or melt from an orifice to a collector (Figure 2.9). High voltages (10-20 kV) are used to generate sufficient surface charge to overcome the surface tension of the solution and a jet then erupts from the tip of the spinneret. The jet is only stable near the tip of the spinneret, after which the jet undergoes bending instability (Yarin *et al.*, 2001). As the charged jet accelerates toward regions of lower potential, the entanglements of the polymer chain will prevent the jet from breaking up while the solvent evaporates resulting in fiber formation. Generally, a grounded plate is used to collect the fibers (Figure 2.9) (Ramakrishna *et al.*, 2006). The diameters of the electrospun fibers are at least one order of magnitude smaller than those made by conventional extrusion techniques.

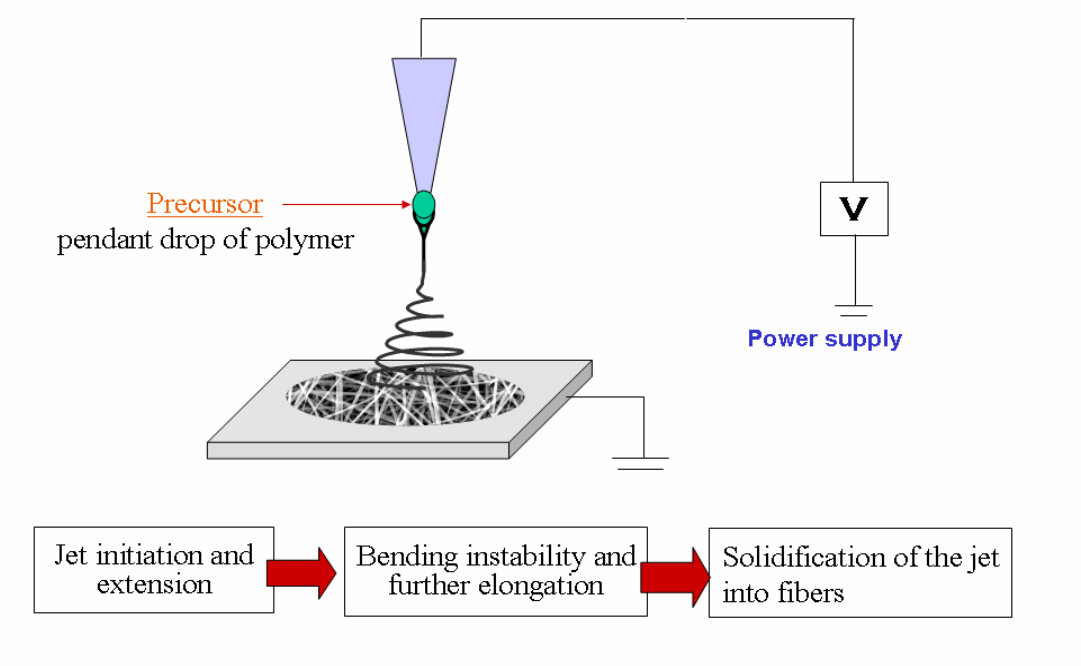

Figure 2.9. Electrospinning basic principles (Ramakrishna *et al.*, 2006).

Electrospinning usually produces non-woven sheet with a flat profile due to the ejection rate of the polymer solution through the orifice must be controlled at a low value if nanoscaled fiber diameter is desired. However, 3-D non-woven fibrous mesh can be obtained if the electrospinning time is long enough. Our experiences show that the thickness of the nanofiber increases with the electrospinning time at a typical speed of 20 μm/h. One effective method to increase the thickness of the non-woven sheet is to use more than one orifice simultaneously, in which the electrospinning speed will be proportional to the number of the orifices. This method may produce 3-D nanofibrous scaffold in a short time in the future (Ma *et al.*, 2005b).

2.4.2 Nanofiber scaffolds

The principle of designing tissue engineered scaffolds is clear: the scaffold should mimic the structure and biological function of native extracellular matrix (ECM) as much as possible, both in terms of chemical compositions and physical structures. In terms of chemical compositions, ECM is mainly composed of three major classes of biomolecules: structural proteins like collagen and elastin, specialized proteins like fibronectin and laminin, and proteoglycans composed of a protein core and glycosaminoglycans (GAGs). In terms of physical structures, ECM is consisted of various protein fibrils interwoven within a hydrated network of GAG chains (Lutolf and Hubbell, 2005). The function of the ECM is far more than providing a physical support for cells. It also provides a substrate with specific ligands for cell adhesion and migration, and regulates cellular proliferation and functions by storing and presenting various growth factors (Alberts *et al.*, 2002). It is reasonably expected that an ECM-mimic tissue engineered scaffold may play a similar role to promote tissue regeneration *in vitro* as the native ECM does *in vivo*.

Polymer nanofiber scaffold is among the most promising biomaterials for native ECM analogues (Ma *et al.*, 2005b). The potential of applying electrospinning in tissue engineered scaffolds is enormous since nanofiber scaffolds can mimic the nanoscaled dimension of the natural ECM and mesoscopic scale of ECM's spatial organization by controlling fiber's orientation and spatial placement. Moreover, nanofiber scaffolds can emulate chemical compositions of ECM by including

biomolecules into fibers. We found that there is a vivid similarity between the electrospun polycaprolactone (PCL) nanofiber scaffold and native ECM in rat cornea (Figure 2.10) (Nishida *et al.*, 1988). Another example is the apparent similarity between the electrospun collagen nanofibers and the ECM of the small intestine, which is composed of collagen bundles, in terms of both physical structure and chemical composition (Figure 2.11) (Teo *et al.*, 2006). In fact, non-woven microscaled polymer scaffolds have already been widely used in tissue engineering for a long time due to their high surface area and high porosity (Cao *et al.*, 1997).

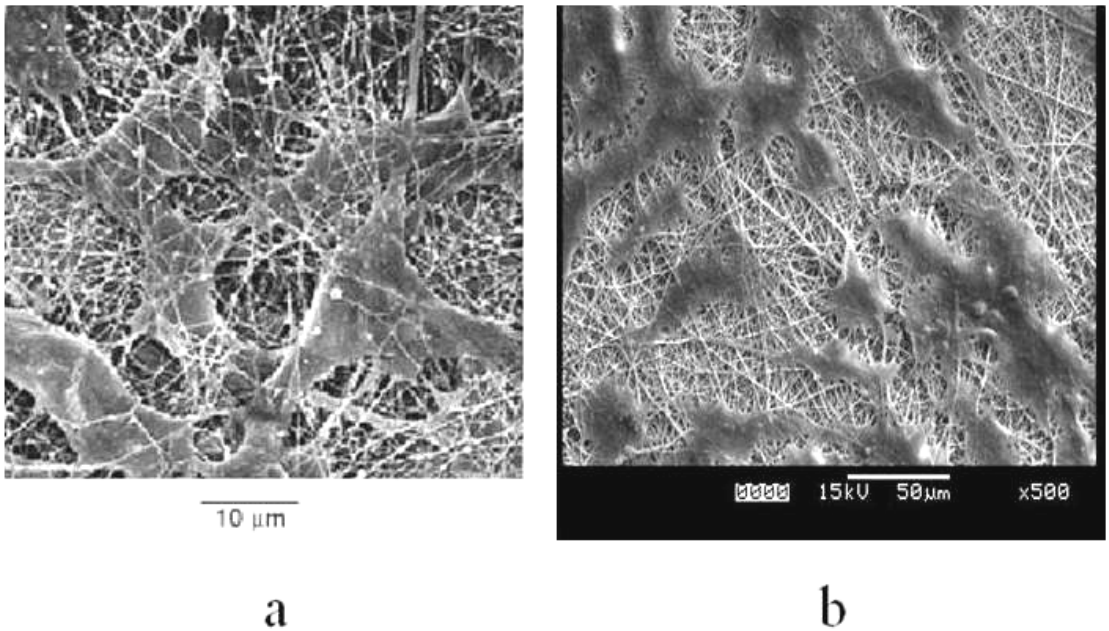

Figure 2.10. Similarity between the native ECM protein structure and the electrospun polymer nanofiber scaffold. (a) Fibroblasts grown *in vivo* on collagen fibrils of rat cornea (Nishida *et al.*, 1988); (b) ECs cultured *in vitro* on the electrospun PCL nanofiber scaffold. Reprint with permission from (Ma *et al.*, 2005b).

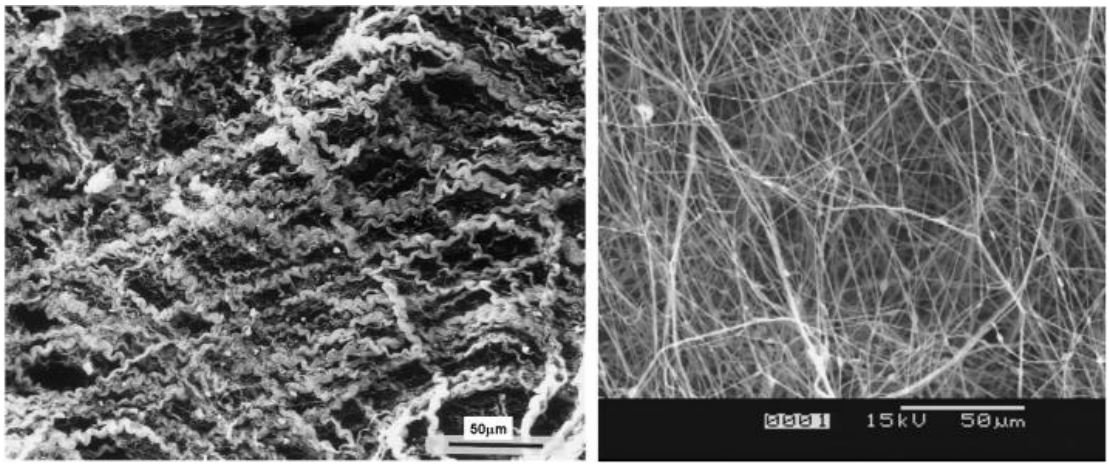

a **b**

Figure 2.11. Similarity between (a) the natural collagen bundles of the connective stroma of the small intestine (Ottani *et al.*, 2001) and (b) the electrospun collagen nanofibers. Reprint with permission from (Teo *et al.*, 2006).

Most of widely used biomaterials have been fabricated into electrospun nanofiber scaffolds. Typical biodegradable polymers like PLGA or PCL and water soluble polymers like poly(ethylene oxide) (PEO) and poly (vinyl alcohol) (PVA) can be easily electrospun into nanofibers using organic or water solvent (Jaeger *et al.*, 1998;Li *et al.*, 2002;Li *et al.*, 2003;Drew *et al.*, 2003). Natural occurred biomaterials like collagen (Huang *et al.*, 2001;Matthews *et al.*, 2002;Matthews *et al.*, 2003;Rho *et al.*, 2006;Chen *et al.*, 2006;Yoo *et al.*, 2006), silk protein (Jin *et al.*, 2002;Kim *et al.*, 2003;Min *et al.*, 2004;Jin *et al.*, 2004;Kim *et al.*, 2005b), elastin-mimic peptide (Huang *et al.*, 2000), fibrinogen (Wnek *et al.*, 2003), casein and lipase enzyme (Xie and Hsieh, 2003) and even DNA (Fang and Reneker, 1997) have also been electrospun into nanofibers. Electrospinning of the natural occurred biomaterials is much more challenging compared with the synthetic polymers for the difficulties in looking for appropriate solvent. 1,1,1,3,3,3-hexafluoro-2-propanol (HFP) is a commonly used solvent for electrospinning of proteins (Matthews *et al.*, 2002;Wnek

et al., 2003). Electrospinning of silk fibroin has been performed with formic acid as the solvent (Kim *et al.*, 2003;Min *et al.*, 2004). The silk fibroin can also be mixed with PEO in water and electrospun, followed by washing with methanol to remove the PEO (Jin *et al.*, 2002;Jin *et al.*, 2004). Huang *et al* prepared polypeptides containing repeated elastomeric peptide sequence of elastin by genetic engineering method. The polypeptide was dissolved in water and electrospun into nanofibers with diameter from 200 to 300 nm under appropriate conditions (Huang *et al.*, 2000). Fang X *et al* reported the electrospinning of calf thymus Na-DNA aqueous solutions with concentrations from 0.3% to 1.5% into nanofibers with diameters around 50 to 80 nm (Fang and Reneker, 1997).

The simplicity and reproducibility of fabricating well-controlled polymer nanofiber scaffolds by electrospinning have invigorated big interests in the field of tissue engineering. In addition to the ECM-like architecture, polymer nanofibers have other desired features for tissue engineered scaffolds such as biocompatibility, high porosity for tissue ingrowth, high surface area-to-volume ratio, adjustable mechanical and biodegradable properties, capability of surface modification (Ma *et al.*, 2005c), and flexibility of loading drugs or genes (Luu *et al.*, 2003). Studies have been carried out in the application of polymer nanofiber scaffolds as tissue engineered bone (Yoshimoto *et al.*, 2003), blood vessel (Mo *et al.*, 2004;Xu *et al.*, 2004a;Xu *et al.*, 2004b;Ma *et al.*, 2005c), cartilage (Li *et al.*, 2002;Li *et al.*, 2005), cardiac tissue (Shin *et al.*, 2004), peripheral nerve system (PNS) (Bini *et al.*, 2004;Yang *et al.*, 2005), ligament (Lee *et al.*, 2005), liver (Chua *et al.*, 2005), and skin (Li *et al.*, 2002) *etc*.

2.4.3 Surface modifications of polymer nanofibers

It has been well known that the interactions between cells and their environments are meditated by the "bio-recognition processes", the specific binding of the receptors on cell surfaces with their corresponding ligands (Elbert and Hubbell, 1996). In native tissues *in vivo*, cell attachment on ECM is mediated by the binding between integrins (receptors on cell surfaces) and ECM adhesion proteins such as collagen, fibronectin, vitronectin, and laminin *etc*. On biomaterial surfaces *in vitro*, the same mechanisms also apply. When foreign materials come into contact with body fluids or cell culture mediums, the initial response is protein adsorptions atop material's surfaces. Thus materials interact with cells through the adsorbed protein layer. The composition and structure of this protein layer play critical roles in determining subsequent cell behaviors (Elbert and Hubbell, 1996). A successful tissue engineering scaffold should have cell compatible surface to allow cell attachment and proliferation.

There are advantages and disadvantages for both synthetic and natural polymers when used as tissue engineering scaffolds (Table 2.3). Synthetic polymers often do not possess surface properties needed for tissue engineering applications. Actually, most mechanically strong and chemically stable synthetic polymers often have inert surfaces both chemically and biologically. In contrast, those natural polymers having active surfaces usually do not possess excellent mechanical

properties which are critical for their successful applications as tissue engineering scaffolds.

Table 2.3. Comparison between synthetic and natural polymers

Polymers	Advantages	Disadvantages
Synthetic	Easily synthesized with controlled molecular weight and other physical properties like mechanical properties	Lack of intrinsic biological activity
Natural	Possess intrinsic biological activity; enzymatically degradable	Source-related variability and contamination; limited control over parameters such as molecular weight; the potential for adverse immunological responses; variation in degradation rates due to difference in host enzyme levels; inferior mechanical properties

The same problem is also faced by electrospun synthetic polymer nanofibers when used as tissue engineering scaffolds. Thus surface modifications of synthetic polymer nanofibers were widely studied. Functionalization of polymer nanofibers is typically carried out either through direct incorporating biomolecules into the spinning solution during electrospinning process or through immobilizing biomolecules onto the surface of nanofibers during the postprocessing step (Pham *et al.*, 2006). Special attentions are required to protect biodegradable polymer nanofibers from rapid degradation and destruction during surface modification process. Strong reaction conditions such as plasma, ultraviolet (UV), γ radiation, high temperature, and acidic or basic environments may destroy degradable nanofibers to some extent. Because of the high surface area-to-volume ratio, biodegradable polymer nanofibers may degrade much faster than bulk materials due to the larger

contact area between nanofibers and the environment. It was found that even poly(ethylene terephthalate) (PET) nanofibers showed considerable degradation in acidic or basic solutions. Some surface modification methods, such as physical coating and "layer by layer" electrostatic interaction, can immobilize biomolecules onto nanofiber surfaces under very moderate conditions, and thus may be the most ideal methods in future (Ma *et al.*, 2005b).

2.4.3.1 Physical methods

The easiest and the most straightforward way to modify polymer surfaces is coating biomolecules onto polymer surfaces or just blending biomolecules into bulk polymers. Although the biggest limitation of this technique is the instability of the polymer surface compositions caused by the losing of biomolecules from polymers, it is still a good choice if this losing is too slow to be considered, or not fast enough to affect applications of surface modified polymers. For example, collagen, fibronectin and laminin have been coated onto the electrospun silk fibroin (SF) nanofiber surfaces to promote cell adhesion (Min *et al.*, 2004). Human keratinocytes and fibroblasts showed spreading morphology and good attachment on the modified SF nanofibers. Similar results were also reported on collagen-coated poly(ε-caprolactone) (PCL) nanofibers, which showed improved smooth muscle cell growth and attachment (Venugopal *et al.*, 2005). Similar to coating, blending is another physical method of modifying nanofiber surfaces. Differently, blending is carried out during

the electrospinning process, while coating is carried out in the postprocessing of electrospun nanofibers.

Due to the simplicity and flexibility of blended electrospinning, different combinations of biomolecules and polymers were blended and electrospun into nanofibers for various tissue engineering applications (Table 2.4). For example, polyanifine (PANi)/gelatin and poly(lactide-co-glycolide)/gelatin/elastin blended nanofibers were investigated for the potential application of supporting rat cardiac myoblast growth (Li *et al.*, 2006b;Li *et al.*, 2006c). Results indicated that those blended nanofibers supported cell attachment and proliferation. In another study, human epidermal fibroblasts were cultured on poly(glycolic acid) (PGA)/chitin blended nanofibers and showed good cell attachment and spreading (Park *et al.*, 2006b). The same group also studied the behavior of human epidermal keratinocytes and fibroblasts on the chitin/silk fibroin blended nanofibers and observed an excellent cell attachment and spreading (Park *et al.*, 2006a).

Table 2.4. Summary of different combinations of biomolecules and polymers in blended nanofibers and their applications in tissue engineering

Combinations in blended nanofibers	**Application**	**Cells used**
Poly(L-lactide-*co*-epsilon-caprolactone) P(LLA-CL) / collagen and P(LLA-CL) / tri-n-butylamine salt of heparin (heparin-TBA) (Kwon and Matsuda, 2005)	Blood vessel regeneration	Human umbilical vein endothelial cells
Polyaniline (PANi) / gelatin (Li *et al.*, 2006b)	Heart regeneration	Rat cardiac myoblasts
Poly (lactide-*co*-glycolide) (PLGA) / gelatin / elastin (Li *et al.*, 2006c)	Heart regeneration	Rat cardiac myoblasts
Poly(glycolic acid) (PGA) / chitin (Park *et al.*, 2006b)	Skin regeneration	Human epidermal fibroblasts
Silk fibroin / chitin (Park *et al.*, 2006a)	Skin regeneration	Human epidermal keratinocyte and fibroblasts
Poly lactide-*co*-glycolide (PLGA) / dextran (Pan *et al.*, 2006)	Skin regeneration, wound healing	Dermal fibroblasts
Collagen / elastin (Buttafoco *et al.*, 2006)	Blood vessel regeneration	Smooth muscle cells
Collagen / PEO (Huang *et al.*, 2001)	Wound healing, tissue engineering, hemostatic agents	N.A.
Collagen / chondroitin sulfate (CS) (Zhong *et al.*, 2005)	Cornea regeneration	Rabbit conjunctiva fibroblast
Poly (epsilon-caprolactone) (PCL) / collagen (Ekaputra *et al.*, 2006)	Bone regeneration	Porcine mesenchymal progenitor cells

As the kind of special blended nanofibers, composite nanofibers containing both organic and inorganic elements were also fabricated through blended electrospinning (Table 2.5).

Table 2.5. Composite nanofibers fabricated through blended electrospinning

Combination in composite nanofibers	**Application**	**Cells used**
Polycaprolactone (PCL) / calcium carbonate ($CaCO_3$) (Fujihara *et al.*, 2005)	Guided bone regeneration	Osteoblast
Silk fibroin / bone morphogenetic protein 2 (BMP-2) / nanoparticles of hydroxyapatite (nHAP) (Li *et al.*, 2006a)	Bone regeneration	Human bone marrow-derived mesenchymal stem cells
Poly(3-hydroxybutyrate-co-3-hydroxyvalerate) (PHBV) / hydroxyapatite (HA) (Ito *et al.*, 2005)	General tissue regeneration	Cos-7 cells, originating from the kidney of an Africa green monkey
Gelatin / hydroxyapatite (HA) (Kim *et al.*, 2005a)	Guided tissue regeneration	Human osteoblastic cells

Blended electrospinning also offer the flexibility of loading drugs into carrier polymers during electrospinning (Pham *et al.*, 2006). But it is possible that bioactivities of drugs may be destroyed in organic solvents and under high electric field during electrospinning process. For example, Casper *et al*. incorporated heparin into nanofibers of PEO and PLGA by mixing it directly into the spinning solution (Casper *et al.*, 2005). By labeling the heparin with a fluorescent dye, the heparin was found to be distributed both throughout individual fibers and the thickness of NFM. Incorporation of poly (ethylene glycol) PEG-heparin resulted in improved heparin retention in the nanofibers (Pham *et al.*, 2006). Table 2.6 summarizes research on blending heparin into electrospun nanofibers.

Table 2.6. Blended nanofibers containing heparin through blended electrospinning

Combination of blended nanofibers	**Application**	**Release profile**
Heparin (or PEG-Heparin) / PEO / PLGA (Casper *et al.*, 2005)	Drug delivery, tissue engineering, wound healing	Incorporation of PEG-heparin permits retention of the heparin for at least 14 days
Heparin / PCL (Luong-Van *et al.*, 2006)	Drug delivery, blood vessel regeneration	A total of approximately half of the heparin was released by diffusion from the nanofibers after 14 days.
Tri-n-butylamine salt of heparin (Heparin-TBA) / poly(L-lactide-co-epsilon-caprolactone) P(LLA-CL) (Kwon and Matsuda, 2005)	Blood vessel regeneration	The releasing rate, released amount, and surface content of heparin-TBA were increased with increasing heparin-TBA content in blended fibers

Blended electrospinning was also used to overcome the disadvantage of un-spinnabillity of some polymers due to their molecular weight/solubility. Polymers which are well-suited for electrospinning can be blended with the original polymers to facilitate the electrospinning process. For example, PEO was added into the aqueous solution of 3,3'-dithiobis(propanoic dihydrazide)-modified hyaluronic acid (HA-DTPH) at an optimal weight ratio of 1:1. The electrospun HA-DTPH/PEO blend scaffold was subsequently cross-linked through poly (ethylene glycol)-diacrylate (PEGDA) mediated conjugate addition. PEO was then extracted in DI water to obtain an electrospun HA-DTPH nanofibrous scaffold (Ji *et al.*, 2006) .

2.4.3.2 Chemical methods

In addition to physical coating or blending, covalently grafting of ECM proteins like collagen and gelatin onto nanofiber surfaces is another choice with the ultimate goal of the development of biocompatible tissue engineering scaffolds. Grating is the simplified term of graft copolymerization. For initiation of graft copolymerization, radicals or groups which can produce radicals like peroxide groups must be introduced onto polymer surfaces first. For most of chemically inert polymers, this can be achieved via irradiation (γ-ray, electron beams, UV, *etc*), plasma treatment, and Ozone (O_3) or hydrogen peroxide (H_2O_2) oxidization or Ce^{4+} oxidization. Then the polymer to be surface modified is usually immersed in a monomer solution, so that the radicals produced on the polymer surface can immediately initiate the copolymerization of the monomer (Figure 2.12).

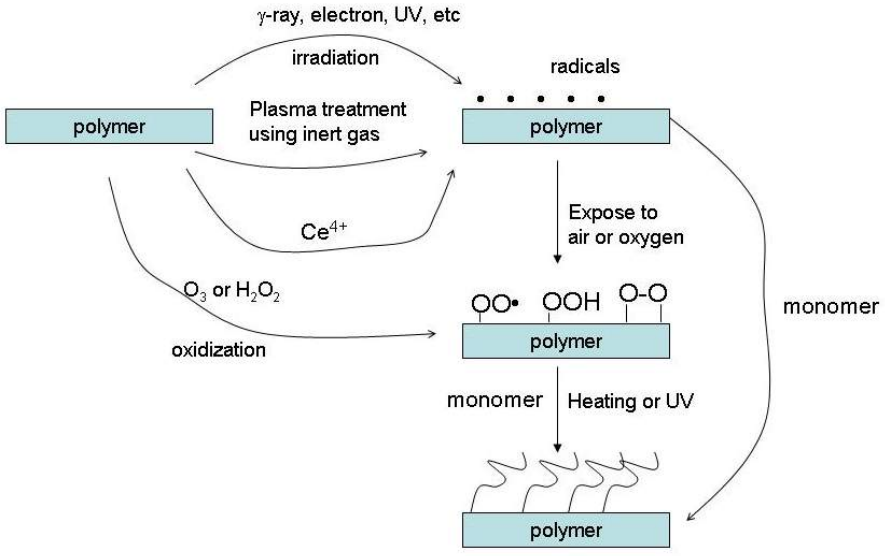

Figure 2.12. General scheme of graft copolymerization on polymer surfaces.

The following are three typical examples of how grafting was applied to modify nanofiber surfaces through the initiation by irradiation, plasma and oxidization respectively (Table 2.7).

Table 2.7. Summary of the three graft copolymerization methods applied to modify nanofiber surface

Materials	**Application**	**Methods**
Poly(e-caprolactone-co-ethyl ethylene phosphate) (PCLEEP) nanofiber surface grafted with Galactose	Artificial liver	Graft copolymerized of PMAA initiated by UV irradiation, followed by immobilization of 1-O-(60-aminohexyl)-D-galactopyranoside (AHG) on carboxyl groups in PMAA
Poly(ε-carprolactone) (PCL) nanofiber surface grafted with gelatin	Blood vessel regeneration	Air Plasma treatment to yield carboxyl groups, followed by immobilization of gelatin on the carboxyl groups
Poly(ethylene terephthalate) (PET) nanofiber surface grafted with gelatin	Blood vessel regeneration	Graft copolymerized of PMMA initiated by Ce^{4+} oxidization, followed by immobilization of gelatin on carboxyl groups in PMMA

Chua *et. al*., used radiation induced graft copolymerization to develop the biofunctional poly(ε-caprolactone-co-ethyl ethylene phosphate) (PCLEEP) nanofiber scaffold for hepatocyte culture (Chua *et al.*, 2005). This was achieved by conjugating hepatocyte-specific galactose ligands onto the nanofiber surface. Poly(acrylic acid) was grafted onto the nanofiber scaffold via UV-induced graft copolymerization using acrylic acid (AAc) monomers. The COOH sites on the grafted scaffold was then used as immobilization sites to conjugate1-O- (6'-aminohexyl)-D-galactopyranoside (AHG) (Figure 2.13). The functionalized AHG-P(AAc)-grafted nanofiber scaffolds exhibited much higher hepatocyte attachment as compared to unmodified scaffold.

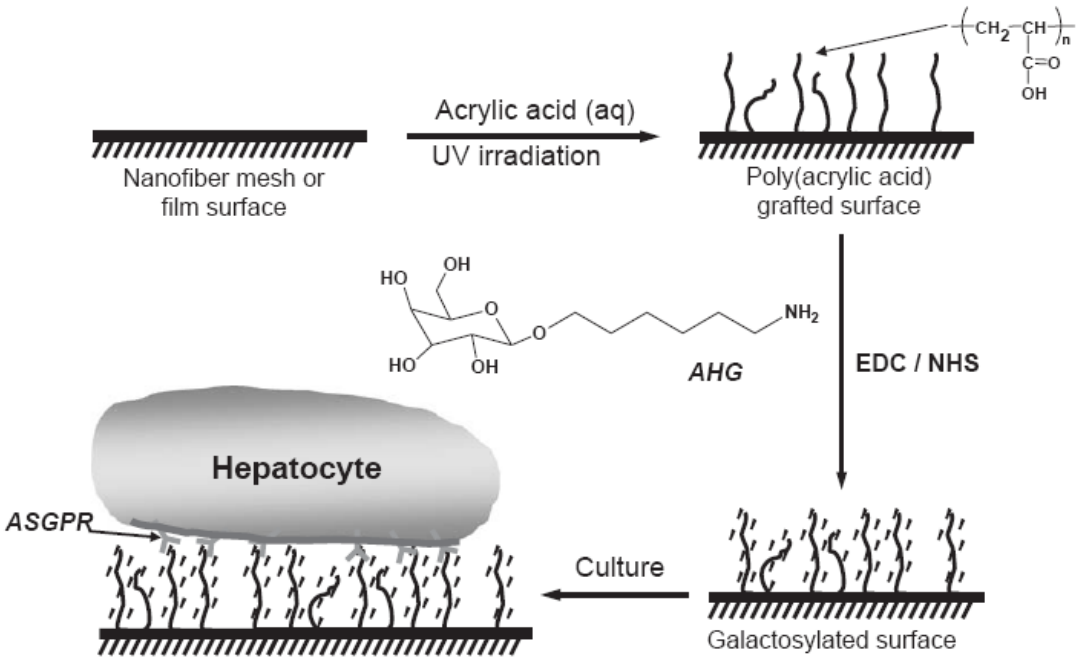

Figure 2.13. Surface modification scheme for galactose conjugation to PCLEEP nanofibers. Reprint with permission from (Chua *et al.*, 2005).

For gelatin grafting on the poly(ε-carprolactone) (PCL) nanofiber surfaces, PCL nanofibers were first treated with air plasma to introduce -COOH groups on the surface followed by covalently grafting of gelatin molecules, using 1-ethyl-3-(3-dimethylamino-propyl) carbodiimide hydrochloride (EDAC) as the coupling agent (Figure 2.14) (Ma *et al.*, 2005a).

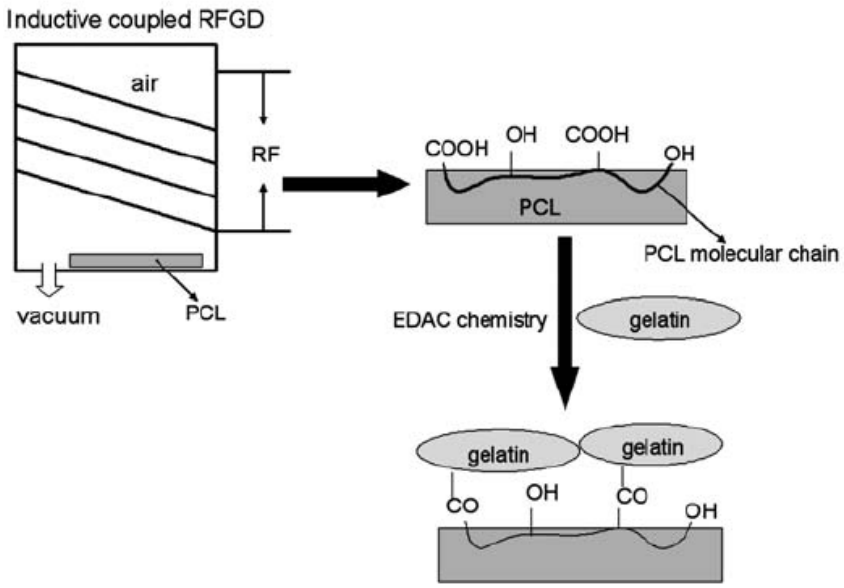

Figure 2.14. Reaction scheme of the surface modification process for PCL nanofiber. RFGD, Radio-frequency glow discharge. Reprint with permission from (Ma *et al.*, 2005a).

One popular method to covalently attach protein molecules on polymer surface is to grafting poly(methacrylic acid) (PMMA) on the biomaterial surface to introduce carboxyl groups at first, followed by the grafting of the protein molecules using water soluble carbodiimide as coupling reagent (Steffens *et al.*, 2002). Electrospun poly(ethylene terephthalate) (PET) nanofibers were grafted with gelatin on the surface. The PET nanofiber was first treated in formaldehyde to yield hydroxyl groups on the surface, followed by the grafting copolymerization of methacrylic acid (MAA) initiated by Ce^{4+} oxidization. Finally the PMAA grafted PET nanofiber was grafted with gelatin using water-soluble 1-ethyl-3-(3-dimethylamino-propyl) carbodiimide hydrochloride (EDAC) as coupling agent (Figure 2.15) (Ma *et al.*, 2005c). Both the gelatin modified PCL and PET nanofibers showed improved EC compatibility than the unmodified nanofibers.

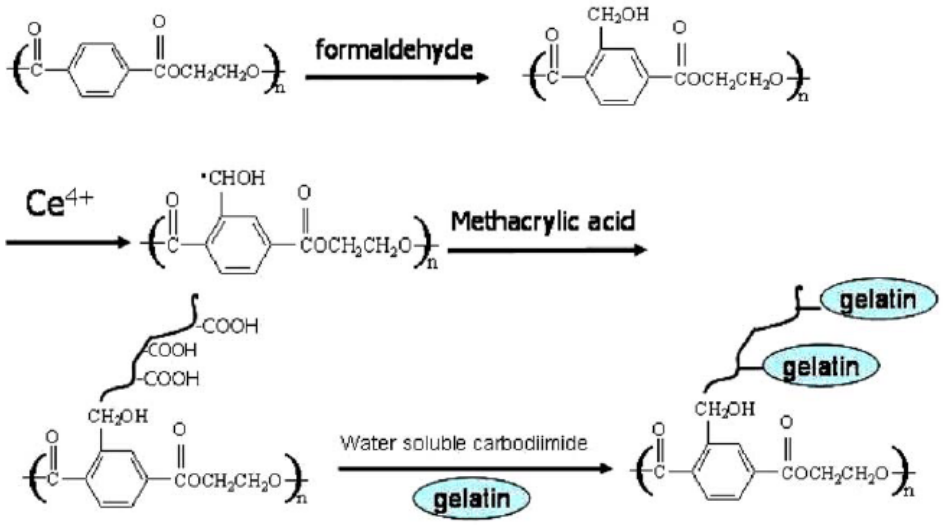

Figure 2.15. Schematic representation of the surface modification process of PET nanofibers. Reprint with permission from (Ma *et al.*, 2005c).

There are several other reports regarding the immobilization of biomolecules onto nanofiber surfaces. Bone morphogenetic protein-2 (BMP-2) immobilized chitosan nanofibers increased osteoblastic cell attachment, proliferation, alkaline phosphatase activity, as well as calcium deposition (Park *et al.*, 2006c). Arg-Gly-Asp (RGD) immobilized poly(D,L-lactic-co-glycolic acid) (PLGA) nanofibers enhanced fibroblasst attachment, spreading, and proliferation (Kim and Park, 2006). Covalent modification of the polyamide nanofibers with neuroactive peptides derived from human tenascin-C significantly enhanced the ability of the nanofibers to facilitate neuronal attachment, neurite generation,and neurite extension *in vitro* (Ahmed *et al.*, 2006) .

2.4.3 Cells-nanofiber scaffolds interactions

The reason why we need to study the interactions between cells and biomaterials *in vitro* is based on the theory that "macroscopic tissue-level events are ultimately derived from, and thus could be controlled by, cellular and molecular level events at the tissue-implant interface" (Giliberti *et al.*, 2002). Thus any implant should be studied *in vitro* first before implantation *in vivo* for the interactions of cells and biomaterials in terms of cell adhesion, proliferation, phenotype maintenance, and functional development.

It has been well established that gross change in ECM affects cell behaviors. However little is known about how cell behaviors will be affected by fine changes at the nanometer scale in the synthetic ECM. Researchers as early as 1960s claimed that nanoscaled features influenced cell behaviors (Rosenberg, 1963). Cells attached and organized well around fibers with diameters smaller than size of cells (Laurencin *et al.*, 1999). Nanoscaled surface roughness with dimensions ranging from 20 to 50 nm produced by chemical etching on Silicone wafer enhanced neural cell adhesion and hydroxylase activity (Fan *et al.*, 2002). Nanoscaled surface topography has been found to promote osteoblast adhesions (Webster *et al.*, 1999). Recent studies reported that osteoblast adhesion, proliferation, alkaline phosphatase activity, and ECM secretion on carbon nanofibers increased with deceasing fiber diameters in the range of 60-200 nm, while the adhesion of other cells like chondrocytes, fibroblasts, and smooth muscle cells was not affected (Elias *et al.*, 2002;Price *et al.*, 2003). It has been

postulated that the nanoscaled surface affects the conformation of the adsorbed adhesion proteins like vitronectin to affect the cell behaviors (Webster *et al.*, 2001). In addition, the nanoscaled dimension of the cell membrane receptors like integrins should also be considered.

Most of the works about *in vitro* cell culturing on nanofiber scaffolds was to evaluate cell adhesion, proliferation, gene expression and ECM secretion. Li *et al* cultured fibroblasts, cartilage and bone marrow derived mesenchymal stem cells on PLGA or PCL nanofibers (Li *et al.*, 2002;Li *et al.*, 2003;Li *et al.*, 2005). It was found that the nanofiber scaffolds were capable of supporting cell attachment and proliferation. Fetal bovine chondrocytes were cultured on PCL nanofibers and their phenotype was evaluated. The chondrocytes seeded on the PCL nanofibers and cultured in serum-free medium continuously maintained their phenotype by expressing cartilage-specific ECM genes. In addition to promoting phenotypic differentiation, the PCL nanofibers also promoted chondrocyte proliferation when the cultures were maintained in serum-containing medium (Li *et al.*, 2003). Adult bone marrow derived mesenchymal stem cells cultured in the PCL nanofibers were able to be induced to form chondrocytes in the presence of transforming growth factor (TGF-β1), as evidenced by chondrocyte-specific gene expressions and synthesis of cartilage-associated ECM proteins. The chrondrogenic ability of the stem cells cultured in the PCL nanofibers was comparable to that observed for the stem cells maintained as cell aggregates or pellets (Li *et al.*, 2005).

2.4.5 Current research of polymer nanofibers as tissue engineered vascular grafts

As we mentioned before, there are requirements on materials for tissue engineered vascular grafts applications, which is summarized in Table 2.1. Electrospun nanofiber scaffolds have shown the potential to fulfill most of those requirements. Most commonly, synthetic polymers were used to construct nanofiber scaffolds for the application of tissue engineered vascular grafts. Poly(L-lactide-*co*-ε-caprolactone) (PLCL 50/50) were electrospun using 1,1,1,3,3,3-hexafluoro-2-propanol (HFP) as the solvent. Human umbilical vein endothelial cells (HUVECs) were found to adhere well and proliferate on the small-diameter fiber fabrics (0.3 and 1.2 μm in diameter) but not on the large-diameter fiber fabrics (7.0 μm in diameter) (Kwon *et al.*, 2005). Surface modification of electrospun poly(ethylene terephthalate) (PET) and poly(ε-caprolactone) (PCL) nanofibers improved the spreading and proliferation of human coronary artery endothelial cells (HCAECs) (Ma *et al.*, 2005a;Ma *et al.*, 2005c). Both random and aligned electrospun poly(L-lactid-*co*-ε-caprolactone) P(LLA-CL) nanofiber scaffolds supported human coronary artery smooth muscle cells (HCASMCs) attachment and proliferation. Also HCASMCs attached and migrated along the axis of the aligned nanofibers and expressed a spindle-like contractile phenotype (Xu *et al.*, 2004a).

Some researchers also made use of natural polymers to construct nanofiber scaffolds for the application of tissue engineered vascular grafts. Huang *et al.* used

recombinant protein based on repeating elastomeric peptide sequence of elastin (Val-Pro-Gly-Val-Gly)$_4$(Val-Pro-Gly-Lys-Gly) to electrospin a non-woven mesh of fibers. The ultimate tensile strength of the nonwoven fabrics was 35 MPa and the material modulus was 1.8 GPa (Huang *et al.*, 2000). Natural collagen and elastin were also electrospun into nanofiber scaffolds as tissue engineered vascular grafts (Buttafoco *et al.*, 2006).

In order to combine advantages of both synthetic and natural polymers, blended nanofiber scaffolds containing synthetic and natural polymers were constructed as tissue engineered vascular grafts. Kwon and Matsuda reported the fabrication of two kinds of blended nanofibers. The first blended nanofibers consisted of PLCL and collagen fibers, and the second ones consisted of PLCL and tri-n-butylamine salt of heparin (heparin-TBA) (Kwon and Matsuda, 2005). Human umbilical vein endothelial cells cultured on the first type of blended nanofibers containing 5 and 10 wt% collagen were highly elongated and well spread. With the second type of blended nanofibers containing the heparin, a burst release was observed in the first 12 h when they were soaked in PBS at 37^{o}C. After then, relatively sustained release rate was observed for 4 weeks probably due to the degradation of the PLCL. By electrospinning both blends simultaneously on the same collector, it may be possible to fabricate a scaffold that is able to encourage cell adhesion and proliferation, and at the same time exhibit anti-thrombogenic properties. Stitzel *et al.* fabricated vascular grafts using blended nanofiber scaffolds which consisted of Type I collagen, elastin, and poly (D,L-lactide-co-glycolide). The

electrospun scaffold was biocompatible and did not elicit local or systemic toxic effects when implanted (Stitzel *et al.*, 2006).

There are also novel ways to design nanofiber scaffolds with a flexible hierarchical organization in terms of structure, topography and material composition, which may make it possible to better simulate the tri-layer structure of natural blood vessels. The group from Takehisa Matsuda developed the sequential multilayering electrospinning and mixing electrospinning (Kidoaki *et al.*, 2005). By sequential electrospinning of collagen, styrenated gelatin, and segmented polyurethane (SPU) layer by layer, a tri-layered electrospun NFM was constructed. By simultaneous electrospinning of SPU and PEO onto the same collector with high-speed rotation and traverse movement, the mixed electrospun NFM composed of SPU and PEO was prepared. Furthermore, a bi-layered tubular scaffold composed of a thin inner layer of collagen and a thick outer layer of SPU was developed as a prototype of artificial vascular grafts. Similarly, Vaz *et al.* electrospun a bi-layered tubular scaffold composed of an inner layer of random and compliant PCL and a outer layer of oriented and stiff PLA through the sequential multilayering electrospinning as a candidate tissue engineered vascular scaffold (Vaz *et al.*, 2005).

The most attractive option of using electrospinning to fabricate vascular graft is its ability to electrospin small-diameter tubes with uniform thickness and fiber distribution throughout the scaffold. The latest research is summarized in Table 2.8.

Table 2.8. Summary of constructing tubular tissue engineered vascular grafts through electrospinning

Materials	**Tube inner Diameter (mm)**	**Tube wall Thickness (μm)**	**Reference**
Poly(L-lactide-co-ε-caprolactone) P(LLA-CL)	2.3-2.5	50-340	(Inoguchi *et al.*, 2006)
Segmented polyurethane (PSU)	3	250	(Matsuda *et al.*, 2005)
Inner: collagen; outer: PSU	3	500	(Kidoaki *et al.*, 2005)
Collagen, elastin and poly (D,L-lactide-co-glycolide) (PLGA)	4.75	N.A	(Stitzel *et al.*, 2006)
Inner: PCL; outer: polyurethane (PU)	N.A	250	(Williamson *et al.*, 2006)

A very recent study by Prof. Li's group in UC Berkeley showed that human bone marrow mesenchymal stem cells (MSC) inoculated nanofiber scaffolds displaced excellent long-term patency and exhibited well organized layers of ECs and SMCs when implanted to replace the common carotid artery in athymic rats for 60 days. While acellular grafts (without MSCs) resulted in significant intimal thickening. These results demonstrate several favorable characteristics of nanofibrous scaffolds and the important role of seeded cells in the scaffolds towards *in vivo* patency of scaffolds (Hashi *et al*., 2007).

Chapter 3

Collagen-Blended P(LLA-CL) Nanofiber Meshes (NFM)

Many studies have been carried out to apply electrospun nanofibers as tissue engineered scaffolds. In most of these studies, synthetic polymers such as poly(caprolactone) (PCL), poly(L-lactide) (PLA), and poly(glycolide) (PGA) *etc* were widely used. In parallel, natural materials like collagen, silk protein, elastin-mimic peptide, fibrinogen *etc* have also been used. The disadvantage for synthetic polymers is their lack of cell-recognition signals, which can be found in natural materials. This problem could be overcome by modification of synthetic polymer nanofibers with natural materials, either through blending natural materials into the spinning solution prior to electrospinning, or immobilizing natural materials onto the surface of polymer nanofibers after electrospinning (Pham *et al.*, 2006).

Although previous studies in our laboratory have demonstrated that human coronary artery smooth muscle cells (HCASMCs) cultured on the P(LLA-CL) NFM showed normal morphology and good proliferation, human coronary artery endothelial cells (HCAECs) were found not to be able to grow well on the P(LLA-CL) NFM (Xu *et al.*, 2004b), which may be due to the lack of ECs recognition sites on pure polymer NFM. Collagen is a native adhesion protein, interacting through RGD domain with integrins receptors in cell membranes (Ruoslahti and Pierschbacher, 1987). This interaction results in focal adhesion of cells on substrates, which benefits

cell attachment and movement. Therefore it is probable that inclusion of collagen into the P(LLA-CL) NFM would increase their bioactivity. In this chapter, collagen-blended P(LLA-CL) NFM were fabricated by electrospinning a mixture of collagen and P(LLA-CL) dissolved in 1,1,1,3,3,3-hexafluro-2-propanol (HFP). Morphology, porosity, mechanical properties, and surface chemistry of the collagen-blended NFM were studied. Behaviors of HCAECs on the collagen-blended NFM were analyzed in terms of morphology, viability, attachment, and phenotype.

3.1 Materials and methods

3.1.1 Materials

Poly(L-lactic acid)-*co*-poly(epsilon-caprolactone) random copolymer [P(LLA-CL), 70:30] was bought from Boehringer (Ingelheim, Germany), with a molecular mass of 150 kDa. 1,1,1,3,3,3-hexafluro-2-propanol (HFP) and Collagen Type I from calf skin were purchased from Sigma-Aldrich (St. Louis, MO, USA). CMFDA fluorescent CellTracker probe was purchased from Molecular Probe (Eugene, OR, USA). CellTiter 96® AQueous One Solution assay was purchased from Promega (Madison, WI, USA)

3.1.2 Fabrication of collagen-blended P(LLA-CL) NFM

P(LLA-CL) and collagen were dissolved in HFP with different weight ratios (4:1, 2:1, 1:1, 1:2) while maintaining the total weight concentration as 5 wt%. The solution was then filled in a syringe. With the aid of a syringe pump, the solution was ejected out through a needle tip with an inner diameter of 0.21 mm at a constant feed-rate of 1.2 mL/h. A high DC voltage of 12 kV (Gamma High Voltage Research, Ormond Beach, FL, USA) was applied between the needle and a grounded aluminum plate which was 12cm below the needle. The electric field generated by the surface charge caused the solution drop at the tip of the needle to distort into a Taylor cone. Once the electric potential at the surface charge exceeded a critical value, the electrostatic forces would overcome the solution surface tension and a thin jet of solution would erupt from the surface of the cone. The schematic setup and the optimized parameters for fabrication of the collagen-blended P(LLA-CL) NFM are shown in Figure 3.1. The nanofibers were collected on an aluminum collector. For future cell culturing in 24-well tissue culture polystyrene (TCPS) plate, coverslips (Assistent, 15 mm in diameter; Karl Hecht, Sondheim, Germany) were placed on top of the aluminum foil to collect the NFM directly. Pure collagen NFM was fabricated by dissolving collagen in HFP and then electrospun into nanofibers.

Uniform smooth films of the P(LLA-CL)-collagen (1:1 w/w) were prepared by a solvent casting method. Briefly, P(LLA-CL) and collagen were first dissolved at a concentration of 5 wt% in HFP. The resulting solution was then cast onto the 15

mm coverslips which were put into a 24-well TCPS plate. After solvent evaporation in open air, the P(LLA-CL)-collagen coated coverslips [hereafter referred to as P(LLA-CL)-collagen film] was finally placed in a vacuum dryer overnight to remove residual solvent.

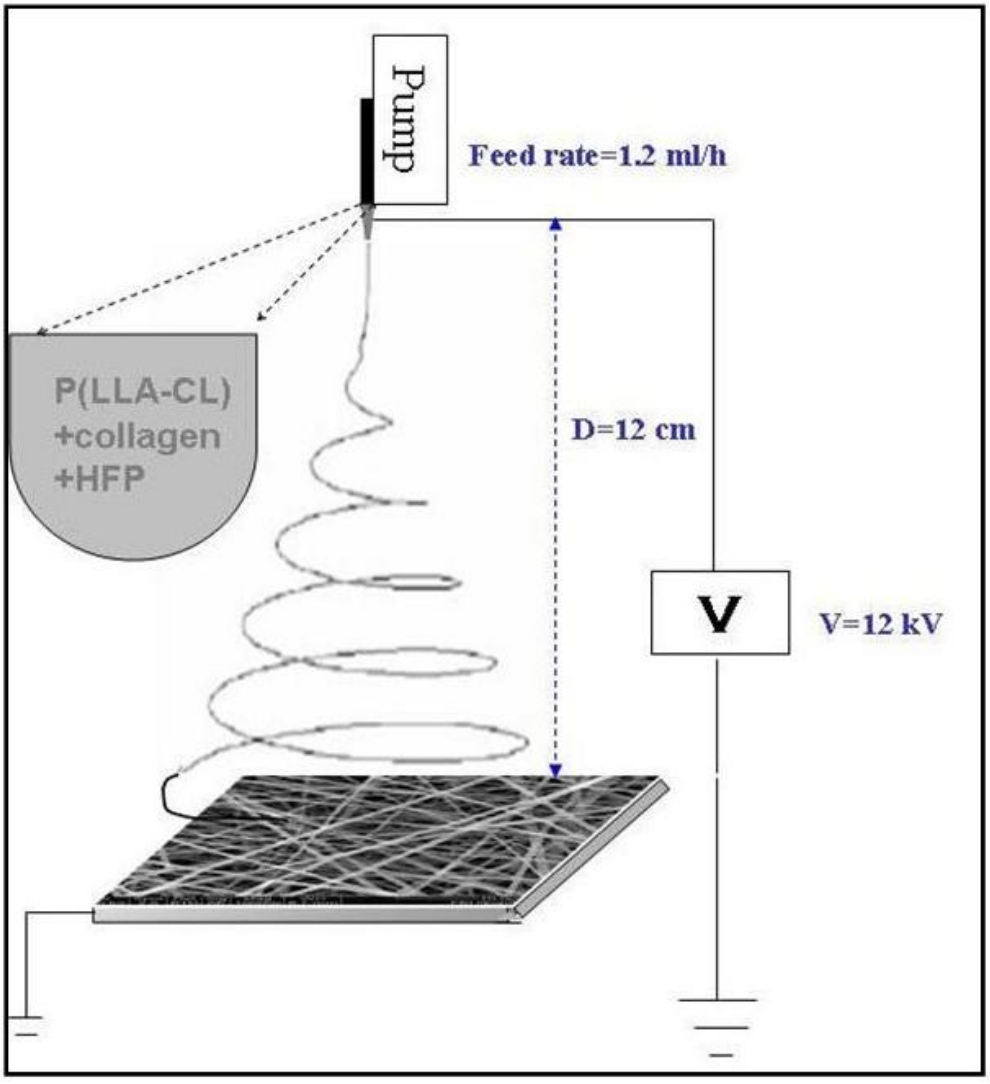

Figure 3.1.Schematic setup and optimized operation parameters for fabrication of the collagen-blended P(LLA-CL) NFM.

3.1.3 Material characterization

3.1.3.1 Physical properties

Scanning electron microscopy (SEM) micrographs of the collagen-blended P(LLA-CL) NFM were obtained with a JSM-5800LV SEM (JEOL, Tokyo, Japan). Transmission electron microscopy (TEM) micrographs of the NFM were obtained with a JEM-2010F FasTEM field emission electron microscope (JEOL) operated at 100 kV. The NFM for the TEM observation were prepared by directly depositing the as-spun NFM onto copper grids that had been coated with a supportive Formvar film (Structure Probe, SPI Supplies Division, West Chester, PA, USA).

Diameter range of the fabricated NFM was measured using image analysis software (Image J, National Institutes of Health, Bethesda, MD, USA) by random counting of 60 nanofibers on the SEM images. The thickness of the collagen-blended P(LLA-CL) NFM was measured with a micrometer (Mitutoyo, Kawasaki, Japan) and its apparent density and porosity were calculated according to the following equations (Ma *et al.*, 2005c):

$$NFM\ \ apparent\ \ density\ (g/cm^3) = \frac{NFM\ \ Mass(mg) \times 10}{NFM\ \ thickness\ (\mu m) \times NFM\ \ area(cm^2)},$$

$$NFM\ \ porosity = \left(1 - \frac{NFM\ \ apparent\ \ density\ (g/cm^3)}{bulk\ density\ of\ \ P(LLA-CL)-collagen(g/cm^3)}\right) \times 100\%$$

3.1.3.2 Surface chemistry

Attenuated total reflectance Fourier transform infrared (ATR-FTIR) spectra were obtained using an AVATAR 380 FTIR machine (Thermo Electron, Waltham, MA, USA). Surface chemistry analysis of the NFM was performed by X-ray photoelectron spectroscopy (XPS) (VG Escalab 2201-XL, Thermo VG Scientific/Thermo Electron, East Grinstead, UK) with a take off angle of 90^{o}. The binding energy was referenced to the $C1_S$ of saturated hydrocarbon at 285.0 eV.

3.1.3.3 Mechanical properties

Tensile tests were carried out with a 5848 microtester (Instron, Norwood, MA, USA) at a stretching speed of 10 mm/min and with a 40 mm gauge length. NFM samples were cut into a rectangular (10 × 60 mm) shape. The NFM thickness measured by a micrometer and the NFM width (10 mm) was input into the computer to calculate the tensile strengh and strain.

3.1.4 Characterization of cellular behaviors

3.1.4.1 *In vitro* cell culture

Collagen-blended P(LLA-CL) NFM were deposited on round 15 mm diameter coverslips, which fits nicely into the bottom of 24-well TCPS plate. A small amount

of implant-grade silicon adhesive (Silbione, MED ADH 4300 RTV; Rhodia, Boulogne-Billancourt, France) was applied along the edge of the NFM to immobilize them on the coverslip surface. The highly inert silicon adhesive has no toxic effects on cells (Ma *et al.*, 2005c). Ethanol solution (75%) was used to sterilize samples and was removed by rinsing with phosphate buffered saline (PBS).

Human coronary artery endothelial cells (HCAECs) obtained at passage 3 from Biowhittaker (New Jersey, USA) were seeded into the 24-well plate containing NFM at given seeding densities. Cells were cultured in endothelial cell basal medium (Clonetics™ EBM®-2) supplemented with EC growth supplements (vascular endothelial growth factor [VEGF], human epidermal growth factor [hEGF], human fibroblast growth factor-B [hFGF-B] insulin-like growth factor type I [IGF-I], hydrocortisone, and ascorbic acid) purchased from Cambrex (North Brunswick, NJ, USA), 5% fetal bovine serum (FBS), penicillin (100 units/mL), and streptomycin (100 μg/mL). Medium was replaced every 4 days and cultures were maintained in a humidified incubator at 37°C with 5% CO_2. When the cells reached 80-90% confluence (confluence density, 5×10^4 cells/cm^2), they were trypsinized and sub-cultured at a 1:3 ratio.

3.1.4.2 Cellular morphology

Cellular morphology was either studied by laser scanning confocal microscope (LSCM, Leica Microsystems, Wetzlar, Germany) or using a scanning

electron microscope (SEM) (JSM-5800LV, JEOL). For LSCM observation, live cells were stained with green fluorescent probe CMFDA (5-chloromethyl fluorescein diacetate). A stock solution of CMFDA (25 μM in dimethyl sulfoxide [DMSO]) was diluted with serum-free cell culture medium to obtain a 2.5 μM working solution. Prewarmed CMFDA working solution (200 μL) was added to cover the bottom of the wells of 24-well plate for 45 min. Cells were washed three times with 1 × PBS and incubated with 200 μL of EC culture medium for another 30 min. Subsequently, the culture medium was replaced with another 1 mL of culture medium, in which the cells were cultured further. Cells were observed by LSCM (excitation, 492 nm; emission, 517 nm).

SEM micrographs were taken for cell morphology studies on different substrates. Cells were washed with 1 × PBS to remove nonadherent cells and then fixed with 2.5% glutaraldehyde for 45 min at 4 °C. Thereafter, the samples were dehydrated in 75% alcohol solutions and dried under vacuum. The samples were sputter coated with gold (JFC-1200 Fine Coater, JEOL, Japan) and observed with an SEM at an accelerating voltage of 15 or 20 kV.

3.1.4.3 Cellular attachment and viability

Cellular attachment and viability on the NFM were determined by the colorimetric MTS assay (CellTiter 96® AQ_{ueous} One Solution cell proliferation assay, Promega, USA). Briefly, cells were incubated with 20% 3-(4,5-dimethylthiazol-2-yl)-

5-(3-carboxymethoxyphenyl)-2-(4-sulfophenyl)-2H-tetrazolium) (MTS) reagent in cell culture medium for 4 h. Thereafter, 100µl aliquots were pipetted into the wells of a 96-well plate and placed into a spectrophotometric plate reader (FLUOstar OPTIMA, BMG Labtech, Offenburg, Germany), and the absorbance at 490 nm for each well was measured.

For cellular viability test, cells were seeded onto the NFM at a density of 1.5×10^4 cells/cm^2 (30% confluence). On day 1, 3, 5, and 7 after cell seeding, unattached cells were washed out and the attached cells were quantified by MTS assay. For cellular attachment study, cells were seeded at the density of 3×10^4 cell/cm^2 (60% confluence). At 1, 2, 4, 6 and 8 h after cell seeding, unattached cells were washed out and the attached cells were quantified by MTS assay. A lower seeding density was used for viability studies as compared with attachment studies. This is to provide more area for cells to proliferate to avoid reaching confluence prematurely. For both cellular viability and attachment test, TCPS was used as a control. Data are representative of three independent experiments and all data points are plotted as means ± SD (n=3)

3.1.4.4 RT-PCR analysis

Four typical cell adhesion molecules (CAMs) characteristic of ECs (platelet endothelial cell ad adhesion molecule-1 [PECAM-1 or CD31], intercellular adhesion molecule-1 [ICAM-1 or CD54], vascular cell adhesion molecule-1 [VCAM-1 or CD106], and E-selectin [or CD62E]) and the ECs universal marker, von Willebrand

Factor (vWF), were studied by reverse transcription-polymerase chain reaction (RT-PCR) for gene expression analysis. Total RNA was extracted from 2.5×10^6 subconfluent HCAECs cultured in a 75 cm^2 TCPS flask or from NFM deposited on a petri-dish (86 mm in diameter, 58 cm^2 in area) using an RNeasy Mini Kit (Qiagen, Hilden, Germany). Cells were lysed and homogenized in the guanidine isothiocyanate (GITC)-containing buffer, and then applied to a column where the total RNA bound to the silica-gel-based membrane and impurities were effectively washed away. Lastly, high-quality RNA was eluted in 30 μL RNase-free water and RNA yields were measured on the basis of absorbance at 260 nm.

For reverse transcription (RT), cDNA was reverse transcribed from 1 μg of total RNA and then stored at -20 °C. Briefly, a 10.5 μL reaction mixture containing 1 μg of total RNA, 0.5 μg of oligodeoxythymidine ($oligo(dT)_{18}$, 1_{st} BASE, Singapore) and distilled water was heated at 75 °C for 5 min and then put on ice for 5 min. Next, dNTPs (dATP, dTTP, dGTP, dCTP, 2mM each), 20 units of recombinant ribonuclease inhibitor (RNasin, Promega, USA), and 200 units of Moloney murine leukemia virus (M-MLV) reverse transcriptase (Promega, USA) were added in a final 20 μL reaction mixture. This mixture was incubated for 1 h at 37 °C followed by heating for 5 min at 95 °C, and then put on ice for 5 min.

For PCR, a 1 μL aliquot of the reaction mixture was subjected to PCR amplification in a final 20 μL reaction mixture that contained 20 pmol of each forward and reverse primer (Table 3.1), 1.5 mM $MgCl_2$, a 0.3 mM concentration of

each of the four deoxynucleotides, and 1 unit of *Taq* polymerase (Promega, USA). Amplification of ECs specific genes by PCR was carried out in a PTC-100 Peltier Thermal Cycler (MJ Research, Waltham, USA) for 30 cycles. In each cycle, an initial denaturation at 94 °C for 1 min was carried out, followed with primers annealing at 55 °C for 1 min and polymerization at 72 °C for 1 min. This was followed with a final extension step at 72 °C for 10 min and stored at 4 °C. The PCR products were analyzed by electrophoresis of 10 μL of each sample in a 1% agarose gel, with the bands visualized under ultraviolet light by ethidium bromide staining, using the Gel Doc 2000 gel documentation system (Bio-Rad, Hercules, CA, USA).

Table 3.1. PCR primers for RT-PCR analysis

Gene	Genebank No.	size (bp)	Primer pair sequences
β-actin	BC002409	318	5’ GAG TCC TGT GGC ATC CAC G 3’
			5’ GAA GCA TTT GCG GTG GAC G 3’
PECAM-1 (CD31)	BC051822	367	5’ TCA TCG GAG TGA TCA TTG CTC 3’
			5’ CTA GAG TAT CTG CTT TCC ACG 3’
von Willebrand Factor (vWF)	BC022258	274	5’ TGA GGC TGG GTA CTA CAA GC 3’
			5’ GGA GAT GTT GCA TGA GCT GC 3’
ICAM-1 (CD54)	J03132	352	5’ GCT TCG TGT CCT GTA TGG C 3’
			5’ CTG GCG GTT ATA GAG GTA CG 3’
VCAM-1 (CD106)	X53051	297	5’ TTC TGA GAG TGT CAA AGA AGG 3’
			5’ AAG GAG GAT GCA AAA TAG AGC 3’
E-selectin (CD62E) (E-SEL)	NM_000450	280	5’ GCA CTG TGT GCA AGT TCG C 3’
			5’ GGC TTT TGG TAG CTT CCG TC 3’

3.1.5 Statistical analysis

Values (at least triplicate) were averaged and expressed as means ± standard deviation (SD). Each experiment was repeated three times. Statistical analysis was carried out for HCAECs viability and attachment studies using One-Way ANOVA testing by SPSS for Windows (SPSS Inc., Copyright 1989-2002) version 11.5.0. Significant difference between data groups was determined by the Student-Newman-Keuls (SNK) post hoc test ($p < 0.05$).

3.2 Results and discussions

3.2.1 Material characterization

3.2.1.1 Physical properties

SEM and TEM micrographs of the collagen-blended P(LLA-CL) NFM with various weight ratios of P(LLA-CL) to collagen (4:1, 2:1, 1:1, and 0:1) are shown in Figure 3.2, revealing the non-woven and interconnected-pore structure of the NFM. Similar morphologies of the NFM, with various weight ratios of P(LLA-CL) to collagen at the same total concentration (5 wt%), were observed, suggesting that the weight ratio did not affect the NFM' morphology (Figure 3.2 A-D). Typical smooth nanofibers had diameters between 100-200 nm, as shown in Figure 3.2 E and F.

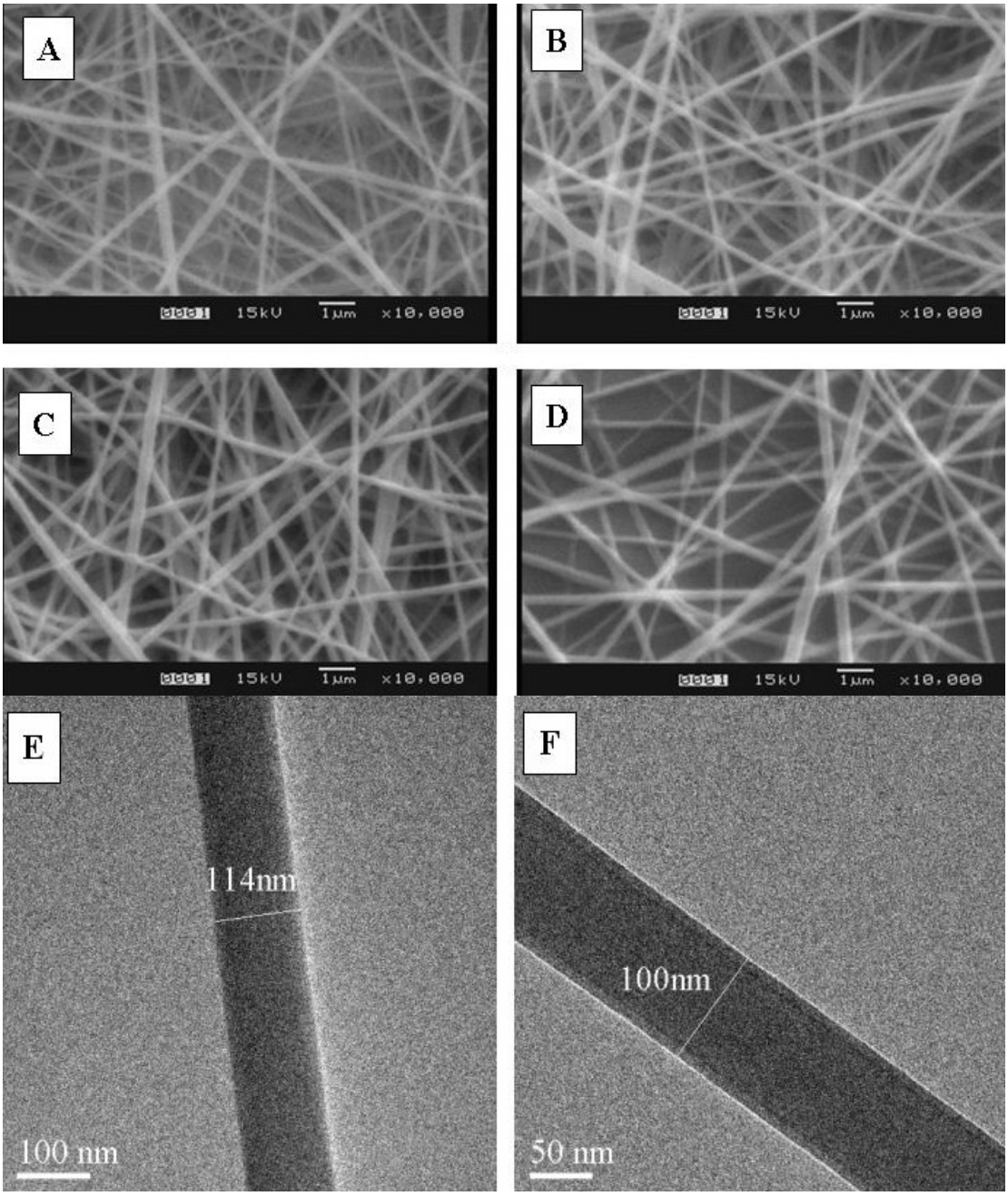

Figure 3.2. SEM (A-D) and TEM (E and F) micrographs of collagen-blended P(LLA-CL) NFM with various weight ratios of P(LLA-CL) to collagen. Weight ratios of P(LLA-CL) to collagen: (A) 4:1; (B) 2:1; (C and E) 1:1; (D and F) 0:1 Total concentration of the electrospinning solution is 5 wt%.

Diameter distributions of the collagen-blended NFM were determined by directly measuring nanofiber's diameter from SEM images in Figure 3.2 by image analysis software (Image J), which is shown in Figure 3.3. It shows quite narrow

diameter distributions for the collagen-blended NFM at various weight ratios of P(LLA-CL) to collagen. Basically, more than 60% of nanofiber's diameters ranged from 100 to 200 nm, with about 20% of nanofiber's diameters ranging from 200 to 300 nm, which was much smaller and better distributed than those of most nanofibers we had reported previously. This may be because that the high molecular weight of collagen (285k) could enhance the viscosity of spinning solution at a low concentration, facilitating the production of small nanofibers. Further, HFP is a polar solvent with a low boiling temperature (58.5 °C) and a high dielectric constant (17.8), which could further enhance spinnabillity of nanofibers (Matthews *et al.*, 2002b).

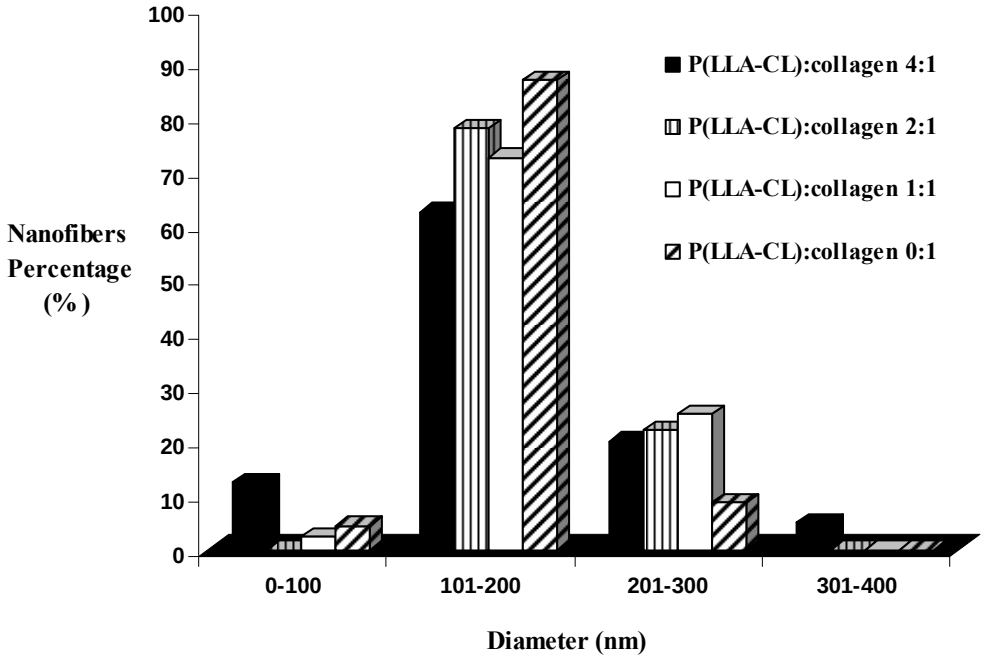

Figure 3.3. Diameter distributions of the collagen-blended P(LLA-CL) NFM with various weight ratios of P(LLA-CL) to collagen.

Diameter, thickness, apparent density, and porosity of the collagen-blended NFM with various weight ratios of P(LLA-CL) to collagen are summarized in Table 3.2. Thickness of the collagen-blended NFM was mainly controlled by electrospinning time if operation parameters such as voltage, feed rate, and collector distance were fixed. Table 3.2 shows that the collagen-blended NFM [P(LLA-C):Collagen, 1:1 (wt:wt)] deposited for 1 h were thicker than others deposited for 30 min. Apparent density of all the collagen-blended NFM was in the range of 0.3-0.4 g/cm^3. No obvious relationship existed between the apparent density and weight ratio of P(LLA-CL) to collagen. This may be because that density of collagen (1.3-1.4 g/cm^3) is close to the density of the P(LLA-CL) (1.2-1.3 g/cm^3). As the collagen-blended P(LLA-CL) NFM are highly porous materials, with the known bulk density of the P(LLA-CL)-collagen blends, porosity of the collagen-blended NFM can be calculated based on the apparent density. The bulk density of the collagen-P(LLA-CL) blends were estimated to be in the range of 1.2-1.4 g/cm^3 based on the bulk density range of the P(LLA-CL) and collagen, and the porosity of the collagen-blended NFM was calculated to be around 70%.

Table 3.2. Diameter, thickness, apparent density, and porosity of collagen-blended P(LLA-CL) NFM with various weight ratios of P(LLA-CL) to collagen[a]

P(LLA-CL) : Collagen (wt : wt)	Diameter (nm)	Thickness (μm)	Apparent density (g/cm^3)	Porosity (%)
4:1	160 ± 68	9 ± 2	0.31 ± 0.01	74-78
2:1	168 ± 40	6 ± 1	0.39 ± 0.05	68-72
1:1[b]	181 ± 47	15 ± 3	0.38 ± 0.08	68-73
1:2	191 ± 63	9 ± 0	0.33 ± 0.06	73-76

[a]Data are representative of three independent experiments and represented as means ± SD (n=5).
[b] Electrospinning deposition time is 60 min. For others, deposition time is 30 min.

3.2.1.2 Surface chemistry

Surface chemistry of biomaterials mediates protein adsorption, which regulates cell adhesion, proliferation, and migration and affects tissue regeneration rate (Li *et al.*, 2002). Regarding the collagen-blended P(LLA-CL) NFM, it is expected that some of the collagen would be present on the surface of the nanofibers, which could promote cell attachment and proliferation. Chemical compositions of the collagen-blended P(LLA-CL) NFM were studied by attenuated total reflectance Fourier transform infrared (ATR-FTIR) spectrometry (Figure 3.4). The spectra of the collagen-blended NFM (Figure 3.4C) revealed peaks characteristic of collagen at wave-numbers of 1651cm^{-1} (amide I band) and 1537 cm^{-1} (amide II band) (Figure 3.4B), and a P(LLA-CL) peak at 1747 cm^{-1} (Figure 3.4A), together with a peak at 3310 cm^{-1} (N-H stretch). ATR-FTIR is not a very surface specific characterization

method because it has a probe depth of about 1 μm. For the NFM with the diameters ranging from 100 to 200 nm, ATR-FTIR may show the compositions inside the nanofibers. Therefore x-ray photoelectron spectroscopy (XPS), which has a probe depth of only tens of nanometers, was used to check whether collagen was present on the surface of nanofibers. The XPS results are summarized in Table 3.3. Appearance of N1S peak represents the presence of collagen on the nanofiber surface. More collagen (higher N atomic ratio) was found to be present on the surface of the collagen-blended P(LLA-CL) NFM with increased collagen weight ratios. The pure collagen NFM showed the highest amount of surface collagen compared with other collagen-blended NFM. There was no collagen present on the surface of the pure P(LLA-CL) NFM.

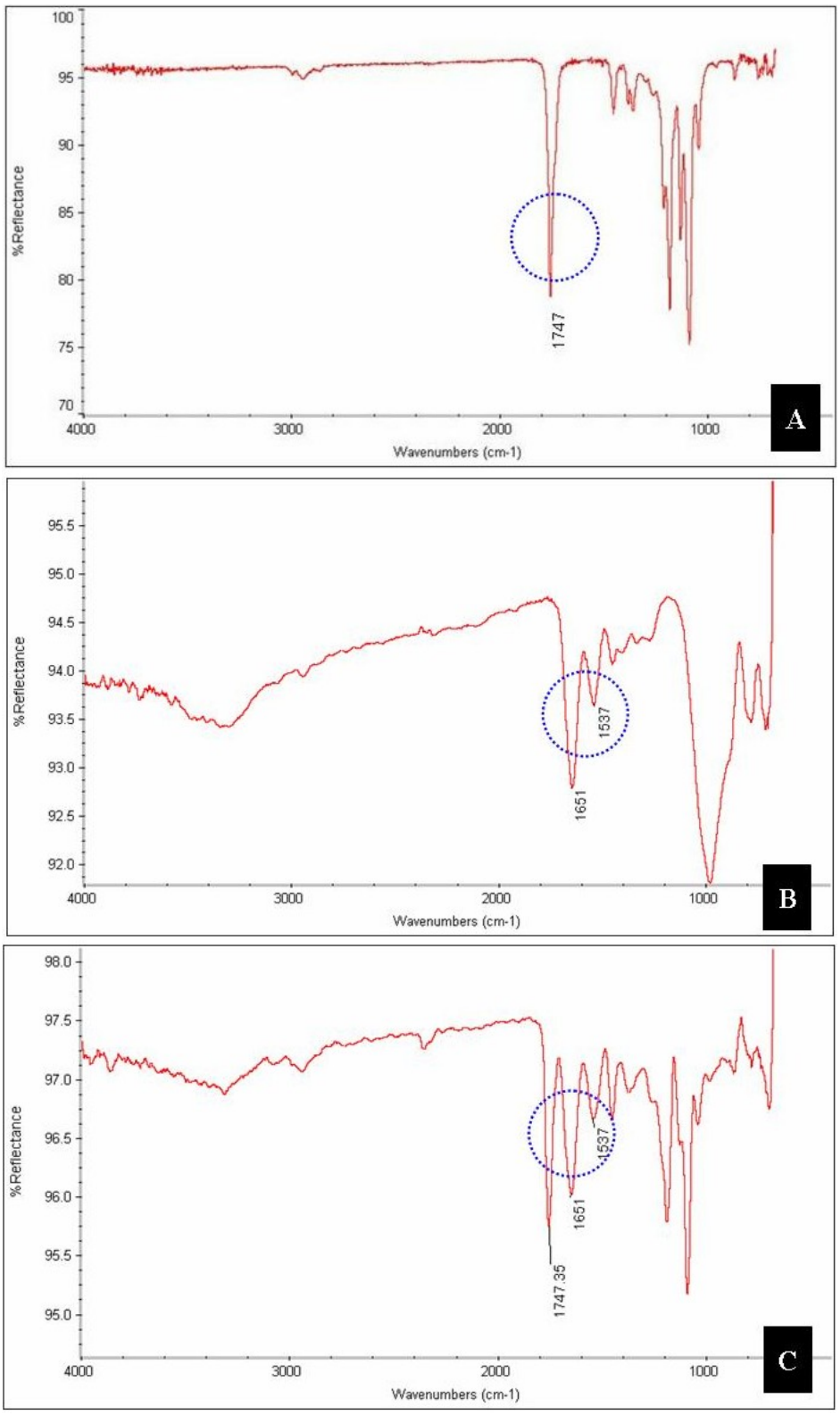

Figure 3.4. ATR-FTIR spectra of (A) P(LLA-CL) NFM, (B) collagen NFM, and (C) collagen-blended P(LLA-CL) NFM with a 1:1 weight ratio of P(LLA-CL) to collagen.

Table 3.3. Atomic ratios of carbon (C), nitrogen (N), and oxygen (O) on the surface of P(LLA-CL) NFM, collagen-blended P(LLA-CL) NFM with various weight ratios of P(LLA-CL) to collagen, and collagen NFM as determined by XPS

NFM	C atomic ratio (%)	N atomic ratio (%)	O atomic ratio (%)
P(LLA-CL)	65.9	0	34.1
P(LLA-CL): collagen=4:1	67	Not Detectable	33
P(LLA-CL): collagen=2:1	56.2	9.2	34.6
P(LLA-CL): collagen=1:1	59	11.7	29.3
P(LLA-CL): collagen=1:2	63.3	13.3	23.4
Collagen	61.6	15.1	23.3

3.2.1.3 Mechanical properties

One of the main failure modes of synthetic vascular grafts is intimal hyperplasia (IH), which is partly due to shear stress disturbances caused by the compliance mismatch at the end-to-end anastomosis between arteries and rigid grafts (Salacinski *et al.*, 2001a). Thus the mechanical property of NFM is critical for their successful application as tissue engineered vascular grafts. Compliance is a mechanical property of a tubular structure which depends on the tube dimensions and modulus. In this study we mainly studied the tensile modulus, tensile strength, and ultimate strain of NFM which all have impact on the compliance of tubelike structures.

Mechanical evaluation of both P(LLA-CL) NFM and collagen-blended P(LLA-CL) NFM revealed the nonlinear stress-strain behavior (Figure 3.5). It shows

that incorporation of collagen at a P(LLA-CL)-to-collagen weight ratio of 1:1 led to a decrease in mechanical properties of the P(LLA-CL) NFM. It was also found that tensile strength of both NFM was in the range of that of a human coronary artery (Table 3.4). Moreover, both NFM had much less stiffness compared with Dacron® (PET; commonly used in large-diameter vascular grafts), which has a tensile strength of 170-180 MPa in orientated form and a tensile modulus of about 14, 000MPa (Salacinski *et al.*, 2001a). Ideally, less stiff (more compliant) and biodegradable scaffolds are a better choice for constructing tissue engineered vascular grafts.

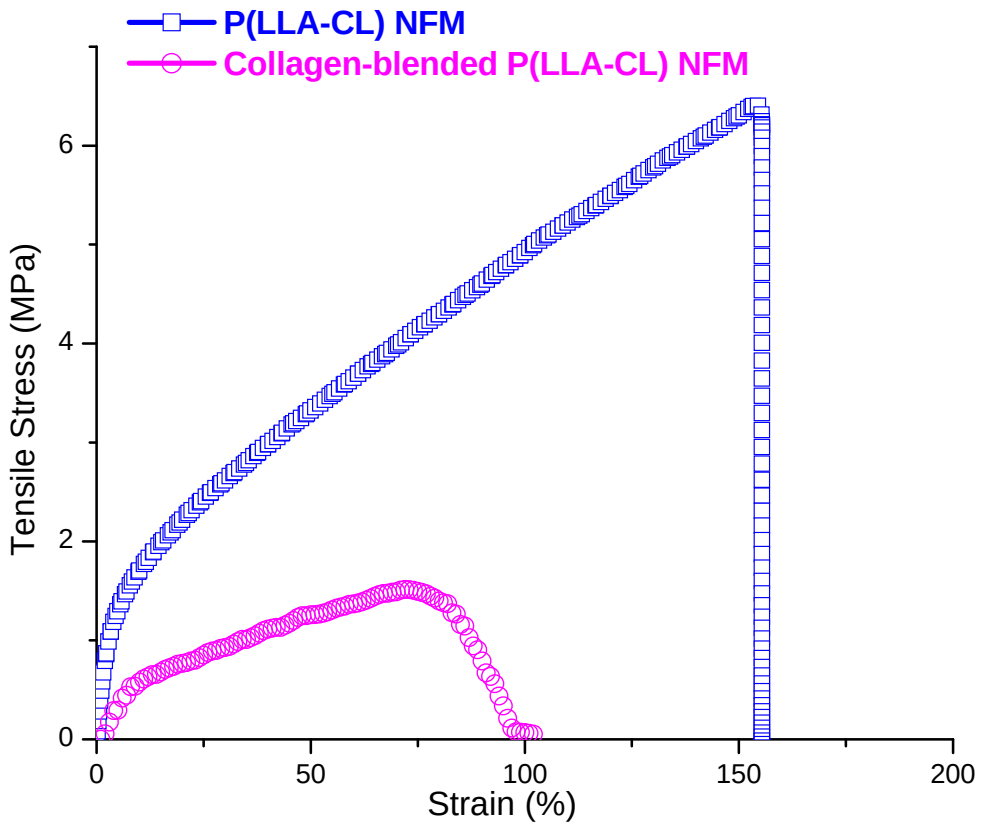

Figure 3.5. Typical stress-strain curves of the P(LLA-PCL) NFM and collagen-blended P(LLA-CL) NFM with the weight ratio of P(LLA-CL) to collagen 1:1 under tensile loading.

Table 3.4. Tensile properties of collagen-blended P(LLA-CL) NFM, with the weight ratio of P(LLA-CL) to collagen 1:1, P(LLA-CL) NFM, and coronary artery[a]

	Collagen-blended P(LLA-CL) NFM	**P(LLA-CL) NFM**	**Coronary artery[b]**
Tensile Modulus (MPa)	26 ± 7	44 ± 4	-
Tensile strength (MPa)	1.54 ± 0.32	6.27 ± 1.38	1.40-11.14
Ultimate strain (%)	66 ± 22	176 ± 49	45-99

[a]Data is representative of three independent experiments and represented as means ± SD (n=3).
[b]See Ref (Xu *et al.*, 2004b).

3.2.2 Cellular behaviors characterization

3.2.2.1 Cellular viability

For cellular viability test, HCAECs were seeded onto the NFM at a density of 1.5×10^4 cells/cm^2 (30% confluence). On day 1, 3, 5, and 7 after cell seeding, unattached cells were washed out and the attached cells were quantified by MTS assay. Figure 3.6 shows viability of HCAECs cultured on (1) collagen-blended P(LLA-CL) NFM, (2) TCPS, (3) collagen NFM, (4) P(LLA-CL) NFM, and (5) P(LLA-CL)-collagen film (blended film) on days 1, 3, 5, and 7 after seeding. Results from day 3 and day 7 are particularly summarized into Figure 3.7 for clarity. The viability of HCAECs increased with collagen weight ratio in the collagen-blended NFM, which can be explained by the previous results showing that more collagen was present on the surface of the NFM with higher collagen weight ratios (Table 3.3). The collagen on the nanofiber surface can help to attach more HCAECs and therefore

leads to higher total cellular viability. The results also showed better HCAECs viability on the collagen-blended NFM than on the blended film, which may indicate the advantage of nanofiber structure in supporting ECs growth.

It is crucial to adjust weight ratios of P(LLA-CL) to collagen for optimal cell growth. From Figure 3.7, it can be found that at a P(LLA-CL)-to-collagen weight ratio of 1:1, the collagen-blended NFM have good cell viability which is comparable to pure collagen NFM and TCPS. The following studies therefore focused on collagen-blended NFM at this ratio. Although pure collagen NFM showed the best cell viability among all the samples, it was not chosen because the collagen NFM swollen into hydrogels in cell culture medium and showed poor mechanical strength, leading to a poorly handlable material.

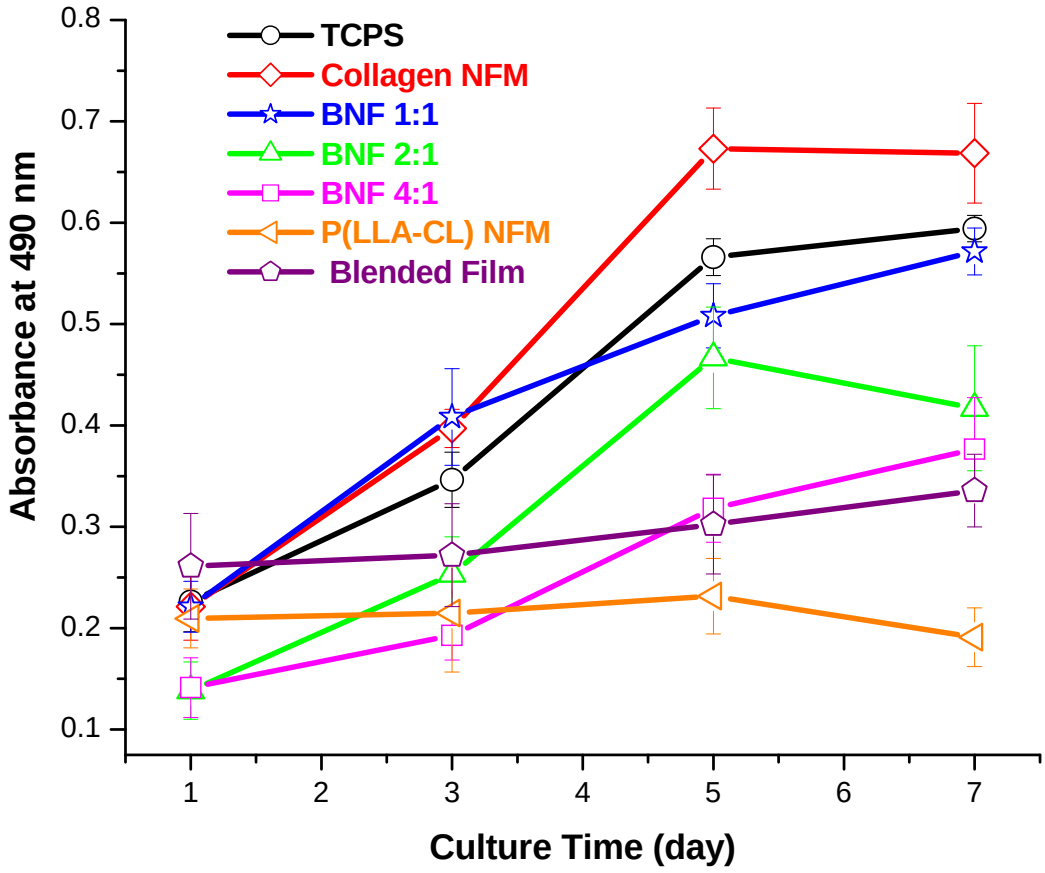

Figure 3.6. Total viability of HCAECs cultured on TCPS, collagen NFM, collagen-blended P(LLA-CL) NFM (BNF) with various weight ratios of P(LLA-CL) to collagen(BNF 1:1, BNF 2:1, BNF 4:1), P(LLA-CL) NFM, and collagen-blended P(LLA-CL) film (Blended film).

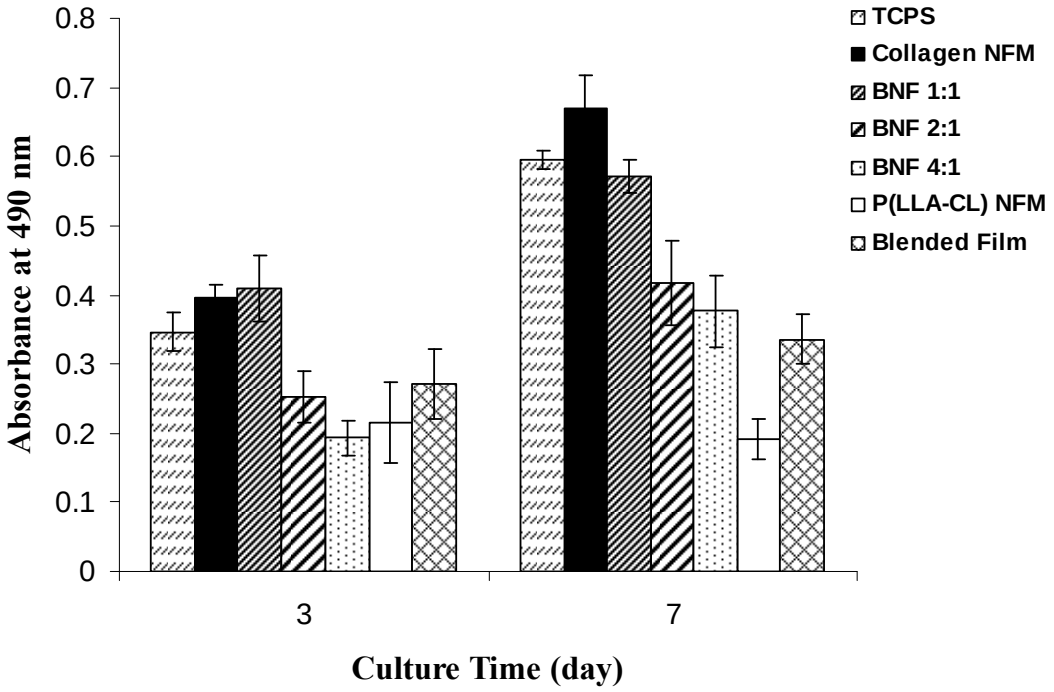

Figure 3.7. Viability of HCAECs on day 3 and 7 shown in Figure 3.6 were summarized here for clarity.

3.2.2.2 Cellular morphology

HCAECs were seeded at a density of 3×10^4 cells/cm^2 and observed on day 5 under laser scanning confocal microscope (LSCM) and SEM (Figure 3.8). It was observed that HCAECs cultured on the P(LLA-CL) NFM were rounded in shape instead of spreading, whereas on the collagen-blended P(LLA-CL) NFM HCAECs adopted a spreading polygonal shape that is typical of normal cell morphology on TCPS. On day 5, HCAECs reached subconfluence on collagen-blended NFM, whereas there were few HCAECs remained on P(LLA-CL) NFM.

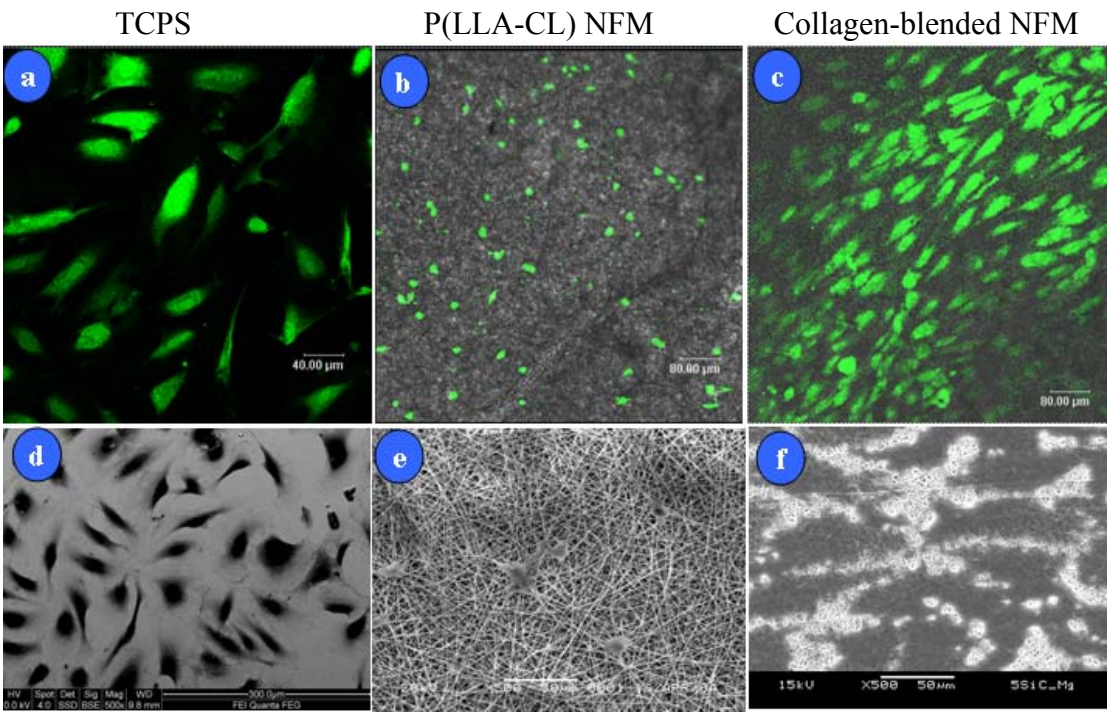

Figure 3.8. LSCM [original magnification: (a): × 400; (b and c): × 200] and SEM [original magnification: (d-f): × 500] images of HCAECs cultured on (a and d) TCPS, (b and e) P(LLA-CL) NFM, and (c and f) collagen-blended P(LLA-CL) NFM.

Figure 3.9 shows interactions between HCAECs and the collagen-blended P(LLA-CL) NFM at higher magnification of SEM. Compared with HCAECs on the P(LLA-CL) NFM which adopted a round shape, HCAECs on the collagen-blended NFM showed better phenotypic spreading. It was also observed that HCAECs interconnected well with the collagen-blended NFM and pseudopods of the cells were oriented along the NFM. Also HCAECs maintained a typical shape of motility, i.e: broad, flat lamella extending in the direction of migration and terminating in a narrow ruffling lamellipodium (Wittmann and Waterman-Storer, 2001).

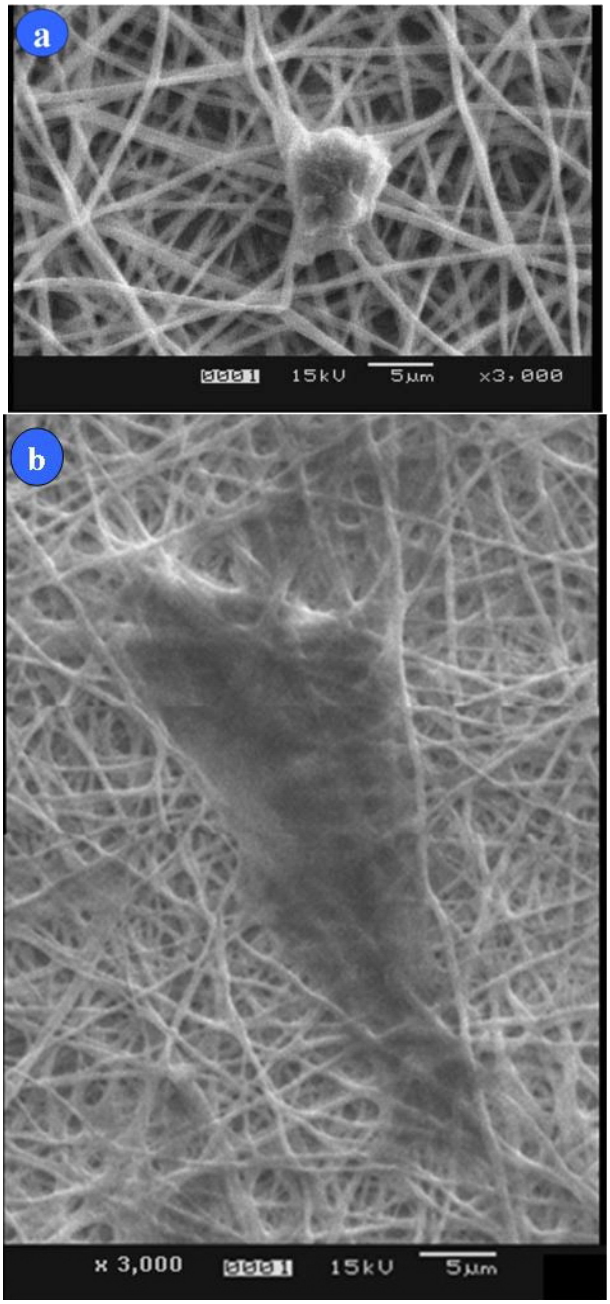

Figure 3.9. Higher magnification of SEM micrographs (original magnification, × 3000), showing the detailed interactions between HCAECs and (a) the P(LLA-CL) NFM and (b) the collagen-blended P(LLA-CL) NFM at 5 days of culture.

3.2.2.3 Cellular attachment

For cellular attachment study, HCAECs were seeded at the density of 3×10^4 cell/cm^2 (60% confluence). At 1, 2, 4, 6 and 8 h after cell seeding, unattached cells were washed out and the attached cells were quantified by MTS assay. Attachment of HCAECs to the TCPS, P(LLA-CL) NFM, and collagen-blended P(LLA-CL) NFM is shown in Figure 3.10. Significantly more HCAECs attached to collagen-blended P(LLA-CL) NFM than P(LLA-CL) NFM in the first 4 h ($p < 0.05$). HCAECs were shown to attach on collagen-blended NFM at a rate similar on TPCS.

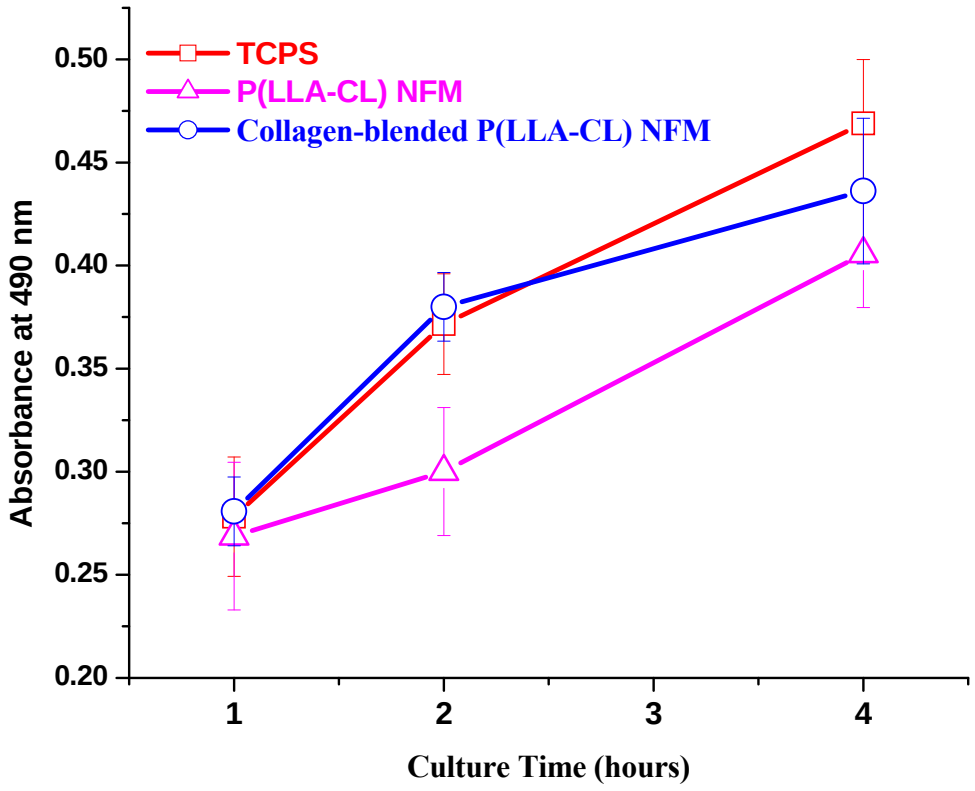

Figure 3.10.Attachment of HCAECs on the TCPS, P(LLA-CL) NFM, and collagen-blended P(LLA-CL) NFM.

3.2.2.4 Cellular phenotype

Tissue engineered vascular grafts should not only support ECs spreading morphology, viability, and attachment but also encourage ECs phenotype maintenance (VanKooten *et al.*, 1997). This is more important because, for suitable vascular grafts, the material should not hamper the adhesion of ECs nor favor the inflammation phenomena (Cenni *et al.*, 1995). Here, ECs phenotype was assessed mainly through RTT-PCR analysis of cell adhesion molecules (CAMs) and EC's universal markers. The functions of CAMs are to mediate cell-cell or cell-matrix interactions. ICAM-1, VCAM-1, and E-selectin are important CAMs expressed by ECs for adhesion and migration of leukocytes or lymphocyte from blood side to tissues during immune responses. Upregulated expression of ICAM-1, VCAM-1, and E-selectin may indicate the onset of the inflammation response (Cenni *et al.*, 1995). PECAM-1 is mainly involved in the homotypic ECs-ECs adhesion, which favors maintenance of endothelium integrity, and can be used to indicate reduced adhesions of ECs to materials (Cenni *et al.*, 1995). Von Willebrand Factor (vWF) is an adhesive glycoprotein synthesized exclusively in ECs and megakaryocytes. It plays a central role in hemostasis by mediating the adhesion of an initial platelet plug to the subendothelium of injured blood vessels and serves as the carrier for factor VIII in plasma (Mohlke *et al.*, 1996). PECAM-1 and vWF are universal EC markers, which can represent the differentiation status of ECs.

Figure 3.11 shows expression of above molecules from HCAECs cultured on the collagen-blended NFM for 10 days. It was found that gene expression levels of the CAMs and vWF from HCAECs cultured on the collagen-blended NFM were comparable to those of cells cultured on TCPS, demonstrating that normal cell phenotype was preserved during *in vitro* culture. Expression of PECAM-1 and vWF revealed that the HCAECs maintained their differentiated status after culturing for 10 days on the collagen-blended NFM. Further, similar expression levels of PECAM-1 represented the normal attachment of HCAECs on the collagen-blended NFM and TCPS, which is especially important for ECs to function well under shear force in a natural environment. The expression of ICAM-1, VCAM-1, and E-selectin indicated that ECs kept the important function of mediating blood cells adhesion in an inflammation response, which further revealed the phenotype maintenance of HCAECs on collagen-blended NFM. Further it shows a higher expression level of VCAM-1 and ICAM-1 from cells grown on blended NFM than on TCPS.

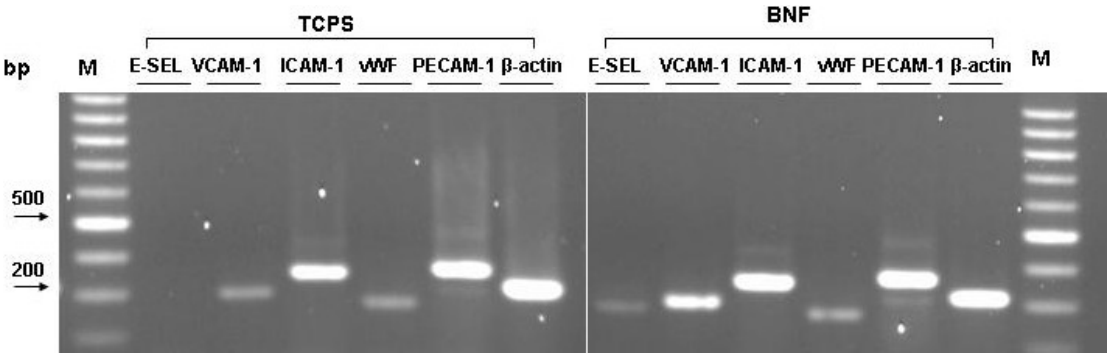

Figure 3.11. Expression of ECs-characteristic genes from HCAECs cultured on TCPS and collagen-blended P(LLA-CL) NFM (BNF) for 10 days. On day 10, total RNA was extracted and RT-PCR was performed with gene-specific primer pairs shown in Table 3.1, including E-Selectin (E-SEL, CD62E), VCAM-1 (CD106), ICAM-1 (CD54), won Willebrand factor (vWF), PECAM-1 (CD31), and β-actin as a housekeeping gene.

3.3 Conclusion

Collagen-blended P(LLA-CL) nanofiber meshes (NFM) were constructed by electrospinning a mixture of collagen and P(LLA-CL) dissolved HFP. The collagen-blended NFM had a well-controlled diameter distribution ranging from 100 to 200 nm and porosity around 70%. Existence of collagen on the surface of the collagen-blended NFM was verified by ATR-FTIR and XPS. The collagen-blended NFM had a decreased tensile modulus, tensile strength, and ultimate strain compared with the P(LLA-CL) NFM. Cell culture showed that the collagen-blended NFM has improved viability and attachment of HCAECs compared with the P(LLA-CL) NFM. HCAECs adopted a spreading polygonal shape and interconnected well with the collagen-blended NFM, whereas HCAECs had a round non-spreading shape on the P(LLA-CL) NFM. Moreover, HCAECs maintained phenotypic expression of cell adhesion molecules such as PECAM-1, ICAM-1, VCAM-1, E-Selectin, and vWF on the collagen-blended NFM.

Chapter 4

Collagen-Coated P(LLA-CL) Nanofiber Meshes (NFM)

The results in chapter 3 showed that blending with collagen type I into electrospun P(LLA-CL) nanofiber meshes (NFM) is a simple method to improve endothelialization ability of the material. But the collagen must be dissolved in organic solvent (HFP) with the polymer prior to the electrospinning process, which may be a harsh environment for the collagen. Secondly, consuming quite a lot of expensive collagen (500 μg collagen per mg NFM) is also a concern. Further, blending with collagen resulted in decreased mechanical properties of the P(LLA-CL) NFM, as was observed in the chapter 3. Most importantly, due to the collagen type I was extracted from natural animal tissues (calf skin), the material's molecular structure is far from as repeatable as synthetic polymers. It was found that the batch difference of the collagen type I even from the same manufacturer (Sigma-Aldrich) often leaded to variable solubility in the HFP, resulting in poor repeatability of the electrospinning conditions. To overcome above problems, in this chapter, collagen-coated P(LLA-CL) NFM were fabricated. P(LLA-CL) NFM were first treated by inductive coupled radiofrequency glow discharge plasma to improve the wettability, followed by collagen coating. The morphology, porosity, mechanical properties, and surface chemistry of the collagen coated P(LLA-CL) NFM were studied. Behaviors of human coronary artery endothelial cells (HCAECs) on the collagen-coated P(LLA-

CL) NFM were evaluated in terms of morphology, viability, attachment, phenotype, and functional maintenance.

4.1 Materials and methods

4.1.1 Materials

Dichloromethane (DCM), *N*,*N*-dimethylformamide (DMF), and hydrochloric acid (HCl) were from Merk & Co.(Whitehouse Station, NJ, USA). The mouse monoclonal antibody to human platelet endothelial cell adhesion molecule-1 (PECAM-1, CD 31) was from Cymbus Biotechnology (Hants, UK). The mouse monoclonal antibodies to human fibronectin and collagen type IV were from Acris (Hiddenhausen, Germany). Other chemical and biological reagents and materials were all the same as used in chapter 3 (see section 3.1.1)

4.1.2 Fabrication of P(LLA-CL) NFM

For electrospinning of the P(LLA-CL) NFM, P(LLA-CL) (10 wt%) solution in DCM and DMF (70:30 wt:wt) was added into a plastic syringe with a needle (inner diameter, 0.21 mm). With the aid of a syringe pump, the solution was injected out at a feed rate of 0.5 mL/h. Electrospinning voltage was applied to the needle at 10 kV using a high-voltage power supply (Gamma High Voltage Research, Ormond Beach, FL, USA). The nanofibers were collected on an aluminum collector which was 10 cm

below the needle. For colleting the random NFM, a static flat alumina plate was used; while for colleting the aligned NFM, a rotating disk (1000 rpm) was used. The rotating plate had a sharpen edge that can strengthen the electric field near the collector. The experiment setups are showed in Figure 4.1.

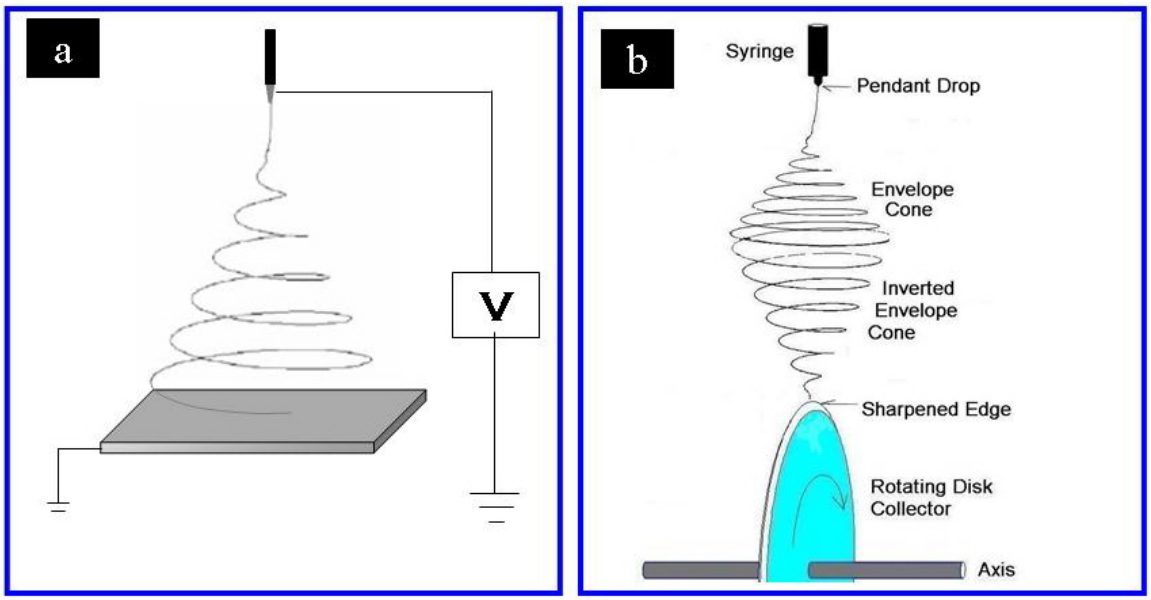

Figure 4.1. Experimental setups for fabricating the random and aligned P(LLA-CL) NFM, which were collected with a static plate (a) and rotating disk (b), respectively.

4.1.3 P(LLA-CL) NFM modification by collagen coating

Air plasma treatment of P(LLA-CL) NFM was performed in an inductive coupled radiofrequency glow discharge plasma cleaner (PDC-001, Harrick Plasma, Ithaca, NY, USA) with the radiofrequency power of 30 W. The plasma treatment increased the surface hydrophilicity of the nanofiber significantly (Chan *et al.*, 1996;Wang *et al.*, 2004), making the P(LLA-CL) NFM easily wettable by collagen solution. The plasma-treated P(LLA-CL) NFM were then immersed in a collagen

solution in 0.01 M hydrochloride (HCl) with a concentration of 290 µg/mL at 4°C overnight. They were then dried at room temperature. The complete surface modification scheme for P(LLA-CL) NFM is shown in Figure 4.2.

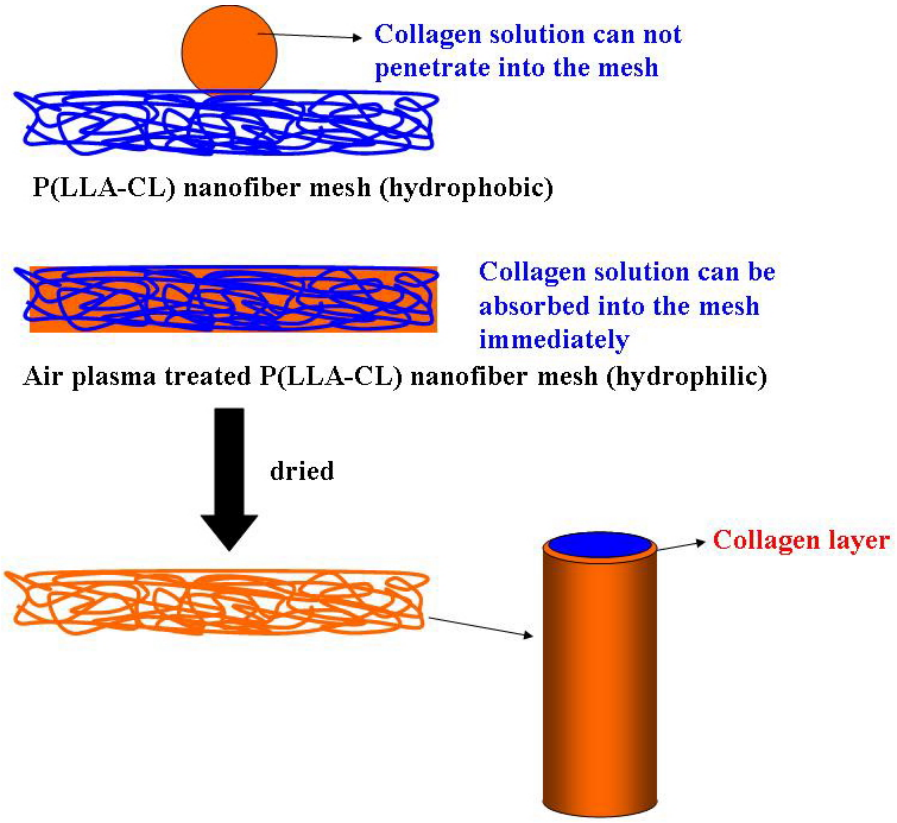

Figure 4.2. Schematic representation of the plasma treatment and collagen coating of the electrospun P(LLA-CL) nanofiber mesh.

4.1.4 Material characterization

4.1.4.1 Physical properties

SEM micrographs of the collagen-coated P(LLA-CL) NFM were obtained on a JSM-5800LV SEM (JEOL, Tokyo, Japan). Diameter range and pore size (the length

of the diagonals of the pore square) of the NFM were measured from the SEM images by random counting of 60 nanofibers using image analysis software (ImageJ, Bethesda, USA). Thickness of the NFM was measured using a micrometer (Mitutoyo, Kawasaki, Japan). Tensile tests were carried out in the same way as described in chapter 3 (see section 3.1.3.3).

4.1.4.2 Surface chemistry

Wettability of the P(LLA-CL) NFM and films before and after air plasma treatment were measured by sessile drop contact angle measurement using a VCA Optima Surface Analysis System (AST products, Billerica, MA). Briefly, 7.5 μL water was dropped onto the material surface and the water drop shape was recorded in 30 seconds. Six independent determinations at different sites of one sample were averaged. To get water contact angle on plane P(LLA-CL) surface, P(LLA-CL) films were prepared by a solvent casting method described in chapter 3 (see section 3.1.2) in detail. XPS spectra of the NFM were obtained in a same way as described in chapter 3 (see section 3.1.3.2).

4.1.4.3 Collagen distribution and quantification

To visualize the collagen distribution on the P(LLA-CL) NFM, P(LLA-CL) NFM coated with rhodamine B isothiocyanate (RBITC, Sigma, USA)-labeled collagen were observed under a laser scanning confocal microscope (LSCM, Leica

Microsystems, Wetzlar, Germany). Depth projection images for three-dimensional (3-D) micrographs were constructed from 20 horizontal slices of step size 1 μm. The RBITC-labeled collagen was prepared as follows: collagen (M*w*=285 k) solution (1 mg/mL) in 0.01M HCl was mixed with the RBITC (M*w*=536.1) with the molar ratio of RBITC to collagen 50:1. The mixed solution was incubated in darkness at room temperature for 3 h and then added into a dialysis tubing cellulose membrane (molecular weight cutoff = 12,400) and dialyzed in 0.01 M HCl solution for 30 days until no more RBITC could be released into the HCl solution.

The amount of collagen coated onto the P(LLA-CL) NFM was quantified by bicinchoninic acid (BCA) Protein Assay Kit (Pierce, USA) with the protocol provided by the manufacture. Briefly, the collagen-coated NFM were immersed in 0.1 mL PBS together with 2 mL working reagent at room temperature for 2 hours under gentle shaking, and then the absorbance at 562 nm of the supernatant was measured. The collagen concentration was calculated from the collagen standard curve.

4.1.5 Characterization of cellular behaviors

4.1.5.1 *In vitro* cell culture

HCAECs culture, HCAECs morphology studies by SEM and green fluorescent probe CMFDA (5-chloromethyl fluorescein diacetate) staining, and

HCAECs viability and attachment studies by MTS assay were all the same as described in chapter 3 (see section 3.1.4.1, 3.1.4.2, and 3.1.4.3).

4.1.5.2 Immunostaining

After 5 days of culture with seeding density of 1.5×10^4 cells/cm^2, the HCAECs cultured on NFM were washed with 1 × PBS, fixed with 2.5% paraformaldehyde, and blocked by 2% bovine serum albumin (BSA). The HCAECs-NFM constructs were then incubated for 2 h at 37^{o}C with primary antibody. After washing with 0.02% BSA, fluorescein isothiocyanate (FITC) labeled rabbit anti-mouse IgG (Chemicon, Temecula, CA, USA) was added and incubated for 2 h at 37^{o}C in dark, followed by washing with 0.02% BSA and counterstaining with propidium iodide (PI, 2.5 μg/mL) for 1 min at 37^{o}C. The immunostained construct samples were then mounted on glass slides. 7 μL FluorSave reagent (Calibiochem, Germany) was dropped onto the samples to prevent photo-bleaching. The samples were viewed under laser scanning confocal microscope (LSCM).

4.1.5.3 RT-PCR analysis

PECAM-1, fibronectin, and collagen type IV were studied by reverse transcriptase polymerase chain reaction (RT-PCR) for gene expression analysis in mRNA level. Forward and reverse primers of each gene are listed in Table 4.1. Total RNA was extracted from subconfluent 2.5×10^6 HCAECs using RNeasy Mini Kit

(Qiagen, Hilden, Germany). For RT-PCR, complementary DNA (cDNA) was reverse transcribed from 1 μg of total RNA. Further information was described in chapter 3 (see section 3.1.4.3) in details. The PCR products were analyzed by electrophoresis of 10 μL of each sample in a 1% agarose gel, and the bands were visualized under ultraviolet light by ethidium bromide staining with a gel documentation system (Gel Doc 2000, BioRad, Hercules, CA, USA).

Table 4.1. PCR primers for RT-PCR analysis

Gene	Genebank No.	size (bp)	Primer pair sequences
β-actin	BC002409	318	5' GAG TCC TGT GGC ATC CAC G 3'
			5' GAA GCA TTT GCG GTG GAC G 3'
PECAM-1 (CD31)	BC051822	367	5' TCA TCG GAG TGA TCA TTG CTC 3'
			5' CTA GAG TAT CTG CTT TCC ACG 3'
Fibronectin	M10905	276	5' TGA CCC TCA TGA GGC AAC G 3'
			5' TCA GCC TGT ACA TCT AAA GGC 3'
Collagen Type IV	NM_001845	257	5' CTT TTG TGA TGC ACA CCA GC 3'
			5' TCT CAT ACA GAC TTG GCA GC 3'

4.1.5.4 cDNA microarray analysis

Total RNA was extracted from the HCAECs cultured for 5 days on tissue culture polystyrene (TCPS), the random and aligned collagen-coated P(LLA-CL) NFM using RNeasy Mini Kit. A biotin-2'-deoxyuridine (dUTP) (Roche, Pleasonton, CA, USA) labeled cDNA probe was synthesized according to GEArray™ probe synthesis kits (GEArray Ampolabeling-LPR kit, SuperArray®, Frederick, MD, USA)

and stored at -20^{o}C. Hybridization with a 2.5 μg biotinylated cDNA probe was done on a nylon membrane printed with the GEArray™ S series (human endothelial cell biology gene array, SuperArray®), which contained 112 genes associated with major functions of ECs. Prehybridization and hybridization were carried out in a hybridization oven (Biometra, Goettingen, Germany) for 2 h and overnight respectively. Finally, the chemiluminescent membranes were scanned by ScannArray® (GSI Lumonics, Billerica, MA, USA).

4.1.6 Statistical analysis

Data were made at least in triplicate and expressed as mean ± standard deviation (SD). Each experiment was repeated three times. Statistical analysis was carried out for HCAECs viability and attachment studies using One-Way ANOVA testing by SPSS for Windows (SPSS Inc., Copyright 1989-2002) version 11.5.0. Significant difference between data groups was determined by the Student-Newman-Keuls (SNK) post hoc test ($p < 0.05$).

4.2 Results and discussions

4.2.1 Material characterization

4.2.1.1 Physical properties

Morphology of the random and aligned collagen-coated P(LLA-CL) NFM is shown in Figure 4.3. Diameter and distribution of the random and aligned collagen-coated P(LLA-CL) NFM are shown in Figure 4.4 and Table 4.2. More uniform diameter distribution was found for the random NFM than the aligned NFM (Figure 4.4 a). The diameter of the aligned NFM (406 ± 126 nm) was smaller than that of the random NFM (470 ± 80 nm). Similar results were also reported for aligned PCL (Ma *et al.*, 2005a) and PLLA NFM (Yang *et al.*, 2005). This might be due to stretching tangential force exerted by the high-speed rotating disk on the nanofiber produced (Ma *et al.*, 2005a).

The pore size for the random NFM was defined as length of diagonal of the pore polygon, which is not applicable for the aligned NFM. Figure 4.4 b and table 4.2 shows pore size of the random NFM to be mainly between 5 and 10 μm. The thickness, apparent density, and porosity of the random and aligned collagen-coated P(LLA-CL) NFM are summarized in Table 4.2. With the known bulk density of P(LLA-CL) (1.2-1.3 g/cm^3) and collagen (1.3-1.4 g/cm^3), the porosity of the collagen-coated P(LLA-CL) NFM can be estimated by measuring their apparent density. Porosity for both NFM was found to be approximately 70%. Porosity is an important measure for tissue engineering scaffolds. Vascular grafts should be porous, and the porosity should allow cells infiltration from the adventitial side and maintain hemostasis, as well as allow sufficient mass transfer of gases and nutrients (Sullivan and Brockbank, 2002). It is generally accepted that a high porosity vascular graft exhibits high patency (Niklason and Seruya, 2002).

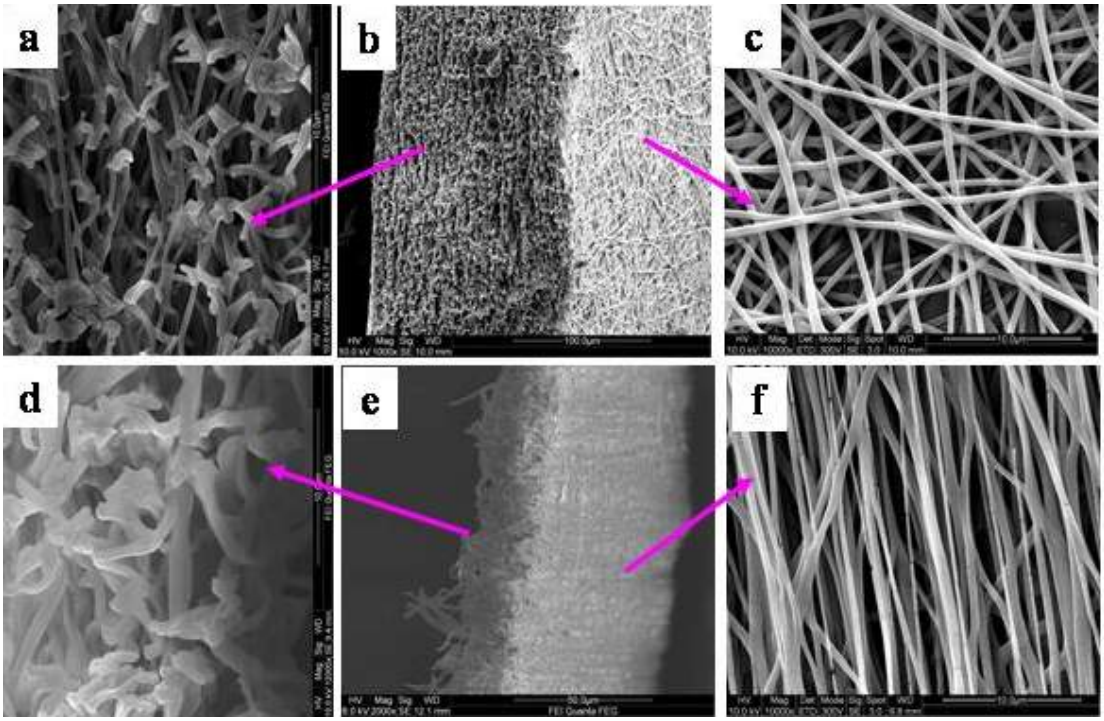

Figure 4.3. SEM pictures of the cross section (a and d), 3-dimensional structure (b and e), and top view (c and f) of the random (a-c) and aligned (d-f) collagen-coated P(LLA-CL) NFM.

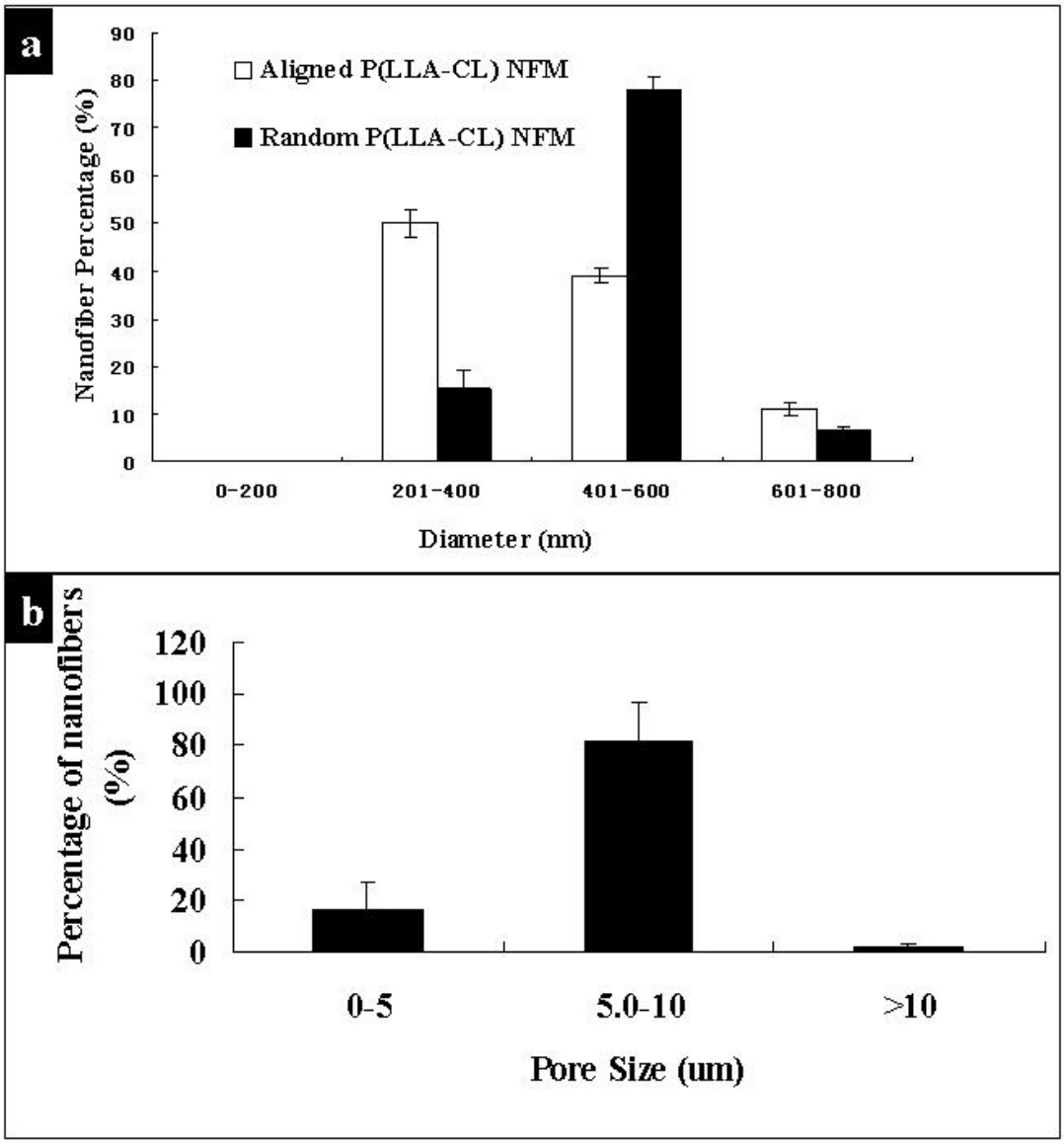

Figure 4.4. (a) Diameter distribution of the random and aligned collagen-coated P(LLA-CL) NFM. (b) Pore size distribution of the random collagen-coated P(LLA-CL) NFM.

Table 4.2. Diameter, thickness, apparent density, porosity, and pore size of the random and aligned collagen-coated P(LLA-CL) NFM[a]

Collagen-coated P(LLA-CL) NFM	Diameter (nm)	Thickness (μm)	Apparent density (g/cm^3)	Porosity (%)	Pore Size (μm)
Random	470 ± 80	26 ± 5	0.43 ± 0.08	64-69	6 ± 2
Aligned	406 ± 126	24 ± 2	0.37 ± 0.02	69-74	N.A.

[a] Data are representative of three independent experiments and are presented as mean ± SD (n=5)

4.2.1.2 Collagen coating

As an adhesion protein that facilitates cell attachment and proliferation (Ruoslahti and Pierschbacher, 1987a), collagen is commonly used to modify the surface of vascular grafts. The first complete tissue engineered vascular graft was fabricated with collagen gel (Weinberg and Bell, 1986). However, pure collagen scaffolds always encountered mechanical limitation (L'Heureux *et al.*, 1993). Electrospinning of collagen nanofibers and modification of nanofibers with collagen are new approaches that may improve scaffold strength (Matthews *et al.*, 2002a)

Due to the hydrophobic nature of the P(LLA-CL), collagen solution stayed on the top surface of the P(LLA-CL) NFM and could not be absorbed into the NFM, which made collagen coating of the NFM not efficient or even. To help the collagen solution easily go into the porous P(LLA-CL) NFM, the hydrophobic P(LLA-CL) NFM was treated with air plasma to make it highly wettable. The effectiveness of the

plasma treatment to increase P(LLA-CL) NFM' wettability was verified by water contact angle measurement. Water contact angles of the random P(LLA-CL) NFM and films before and after plasma treatment are summarized in Table 4.3. The P(LLA-CL) NFM exhibited different water contact angles from the films due to different surface structure. The P(LLA-CL) NFM and films were both hydrophobic in nature before plasma treatment and the NFM showed higher contact angle than the films. Although the original P(LLA-CL) NFM showed high water contact angle, after plasma treatment, they became highly wettable. The water drop, upon contact with the plasma treated P(LLA-CL) NFM, was immediately absorbed into the NFM, giving a zero apparent water contact angle. Although the films also tended to be more hydrophilic after plasma treatment, the contact angle change after the air plasma treatment was not as big as that for the P(LLA-CL) NFM. It's also shown in Table 4.3 that plasma treatment of 5 min was enough to increase the P(LLA-CL) NFM' wettability.

Table 4.3. Water contact angles of the P(LLA-CL) NFM and films before and after plasma treatment for various time[a]

Plasma Treatment Time (min)	**P(LLA-CL) NFM (deg)**	**P(LLA-CL) films (deg)**
0	129 ± 1	96 ± 6
5	0 ± 0	60 ± 1
15	0 ± 0	57 ± 3
30	0 ± 0	55 ± 3

[a] Data are representative of three independent experiments and represented as mean ± SD (n=6).

The big difference of the P(LLA-CL) NFM' wettability before and after plasma treatment can be explained as the following. The water contact angle of a solid surface is affected by surface roughness in such a manner: if the material is intrinsically hydrophobic, the water will not be able to penetrate into the hollows and pores on the rough surface and can be regarded as resting on a semi-solid and semi-air plane surface, which will increase the contact angle significantly. In contrast, the water will penetrate and fill up most of the hollows and pores formed by an intrinsically hydrophilic material, forming a surface which is partly solid and partly liquid and therefore leading to a low water contact angle. Having a highly rough surface, the P(LLA-CL) NFM experienced a big improvement in wettability after they were plasma treated from hydrophobic to hydrophilic (Ma *et al.*, 2005b).

After the plasma treatment, the P(LLA-CL) NFM were then immersed in a collagen solution in 0.01 M hydrochloride (HCl) with a concentration of 290 μg/mL at 4 ^{o}C overnight. They were then dried at room temperature.

4.2.1.3 Surface chemistry

The presence of the collagen on the P(LLA-CL) NFM's surface was confirmed by the appearance of the N1S peak (indicated in nitrogen [N] atomic ratio) in the XPS spectrum of the collagen-coated P(LLA-CL) NFM (Table 4.4), while no N1S peak was found in the spectrum of the pure P(LLA-CL) NFM. Compared with

the pure electrospun collagen NFM (15.1%), less nitrogen was found on the collagen-coated NFM (5.2%).

Table 4.4. Atomic ratio of C, N, and O on the surface of the P(LLA-CL) NFM, the collagen-coated P(LLA-CL) NFM, and the pure collagen NFM determined by XPS

NFM	C atomic ratio (%)	N atomic ratio (%)	O atomic ratio (%)
P(LLA-CL)	65.9	0	34.1
Collagen-coated P(LLA-CL)	61.5	5.2	33.3
Collagen	61.6	15.1	23.3

To visualize spatial distribution of the collagen coated onto the P(LLA-CL) NFM, rhodamine-labeled collagen was coated onto the P(LLA-CL) NFM and observed under laser scanning confocal microscope (LSCM). It shows in 3-dimensional (3-D) images of the NFM that collagen was uniformly distributed on the surface of every nanofiber in both random (Figure 4.5 a) and aligned (Figure 4.5 b) NFM. There was no auto-fluorescence observed on the P(LLA-CL) NFM without collagen-coating under LSCM (data not shown).

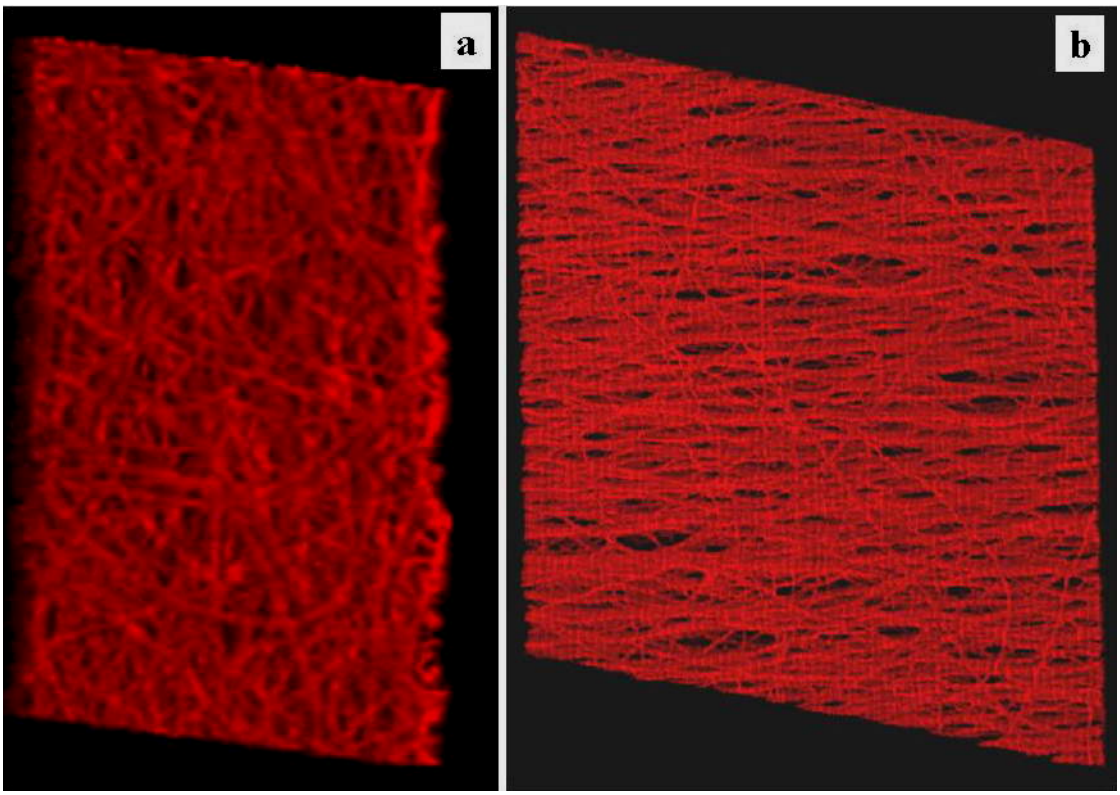

Figure 4.5. 3-D laser scanning confocal microscopy (LSCM) (original magnification, × 600) of the collagen-coated random (a) and aligned (b) P(LLA-CL) NFM. Existence of rhodamine-labeled collagen was identified by its red fluorescence.

By BCA protein assay analysis, the amount of collagen coated onto the P(LLA-CL) NFM was measured and normalized by NFM' weight. It was found that 15 ± 5 μg collagen was coated per 1 mg NFM. Compare with the collagen amount used in the collagen-blended P(LLA-CL) NFM at P(LLA-CL)-to-collagen weight ratio of 1:1 (500 μg collagen per 1 mg NFM), collagen coating used much less amount of collagen.

4.2.1.4 Mechanical properties

Figure 4.6 shows the stress-strain curves for the random and aligned P(LLA-

CL) NFM under tensile loading. The stretching direction for the aligned NFM is in the fiber alignment direction. Mechanical strength of the aligned P(LLA-CL) NFM were higher compared with the random NFM. Tensile properties of the NFMs are further summarized in Table 4.5, which also shows that aligned NFM has larger tensile modulus and tensile strength but smaller ultimate strain than the random NFM. This finding correlates to the report that orientation of the fibers directly enhanced the mechanical properties of the nanofibers along the fiber alignment direction (Matthews *et al.*, 2002b).

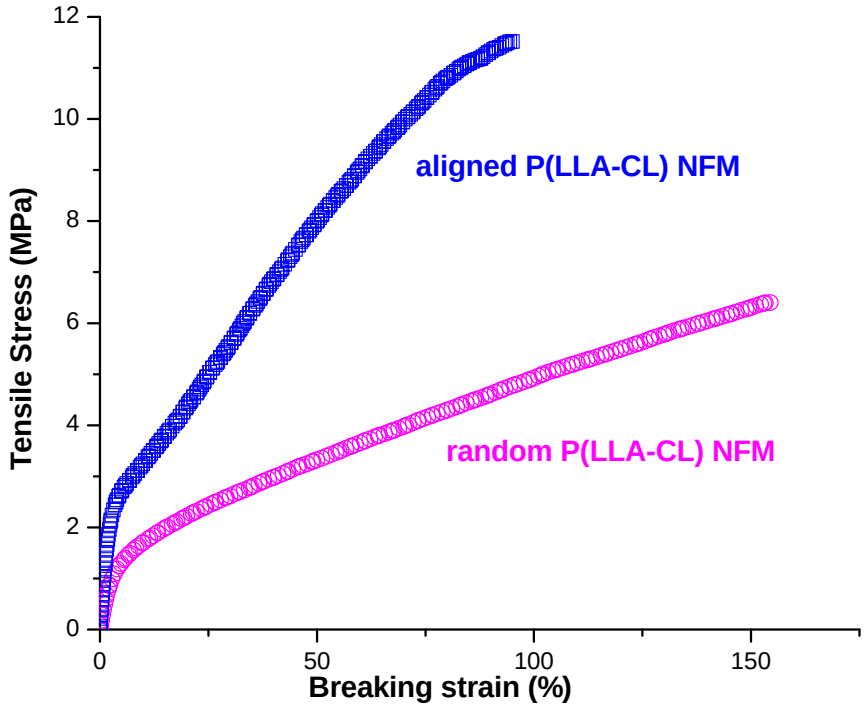

Figure 4.6. Stress-strain curves for the random and aligned P(LLA-PCL) NFM under tensile loading.

Table 4.5. Tensile properties of the random and aligned P(LLA-CL) NFM[a]

	Random	**Aligned**
Tensile Modulus (MPa)	44 ± 4	103 ± 6
Tensile strength (MPa)	6.3 ± 1.4	10.6 ± 1.3
Ultimate strain (%)	176 ± 49	99 ± 5

[a] Data are representative of three independent experiments and represented as mean ± SD (n=3)

4.2.2 Characterization of cellular behaviors

4.2.2.1 Cellular morphology

HCAECs were seeded at a seeding density of 3×10^4 cells/cm^2 and observed 3 days later by CMFDA staining for fluorescent microscopy or fixed by glutaraldehyde for SEM study (Figure 4.7). HCAECs cultured on the P(LLA-CL) NFM were rounded in shape instead of a spreading morphology, whereas on the collagen-coated P(LLA-CL) NFM HCAECs adopted a spreading polygonal shape which is typical of the normal ECs morphology as on TCPS. Further, immunostaining of PECAM-1 from HCAECs cultured on TCPS and collagen-coated P(LLA-CL) NFM showed similar pattern of PECAM-1 expression which occurred mainly at cell-cell interfaces. The P(LLACL) NFM was red in color due to the presence of rhodamine-labeled collagen being coated on NFM's surface (Figure 4.8).

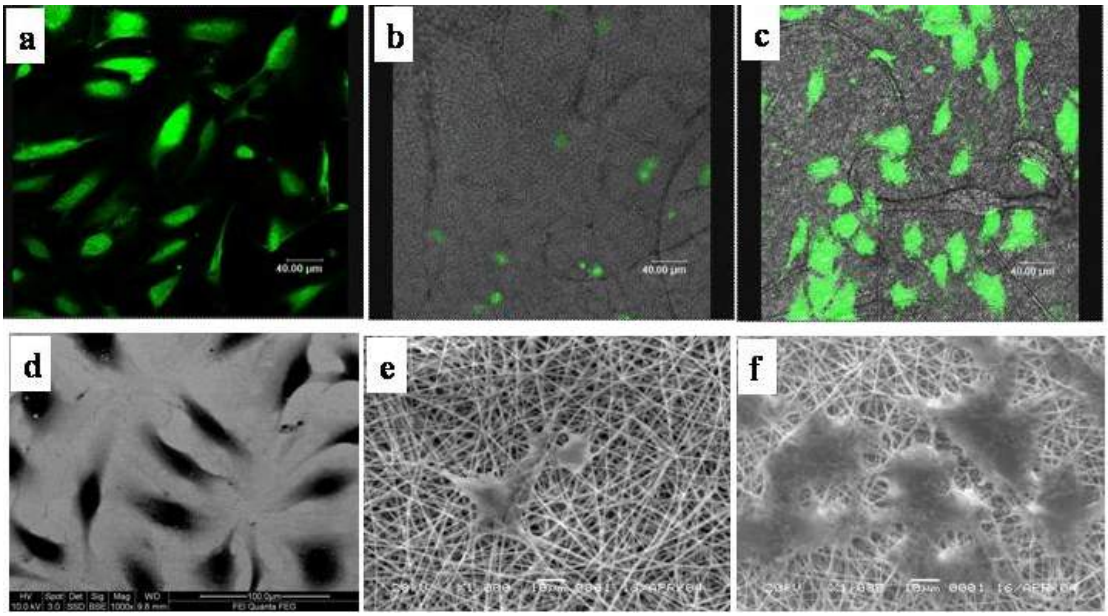

Figure 4.7. LSCM (original magnification, × 400) and SEM (original magnification, × 1000) images of HCAECs cultured on (a, d) TCPS, (b, e) P(LLA-CL) NFM, and (c, f) collagen-coated P(LLA-CL) NFM.

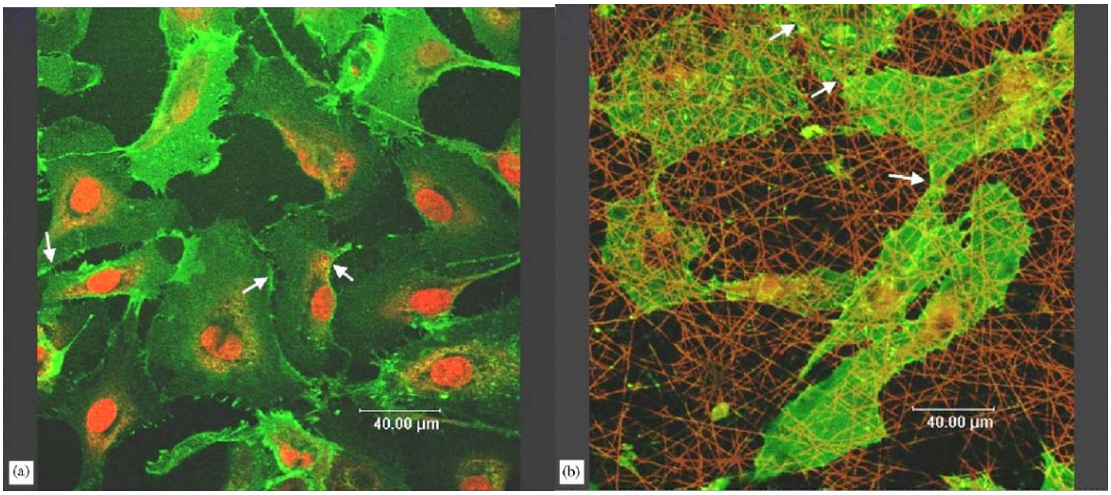

Figure 4.8. Immunofluorescent staining of PECAM-1 from HCAECs cultured on TCPS (a) and the collagen-coated P(LLA-CL) NFM (b). Existence of rhodamine-labeled collagen was identified by its red fluorescence in (b). White arrows indicate strong PECAM-1 expression at cell-cell interfaces.

4.2.2.2 Cellular viability and attachment

Total viability of HCAECs at day 1, 3, 5, and 7 cultured on the TCPS, collagen-coated P(LLA-CL) NFM, and pure P(LLA-CL) NFM is shown in Figure 4.9. Viability of HCAECs on the collagen-coated P(LLA-CL) NFM was obviously increased compared with that on the pure P(LLA-CL) NFM from day 3 onwards ($p < 0.05$).

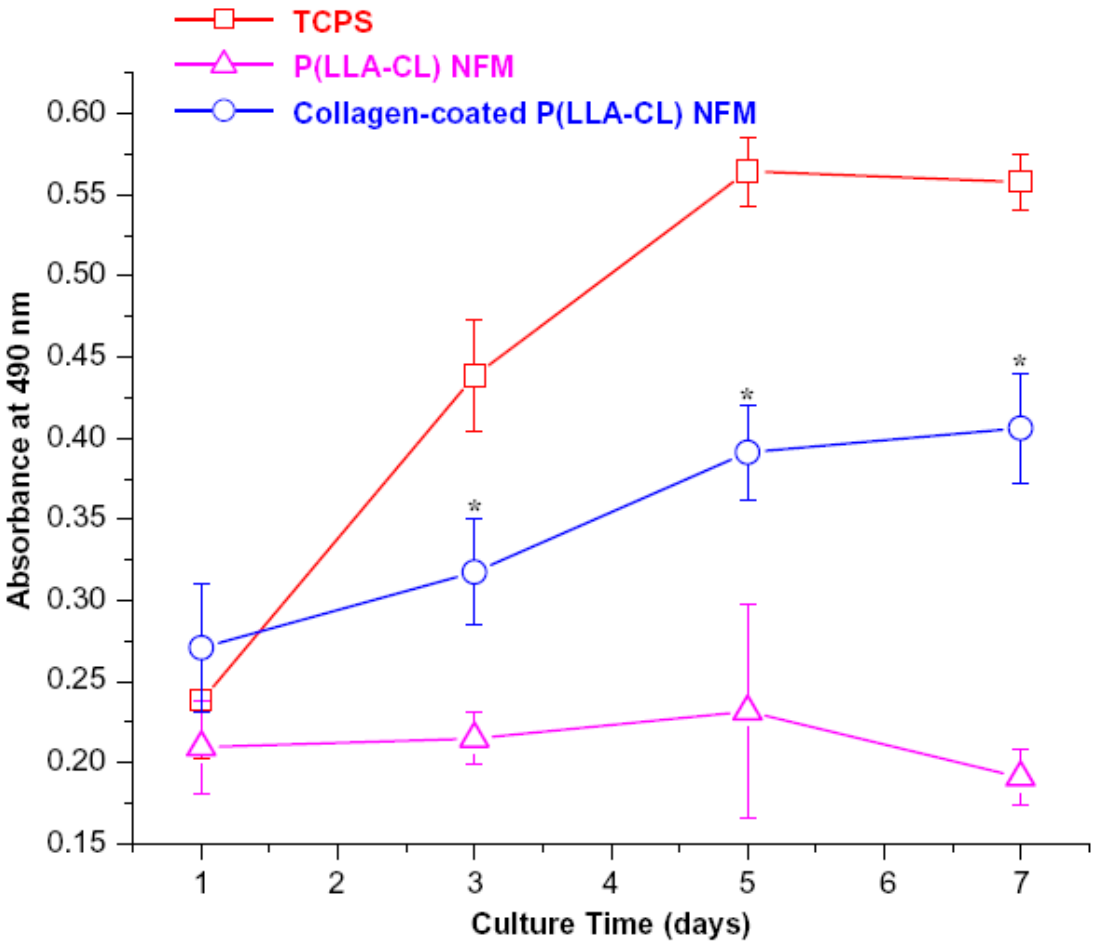

Figure 4.9. Viability of HCAECs on the TCPS, P(LLA-CL) NFM, and collagen-coated P(LLA-CL) NFM. (* $p < 0.05$ compared with the P(LLA-CL) NFM).

The attachment of HCAECs to the TCPS, collagen-coated P(LLA-CL) NFM, and pure P(LLA-CL) NFM is shown in Figure 4.10. Significantly higher cellular viability on the collagen-coated P(LLA-CL) NFM than the pure P(LLA-CL) NFM, which may indicate more attached cells, was found 2 h after cells seeding ($p < 0.05$). HCAECs were found to attach on the collagen-coated P(LLA-CL) NFM at a very similar rate as that they attached on the TPCS. This is because collagen is the most abundant ECM protein with both structural and adhesive functions, facilitating cell adhesion through the integrin receptors (Ruoslahti and Pierschbacher, 1987b).

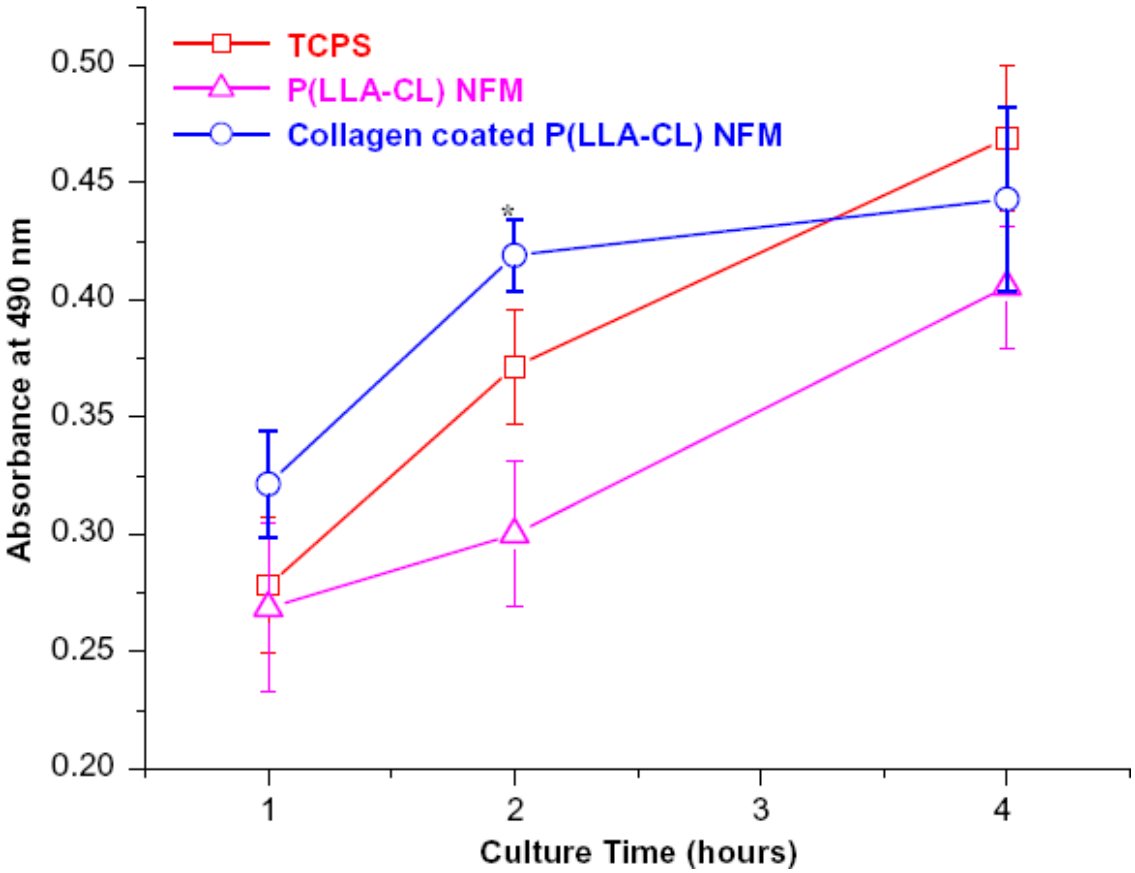

Figure 4.10. Attachment of HCAECs on the TCPS, P(LLA-CL) NFM, and collagen-coated P(LLA-CL) NFM. (* $p < 0.05$ compared with the P(LLA-CL) NFM).

4.2.2.3 Cellular Phenotype

In order to study phenotypic and functional maintenance of HCAECs on the collage-coated P(LLA-CL) NFM, we performed a series of studies ranging from ECs morphology, and ECs phenotype studies through immunostaining and RT-PCR, to a deeper analysis of gene expression by cDNA microarray.

Morphology of HCAECs was studied first. Figure 4.11A shows HCAECs adopted a spindle shape on the aligned NFM in the direction of fiber alignment. This finding was distinct from the polygonal shape of HCAECs on the TCPS and random NFM. Ability of the aligned NFM to control cell orientation is meaningful for tissue engineered vascular grafts (Nerem and Seliktar, 2001). Shear stress caused by blood flow *in vivo* orientates ECs growth along the direction of blood flow (Dewey *et al.*, 1981), which may increase the ability of ECs to resist shear stress and decrease desquamation of these cells from vascular grafts. One way to orientate cells *in vitro* is through dynamic cell culture in a bioreactor. It was reported that smooth muscle cells (SMCs) cultured in a perfusion bioreactor showed contractile phenotype, significant cell alignment, and increased collagen production (Jeong *et al.*, 2005). Similarly, Lee *et al* found human ligament fibroblast cultured on the aligned polyurethane nanofibers were orientated along the fiber direction and secreted more collagen than on the randomly orientated nanofibers (Lee *et al.*, 2005). Thus, aligned NFM might be used as substitute for a bioreactor which necessitates a complicated fluid system in a specific application where cell alignment is important.

Phenotype studies of HCAECs were then carried out by immunostaining and RT-PCR analysis. First, immunostaining of PECAM-1, a universal EC marker, showed the differentiation status and phenotypic maintenance of HCAECs on both TCPS and random and aligned NFM (Figure 4.11 A, top). Second, Figure 4.11 B showed immunostaining of fibronectin and collagen IV for HCAECs on the TCPS, random and aligned NFM. HCAECs cultured on the collagen-coated P(LLA-CL) NFM expressed the ECs-characteristic ECM proteins, indicating the potential capability of HCAECs to build ECM *in vitro*. Finally, Figure 4.11 C further revealed the expression of these three molecules (PECAM-1, fibronectin, and collagen IV) at the gene level by RT-PCR analysis.

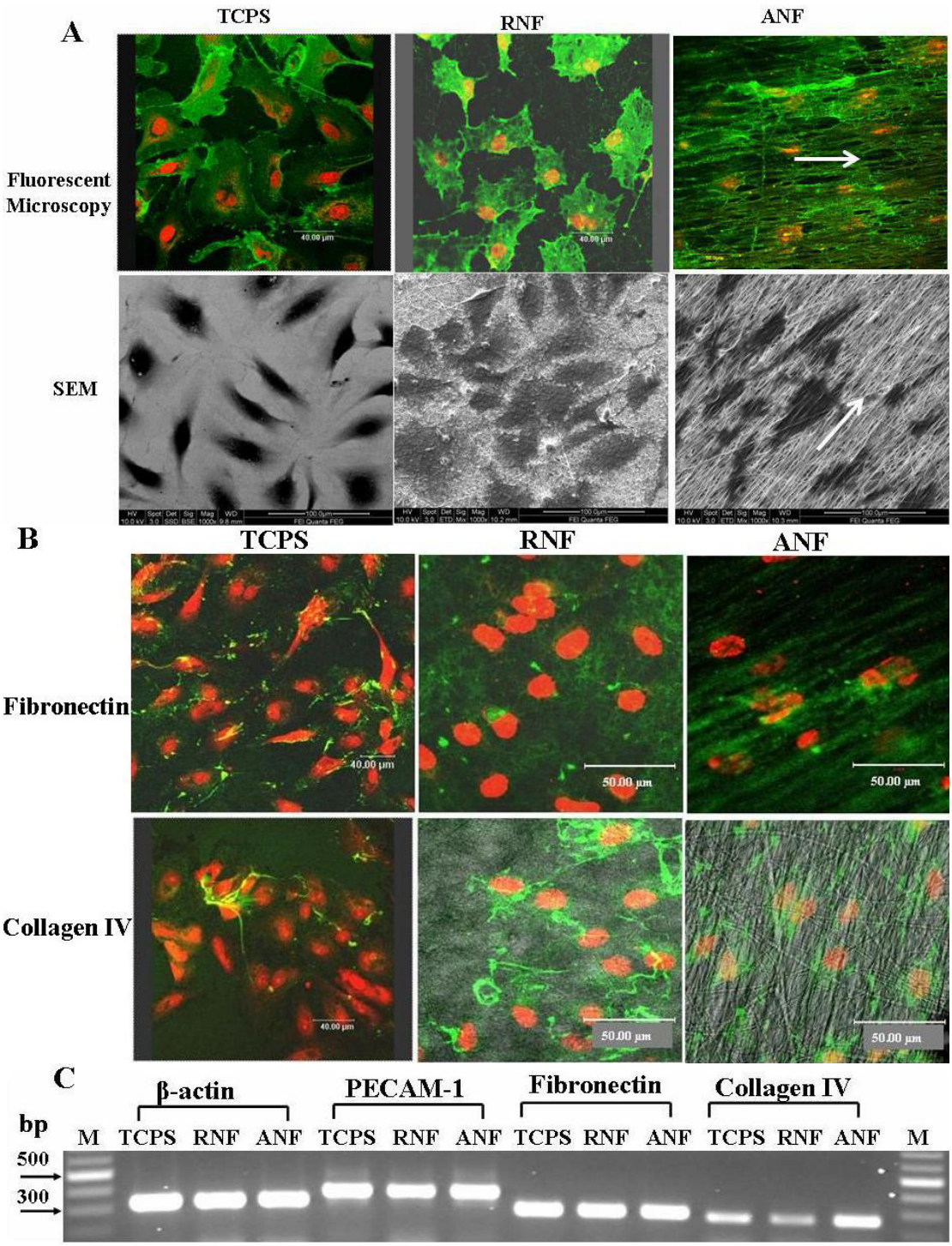

Figure 4.11. (A) Fluorescent microscopy (original magnification, × 600) and SEM (original magnification, × 1000) images from HCAECs on TCPS, random NFM (RNF) and aligned (ANF) collagen-coate P(LLA-CL) NFM. (B) LSCM images of fibronectin and collagen type IV expressions from HCAECs on the TCPS, RNF, and ANF. (C) RT-PCR analysis of expressions of PECAM-1, fibronectin, and collagen type IV from HCAECs on the TCPS, RNF, and ANF.

4.2.2.4 Gene expression

In order to study functional maintenance of HCAECs, cDNA microarray was applied to study gene expression profiles of HCAECs cultured on the TCPS, collagen-coated random and aligned P(LLA-CL) NFM. Figure 4.12 A shows the expression profile of 112 genes, printed onto a nylon membrane in the form of 8×14 grid, which are associated with four major functions of ECs, i.e., permissibility and tone, angiogenesis, ECs activation, and ECs injury. Figure 4.12 B shows three groups of comparison by scatter plots: random NFM (RNF) versus TCPS; aligned NFM (ANF) versus TCPS, and ANF versus RNF. Quantitative analysis of the scatter plot revealed similarities of 87.5%, 89.3%, and 94.6%, respectively. This means, for example, that 87.5% of the genes from HCAECs cultured on random NFM have an expression level similar to that on TCPS. So is for the other two. The results are further summarized in Table 4.6. It shows the functional maintenance of HCAECs on TCPS, and random and aligned NFM. RT-PCR analysis (Figure 4.12 C) was further performed to verify gene expression profile from the cDNA microarray. Three continuous spotted genes from the integrin family (integrin α5, integrin αV, and integrin β1) were chosen, highlighted by a red quadrangle in Figure 4.12A. The cDNA microarray results showed a clear pattern of higher expression levels of integrin α5 and integrin β1 compared with integrin αV. Accordingly, RT-PCR results (Figure 4.12 C) also displayed the highest expression level of integrin α5 amongst the 3 integrins. However integrin β1 and integrin αV seemed to have the same expression level.

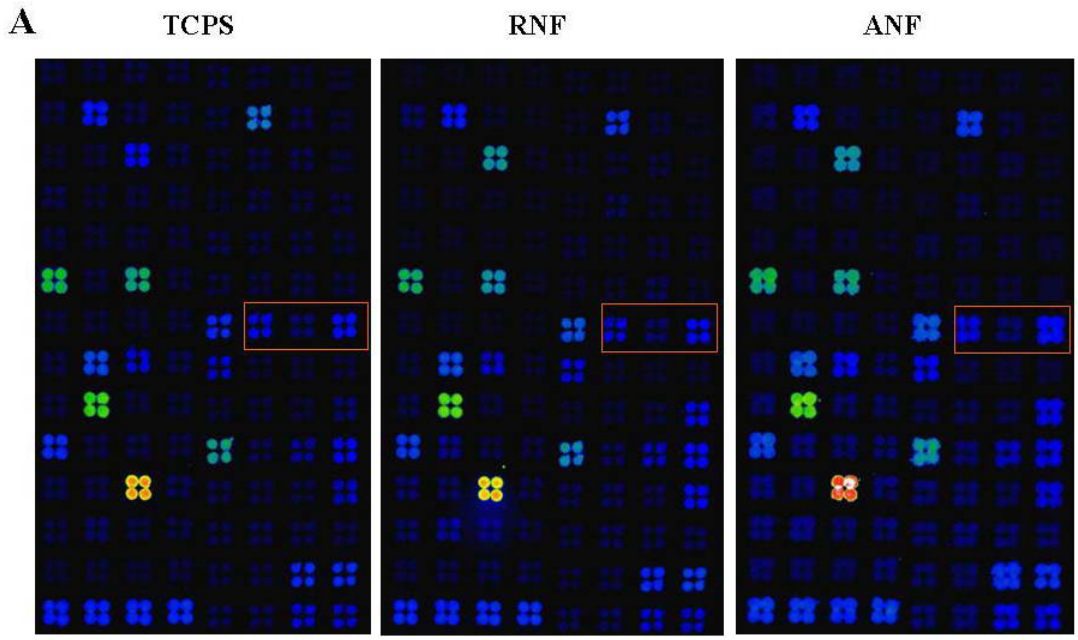
A
TCPS
RNF
ANF

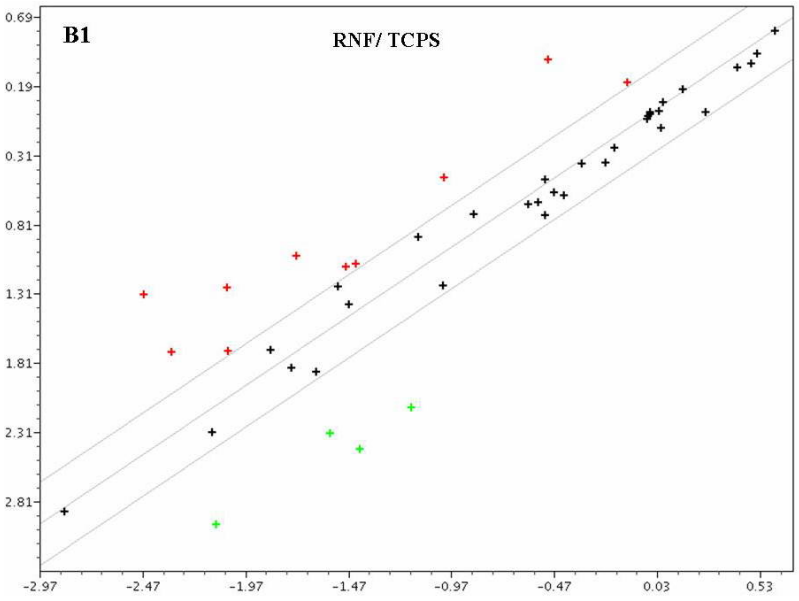
B1
RNF/ TCPS
0.69
0.19
0.31
0.81
1.31
1.81
2.31
2.81
-2.97
-2.47
-1.97
-1.47
-0.97
-0.47
0.03
0.53

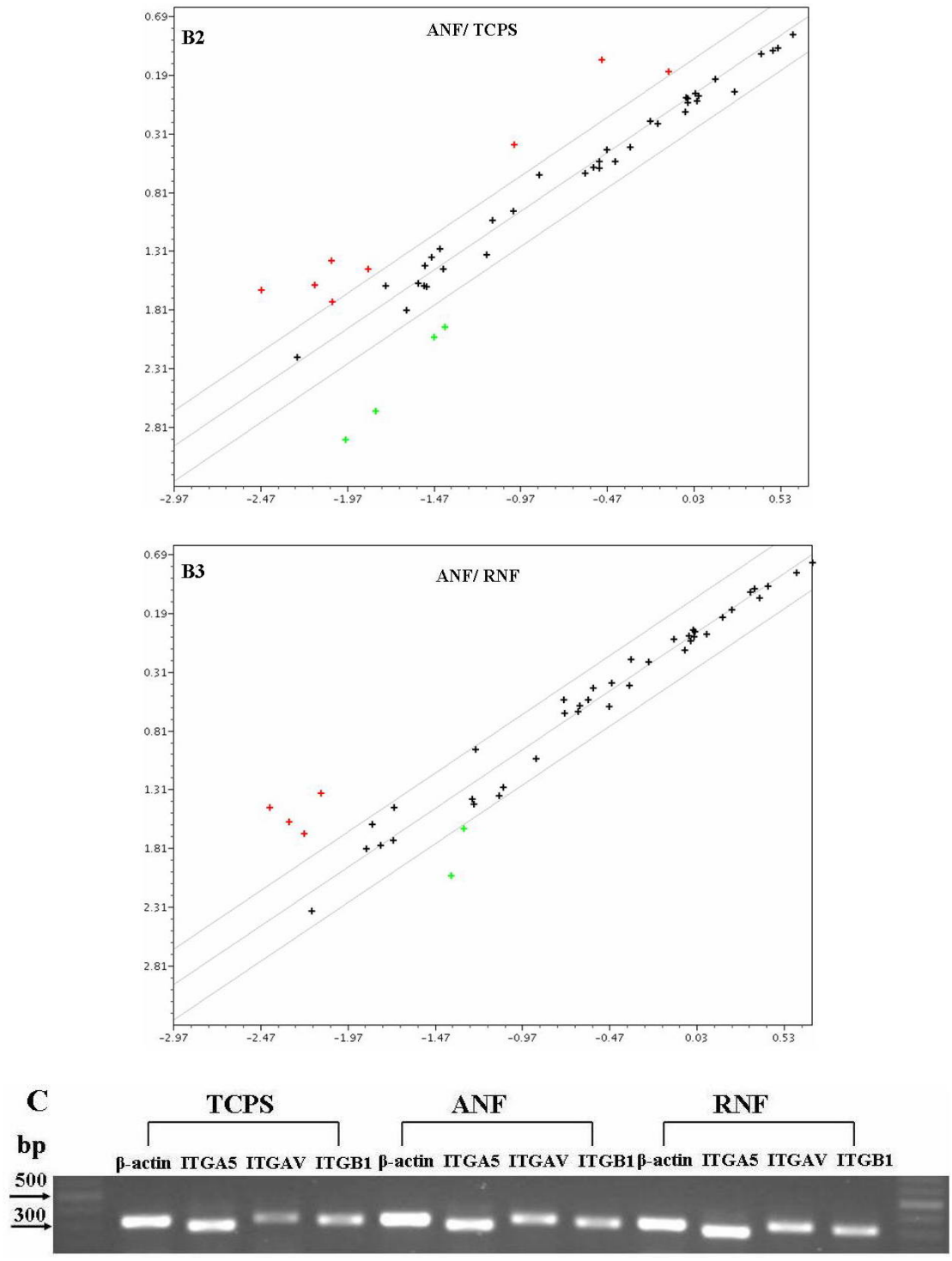

Figure 4.12. (A) Gene expression profiles of HCAECs on TCPS, random (RNF), and aligned (ANF) collagen-coated P(LLA-CL) NFM by cDNA microarray analysis. Expression of each gene is represented by the fluorescence of a tetra-spot. (B) Scatter plots showing the relative gene expression of (B1) RNT versus TCPS, (B2) ANF versus TCPS, and (B3) ANF versus RNF. (C). RT-PCR analysis of integrin α5 (ITGA5), αV (ITGAV), and β1 (ITGB1) expression from HCAECs cultured on TCPS, RNF, and ANF, which correlate to the genes in a red frame in (A).

Table 4.6. Percentage (%) of genes with over-expressed, similar-expressed, and less-expressed levels between HCAECs grown on TCPS, random (RNF) and aligned (ANF) collagen-coated P(LLA-CL) NFM

Comparison groups	Over-expressed genes	Genes with similar expression level	Less-expressed genes
RNF/TCPS	8.9	87.5	3.6
ANF/TCPS	7.1	89.3	3.6
ANF/RNF	3.6	94.6	1.8

4.3 Comparison between collagen-blended and collagen-coated NFM

The comparison between the two collagen-modified NFMs is summarized in Table 4.7. Both the collagen-coated and the collagen-blended NFM showed similarly improved ECs growth compared with the pure polymer NFM. However, the collagen-coated NFM has several advantages over the collagen blended NFM. First, the collagen coating process consumes less amount of collagen than the collagen blending process. It was found 25-50 times more collagen was used in the blending process than that was used in the coating process, which is a disadvantage for mass production of collagen-blended NFM. Second, collagen-coated NFM had higher mechanical properties compared with the collagen-blended NFM as is shown in Table 4.7. Third, as to collagen-blended NFM, the collagen must be dissolved in organic solvent (HFP) with the polymer prior to the electrospinning process (Matthews *et al*., 2002b), which may be a harsh environment for the collagen. In parallel, the collagen can be dissolved in aqueous solvent (HCl) in the coating process, which is a mild condition for collagen. Further, the batch difference of collagen will affect the viscosity and solubility of collagen solution which would affect the electrospinnability because electrospinning process is highly dependent on the

character of spin solution (Huang *et al*., 2003). However characteristics of collagen solution would not affect the coating process. For this reason, the repeatability of fabrication of collagen-coated NFM was much better than that of the collagen-blended NFM. Based on above reasons, collagen coating was used in the following study to modify the 3-D tubular nanofiber scaffolds.

Table 4.7. Comparison between the collagen-blended NFM and collagen-coated NFM

	Collagen blended NFM	Collagen coated NFM
Amount of collagen used	500 μg collagen in 1 mg NFM	10-20 μg collagen in 1 mg NFM
Mechanical properties	Tensile modulus, 26 MPa; tensile strength, 1.5 Mpa	Tensile Modulus, 44 MPa; tensile strength, 6.3 MPa
Organic solvent used	HFP	No
Cell behaviors	Spreading morphology, good viability and attachment, and preserved phenotype	Spreading morphology, good viability and attachment, and preserved phenotype
Others	Batch difference will affect collagen solubility in HFP	Batch difference won't affect collagen solubility in HCl

4.4 Conclusion

P(LLA-CL) NFM were treated by inductive coupled radiofrequency glow discharge plasma, followed by collagen coating. The collagen-coated P(LLA-CL) NFM displayed the features of ECM-like non-woven architecture, high porosity, proper mechanical properties, bioactive surface, and controllable fiber alignment. Collagen was found to be evenly coated throughout the surface of nanofibers.

Collagen coating improved the viability and attachment of HCAECs on P(LLA-CL) NFM. Immunostaining and RT-PCR analysis showed that HCAECs maintained the phenotypic expression of PECAM-1, fibronectin, and collagen IV. cDNA microarray analysis further indicated that HCAECs kept the expressions of 112 function-related genes. Particularly, aligned collagen-coated P(LLA-CL) NFM were constructed. The aligned NFM have higher mechanical strength and modulus than the random NFM. HCAECs grew along the direction of nanofiber alignment and showed elongated morphology.

Chapter 5

3-D Tubular Nanofiber Scaffolds

The works in chapter 3 and 4 achieved the flat P(LLA-CL) nanofiber meshes (NFM) with effective endothelialization. In order to approach the long-term goal of constructing blood vessel-like scaffolds, 3-D tubular nanofiber scaffolds should be fabricated. An attractive feature of electrospinning process is its ability to deposit nanofibers onto a rotational mandrel to get a tubular scaffold. In this chapter we studied fabrication of electrospun tubular nanofiber scaffolds and HCAECs seeding onto their lumens. Collagen coating technique developed in chapter 4 was used to surface modify the tubular nanofiber scaffolds. One big difference between ECs culturing on the flat NFM and the tubular nanofiber scaffolds is the cell seeding method. In this chapter, a special cell seeding technique was developed to seed cells evenly distributed onto the lumen of the scaffolds. Mechanical properties of the tubular nanofiber scaffolds and HCAECs' morphology and phenotypic maintenance were studied with commercialized ePTFE 3 mm vascular grafts as a control.

5.1 Materials and Methods

5.1.1 Materials

P(LLA-CL), collagen Type I (calf skin), and HCAECs were as same as those used in chapter 3 (see section 3.1.1). ePTFE (Gore-Tex®)3 mm vascular grafts were obtained from Professor Peter Ashley Robless, a vascular surgeon of National University of Hospital in Singapore.

5.1.2 Fabrication of P(LLA-CL) tubular nanofiber scaffolds

For electrospinning of the P(LLA-CL 70:30) tubular nanofiber scaffolds, P(LLA-CL) (10 wt%) solution in DCM and DMF (70:30 wt:wt) was added into a plastic syringe with a needle (inner diameter, 0.21 mm). With the aid of a syringe pump, the solution was injected out at the feed-rate of 1 mL/h. Electrospinning voltage was applied to the needle at 10 kV using a high voltage power supply (Gamma High Voltage Research, USA). The nanofibers were collected onto a rotating metallic mandrel (3 mm in outer diameter, 12 cm in length) at the speed of 150 rpm. The electrospinning setup is shown in Figure 5.1. SEM micrographs of the tubular scaffold were obtained on a FEI Quanta 200F SEM (Japan). Collagen was coated onto surface of nanofibers in a method reported in chapter 4 (see section 4.1.3). Briefly, P(LLA-CL) tubular nanofiber scaffolds were treated by air plasma to increase the hydrophilicity. The 3-D tubular nanofiber scaffolds were treated for a longer time (15 min) than the nanofiber meshes (5 min). The plasma-treated scaffolds were then immersed in a collagen solution with a concentration of 290 μg/mL at 4^{o}C overnight, and then were dried at room temperature.

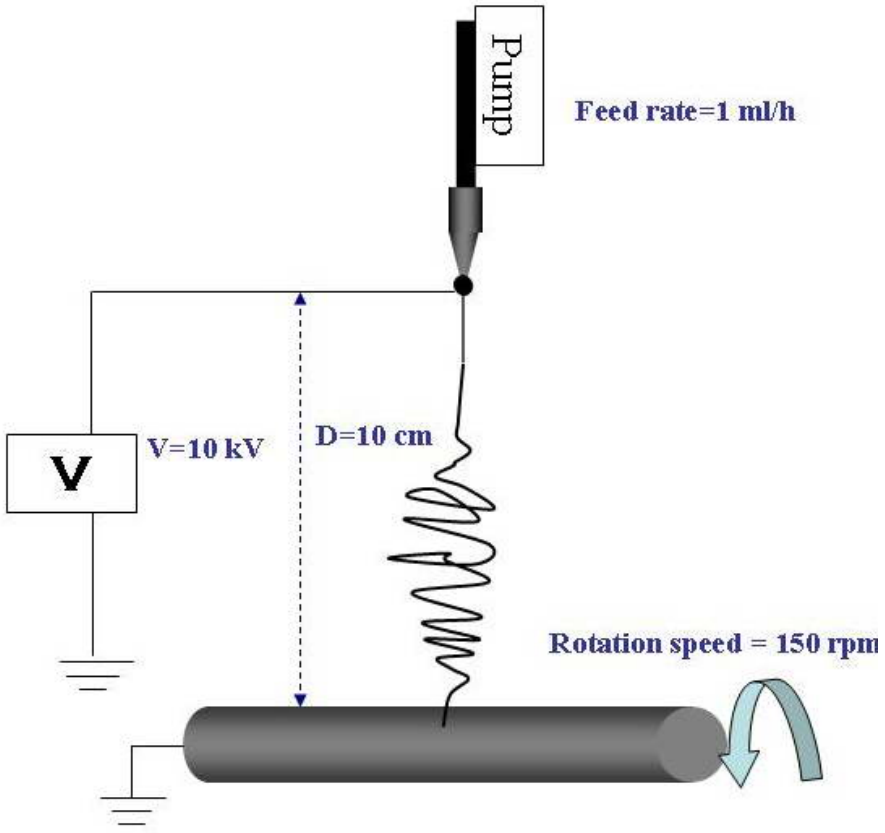

(A)

(B)

Figure 5.1. (A) Setup and operation parameters for fabrication of the P(LLA-CL) tubular nanofiber scaffolds. (B) The electrospun tubular nanofiber scaffold collected on the mandrel.

5.1.3 Mechanical properties

Tensile tests were carried using a 5848 microtester (Instrom, Canton, MA) at a stroke rate of 3 mm/min with a 5 mm gauge length. The collagen-coated P(LLA-CL)

tubular nanofiber scaffolds were unfolded and prepared in a rectangular (5 × 5 mm) shape for the tensile test in both circumferential and longitudinal directions.

5.1.4 Cellular behaviors characterization

5.1.4.1 Rotational cell seeding

HCAECs suspension to be seeded into the lumen of the tubular scaffolds was prepared first. To determine the cell suspension concentration, the following method was used. The desired seeding density of HCAECs onto the lumen surface of the scaffolds is 4×10^4 cellls/cm^2, which is about 80% of the confluence density (5×10^4 cellls/cm^2). So the cell suspension concentration can be calculated by the following equation.

$$V(cm^3) \times Conc(cells/cm^3) = A(cm^2) \times 4 \times 10^4 (cells/cm^2)$$

Where V is the volume of the tubular nanofiber scaffold and A is the lumen area of the scaffold. For the tubular nanofiber scaffolds with length of 3 cm and inner diameter of 3 mm, A is $\pi \times 3$ mm $\times$ 3 cm = 2.8 cm^2 and V is $\pi \times (1.5 \text{ mm})^2 \times 3$ cm = 0.2 cm^3. Thus seeding concentration (*Conc*) was calculated to be 6×10^5 cells/cm^3 based on the above equation. The suspension of HCAECs at this concentration was injected into the collagen-coated P(LLA-CL) tubular nanofiber scaffolds, the ends of which were connected to PTFE tubes. Because of the high hydrophobicity of PTFE tubes, the HCAECs suspension was limited in the lumen of the tubular nanofiber scaffolds. The cells-scaffold constructs were rotated at the speed of 6 rpm for 4 h, and

then taken out and cultured in a normal static environment. On day 1, 5, 7, and 10 after culture, the HCAECs-scaffolds constructs were taken out for morphology and phenotype studies. The schematic representation of HCAECs seeding is shown in Figure 5.2. HCAECs culture and morphology studies by SEM were the same as described in chapter 3 (see section 3.1.4.1 and 3.1.4.2).

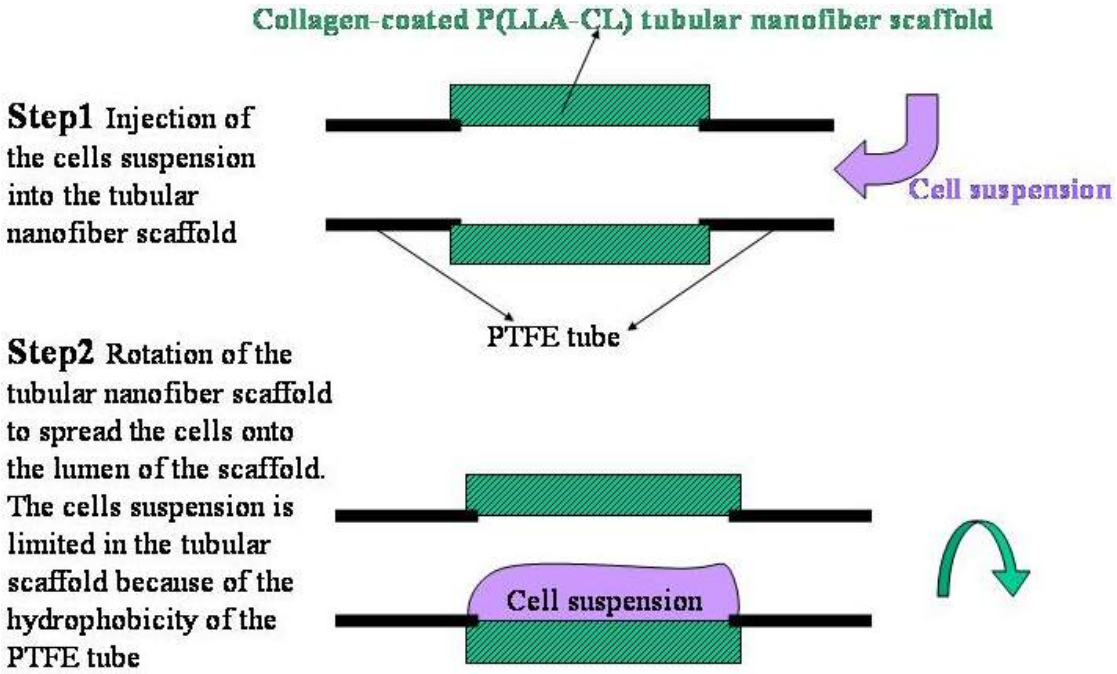

Figure 5.2. Schematic illustration of HCAECs seeding onto the lumen of the collagen-coated P(LLA-CL) tubular nanofiber scaffold.

5.1.4.2 Hematoxylin & Eosin (H&E) staining

After 10% formalin fixation, ethanol dehydration, and toluene immersion, the HCAECs-scaffold constructs cultured for 10 days were embedded in the paraffin by the Leica EG 1160 tissue embedding center (Leica, Germany). The paraffin-embedded constructs were cross-sectioned by the microtome (Leica RM2135,

Germany) into slices with 10 μm in thickness. After de-paraffinization in xylene and rehydrate in ethanol, the slices were stained with Hematoxyline (Sigma, USA) for 70 seconds and Eosin (Sigma, USA) for another 10 seconds. The slices were mounted onto glassslides and observed under optical microscope.

5.1.4.3 Immunostaining

For immunostainning, the de-paraffinized slices were immersed into 1 × PBS for half an hour then blocked by 2% BSA. The slices were then incubated for 2 h at 37^{o}C with primary antibody (mouse anti-human Platelet Endothelial Cell Adhesion Molecule-1 (PECAM-1, CD 31)) (Cymbus Biotechnology, UK) diluted at 1:50. After washing, fluorescein isothiocyanate (FITC) labeled rabbit anti-mouse IgG (Chemicon, USA) diluted at 1:50 was added and incubated for 2 h at 37 ^{o}C. The immunostained slices were then mounted onto glassslides with FluorSave™ reagent (Calibiochem, Germany), and viewed under LSCM.

5.2 Results and discussions

5.2.1 Material characterization

5.2.1.1 Morphology

Collagen-coated P(LLA-CL) tubular nanofiber scaffolds with inner diameter of 3 mm and wall thickness of about 100 μm were fabricated from 2 h electrospining at the condition shown in Figure 5.1. Length and inner diameter of the scaffolds can be readily adjusted by choosing mandrel with different sizes to collect nanofibers. In our lab, tubular nanofiber scaffolds with length up to 8 cm and inner diameter in the range of 1-6 mm have been successfully fabricated. Wall thickness of the tubular nanofiber scaffolds can be controlled by electrospinning time at the rough relationship of 50-60 μm/h.

Morphology of the collagen-coated P(LLA-CL) tubular nanofiber scaffolds (Figure 5.3) were compared with that of the commercialized ePTFE 3 mm vascular grafts (Figure 5.4) for macroscopic and microscopic structure analysis. ePTFE vascular grafts are generally recognized as the gold standard for vascular surgeries in medium-diameter (inner diameter 6-12 mm) blood vessel replacements and have a 5 year patency rate of 91-95% in aortic sites (Pourdeyhimi, 1986). However, synthetic vascular grafts, including ePTFE, have rarely been proved successful in small-diameter blood vessel replacement (inner diameter < 6 mm) (Seal *et al.*, 2001).

For macroscopic structures, the tubular nanofiber scaffold showed the same length and inner diameter as the EPTFE® vascular graft (Figure 5.3 and 5.4 a and b). The ePTFE vascular graft was thicker in wall than the tubular nanofiber scaffold (Figure 5.3 and 5.4 d). For microscopic structures, there were some differences. First, the inner surface of the ePTFE vascular graft is composed of relatively large and

circumferentially orientated nodes from which extend fine longitudinal fibrils at the nanometer scale (Figure 5.4 e), whereas the inner surface of the tubular nanofiber scaffold was only composed of nanofiber network (Figure 5.3 e). This indicates that both grafts had nanoscale fibers at similar dimensional scale, which may increase the surface area for cell attachment. Second, the tubular nanofiber scaffold has interconnected pores in the whole structure (Figure 5.3 f), whereas the ePTFE vascular graft is not porous in the outer layer (Figure 5.4 f). To make it clearer, major properties such as inner diameter, wall thickness, pore size, and fabrication methods of the ePTFE vascular grafts and tubular nanofiber scaffolds are summarized in Table 5.1.

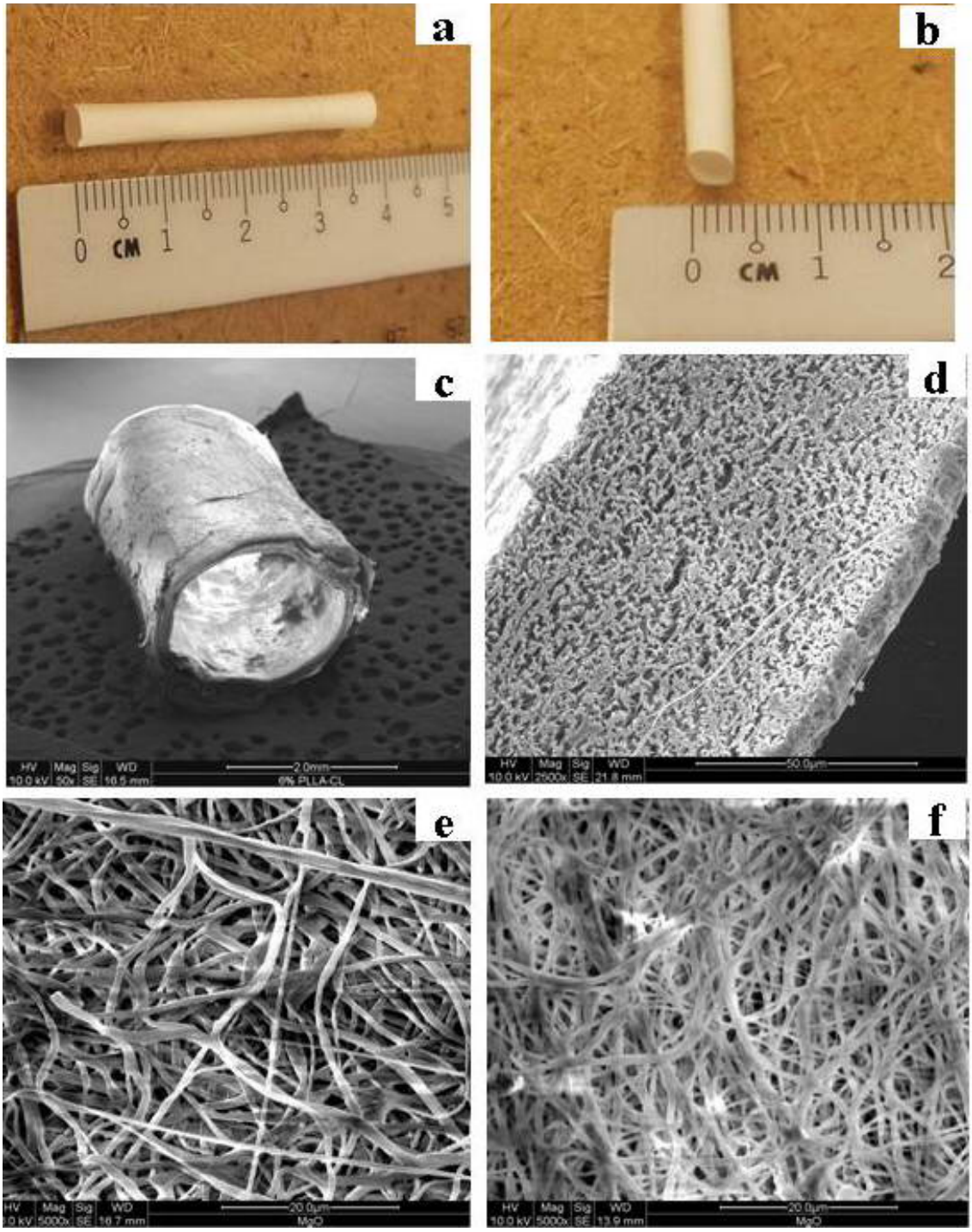

Figure 5.3. Macroscopic and microscopic structures of the collagen-coated P(LLA-CL) tubular nanofiber scaffolds . (a, b) optical images of macroscopic structures. (c, d, e, f) SEM photographs: (c) whole structure; (d) enlarged cross-section of wall; (e) inner layer; (f) out layer. Original magnification: × 50, × 2500, × 5000, × 5000 for c, d, e, f, respectively.

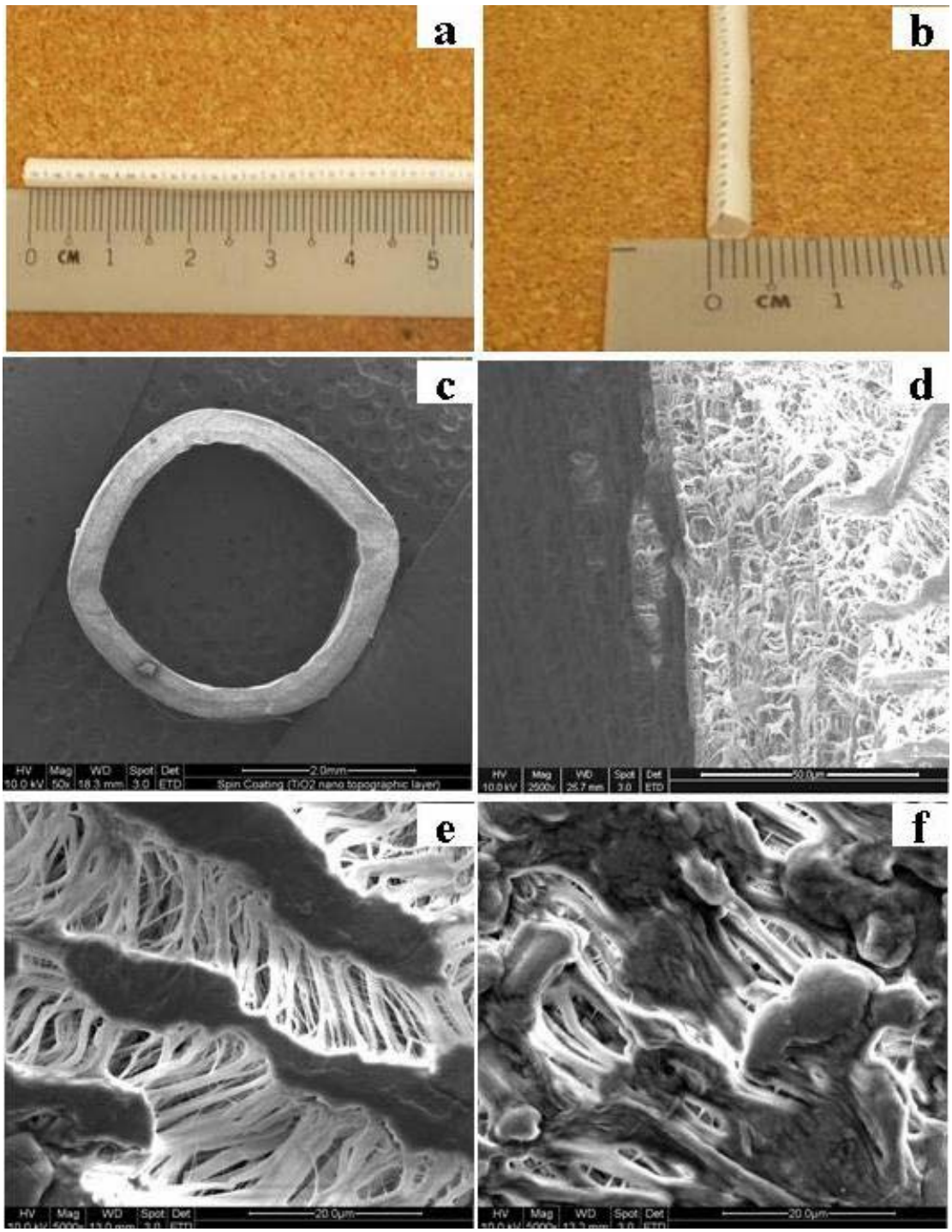

Figure 5.4. Macroscopic and microscopic structures of the ePTFE vascular grafts. (a, b) optical images of macroscopic structures. (c, d, e, f) SEM photographs: (c) cross section; (d) enlarged cross-section of wall; (e) inner layer; (f) out layer.

Table 5.1. Comparison between the ePTFE vascular grafts and the tubular nanofiber scaffolds in terms of inner diameter, wall thickness, pore size, and fabrication methods

Vascular Grafts	Inner Diameter (mm)	Wall thickness (mm)	Pore size (μm)	Fabrication Methods
Tubular nanofiber scaffold: collagen-coated P(LLA-CL)	3 mm	Controllable	Around 5 μm	Polymer is dissolved in organic solvent and then is electrospun into nanofibers
Gore-Tex®: ePTFE	3 mm	0.3-0.5	10-30 μm (Pourdeyhimi, 1986)	Materials are initially produced as a non-porous film and subsequently stretched to produce micro-porous structures (Pourdeyhimi, 1986)

One distinct character of the collagen-coated P(LLA-CL) tubular nanofiber scaffolds compared with the ePTFE vascular grafts is biodegradability. ePTFE vascular grafts are non-biodegradable. Nowadays it is generally believed that a biodegradable graft is superior to a non-biodegradable graft because scaffold that degrades over time will allow natural tissue in-growth and healing in time. Also a biodegradable graft can reduce the possibility of infection from a non-biodegradable graft due to shorter existence in human body. Thus it could be the trend for the replacement of biodegradable grafts for the current commercially available non-biodegradable grafts.

5.2.1.2 Surface chemistry

To visualize spatial distribution of the collagen coated on the P(LLA-CL) tubular nanofiber scaffolds, rhodamine-labeled collagen was coated onto the tubular scaffolds and observed under laser scanning confocal microscope (LSCM). Figure 5.5 (left) is the picture of 3-D reconstruction of surface part of the tubular nanofiber scaffold. It shows clearly that collagen was uniformly coated on the surface of nanofibers in a larger magnification image (Figure 5.5 right), which correlated with the results in chapter 4 (Figure 4.5). This implies that plasma treatment was not only effective for modifying the flat nanofiber meshes but also the 3-D tubular nanofiber scaffolds. There was no auto-fluorescence observed on the P(LLA-CL) tubular nanofiber scaffolds without collagen-coating under LSCM (data not shown).

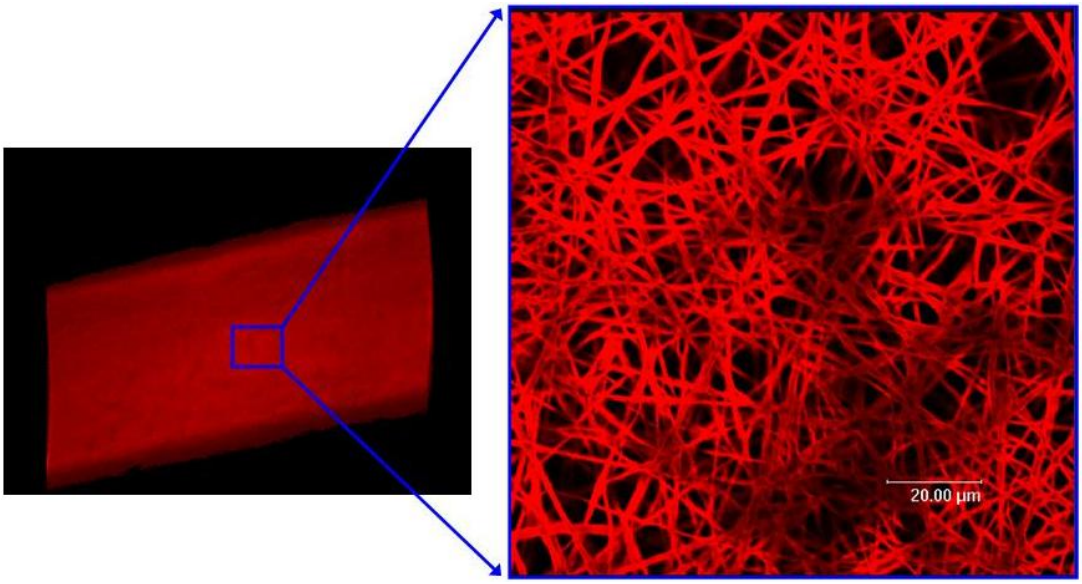

Figure 5.5. (Left) 3-D LSCM (original magnification, × 600) image of the collagen-coated P(LLA-CL) tubular nanofiber scaffolds. (Right) Enlarged LSCM image of the frame in (A). Rhodamine-labeled collagen was identified by its red fluorescence.

5.2.1.3 Mechanical properties

Vascular grafts should have enough strength to resist rupture or excessive dilation when subjected to pulsatile pressure *in vivo*. They should also have stable mechanical properties during their expected life time. Although it is generally accepted that mechanical properties of vascular grafts should match those of natural blood vessels, current commonly used commercialized vascular grafts made from PET and PTFE have much stronger mechanical properties than that of aortic tissues (How, 1992). Figure 5.6 shows the typical stress-strain curves of the collagen-coated P(LLA-CL) tubular nanofiber scaffolds in both circumferential and longitudinal directions. The results suggested that tensile strength at the longitudinal direction was larger than that at the circumferential direction. The ultimate strain in both directions was similar to each other. Tensile properties of the tubular nanofiber scaffolds are further summarized in Table 5.2. Particularly, the longitudinal and circumferential tensile strength of the tubular nanofiber scaffolds were compared with that of the Teflon® (TF-208), another kind of commercialized vascular graft, and natural abdominal aorta, results of which are shown in Table 5.3. We could not find the detailed mechanical properties of the ePTFE (Gore-Tex®)3 mm vascular graft, thus Teflon® (TF-208), which is also made from ePTFE, was used for comparison. It can be found that tensile properties of the tubular nanofiber scaffolds were closer to that of the natural human artery than the Teflon® (TF-208).

It was reported that larger anisotropic property (defined as the ratio of

circumferential tensile strength to the longitudinal tensile strength) of the tubular nanofiber grafts was noticed at mandrel rotation speed of 150 rpm compared with that at the speed of 3400 rpm (Matsuda *et al.*, 2005). This may indicate that fiber orientation induced by the mandrel rotation of a fiber might affect the anisotropic mechanical properties of a graft wall. Our results were consistent with the above studies regarding to the point of larger tensile stress in the longitudinal direction than the circumferential direction at the mandrel rotational speed of 150 rpm.

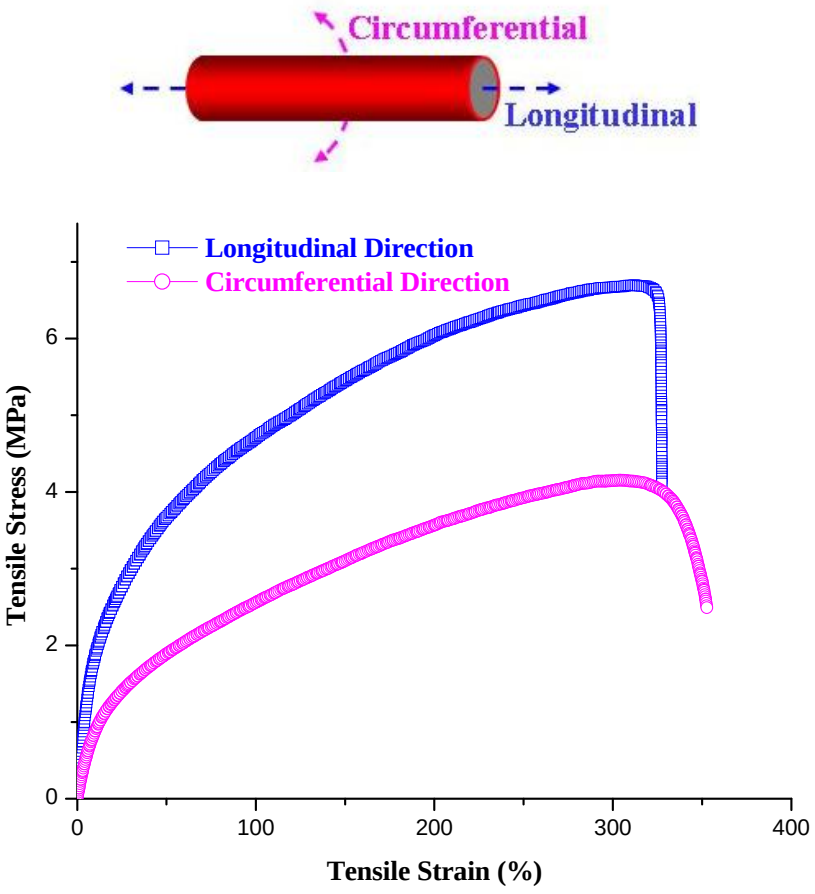

Figure 5.6. Typical uniaxial stress-strain curves for the collagen-coated P(LLA-CL) tubular nanofiber scaffolds under tensile loading in longitudinal and circumferential directions.

Table 5.2. Tensile properties of the collagen-coated P(LLA-CL) tubular nanofiber scaffolds in both longitudinal and circumferential directions[a]

	Longitudinal direction	**Circumferential direction**
Tensile modulus (MPa)	16 ± 7	17 ± 4.4
Tensile strength (MPa)	7.0 ± 0.4	3.9 ± 0.3
Ultimate strain (%)	289 ± 55	292 ± 87

[a]Data is representative of 3 independent experiments and represented as mean ± SD (n=3)

Table 5.3. Longitudinal and circumferential tensile strength of the tubular nanofiber scaffolds, Teflon® (TF-208), and natural abdominal aorta

Materials	**Longitudinal directions (MPa)**	**Circumferential directions (MPa)**
Tubular nanofiber scaffolds	7.0	3.9
Teflon® (TF-208) (How, 1992)	85.2	66.7
Abdominal aorta (How, 1992)	1.47	5.29

5.2.2 Characterization of cellular behaviors

5.2.2.1 Morphology and phenotype

HCAECs were seeded into the lumen of the collagen-coated P(LLA-CL) tubular nanofiber scaffolds connected in a customized seeding device at a speed of 6 rpm for 4 h. By optical microscope observation, there was neglected number of cells

remained in the cell suspension after seeding. So the cell seeding efficiency, which is defined as the percentage of attached cells of the total seeded cells, can be assumed to be 100% after the 4 h rotational seeding. Then the cells-scaffolds constructs were put into an incubator for further static culture after the rotational seeding. On day 1, 5, and 7 the HCAECs-scaffolds constructs were taken out for morphology studies (Figure 5.7), and for phenotype studies on day 10 (Figure 5.8). For SEM studies of HCAECs morphology on the lumen of the tubular nanofiber scaffolds, the HCAECs-scaffold constructs were cut open into flat meshes to expose the lumen side for direct SEM observations (Figure 5.7). It was found that seeded at 80% of confluence density, HCAECs grew into sub-confluence immediately in 1 day's time (Figure 5.7a and b). Further, HCAECs spread well and evenly on the lumen of the tubular nanofiber scaffolds from day 1 onwards to day 7 after culture. These results indicated that the tubular nanofiber scaffolds facilitated quick and stable *in vitro* endothelialization. There are still gaps between cells indicating cells have yet reached confluence which could be readily improved by using a higher concentration of cell suspension for seeding.

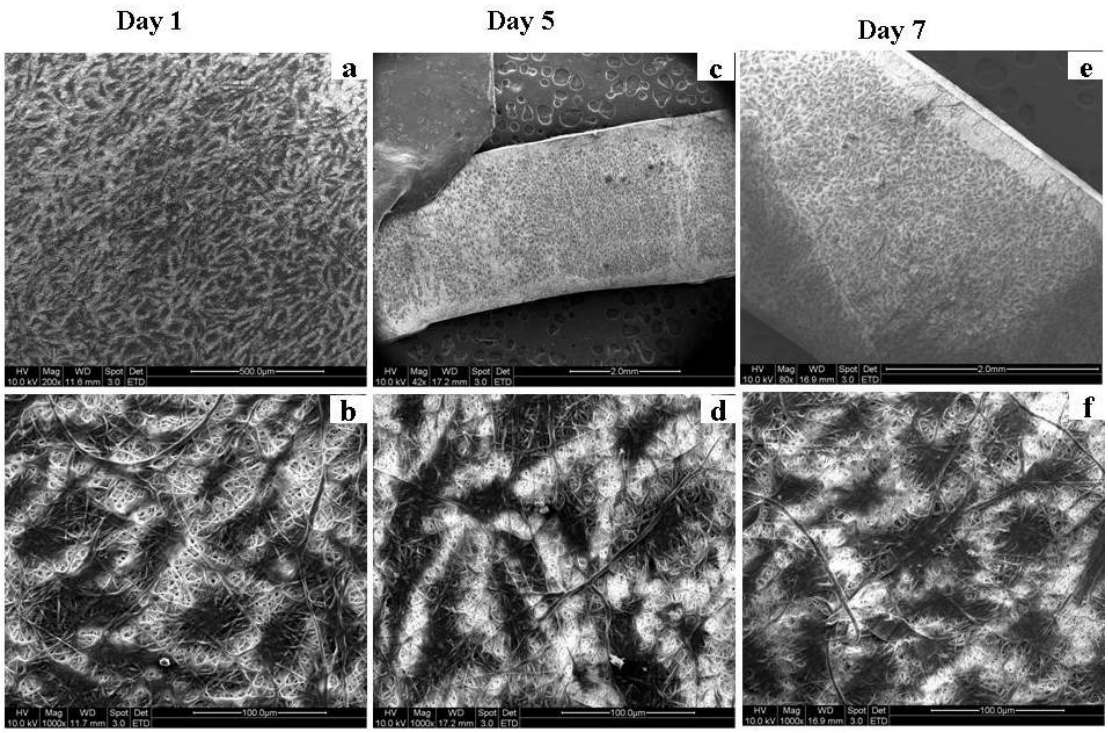

Figure 5.7. HCAECs grew on the lumen of the tubular nanofiber scaffolds for 1 day (a and b), 5 days (c and d), and 7 days (e and f) after seeding at the density of 6×10^5 cells/cm^3. (b, d, and f): higher magnification images of (a, c, and e) respectively. Original magnification: a, × 200, c, × 42, e, × 80, b, d and f, × 1000.

Figure 5.8 further revealed that HCAECs existed as a thin layer covering the lumen of the tubular nanofiber scaffolds (Figure 5.8 b) and there was no cells infiltration in the scaffolds (Figure 5.8 c) after 10 days' culture. Further, HCAECs possessed the phenotypic expression of PECAM-1(Figure 5.8 d), indicating no de-differentiation of ECs occurred. On the control group, the ePTFE vascular grafts, there were no HCAECs found from day 1 onwards after the rotational seeding of HCAECs (data not shown). Although successfully used as large and medium size vascular grafts, ePTFE vascular grafts did not favor ECs growth because of negative surface charge, which is an important property against platelet deposition but also obstruct the negatively charged ECs from accessing graft surface (Xue.L, 2000).

It needs to be noticed that SMCs and fibroblasts, another two types of vascular cells, grow as multi-layers on the media and adventitia of blood vessels, which is different from mono-layer growth of ECs in the intima. To encourage the infiltration of SMCs and fibroblasts, an approach is to electrospray the cells during electrospinning process. It has been reported that after electrospraying, vascular smooth muscle cells remained their viability and proliferation compared with the unprocessed cells (Stankus *et al.*, 2006).

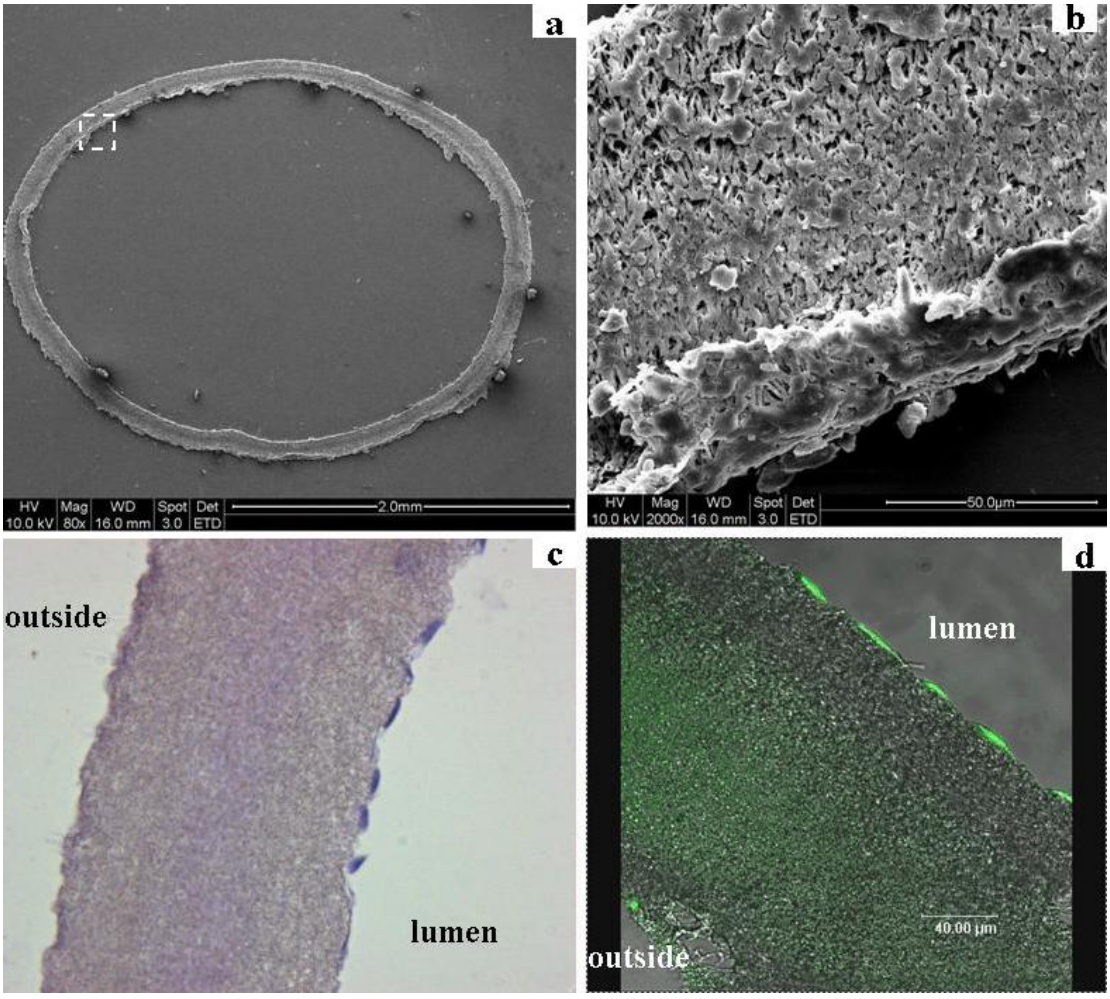

Figure 5.8. HCAECs grew on the lumen of the tubular nanofiber scaffolds for 10 days after seeding. (a, b) SEM images showing the overall structure of the HCAECs-scaffold constructs: (a) cross-section of wall of the constructs; (b) enlarged quadrangle in (a). (c) H&E staining of the cross-section of the constructs. (d) Immunostaining of PECAM-1 from HCAECs on the lumen of the tubular nanofiber scaffolds. Original magnification: a, × 80, b, × 2000, c, × 200, d, × 630.

The good HCAECs attachment on lumen of the tubular nanofiber scaffolds may be due to two important cues presented by the scaffolds: 1). physical cues of high porosity, high spatial interconnectivity, and high surface area to volume ratio for cells attachment; 2). chemical cues of collagen, which is the main type of collagen in connective tissue and is present throughout the arterial wall. Study in chapter 4 have already shown that collagen-coating improved spreading, viability, and attachment of HCAECs on the pure P(LLA-CL) NFM. Because of co-existence of the two cues, tubular nanofiber scaffolds provide ECs an environment similar as the basement membrane where ECs grow above in a natural condition.

5.3 Conclusion

3-D P(LLA-CL) tubular nanofiber scaffolds (inner diameter 3 mm) were fabricated by electrospinning onto a rotating metallic mandrel. Collagen was coated onto the scaffolds after air plasma treatment. Tensile properties of the tubular nanofiber scaffold were closer to that of the natural human arteries compared with the ePTFE vascular grafts. HCAECs were seeded onto the lumen of the scaffolds and rotated at the speed of 6 rpm for 4 h, followed by normal static culture. It was found that HCAECs spread evenly on the lumen of the P(LLA-CL) tubular nanofiber scaffolds and reached sub-confluence immediately after seeding. After 10 day's culture, HCAECs possessed the phenotypic expression of PECAM-1 and existed as a thin layer covering the lumen of the scaffolds. On the ePTFE vascular grafts, there

were no HCAECs present after rotational seeding of HCAECs onto lumen of the grafts.

Chapter 6

In Vivo Rabbit Model

The works in chapter 5 achieved tubular nanofiber scaffolds with good attachment and phenotypic maintenance of ECs *in vitro*. However, there are several concerns from vascular surgeons' point of views regarding the feasibility of the tubular nanofiber scaffolds to be used as tissue engineered vascular grafts *in vivo*. For example, are the tubular nanofiber scaffolds easy to be connected with natural blood vessels by suturing? Will blood leak from the porous nanofiber scaffolds after implantation? In order to answer these basic questions, in this chapter, an animal model which can test the feasibility and in *vivo* patency of the tubular nanofiber scaffolds was established, and short-term (7 weeks) implantation of the tubular nanofiber scaffolds into the animal model was evaluated. We chose a well-established and reliable flap, the rabbit epigastric flap, as the animal model because thrombogenically, the rabbit resembles the human more closely than does the rat. The viability of a rabbit epigastric free flap has been described as a good indicator of vascular graft patency (Terada *et al.,* 1999). As an initial study, ECs-seeded tubular nanofiber scaffolds were not used for the implantation. It is hoped that with the advanced development in autologous ECs extraction technique, results from the non ECs-seeded tubular nanofiber scaffolds could demonstrate the basic possibility for further study using ECs-seeded scaffolds.

6.1 Materials and methods

The rabbit epigastric free flap model has been approved from the Institutional Animal Care and Use Committee (IACUC) of National University of Singapore. All animals received humane care in compliance with the "Guide for the Care and Use of Laboratory Animals" published by the National Institutes of Health (NIHpublication no. 85-23, revised 1985).

Male New Zealand white rabbits (n=3) were operated on under sterile conditions and general anaesthesia with a halothane/oxygen mixture (2.5%) at 2 L/min using a standard anaesthetic machine after induction with intramuscular ketamine/xylazine at 35/5 mg/kg. After shaving and prepping, an epigastric flap measuring 2 × 2 cm was outlined on the rabbit's lower abdomen. Using an operating microscope, the flap was raised and the pedicle consisting of the inferior superficial epigastric vein, which is shown in Figure 6.1, was exposed and dissected to its origin from the superficial femoral vessels. The flap was completely detached and a segment of the venous pedicle of 1 cm in lengths was completely excised and replaced with the tubular nanofiber scaffold, which is shown in Figure 6.2. The inner diameter of the tubular scaffolds was 1 mm to match the size of the veins. End-to-end anastomosis was performed with 9-0 nylon using interrupted sutures. Once the anastomosis was completed, the microvascular clamp was released and flap perfusion was observed. The skin portion was closed with 4-0 Prolene running suture. The flap was then covered with Opsite spray to help prevent self-mutilation. Antibiotics

(cephalexin 500 mg/day) was administered in the drinking water postoperatively for 7 days. Flap was also checked daily for signs of ischaemia and/or venous congestion or infection. The rabbits were housed singly after surgery and received human care in compliance with the guidelines from National University of Singapore for the care and use of laboratory animals. At 7 weeks post procedure, the rabbits were anaesthetized using the same procedure and the tubular nanofiber scaffolds were explanted for histological analysis.

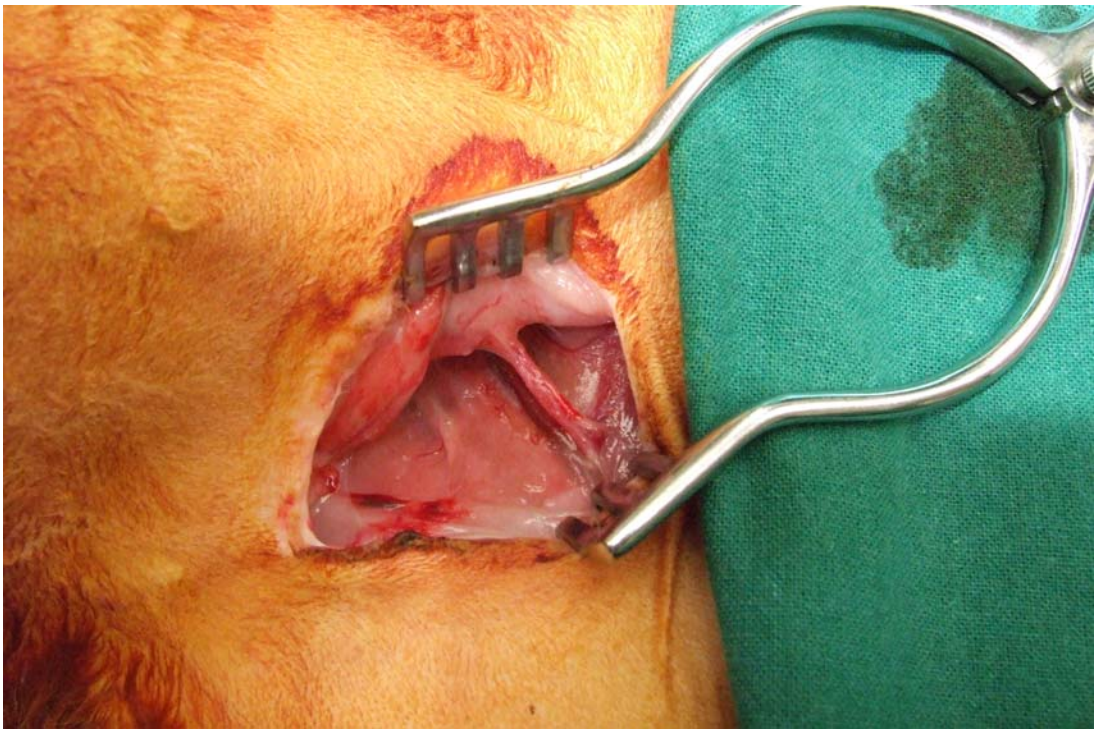

Figure 6.1 Image of the exposed inferior superficial epigastric vein in the rabbit model.

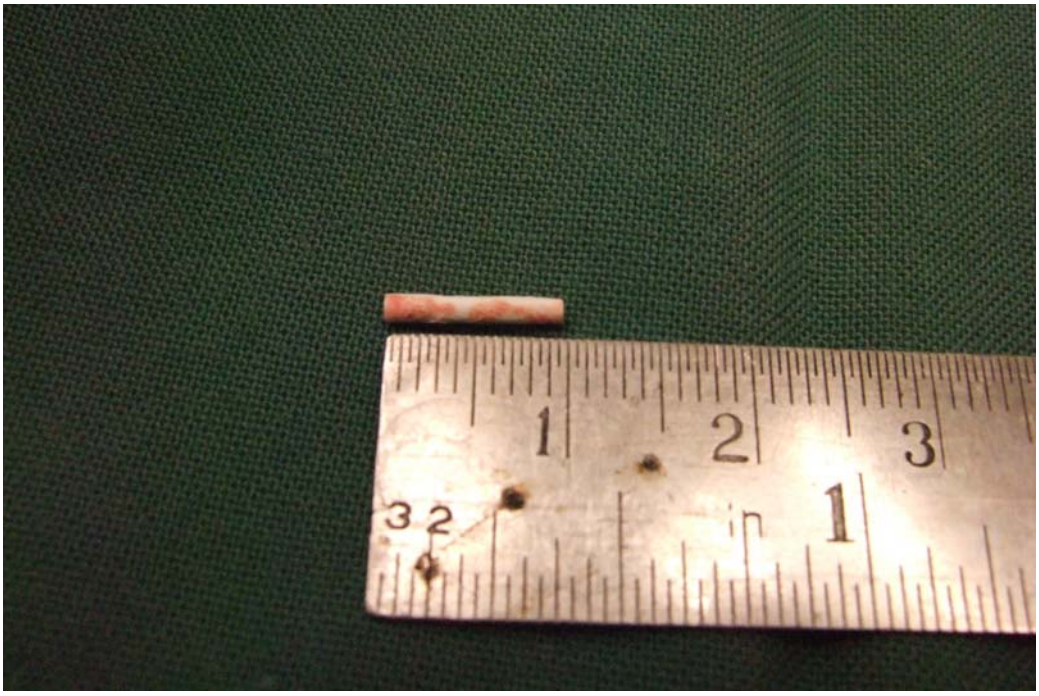

Figure 6.2. Image of the P(LLA-CL) tubular nanofiber scaffold (length: 1 cm, inner diameter: 1 mm) before implantation.

6.2 Results and discussion

Without ECs covering, collagen might be a thrombogenic surface, being adhesive to other types of cells like platelets. Thus, pure P(LLA-CL) tubular nanofiber scaffolds without collagen coating and without ECs seeding were implanted into the rabbit model to replace the 1 cm segments of the excised inferior superficial epigastric veins (Figure 6.3). The implantation showed that the tubular nanofiber scaffolds are suturable, and did not show dehiscence at the anastomosis or blood leaking from the inside of the scaffolds. As a porous material with a possibility of blood leaking, nanofiber meshes were reported to be able to stop the filtration of micro-particles with 1 μm in diameter (Gopal et al., 2006). Therefore being larger than 1 μm, blood cells which include red blood cells, white blood cells, and platelets

would not leak from the scaffolds. Plus, adhesions of plasma (cell free serum in blood) proteins to the lumen surfaces of the tubular scaffolds may further prevent the infiltration of blood cells.

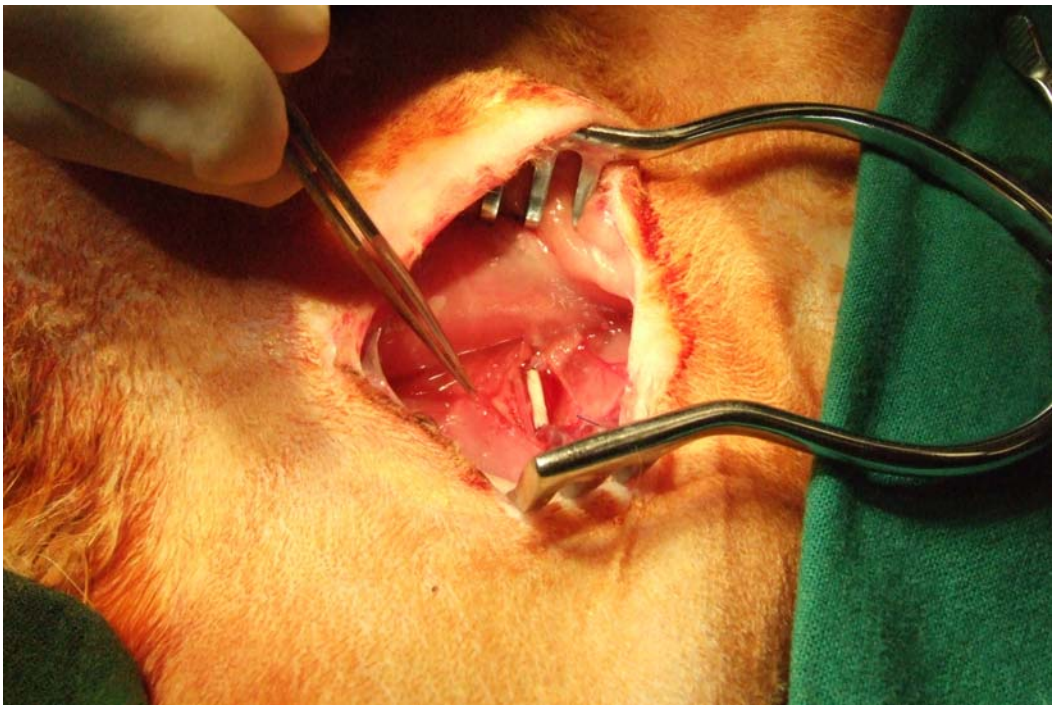

Figure 6.3. Image of the replacement of the inferior superficial epigastric vein with the P(LLA-CL) tubular nanofiber scaffold.

After 7 weeks' implantation into the rabbit model, the tubular nanofiber scaffolds were explanted for macroscopic structure and histochemical analysis. First, macroscopically, the explanted scaffolds kept the structure integrity and no deformation was found, which correlated with our observation from *in vitro* biodegradation study of the electrospun P(LLA-CL) NFM: no weight loss or morphology change for the NFM immersed in 1 × PBS for 3 month at 37 ^{o}C (Figure 6.4 c and d). The P(LLA-CL) NFM did not lost the total weight and structure integrity until 8 months later. It was found that most of nanofibers broke into small

segments of fibers (Figure 6.4 e and f) probably because the materials became more brittle, resulting in very poor handability of the P(LLA-CL) NFM.

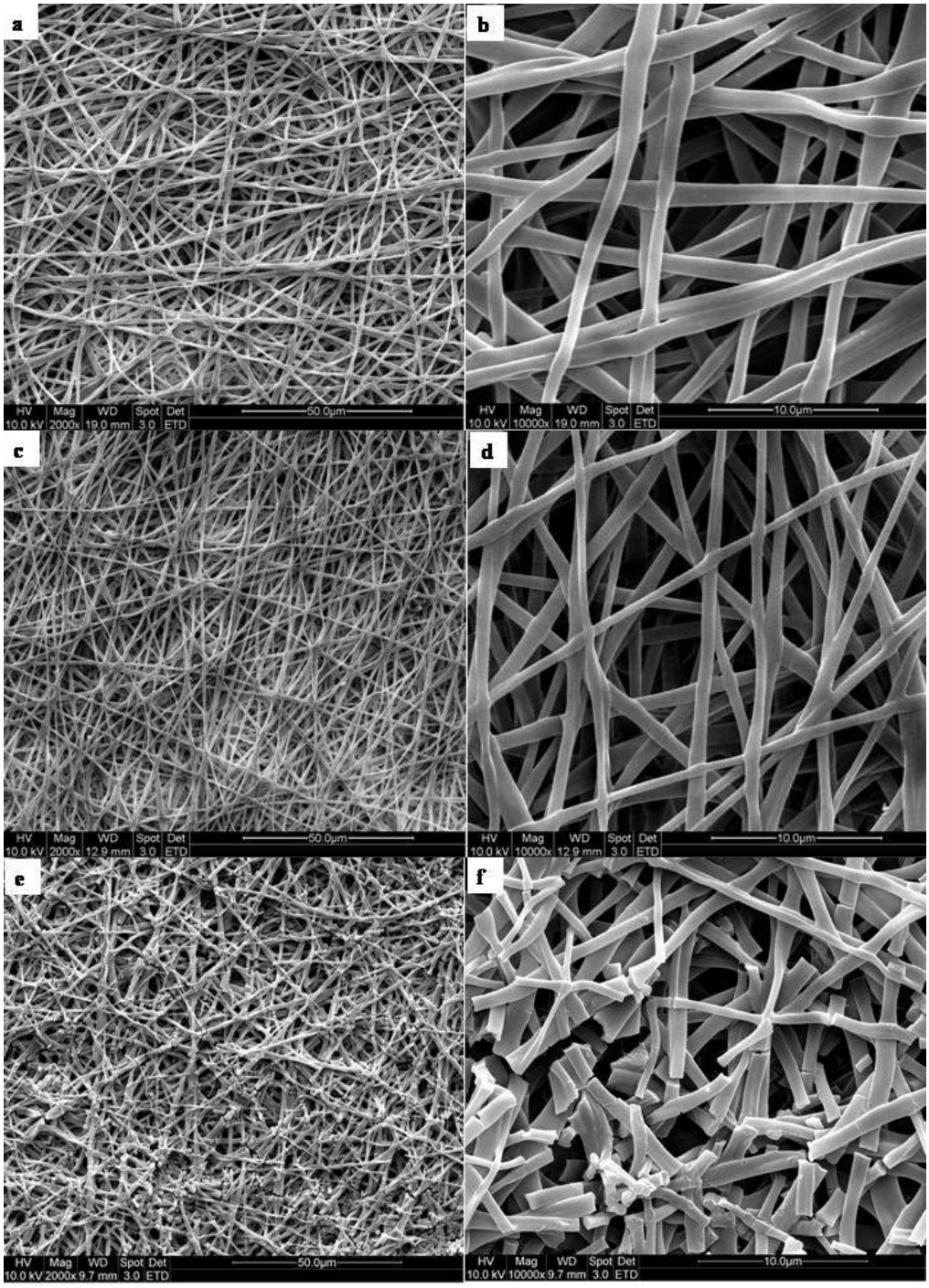

Figure 6.4. SEM images showing morphology of the P(LLA-CL) NFM biodegraded in 1 × PBS at 37 ^{o}C for (a and b) 0 month, (c and d) 3 month, and (e and f) 8 month. (b, d, and f) are magnified images of (a, c, and e) respectively.

Second, H&E staining from the oblique-section of the paraffin-embedded tubular nanofiber scaffolds revealed a thick fibrous tissue, indicating a natural host-tissue foreign body response towards the scaffolds, around the scaffolds but no cell infiltration was found (Figure 6.5). This was similar as the previous results in Figure 5.7c, showing there was no ECs infiltration into the tubular scaffolds after 10 days' *in vitro* culture.

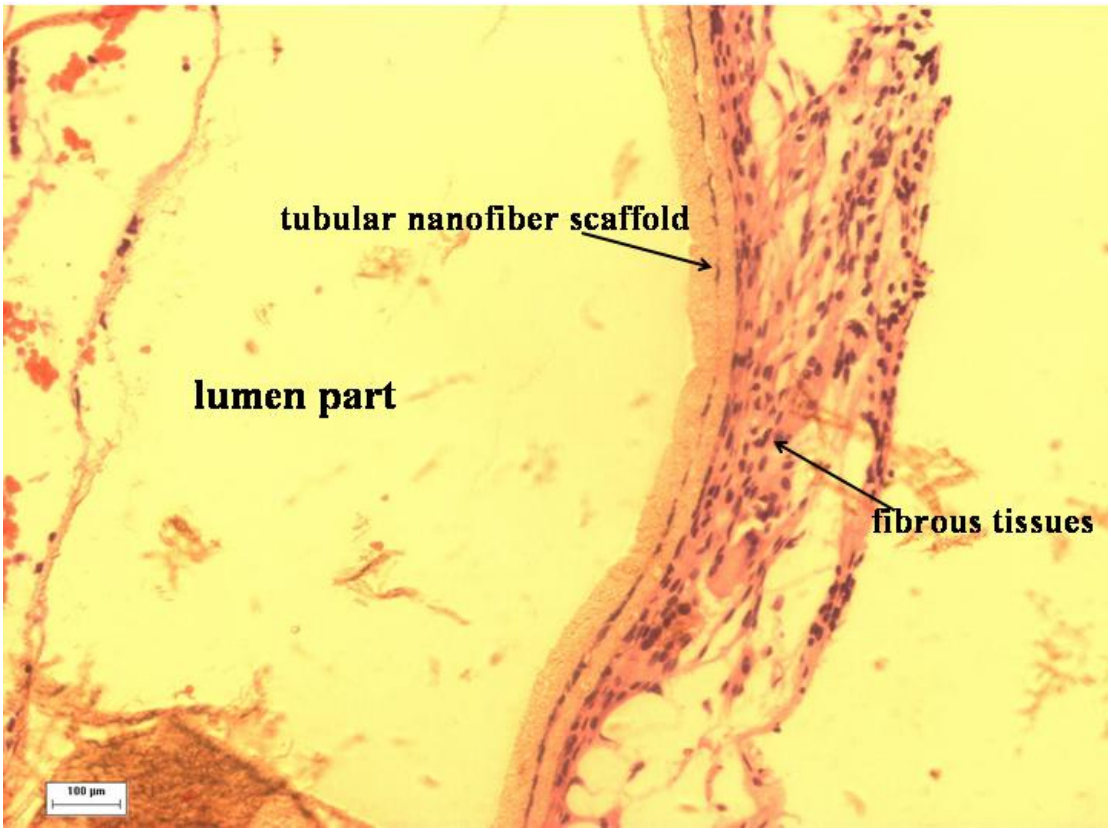

Figure 6.5. H&E staining image of the oblique-section of the explanted tubular nanofiber scaffold after 7 weeks' implantation in the rabbit model.

Third, it was found that no ECs-like cells were present on the lumen of the tubular nanofiber scaffolds, indicating the challenge of immediate *in vivo* endothelialization and the necessity of *in vitro* ECs-seeding of vascular grafts.

Although no blood coagulation occurred in the lumen of the scaffolds for 7 weeks' implantation, it is highly possible that blood coagulation (thrombosis) would occur in a later phase due to the lack of anti-thrombogenic ECs layer. Thus EC-seeded vascular grafts should be implanted into the rabbit to test the patency in the future. There are several approaches regarding where and how to extract ECs. Autologous ECs could be harvested from veins, arteries, capillaries, and fatty tissues *etc*. Recent advances in stem cell technology also provide alternative ECs sources. It was reported that endothelial progenitor cells (EPCs), circulating in the peripheral blood, could be differentiated into ECs with comparable antithrombogenic potential (Lin *et al.*, 2000). Further, human embryonic stem cells were shown to be differentiated into ECs forming vascular-like structures successfully (Levenberg *et al.*, 2002).

6.3 Conclusion

To prove the basic concept of using the tubular nanofiber scaffolds as vascular grafts, the tubular P(LLA-CL) nanofiber scaffolds (inner diameter 1 mm) without collagen coating and without ECs seeding were implanted *in vivo* into a rabbit model to replace the inferior superficial epigastric veins. Results showed the scaffolds could sustain the suturing during the implantation process and there was no blood leaking from the scaffolds. After 7 weeks, the explanted scaffolds kept the structure integrity. There was a thick fibrous tissue around the scaffolds. No ECs layer or blood coagulation occurred in the lumen of the scaffolds. The lack of ECs layer in the

lumen indicated the necessity of ECs seeding *in vitro* onto the scaffolds before implantation.

Chapter 7

Conclusion and Recommendations

The scope of this research encompasses modification of electrospun P(LLA-CL) nanofiber scaffolds with natural collagen type I and construction of tissue engineered small-diameter vascular grafts by hybridizing the scaffold and endothelial cells (ECs).

7.1 Main conclusions

1. Flat collagen-modified P(LLA-CL) nanofiber meshes (NFM) were successfully fabricated by two ways: (1) electrospinning a mixture of collagen and P(LLA-CL) dissolved in a polar organic solvent, HFP; (2) collagen coating on the electrospun P(LLA-CL) NFM after air plasma treatment. The modified NFM had diameter range between 100 to 800 nm and displayed features of ECM-like non-woven architecture, high porosity (around 70%), bioactive surface, proper mechanical properties (tensile strength, 1-10 MPa), and controllable fiber alignment. Collagen coated aligned NFM have higher mechanical strength and modulus in the fiber alignment direction than the random NFM.

2. The collagen-blended P(LLA-CL) NFM has improved viability and attachment of HCAECs compared with the unmodified P(LLA-CL) NFM. HCAECs adopted a

spreading polygonal shape and interconnected well with the collagen-blended NFM, whereas HCAECs had a round non-spreading shape on the P(LLA-CL) NFM. Further, HCAECs maintained phenotypic expressions of cell adhesion molecules such as PECAM-1, ICAM-1, VCAM-1, E-Selectin, and von Willebrand factor on the collagen-blended NFM.

3. The collagen coating treatment improved the viability and attachment of HCAECs on the P(LLA-CL) NFM. HCAECs maintained the phenotypic expression of PECAM-1, fibronectin, and collagen IV. Furthermore, HCAECs kept the expressions of 112 function-related genes. On the collagen coated aligned NFM, HCAECs grew along the direction of nanofiber alignment and showed elongated morphology.

4. 3-D P(LLA-CL) tubular nanofiber scaffolds were fabricated by electrospinning onto a rotating metallic mandrel. The tubular scaffolds were then modified with collagen by coating method. A rotational seeding technique can be used to seed HCAECs on the lumen of the scaffolds with even cell distribution. The collagen coated scaffolds possessed quick and stable endothelialization and reached sub-confluence of HCAECs immediately after seeding. After 10 day's culture, HCAECs existed as a thin layer covering the lumen of the scaffolds. Further, the cells showed the phenotypic expression of PECAM-1. On the control (Gore-Tex® vascular grafts) there were no HCAECs present after rotational seeding.

5. The pure P(LLA-CL) tubular nanofiber scaffolds without collagen modification showed an *in vivo* patency for 7 weeks when implanted into a rabbit model. The scaffolds sustained the suturing and no blood leaked from the scaffolds. After 7 weeks, the scaffolds kept the structure integrity and no blood coagulation occurred in the lumen. A thick fibrous tissue was observed to be around the out layer of the scaffolds.

7.2 Limitations

What's left in this study is that some experiment designs are not optimized to a satisfied level. First of all, only one cell type, i.e. human coronary artery endothelial cells (HCAEC), has been studied. Other cell candidates such as human umbilical vein endothelial cells (HUVEC) and stem cells should been explored as they're extensively used in literature. Secondly, the ePTFE graft should not act as a control for a viable TEVG because it's made of synthetic and non-biodegradable materials. Ideally a natural vein/artery from humans could better show the existing "gap" between a TEVG and a conduit routinely used in clinical practice. Lastly, the very basic question which is why and how nanostructure topography affects cellular behavior remains unknown. We used cell grown on TCPS as a control to study cellular behavior on nanofiber scaffolds. However, as a hard surface with different chemical composition, TCPS could not theoretically act as a good control for nanofiber surface.

7.3 Recommendations

7.3.1 Advanced mechanical properties studies

In this study, the mechanical properties of the flat nanofiber meshes were studied but they could not reflect other important mechanical properties of the 3-D tubular nanofiber scaffolds such as burst pressure and compliance, which need be studied using professionally customized apparatus. Burst pressure is a pressure under which vascular grafts rupture. It can be measured by affixing the tubular scaffold to a nozzle connected to a pressure gauge, pressure regulator, and filled with liquid. The pressure will be then increased slowly until the scaffold bursts. The burst pressure will be recorded and expressed in mmHg. Compliance is defined as the volume change of vascular grafts, usually expressed as percentage of radius change versus pressure change. For compliance test, the tubular scaffold will be immersed in a water bath and cannulated at either end. One cannula will be connected to a column of water and the other to a drainage tube. The column of water should create a pressure within the scaffold as high as 120 mmHg. Water can be then drained from the scaffold to lower the pressure in decrements of 10 mmHg. At each decrement, the diameter of the scaffold will be recorded using a digital camera. This process will be repeated until the pressure reaches 0 mmHg.

7.3.2. Introducing growth factors into the nanofiber scaffolds

A recently developed core-shell nanofibers in our lab have the potential of carrying proteins and growth factors into nanofibers (Figure 7.1) (Zhang *et al.*, 2004). Initial study of release kinetic of core-shell nanofibers with fluorescein-isothiocyanate-conjugated bovine albumin (FITC-BSA) encapsulated in the core showed a control release pattern (Ramakrishna *et al.*, 2006). The drug release rate could be adjusted by the ratio of thickness of the shell to core. In the future, ECs chemokine such as vascular endothelial growth factor (VEGF) can be loaded into the core of the nanofibers. The gradually released VEGF may recruit host ECs onto lumen of the tubular scaffolds.

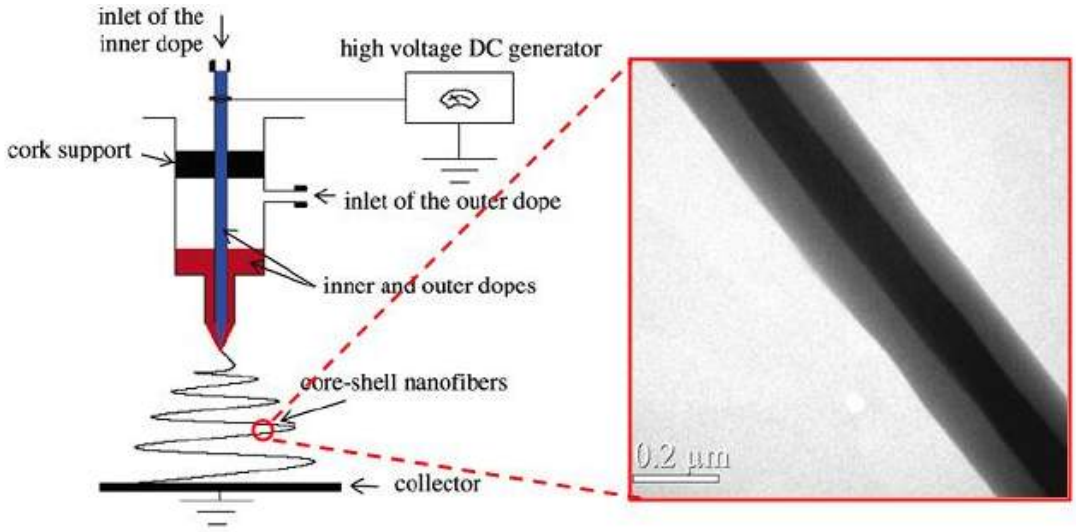

Figure 7.1. Experimental setup for electrospinning core-shell nanofibers (Zhang *et al.*, 2004).

7.3.3 Constructing tubular nanofiber scaffolds with hierarchical structure

It is important to design tubular nanofiber scaffolds with a controllable hierarchical organization which would better simulate the tri-layer structure of natural blood vessels. In natural blood vessels, the intima layer is for ECs growth and can be fabricated using collagen-modified NFM. The media layer is for SMCs growth and can be constructed by aligned collagen-modified NFM, having the ability to control the alignment of SMCs. The outer layer consists of fibroblasts. Random polymer NFM can be used to construct the outer layer because fibroblasts can easily grow well in a random pattern on surface of polymers. To conclude, ECs-seeded NFM, SMCs-seeded aligned NFM, and fibroblast-seeded NFM can be constructed one by one to obtain vascular grafts with unique mechanical strength (Figure 7.2). It needs to be noticed that SMCs and fibroblasts need to grow into multi-layers on the media and adventitia for functional blood vessels regeneration, which is different from ECs growing as a mono-layer in the intima. To encourage the multilayer growth of SMCs and fibroblasts, pore size of the NFM should be controlled to enable infiltration of the cells into the NFM. Another approach is to electrospray the cells during electrospinning process. It has been reported that after electrospraying, vascular smooth muscle cells remained their viability and proliferation compared with the unprocessed cells (Stankus *et al.*, 2006).

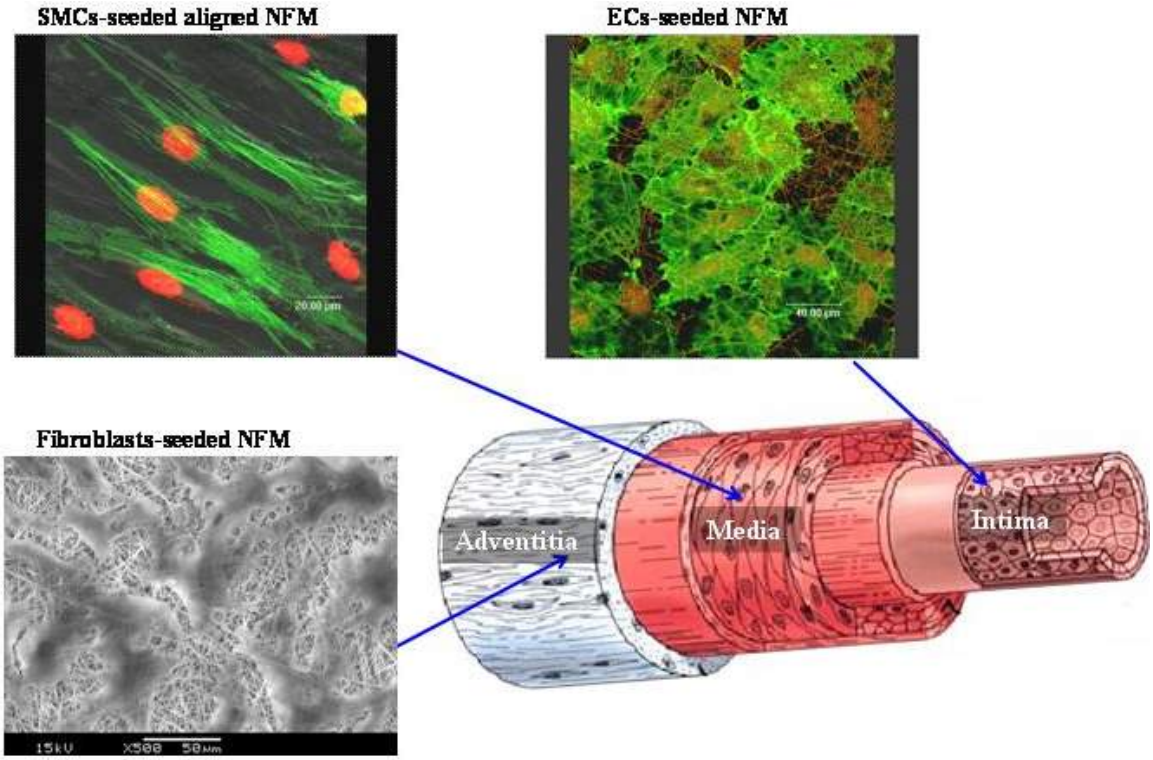

Figure 7.2. Constructing tubular nanofiber scaffolds with hierarchical structure: ECs-seeded NFM, SMC-contained aligned NFM, and fibroblasts-contained NFM can be used to construct the intima, media, and adventitia of blood vessels respectively.

Reference

Ahmed,I., Liu,H.Y., Mamiya,P.C., Ponery,A.S., Babu,A.N., Weik,T., Schindler,M., and Meiners,S. (2006). Three-dimensional nanofibrillar surfaces covalently modified with tenascin-C-derived peptides enhance neuronal growth in vitro. Journal of Biomedical Materials Research Part A 76A, 851-860.

Alberts,B., Johnson,A., Lewis,J., Raff,M., Roberts,K., and Walter,P. (2002). Cells in Their Social Context. In: Molecular Biology of Cell. New York: Garland Science, 1065-1125.

Bini,T.B., Gao,S., Tan,T.C., Wang,S., Lim,A., Hai,L.B., and Ramakrishna,S. (2004). Electrospun poly(L-lactide-co-glycolide) biodegradable polymer nanofiber tubes for peripheral nerve regeneration. Nanotechnology 15, 1459-1464.

Blakemore,A.H. and Voorhees,A.B.Jr. (1954). The use of tubes constructed from vinyon N cloth in bridging arterial defects; experimental and clinical. Annals of Surgery 140, 324-334.

Buttafoco,L., Kolkman,N.G., Engbers-Buijtenhuijs,P., Poot,A.A., Dijkstra,P.J., Vermes,I., and Feijen,J. (2006). Electrospinning of collagen and elastin for tissue engineering applications. Biomaterials 27, 724-734.

Cao,Y.L., Vacanti,J.P., Paige,K.T., Upton,J., and Vacanti,C.A. (1997). Transplantation of chondrocytes utilizing a polymer-cell construct to produce tissue-engineered cartilage in the shape of a human ear. Plastic and Reconstructive Surgery 100, 297-302.

Casper,C.L., Yamaguchi,N., Kiick,K.L., and Rabolt,J.F. (2005). Functionalizing electrospun fibers with biologically relevant macromolecules. Biomacromolecules 6, 1998-2007.

Cenni,E., Granchi,D., Arciola,C.R., Ciapetti,G., Savarino,L., Stea,S., Cavedagna,D., Dileo,A., and Pizzoferrato,A. (1995). Adhesive Protein Expression on Endothelial-Cells After Contact In-Vitro with Polyethylene Terephthalate Coated with Pyrolytic Carbon. Biomaterials 16, 1223-1227.

Chan,C.M., Ko,T.M., and Hiraoka,H. (1996). Polymer surface modification by plasmas and photons. Surface Science Reports 24, 3-54.

Chen,Z.G., Mo,X.M., and Qing,F.L. (2006). Electrospinning of chitosan collagen complex: To mimic the native extracellular matrix. Tissue Engineering 12, 1074.

Chua,K.N., Lim,W.S., Zhang,P.C., Lu,H.F., Wen,J., Ramakrishna,S., Leong,K.W., and Mao,H.Q. (2005). Stable immobilization of rat hepatocyte spheroids on galactosylated nanofiber scaffold. Biomaterials 26, 2537-2547.

Dewey,C.F., Bussolari,S.R., Gimbrone,M.A., and Davies,P.F. (1981). The Dynamic-Response of Vascular Endothelial-Cells to Fluid Shear-Stress. Journal of Biomechanical Engineering-Transactions of the Asme 103, 177-185.

Drew,C., Wang,X.Y., Samuelson,L.A., and Kumar,J. (2003). The effect of viscosity and filler on electrospun fiber morphology. Journal of Macromolecular Science-Pure and Applied Chemistry A40, 1415-1422.

Ekaputra,A.K., Chen,Z.C.C., Cool,S., and Hutmacher,W.D. (2006). Physical characterization and osteogenic induction of porcine mesenchymal progenitor cells on electrospun poly (epsilon-caprolactone)-collagen (PCL-Col) blend nanofiber scaffolds. Tissue Engineering 12, 1080.

Elbert,D.L. and Hubbell,J.A. (1996). Surface Treatments of Polymers for Biocompatibility. Annual Review of Materials Science 26, 365-294.

Elias,K.L., Price,R.L., and Webster,T.J. (2002). Enhanced functions of osteoblasts on nanometer diameter carbon fibers. Biomaterials 23, 3279-3287.

Fan,Y.W., Cui,F.Z., Hou,S.P., Xu,Q.Y., Chen,L.N., and Lee,I.S. (2002). Culture of neural cells on silicon wafers with nano-scale surface topograph. Journal of Neuroscience Methods 120, 17-23.

Fang,X. and Reneker,D.H. (1997). DNA fibers by electrospinning. Journal of Macromolecular Science-Physics B36, 169-173.

Fujihara,K., Kotaki,M., and Ramakrishna,S. (2005). Guided bone regeneration membrane made of polycaprolactone/calcium carbonate composite nano-fibers. Biomaterials 26, 4139-4147.

Giliberti,D.C., White,K.K., and Dee,K.C. (2002). Control of Cell-Biomaterials Interactions. In: Polymeric biomaterials, ed. S.DumitriuNew York: Marcel Dekker Inc, 361-375.

Gopal,R., Kaur,S., Ma,Z.W., Chan,C., Ramakrishna,S., and Matsuura,T. (2006). Electrospun nanofibrous filtration membrane. Journal of Membrane Science 281, 581-586.

Gross,P.L. and Aird,W.C. (2000). The endothelium and thrombosis. Seminars in Thrombosis and Hemostasis 26, 463-478.

Hashi, C.K., Zhu, Y., Yang, G.Y., Young, W.L., Hsiao, B.S., Wang, K., Chu, B., and Li, S. (2007) Antithrombogenic property of bone marrow mesenchymal stem cells in nanofibrous vascular grafts. Proceedings of the National Academy of Sciences 104, 11915-11920.

Hastings,G.W. (1992). Preface. In: Cardiovascular biomaterials, ed. G.W.HastingsNew York: Springer-Verlag.

He,W., Yong,T., Teo,W.E., Ma,Z.W., and Ramakrishna,S. (2005). Fabrication and endothelialization of collagen-blended biodegradable polymer nanofibers: Potential vascular graft for blood vessel tissue engineering. Tissue Engineering 11, 1574-1588.

Herring,M., Gardner,A., and Glover,J. (1978). A single-staged technique for seeding vascular grafts with autogenous endothelium. Surgery 84, 498-504.

How,T.V. (1992). Mechanical Properties of Arteries and Arterial Grafts. In: Cardiovascular biomaterials, ed. G.W.HastingsNew York: Springer-Verlag, 1-35.

Huang,L., McMillan,R.A., Apkarian,R.P., Pourdeyhimi,B., Conticello,V.P., and Chaikof,E.L. (2000). Generation of synthetic elastin-mimetic small diameter fibers and fiber networks. Macromolecules 33, 2989-2997.

Huang,L., Nagapudi,K., Apkarian,R.P., and Chaikof,E.L. (2001). Engineered collagen-PEO nanofibers and fabrics. Journal of Biomaterials Science-Polymer Edition 12, 979-993.

Huang,Z.M., Zhang,Y.Z., Kotaki,M., and Ramakrishna,S. (2003). A review on polymer nanofibers by electrospinning and their applications in nanocomposites. Composites Science and Technology 63, 2223-2253.

Hubbell,J.A., Massia,S.P., Desai,N.P., and Drumheller,P.D. (1991). Endothelial Cell-Selective Materials for Tissue Engineering in the Vascular Graft Via A New Receptor. Bio-Technology 9, 568-572.

Hubbell,J.A., Massia,S.P., and Drumheller,P.D. (1992). Surface-Grafted Cell-Binding Peptides in Tissue Engineering of the Vascular Graft. Annals of the New York Academy of Sciences 665, 253-258.

Hutmacher,D.W., Sittinger,M., and Risbud,M.V. (2004). Scaffold-based tissue engineering: rationale for computer-aided design and solid free-form fabrication systems. Trends in Biotechnology 22, 354-362.

Inoguchi,H., Kwon,I.K., Inoue,E., Takamizawa,K., Maehara,Y., and Matsuda,T. (2006). Mechanical responses of a compliant electrospun poly(l-lactide-co-[epsilon]-caprolactone) small-diameter vascular graft. Biomaterials 27, 1470-1478.

Ishibashi,K. and Matsuda,T. (1994). Reconstruction of a hybrid vascular graft hierarchically layered with three cell types. ASAIO journal 40, 284-290.

Ito,Y., Hasuda,H., Kamitakahara,M., Ohtsuki,C., Tanihara,M., Kang,I.K., and Kwon,O.H. (2005). A composite of hydroxyapatite with electrospun biodegradable nanofibers as a tissue engineering material. Journal of Bioscience and Bioengineering 100, 43-49.

Jaeger,R., Bergshoef,M.M., Batlle,C.M.I., Schonherr,H., and Vancso,G.J. (1998). Electrospinning of ultra-thin polymer fibers. Macromolecular Symposia 127, 141-150.

Jeong,S.I. et al. (2005). Mechano-active tissue engineering of vascular smooth muscle using pulsatile perfusion bioreactors and elastic PLCL scaffolds. Biomaterials 26, 1405-1411.

Ji,Y., Ghosh,K., Shu,X.Z., Li,B.Q., Sokolov,J.C., Prestwich,G.D., Clark,R.A.F., and Rafailovich,M.H. (2006). Electrospun three-dimensional hyaluronic acid nanofibrous scaffolds. Biomaterials 27, 3782-3792.

Jin,H.J., Chen,J.S., Karageorgiou,V., Altman,G.H., and Kaplan,D.L. (2004). Human bone marrow stromal cell responses on electrospun silk fibroin mats. Biomaterials 25, 1039-1047.

Jin,H.J., Fridrikh,S.V., Rutledge,G.C., and Kaplan,D.L. (2002). Electrospinning Bombyx mori silk with poly(ethylene oxide). Biomacromolecules 3, 1233-1239.

Kakisis,J.D., Liapis,C.D., Breuer,C., and Sumpio,B.E. (2005). Artificial blood vessel: The Holy Grail of peripheral vascular surgery. Journal of Vascular Surgery 41, 349-354.

Kidoaki,S., Kwon,I.K., and Matsuda,T. (2005). Mesoscopic spatial designs of nano- and microfiber meshes for tissue-engineering matrix and scaffold based on newly devised multilayering and mixing electrospinning techniques. Biomaterials 26, 37-46.

Kim,H.W., Song,J.H., and Kim,H.E. (2005a). Nanoriber generation of gelatin-hydroxyapatite biomimetics for guided tissue regeneration. Advanced Functional Materials 15, 1988-1994.

Kim,K.H. et al. (2005b). Biological efficacy of silk fibroin nanofiber membranes for guided bone regeneration. Journal of Biotechnology 120, 327-339.

Kim,S.H., Nam,Y.S., Lee,T.S., and Park,W.H. (2003). Silk fibroin nanofiber. Electrospinning, properties, and structure. Polymer Journal 35, 185-190.

Kim,T.G. and Park,T.G. (2006). Biomimicking extracellular matrix: Cell adhesive RGD peptide modified electrospun poly(D,L-lactic-Co-glycolic acid) nanofiber mesh. Tissue Engineering 12, 221-233.

Kwon,I.K., Kidoaki,S., and Matsuda,T. (2005). Electrospun nano- to microfiber fabrics made of biodegradable copolyesters: structural characteristics, mechanical properties and cell adhesion potential. Biomaterials 26, 3929-3939.

Kwon,I.K. and Matsuda,T. (2005). Co-electrospun nanofiber fabrics of poly(L-lactide-co-epsilon-caprolactone) with type I collagen or heparin. Biomacromolecules 6, 2096-2105.

L'Heureux,N. et al. (2006). Human tissue-engineered blood vessels for adult arterial revascularization. Nature Medicine 12, 361-365.

L'Heureux,N., Germain,L., Labbe,R., and Auger,F.A. (1993). In vitro construction of a human blood vessel from cultured vascular cells: a morphologic study. Journal of Vascular Surgery 17, 499-509.

L'Heureux,N., Paquet,S., Labbe,R., Germain,L., and Auger,F.A. (1998). A completely biological tissue-engineered human blood vessel. Faseb Journal 12, 47-56.

Laurencin,C.T., Ambrosio,A.M.A., Borden,M.D., and Cooper,J.A. (1999). Tissue engineering: Orthopedic applications. Annual Review of Biomedical Engineering 1, 19-46.

Lee,C.H., Shin,H.J., Cho,I.H., Kang,Y.M., Kim,I.A., Park,K.D., and Shin,J.W. (2005). Nanofiber alignment and direction of mechanical strain affect the ECM production of human ACL fibroblast. Biomaterials 26, 1261-1270.

Levenberg,S., Golub,J.S., Amit,M., Itskovitz-Eldor,J., and Langer,R. (2002). Endothelial cells derived from human embryonic stem cells. Proceedings of the National Academy of Sciences of the United States of America 99, 4391-4396.

Li,C.M., Vepari,C., Jin,H.J., Kim,H.J., and Kaplan,D.L. (2006a). Electrospun silk-BMP-2 scaffolds for bone tissue engineering. Biomaterials 27, 3115-3124.

Li,M.Y., Guo,Y., Wei,Y., MacDiarmid,A.G., and Lelkes,P.I. (2006b). Electrospinning polyaniline-contained gelatin nanofibers for tissue engineering applications. Biomaterials 27, 2705-2715.

Li,M.Y., Mondrinos,M.J., Chen,X.S., and Lelkes,P.I. (2006c). Co-electrospun poly (lactide-co-glycolide), gelatin, and elastin blends for tissue engineering scaffolds. Tissue Engineering 12, 989. (An abstract for 8th TESI Annual Meeting October 22–25, 2005 Shanghai, China)

Li,W.J., Danielson,K.G., Alexander,P.G., and Tuan,R.S. (2003). Biological response of chondrocytes cultured in three-dimensional nanofibrous poly(epsilon-caprolactone) scaffolds. Journal of Biomedical Materials Research Part A 67A, 1105-1114.

Li,W.J., Laurencin,C.T., Caterson,E.J., Tuan,R.S., and Ko,F.K. (2002). Electrospun nanofibrous structure: A novel scaffold for tissue engineering. Journal of Biomedical Materials Research 60, 613-621.

Li,W.J., Tuli,R., Okafor,C., Derfoul,A., Danielson,K.G., Hall,D.J., and Tuan,R.S. (2005). A three-dimensional nanofibrous scaffold for cartilage tissue engineering using human mesenchymal stem cells. Biomaterials 26, 599-609.

Lin,Y., Weisdorf,D., Solovey,A., and Hebbel,R.P. (2000). Origins of circulating endothelial cells and endothelial outgrowth from blood. Journal of Clinical Investigation 105, 71-77.

Lu,A. and Sipehia,R. (2001). Antithrombotic and fibrinolytic system of human endothelial cells seeded on PTFE: the effects of surface modification of PTFE by ammonia plasma treatment and ECM protein coatings. Biomaterials 22, 1439-1446.

Luong-Van,E., Grondahl,L., Chua,K.N., Leong,K.W., Nurcombe,V., and Cool,S.M. (2006). Controlled release of heparin from poly(epsilon-caprolactone) electrospun fibers. Biomaterials 27, 2042-2050.

Luscher,T.F. and Barton,M. (1997). Biology of the endothelium. Clinical Cardiology 20, 3-10.

Lutolf,M.P. and Hubbell,J.A. (2005). Synthetic biomaterials as instructive extracellular microenvironments for morphogenesis in tissue engineering. Nature Biotechnology 23, 47-55.

Luu,Y.K., Kim,K., Hsiao,B.S., Chu,B., and Hadjiargyrou,M. (2003). Development of a nanostructured DNA delivery scaffold via electrospinning of PLGA and PLA-PEG block copolymers. Journal of Controlled Release 89, 341-353.

Ma,Z.W., He,W., Yong,T., and Ramakrishna,S. (2005a). Grafting of gelatin on electrospun poly(caprolactone) nanofibers to improve endothelial cell spreading and proliferation and to control cell orientation. Tissue Engineering 11, 1149-1158.

Ma,Z.W., Kotaki,M., Inai,R., and Ramakrishna,S. (2005b). Potential of nanofiber matrix as tissue-engineering scaffolds. Tissue Engineering 11, 101-109.

Ma,Z.W., Kotaki,M., Yong,T., He,W., and Ramakrishna,S. (2005c). Surface engineering of electrospun polyethylene terephthalate (PET) nanofibers towards development of a new material for blood vessel engineering. Biomaterials 26, 2527-2536.

Maruyama,I. (1998). Biology of endothelium. Lupus 7, S41-S43.

Matsuda,T. (2004). Recent progress of vascular graft engineering in Japan. Artificial Organs 28, 64-71.

Matsuda,T., Ihara,M., Inoguchi,H., Kwon,K., Takamizawa,K., and Kidoaki,S. (2005). Mechano-active scaffold design of small-diameter artificial graft made of electrospun segmented polyurethane fabrics. Journal of Biomedical Materials Research Part A 73A, 125-131.

Matsuda,T. and Miwa,H. (1995). A hybrid vascular model biomimicking the hierarchic structure of arterial wall: Neointimal stability and neoarterial regeneration process under arterial circulation. The Journal of Thoracic and Cardiovascular Surgery 110, 988-997.

Matthews,J.A., Boland,E.D., Wnek,G.E., Simpson,D.G., and Bowlin,G.L. (2003). Electrospinning of collagen type II: A feasibility study. Journal of Bioactive and Compatible Polymers 18, 125-134.

Matthews,J.A., Stitzel,J.D., Wnek,G.E., Simpson,D.G., and Bowlin,G.L. (2002a). Smooth muscle cell migration in electrospun poly(lactic acid) and collagen/elastin. Cardiovascular pathology 11, 13.

Matthews,J.A., Wnek,G.E., Simpson,D.G., and Bowlin,G.L. (2002b). Electrospinning of collagen nanofibers. Biomacromolecules 3, 232-238.

Mazzucotelli,J.P., Moczar,M., Zede,L., Bambang,L.S., and Loisance,D. (1994). Human Vascular Endothelial-Cells on Expanded Ptfe Precoated with An Engineered Protein Adhesion Factor. International Journal of Artificial Organs 17, 112-117.

Mckeown,N.B., Kalman,P.G., Sodhi,R., Romaschin,A.D., and Thompson,M. (1991). Surface Selective Chemical Modification of Fluoropolymer Using Aluminum Deposition. Langmuir 7, 2146-2152.

Meinhart,J.G., Deutsch,M., Fischlein,T., Howanietz,N., Froschl,A., and Zilla,P. (2001). Clinical autologous in vitro endothelialization of 153 infrainguinal ePTFE grafts. Annals of Thoracic Surgery 71, S327-S331.

Min,B.M., Lee,G., Kim,S.H., Nam,Y.S., Lee,T.S., and Park,W.H. (2004). Electrospinning of silk fibroin nanofibers and its effect on the adhesion and spreading of normal human keratinocytes and fibroblasts in vitro. Biomaterials 25, 1289-1297.

Mitchell,S.L. and Niklason,L.E. (2003). Requirements for growing tissue-engineered vascular grafts. Cardiovascular Pathology 12, 59-64.

Miwa,H. and Matsuda,T. (1994). An Integrated Approach to the Design and Engineering of Hybrid Arterial Prostheses. Journal of Vascular Surgery 19, 658-667.

Mo,X.M., Xu,C.Y., Kotaki,M., and Ramakrishna,S. (2004). Electrospun P(LLA-CL) nanofiber: a biomimetic extracellular matrix for smooth muscle cell and endothelial cell proliferation. Biomaterials 25, 1883-1890.

Mohlke,K.L., Nichols,W.C., Westrick,R.J., Novak,E.K., Cooney,K.A., Swank,R.T., and Ginsburg,D. (1996). A novel modifier gene for plasma von Willebrand factor level maps to distal mouse chromosome 11. Proceedings of the National Academy of Sciences of the United States of America 93, 15352-15357.

Nerem,R.M. and Seliktar,D. (2001). Vascular tissue engineering. Annual Review of Biomedical Engineering 3, 225-243.

Niklason,L.E., Gao,J., Abbott,W.M., Hirschi,K.K., Houser,S., Marini,R., and Langer,R. (1999). Functional arteries grown in vitro. Science 284, 489-493.

Niklason,L.E. and Seruya,M. (2002). Small-Diameter Vascular Grafts. In: Methods of Tissue Engineering, ed. A.Atala and R.P.LanzaSan Diego: Academic Press, 905-913.

Nishida,T., Yasumoto,K., Otori,T., and Desaki,J. (1988). The Network Structure of Corneal Fibroblasts in the Rat As Revealed by Scanning Electron-Microscopy. Investigative Ophthalmology & Visual Science 29, 1887-1890.

Ottani,V., Raspanti,M., and Ruggeri,A. (2001). Collagen structure and functional implications. Micron 32, 251-260.

Pan,H., Jiang,H.L., and Chen,W.L. (2006). Interaction of dermal fibroblasts with electrospun composite polymer scaffolds prepared from dextran and poly lactide-co-glycolide. Biomaterials 27, 3209-3220.

Park,K.E., Jung,S.Y., Lee,S.J., Min,B.M., and Park,W.H. (2006a). Biomimetic nanofibrous scaffolds: Preparation and characterization of chitin/silk fibroin blend nanofibers. International Journal of Biological Macromolecules 38, 165-173.

Park,K.E., Kang,H.K., Lee,S.J., Min,B.M., and Park,W.H. (2006b). Biomimetic nanofibrous scaffolds: Preparation and characterization of PGA/chitin blend nanofibers. Biomacromolecules 7, 635-643.

Park,Y.J., Kim,K.H., Lee,J.Y., Ku,Y., Lee,S.J., Min,B.M., and Chung,C.P. (2006c). Immobilization of bone morphogenetic protein-2 on a nanofibrous chitosan membrane for enhanced guided bone regeneration. Biotechnology and Applied Biochemistry 43, 17-24.

Pearson,J.D. (1999). Endothelial cell function and thrombosis. Best Practice & Research Clinical Haematology 12, 329-341.

Pham,Q.P., Sharma,U., and Mikos,A.G. (2006). Electrospinning of polymeric nanofibers for tissue engineering applications: A review. Tissue Engineering 12, 1197-1211.

Pourdeyhimi,B. (1986). Textiles Structure Used in Vascular Grafts. In: Vascular grafts: textile structures and their performance: a critical appreciation of recent Developments, ed. P.W.HarrisonManchester: The Textile Institute, 1-7.

Price,R.L., Waid,M.C., Haberstroh,K.M., and Webster,T.J. (2003). Selective bone cell adhesion on formulations containing carbon nanofibers. Biomaterials 24, 1877-1887.

Ramakrishna,S., Fujihara,K., Teo,W.E., Yong,T., Ma,Z.W., and Ramaseshan,R. (2006). Electrospun nanofibers: solving global issues. Materialstoday 9, 40-50.

Ratcliffe,A. (2000). Tissue engineering of vascular grafts. Matrix Biology 19, 353-357.

Rho,K.S., Jeong,L., Lee,G., Seo,B.M., Park,Y.J., Hong,S.D., Roh,S., Cho,J.J., Park,W.H., and Min,B.M. (2006). Electrospinning of collagen nanofibers: Effects on the behavior of normal human keratinocytes and early-stage wound healing. Biomaterials 27, 1452-1461.

Rosenberg,M.D. (1963). Cell guidance by alterations in monomolecular films. Science 139, 411-412.

Ross,R. (1993). The Pathogenesis of Atherosclerosis - A Perspective for the 1990S. Nature 362, 801-809.

Ruoslahti,E. and Pierschbacher,M.D. (1987). New perspectives in cell adhesion: RGD and integrins. Science 238, 491-497.

Salacinski,H.J., Goldner,S., Giudiceandrea,A., Hamilton,G., Seifalian,A.M., Edwards,A., and Carson,R.J. (2001a). The mechanical behavior of vascular grafts: A review. Journal of Biomaterials Applications 15, 241-278.

Salacinski,H.J., Tiwari,A., Hamilton,G., and Seifalian,A.M. (2001b). Cellular engineering of vascular bypass grafts: role of chemical coatings for enhancing endothelial cell attachment. Med Biol Eng Comput. 39, 609-618.

Sayers,R.D., Raptis,S., Berce,M., and Miller,J.H. (1998). Long-term results of femorotibial bypass with vein or polytetrafluoroethylene. British Journal of Surgery 85, 934-938.

Schindler,M., Ahmed,I., Kamal,J., Nur-E-Kamal, Grafe,T.H., Chung,H.Y., and Meiners,S. (2005). A synthetic nanofibrillar matrix promotes in vivo-like organization and morphogenesis for cells in culture. Biomaterials 26, 5624-5631.

Schmeichel,K.L. and Bissell,M.J. (2003). Modeling tissue-specific signaling and organ function in three dimensions. Journal of Cell Science 116, 2377-2388.

Seal,B.L., Otero,T.C., and Panitch,A. (2001). Polymeric biomaterials for tissue and organ regeneration. Materials Science & Engineering R-Reports 34, 147-230.

Seeger,J.M. and Klingman,N. (2006). Improved in vivo endothelialization of prosthetic grafts by surface modification with fibronectin. Journal of Vascular Surgery 8, 476-482.

Seliktar,D., Black,R.A., Vito,R.P., and Nerem,R.M. (2000). Dynamic mechanical conditioning of collagen-gel blood vessel constructs induces remodeling in vitro. Annals of Biomedical Engineering 28, 351-362.

Shin'oka,T., Imai,Y., and Ikada,Y. (2001). Transplantation of a tissue-engineered pulmonary artery. New England Journal of Medicine 344, 532-533.
Shin,H., Jo,S., and Mikos,A.G. (2003). Biomimetic materials for tissue engineering. Biomaterials 24, 4353-4364.

Shin,M., Ishii,O., Sueda,T., and Vacanti,J.P. (2004). Contractile cardiac grafts using a novel nanofibrous mesh. Biomaterials 25, 3717-3723.

Sipehia,R., Martucci,G., and Lipscombe,J. (1996). Transplantation of human endothelial cell monolayer on artificial vascular prosthesis: The effect of growth-support surface chemistry, cell seeding density, ECM protein coating, and growth factors. Artificial Cells Blood Substitutes and Immobilization Biotechnology 24, 51-63.

Stankus,J.J., Guan,J.J., Fujimoto,K., and Wagner,W.R. (2006). Microintegrating smooth muscle cells into a biodegradable, elastomeric fiber matrix. Biomaterials 27, 735-744.

Steffens,G.C.M., Nothdurft,L., Buse,G., Thissen,H., Hocker,H., and Klee,D. (2002). High density binding of proteins and peptides to poly(D,L-lactide) grafted with polyacrylic acid. Biomaterials 23, 3523-3531.

Stitzel,J. et al. (2006). Controlled fabrication of a biological vascular substitute. Biomaterials 27, 1088-1094.

Sullivan,S.J. and Brockbank,K.G.M. (2002). Small-Diameter Vascular Grafts. In: Principle of Tissue Engineering, ed. R.P.LanzaSan Diego: Academic Press, 447-454.

Teo,W.E., He,W., and Ramakrishna,S. (2006). Electrospun scaffold tailored for tissue-specific extracellular matrix. Biotechnology Journal 1, 918-929.

Terada,S., Suzuki,K., Nozaki,M., Okano,T., and Sasaki,K. (1999). Experimental study of ectopic-free tissue transfer of rabbit epigastric flap using small-caliber vascular grafts. Journal of Biomedical Materials Research 45, 28-35.

Thomas,A.C., Campbell,G.R., and Campbell,J.H. (2003). Advances in vascular tissue engineering. Cardiovascular Pathology 12, 271-276.

Tomizawa,Y. (2003). Vascular Graft: Basic Research and Clinical Applications. In: Vascular grafts: experiment and modeling, ed. A.Tura Southampton: WIT, 1-39.

Tranquillo,R.T., Girton,T.S., Bromberek,B.A., Triebes,T.G., and Mooradian,D.L. (1996). Magnetically orientated tissue-equivalent tubes: Application to a circumferentially orientated media-equivalent. Biomaterials 17, 349-357.

Unger,R.E., Peters,K., Huang,Q., Funk,A., Paul,D., and Kirkpatrick,C.J. (2005). Vascularization and gene regulation of human endothelial cells growing on porous polyethersulfone (PES) hollow fiber membranes. Biomaterials 26, 3461-3469.

VanKooten,T.G., Klein,C.L., Kohler,H., Kirkpatrick,C.J., Williams,D.F., and Eloy,R. (1997). From cytotoxicity to biocompatibility testing in vitro: cell adhesion molecule expression defines a new set of parameters. Journal of Materials Science-Materials in Medicine 8, 835-841.

Vaz,C.M., van Tuijl,S., Bouten,C.V.C., and Baaijens,F.P.T. (2005). Design of scaffolds for blood vessel tissue engineering using a multi-layering electrospinning technique. Acta Biomaterialia 1, 575-582.

Venugopal,J., Ma,L.L., Yong,T., and Ramakrishna,S. (2005). In vitro study of smooth muscle cells on polycaprolactone and collagen nanofibrous matrices. Cell Biology International 29, 861-867.

Voorhees,A.B.Jr., Jaretzki,A., and Blakemore,A.H. (1952). The use of tubes constructed from vinyon "N" cloth in bridging arterial defects. Annals of Surgery 135, 332-336.

Vroman,L.M. and Adams,A.L. (1969). Identification of rapid changes at plasma-solid interfaces. Journal of Biomedical Materials Research 3, 43-67.

Waddell,W.H., Evans,L.R., Gillick,J.G., and Shuttleworth,D. (1992). Polymer Surface Modification. Rubber Chemistry and Technology 65, 687-696.

Walluscheck,K.P., Steinhoff,G., Kelm,S., and Haverich,A. (1996). Improved endothelial cell attachment on ePTFE vascular grafts pretreated with synthetic RGD-containing peptides. European Journal of Vascular and Endovascular Surgery 12, 321-330.

Wang,Y.Q., Qu,X., Lu,J., Zhu,C.F., Wan,L.J., Yang,J.L., Bei,J.Z., and Wang,S.G. (2004). Characterization of surface property of poly(lactide-co-glycolide) after oxygen plasma treatment. Biomaterials 25, 4777-4783.

Webster,T.J., Schadler,L.S., Siegel,R.W., and Bizios,R. (2001). Mechanisms of enhanced osteoblast adhesion on nanophase alumina involve vitronectin. Tissue Engineering 7, 291-301.

Webster,T.J., Siegel,R.W., and Bizios,R. (1999). Osteoblast adhesion on nanophase ceramics. Biomaterials 20, 1221-1227.

Weinberg,C.B. and Bell,E. (1986). A Blood-Vessel Model Constructed from Collagen and Cultured Vascular Cells. Science 231, 397-400.

William,J.M. Methods of dispersing fluirds. [705,691], 1-4. 1902. New York/USA.
Ref Type: Patent

Williamson,M.R., Black,R., and Kielty,C. (2006). PCL-PU composite vascular scaffold production for vascular tissue engineering: Attachment, proliferation and bioactivity of human vascular endothelial cells. Biomaterials 27, 3608-3616.

Wittmann,T. and Waterman-Storer,C.M. (2001). Cell motility: can Rho GTPases and microtubules point the way? J Cell Sci 114, 3795-3803.

Wnek,G.E., Carr,M.E., Simpson,D.G., and Bowlin,G.L. (2003). Electrospinning of nanofiber fibrinogen structures. Nano Letters 3, 213-216.

Xie,J.B. and Hsieh,Y.L. (2003). Ultra-high surface fibrous membranes from electrospinning of natural proteins: casein and lipase enzyme. Journal of Materials Science 38, 2125-2133.

Xu,C.Y., Inai,R., Kotaki,M., and Ramakrishna,S. (2004b). Electrospun nanofiber fabrication as synthetic extracellular matrix and its potential for vascular tissue engineering. Tissue Engineering 10, 1160-1168.

Xu,C.Y., Inai,R., Kotaki,M., and Ramakrishna,S. (2004a). Aligned biodegradable nanofibrous structure: a potential scaffold for blood vessel engineering. Biomaterials 25, 877-886.

Xue.L,G.H.P. (2000). Blood Vessels. In: Principle of Tissue Engineering, ed. Lanza RPSan Diego: Academic Press, 427-446.

Yang,F., Murugan,R., Wang,S., and Ramakrishna,S. (2005). Electrospinning of nano/micro scale poly(L-lactic acid) aligned fibers and their potential in neural tissue engineering. Biomaterials 26, 2603-2610.

Yarin,A.L., Koombhongse,S., and Reneker,D.H. (2001). Bending instability in electrospinning of nanofibers. Journal of Applied Physics 89, 3018-3026.

Yoo,J.J., Liu,J., Soker,S., Komura,M., Lim,G., Atala,A., and Stitzel,J. (2006). Electrospinning fabrication of collagen-based scaffolds for vascular tissue engineering. Faseb Journal 20, A1101.

Yoshimoto,H., Shin,Y.M., Terai,H., and Vacanti,J.P. (2003). A biodegradable nanofiber scaffold by electrospinning and its potential for bone tissue engineering. Biomaterials 24, 2077-2082.

Zhang,Y.Z., Huang,Z.M., Xu,X.J., Lim,C.T., and Ramakrishna,S. (2004). Preparation of core-shell structured PCL-r-gelatin Bi-component nanofibers by coaxial electrospinning. Chemistry of Materials 16, 3406-3409.

Zhong,S.P., Teo,W.E., Zhu,X., Beuerman,R., Ramakrishna,S., and Yung,L.Y.L. (2005). Formation of collagen-glycosaminoglycan blended nanofibrous scaffolds and their biological properties. Biomacromolecules 6, 2998-3004.

Zhu,Y.B., Gao,C.Y., He,T., and Shen,J.C. (2004). Endothelium regeneration on luminal surface of polyurethane vascular scaffold modified with diamine and covalently grafted with gelatin. Biomaterials 25, 423-430.

TISSUE ENGINEERING
Volume 12, Number 9, 2006

Biodegradable Polymer Nanofiber Mesh to Maintain Functions of Endothelial Cells

WEI HE, M.Sc.,[1] THOMAS YONG, Ph.D.,[1] ZU WEI MA, Ph.D.,[2] RYUJI INAI, Ph.D.,[3] WEE EONG TEO, B.Sc.,[3] and SEERAM RAMAKRISHNA, Ph.D.[1–3]

ABSTRACT

Maintaining functions of endothelial cells *in vitro* is a prerequisite for effective endothelialization of biomaterials as an approach to prevent intimal hyperplasia of small-diameter vascular grafts. The aim of this study was to design suitable nanofiber meshes (NFMs) that further maintain the phenotype and functions of human coronary artery endothelial cells (HCAECs). Collagen-coated random and aligned poly(L-lactic acid)-*co*-poly(ε-caprolactone) (P(LLA-CL)) NFMs were fabricated using electrospinning. Mechanical testing showed that tensile modulus and strength were greater for the aligned P(LLA-CL) NFM than for the random NFM. Spatial distribution of the collagen in the NFMs was visualized by labeling with fluorescent dye. HCAECs grew along the direction of nanofiber alignment and showed elongated morphology that simulated endothelial cells *in vivo* under blood flow. Both random and aligned P(LLA-CL) NFMs preserved phenotype (expression of platelet endothelial cell adhesion molecule-1, fibronectin, and collagen type IV in protein level) and functions (complementary DNA microarray analysis of 112 genes relevant to endothelial cell functions) of HCAECs. The P(LLA-CL) NFMs are potential materials for tissue-engineered vascular grafts that may enable effective endothelialization.

INTRODUCTION

SMALL-DIAMETER (<6 MM) PROSTHETIC VASCULAR GRAFTS remain patent only 15–30% of the time after 5 years[1] and are associated with thrombosis rates greater than 40% after 6 months;[2] these outcomes are due to thrombosis and intimal hyperplasia (excessive tissue ingrowth). Seeding endothelial cells onto the inner surface of a vascular graft is a promising method to improve the antithrombogenicity property of vascular grafts, which is considered the beginning of tissue engineering for the cardiovascular system.[3] However, endothelialization has always been limited because attached endothelial cells often detach from the surface upon exposure to blood circulation.[4] Thus, natural extracellular matrix (ECM) proteins have been used to modify the surface of vascular grafts to introduce cell recognition sites in order to induce cell-material interactions.[5]

Since endothelial cells are locally regulated by ECM, biomimetic and bioactive materials may physically mimic ECM and chemically could be preferred candidates to support normal attachment, proliferation, and phenotypic and functional maintenance of endothelial cells.[6] Polymer nanofiber scaffold is among the most promising biomaterials for native ECM analogues. Biodegradable polymer nanofibers with diameters ranging from 100 to 800 nm have been extensively used as tissue engineering scaffolds[7–11] because they possess many desirable properties: biocompatibility, ECM-like architecture, high porosity, adjustable mechanical and biodegradable properties,[12] capability of surface modification,[10,11] and flexibility of loading drugs or genes.[13,14] We have reported that the random electrospun poly(L-lactic acid)-*co*-poly(ε-caprolactone) P(LLA-CL) nanofiber can better support proliferation, adhesion, and differentiation of vascular smooth muscle cells[7–9] than can the solvent cast polymer film.

[1]Division of Bioengineering, National University of Singapore, Singapore.
[2]Nanoscience and Nanotechnology Initiative, National University of Singapore, Singapore.
[3]Department of Mechanical Engineering, National University of Singapore, Singapore.

The objective of the study was to design nanofiber meshes (NFMs) that had properties suitable for tissue-engineered vascular grafts and could support phenotypic and functional maintenance of endothelial cells. We fabricated collagen-coated random and aligned P(LLA-CL) NFMs with nanoscale dimension, immobilized ECM protein, and adjustable fiber alignment. We chose the copolymer from the biodegradable and bioresorbable aliphatic polyester family, random P(LLA-CL) because the degradation rate of the copolymer can be controlled readily by adjusting the ratio of 2 components. In addition, poly(L-lactic acid) (PLLA) is a semi-crystallized hard and brittle material, while poly(ε-caprolactone) (PCL) is a semi-crystalline material with rubbery properties.[15] Copolymers of PLA and PCL could achieve a balanced mechanical property through the adjustment of the ratio of the 2 components. Collagen type I was chosen as the immobilized ECM protein because it is the main type of collagen in connective tissue and is present throughout the arterial wall. The collagen-coated P(LLA-CL) NFMs were fabricated through plasma treatment, followed by collagen coating. Morphology, porosity, mechanical properties, and surface chemistry of the NFMs were studied with respect to the requirements of vascular grafts. Behaviors of human coronary artery endothelial cells (HCAECs) on the collagen-coated P(LLA-CL) NFMs were analyzed in terms of morphology, phenotypic maintenance, and functional maintenance.

MATERIALS AND METHODS

Materials

The random P(LLA-CL) was bought from Boehringer Ingelheim (Ingelheim, Germany); the molecular weight was 150 kDa. Dichloromethane, *N*, *N*-dimethylformamide, and hydrochloric acid were bought from Merck & Co. (Whitehouse Station, NJ). Collagen type I (calf skin) and 1, 1, 1, 3, 3, 3-hexafluoro-2-propanol were purchased from Sigma-Aldrich (St. Louis, MO). Human HCAECs were obtained from Cambrex Bio Science (Walkersville, NJ). The endothelial cell basal medium (Clonetics EBM-2) and the growth factors were purchased from Cambrex Bio Science. The mouse monoclonal antibody to human platelet endothelial cell adhesion molecule-1 (PECAM-1, CD 31) was bought from Cymbus Biotechnology (Hants, United Kingdom). The mouse monoclonal antibody to human fibronectin and collagen type IV were purchased from Acris (Hiddenhausen, Germany).

Fabrication of the random and aligned P(LLA-CL) NFMs

For electrospinning of the P(LLA-CL) NFMs, random P(LLA-CL) (10 wt%) solution in dichloromethane and *N*, *N*-dimethylformamide (70:30 wt:wt) was added to a plastic syringe with a needle (inner diameter, 0.21 mm). With the aid of a syringe pump, the solution was injected at a feed rate of 0.5 mL/h. Electrospinning voltage was applied to the needle at 10 kV using a high-voltage power supply (Gamma High Voltage Research, Ormond Beach, FL). The resultant nanofibers were collected on an aluminum collector. For collecting the random NFM, a static flat alumina plate was used; for the aligned NFM, a rotating disk (1000 rpm) was used. The rotating plate has a sharpened edge that can strengthen the electric field near the collector. Experiment setups are shown in Fig. 1. Detailed information on the equipment used to fabricate aligned nanofiber is provided in a report by Xu *et al.*[7]

Collagen coating on the P(LLA-CL) NFMs

Air plasma treatment of the P(LLA-CL) NFMs was performed in an inductive coupled radiofrequency glow discharge plasma cleaner (PDC-001, Harrick Plasma, Ithaca,

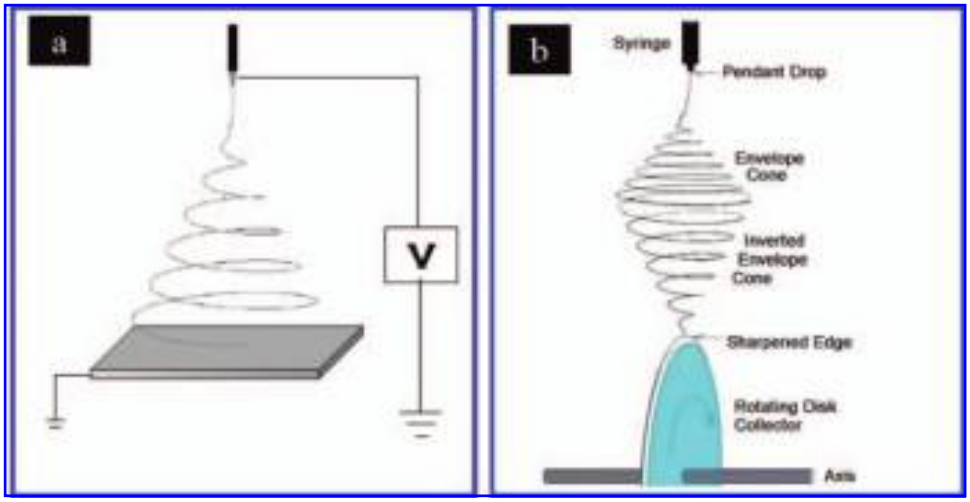

FIG. 1. Experiment setups for electrospinning the random and aligned poly(L-lactic acid)-*co*-poly(ε-caprolactone) nanofiber meshes, which were collected with a static plate (**A**) or rotating disk (**B**), respectively. Color images available online at www.liebertpub.com/ten.

NY) for 5 min with the radiofrequency power set at 30 W. Plasma treatment can increase the surface hydrophilicity of materials,[16,17] which makes the NFMs wettable by collagen solution. The plasma-treated NFMs were immersed in the collagen solution in 0.01 M hydrochloride with a concentration of 290 μg/mL at 4°C overnight. They were then dried at room temperature.

Characterization of the P(LLA-CL) NFMs

Scanning electron micrographs of the NFMs were obtained on a JSM-5800LV scanning electron microscope (JEOL, Tokyo, Japan). Diameter range and pore size (length of the diagonals of the pore square) of the NFMs were measured from the scanning electron microscope images by random counting of 60 nanofibers using ImageJ image analysis software (ImageJ, Bethesda, MD).

Thickness of the P(LLA-CL) NFM was measured by a micrometer (Mitutoyo, Kanagawa, Japan) and its apparent density and porosity were calculated using the following equations:

$$NFM\ apparent\ density\ (g/cm^3) = \frac{NFM\ mass\ (g)}{NFM\ thinckness\ (cm) \times NFM\ area\ (cm^2)}$$

$$NFM\ porosity = \left(1 - \frac{NFM\ apparent\ desnity\ (g/cm^3)}{bulk\ density\ of\ P(LLA\text{-}CL)\ (g/cm^3)}\right) \times 100\%$$

[10].

To visualize the collagen distribution, P(LLA-CL) NFMs coated with rhodamine B isothiocyanate (Sigma)–labeled collagen were observed under a laser scanning confocal microscope (Leica Microsystems, Wetzlar, Germany).

Tensile tests were carried using a 5848 microtester (Instrom, Canton, MA) at a stroke rate of 10 mm/min with a 40-mm gauge length. For the test, the NFMs were prepared in rectangular (10×60 mm) shapes with a thickness of approximately 20 μm.

In vitro *culture of HCAECs*

HCAECs were bought at passage 3. The cells were cultured in Clonetics EBM-2 complete medium supplemented with 5% fetal bovine serum, penicillin (100 units/mL), and streptomycin (100 μg/mL). The medium was replaced every 4 days and cultures were maintained in a humidified incubator at 37°C with 5% carbon dioxide. When the cells reached 80–90% confluence, they were trypsinized and subcultured at 1:3 ratios.

Immunofluorescent staining

After 5 days of culture at seeding density of 1.5×10^4 cells/cm^2, HCAECs were washed with phosphate-buffered saline, fixed with 2.5% paraformaldehyde, and blocked by 2% bovine serum albumin. HCAECs were then incubated for 2 h at 37°C with primary antibody. After washing, fluorescein isothiocyanate–labeled rabbit anti-mouse IgG (Chemicon, Temecula, CA) was added and incubated for 2 h at 37°C, followed by washing and counterstaining with propidium iodide (2.5 μg/mL) for 1 min at 37°C. The immunostained cellular construct samples were then mounted on glass slides with 7 μL FluorSave reagent (Calbiochem, Darmstadt, Germany), and viewed under laser scanning confocal microscope.

Reverse transcriptase polymerase chain reaction analysis

PECAM-1, fibronectin, and collagen type IV were studied by reverse transcriptase polymerase chain reaction (RT-PCR) for gene expression analysis in messenger RNA. Total RNA was extracted from subconfluent 2.5×10^6 HCAECs using RNeasy Mini Kit (Qiagen, Hilden, Germany). For RT-PCR, complementary DNA (cDNA) was reverse transcribed from 1 μg of total RNA. Further information is available in the report by He *et al.*[18]

The PCR products were analyzed by electrophoresis of 10 μL of each sample in 1% agarose gel, and the bands were visualized under ultraviolet light by ethidium bromide staining with a gel documentation system (Gel Doc 2000, BioRad, Hercules, CA).

cDNA microarray analysis

Total RNA was extracted from the HCAECs cultured for 5 days on tissue culture polystyrene, the random and aligned P(LLA-CL) NFMs using RNeasy Mini Kit. A biotin–2′-deoxyuridine 5′-triphosphate (Roche, Pleasonton, CA)–labeled cDNA probe was synthesized according to GEArray probe synthesis kits (GEArray Ampolabeling-LPR kit, Superarray, Frederick, MD) and stored at −20°C. Hybridization with a 2.5-μg biotinylated cDNA probe was done on a nylon membrane printed with the GEArray S series (human endothelial cell biology gene array, Superarray), which contained 112 genes associated with major functions of endothelial cells. Prehybridization and hybridization were carried out in a hybridization oven (Biometra, Goettingen, Germany) for 2 h and overnight, respectively. Finally, the chemiluminescent detection results were scanned using ScannArray (GSI Lumonics, Billerica, MA).

RESULTS

Characterizations of the P(LLA-CL) NFMs

Morphology of the random and aligned P(LLA-CL) NFMs is shown in Fig. 2, which represents the cross-section (parts A and D), 3-dimensional structure (parts B and E), and top view (parts C and F) of the NFMs.

Diameter and pore size distribution of the random and aligned P(LLA-CL) NFMs are shown in Fig. 3. This figure

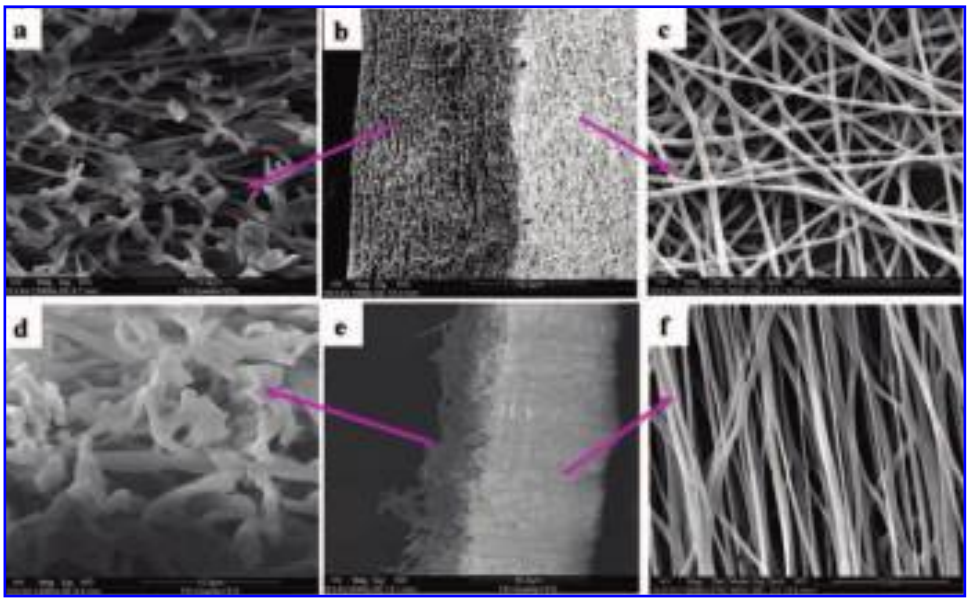

FIG. 2. Scanning electron microscopy pictures of a cross-section (**A** and **D**), 3-dimensional structure (**B** and **E**), and top view (**C** and **F**) of the random (**A–C**) and aligned (**D–F**) poly(L-lactic acid)-*co*-poly(ε-caprolactone) nanofiber meshes. Color images available online at www.liebertpub.com/ten.

reveals a diameter range of 200–800 nm for both NFMs and more uniform diameter distribution for the random NFM than the aligned NFM (Fig. 3A). The pore size for the random NFM was defined as length of diagonal of the pore polygon, which is not applicable for the aligned NFM. Fig. 3B shows pore size distribution of the random NFM to be mainly between 5 and 10 μm.

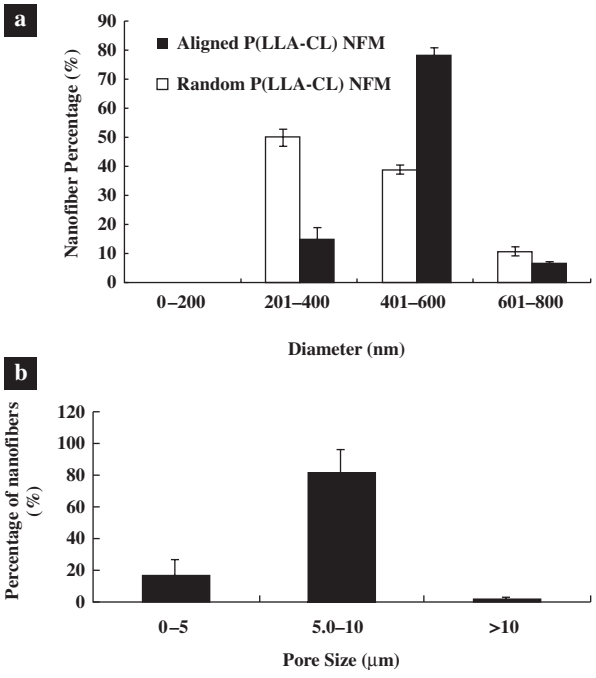

FIG. 3. (**A**) Diameter distribution of the random and aligned poly(L-lactic acid)-*co*-poly(ε-caprolactone) (P(LLA-CL)) nanofiber meshes. (**B**) Pore size distribution of the random P(LLA-CL) nanofiber meshes.

Diameter, thickness, apparent density, porosity, and pore size of the random and aligned P(LLA-CL) NFMs are further summarized in Table 1. This table shows that the diameter of the aligned NFM (mean ± SD, 406 ± 126 nm) is smaller than that of the random NFM (mean ± SD, 470 ± 80 nm). Similar results were reported for aligned PCL[11] and PLLA NFMs.[19] This might be due to stretching tangential force exerted by the high-speed rotating disk on the nanofiber produced.[11] With the known bulk density of P(LLA-CL), the porosity of the NFMs can be calculated by measuring their apparent density. Porosity for both NFMs was found to be approximately 70%.

To visualize spatial distribution of the collagen coated onto the P(LLA-CL) NFMs, rhodamine-labeled collagen was coated onto the NFMs and observed under laser scanning confocal microscope. Collagen was uniformly coated on the surface of every nanofiber in both random (Fig. 4A) and aligned (Fig. 4B) NFMs.

TABLE 1. DIAMETER, THICKNESS, APPARENT DENSITY, POROSITY, AND PORE SIZE OF THE RANDOM AND ALIGNED POLY(L-LACTIC ACID)-*co*-POLY(ε-CAPROLACTONE) NANOFIBER MESH. DATA ARE REPRESENTATIVE OF 2 INDEPENDENT EXPERIMENTS AND ARE PRESENTED AS MEAN ± SD ($n = 5$)

P(LLA-CL) NFM	*Diameter (nm)*	*Thickness (μm)*	*Apparent density (g/cm^3)*	*Porosity (%)*	*Pore size (μm)*
ANF	406 ± 126	24 ± 2	0.37 ± 0.02	69–72	N.A.
RNF	470 ± 80	26 ± 5	0.43 ± 0.08	64–67	6 ± 2

N.A.: not applicable; RNF: random NFM; ANF: aligned NFM.

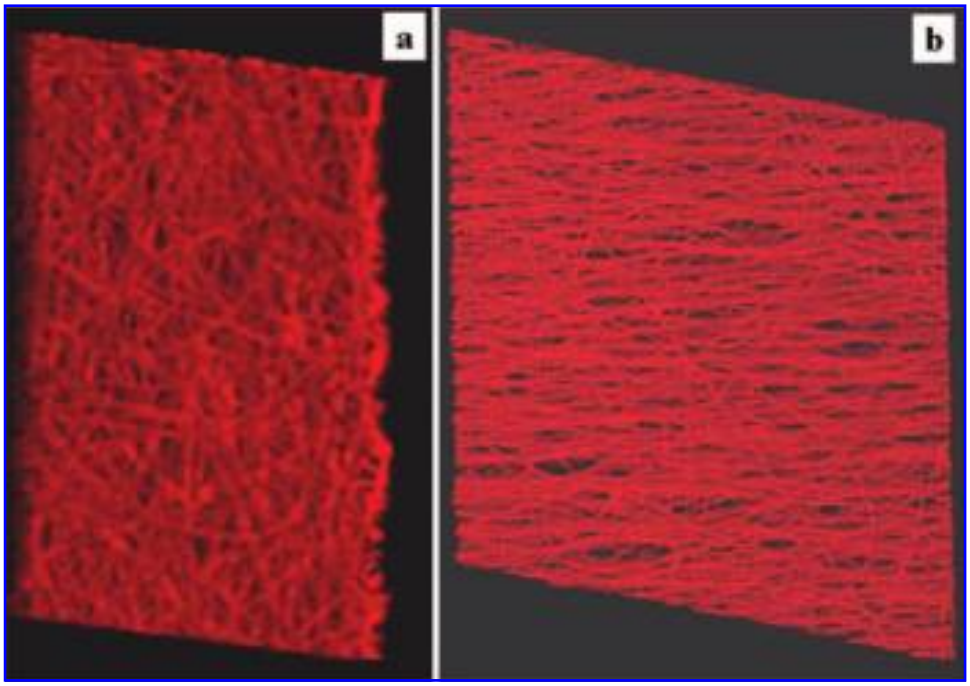

FIG. 4. Three-dimensional laser scanning confocal microscopy (original magnification, ×600) of the collagen-coated random (**A**) and aligned (**B**) poly(L-lactic acid)-*co*-poly(ε-caprolactone) nanofiber meshes. Rhodamine-labeled collagen was identified by its red fluorescence. Color images available online at www.liebertpub.com/ten.

Mechanical properties of the P(LLA-CL) NFMs

Fig. 5 shows the typical stress-strain curves for the random and aligned P(LLA-CL) NFMs under tensile loading. Mechanical strength of the aligned P(LLA-CL) NFM increased compared with the random NFM. This finding correlates to the report that orientation of the fibers directly modulates the mechanical properties of the nanofibers.[20] It also indicates a way to tailor mechanical properties of NFM by changing the fiber alignment. Tensile properties of the NFMs are further summarized in Table 2. This table shows that aligned NFM has larger tensile modulus and tensile strength but smaller ultimate strain than the random NFM.

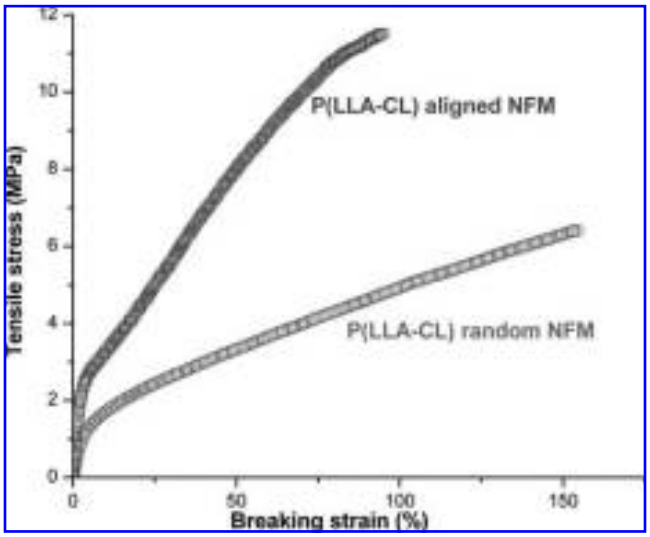

FIG. 5. Typical stress-strain curves for the random and aligned poly(L-lactic acid)-*co*-poly(ε-caprolactone) P(LLA-PCL) nanofiber meshes (NFMs) under tensile loading. Color images available online at www.liebertpub.com/ten.

Morphology and phenotype studies of HCAECs

To study functional development of HCAECs on the NFMs, we performed a series of studies ranging from basic analyses of cell morphology and phenotype to a deeper analysis of functional development by microarray gene expression.

Fig. 6A shows that HCAECs adopted a spindle shape on the aligned NFM, with the long axes parallel to each other and with fibers aligned; this finding is distinct from the polygonal shape on the tissue culture plates and random NFMs.

TABLE 2. TENSILE PROPERTIES OF THE RANDOM AND ALIGNED POLY(L-LACTIC ACID)-*co*-POLY(ε-CAPROLACTONE) NANOFIBER MESH. DATA ARE REPRESENTATIVE OF 2 INDEPENDENT EXPERIMENTS AND ARE PRESENTED AS MEAN ± SD ($n = 3$)

	ANF	*RNF*
Tensile Modulus (MPa)	102.59 ± 5.86	43.99 ± 4.04
Tensile strength (MPa)	10.60 ± 1.29	6.27 ± 1.38
Ultimate strain (%)	99 ± 5	175 ± 49

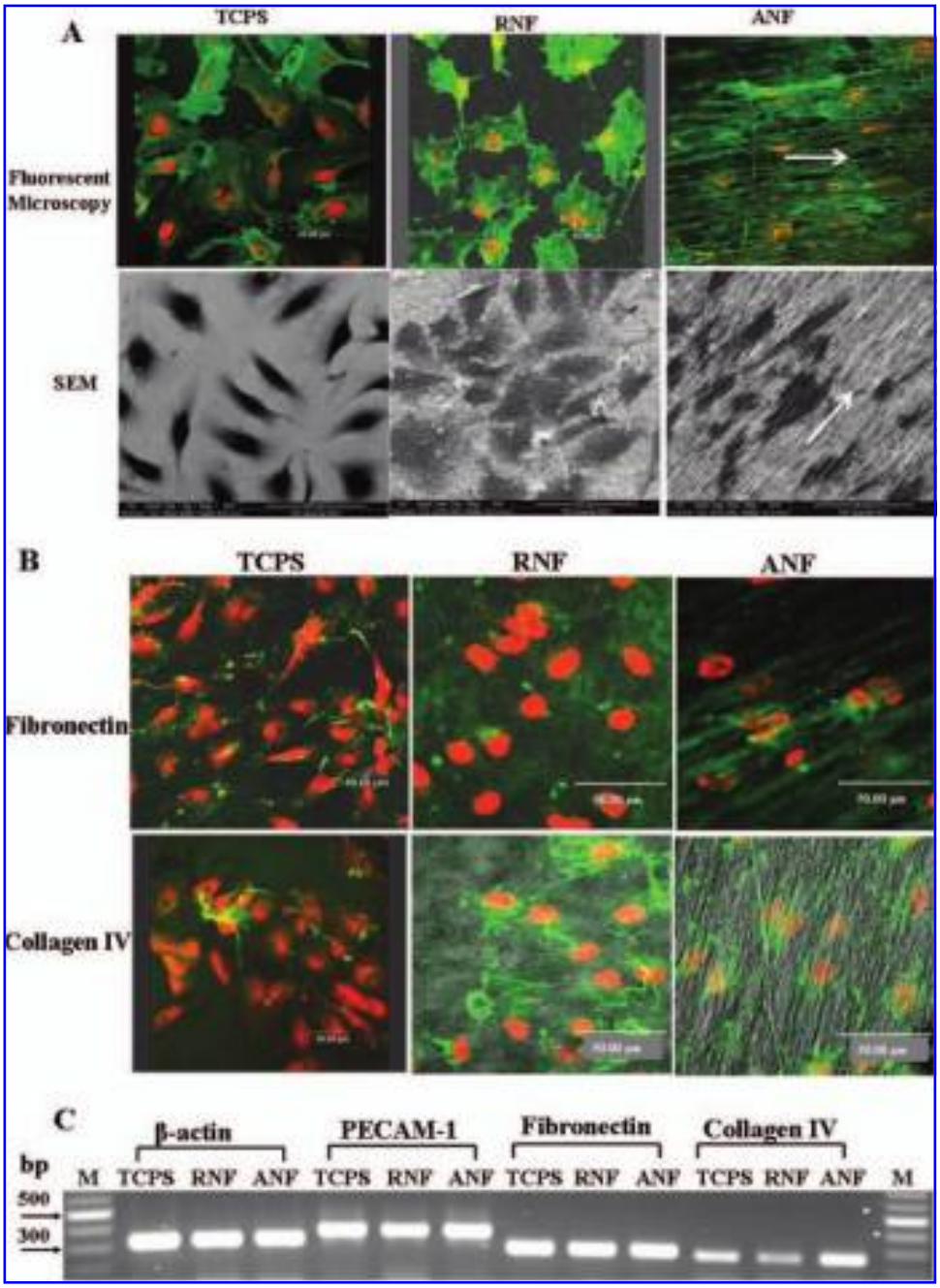

FIG. 6. (**A**) Fluorescent microscopy (original magnification, ×600) and scanning electron microscopy (SEM) (original magnification, ×1000) images of human coronary artery endothelial cells (HCAECs) cultured for 3 days at a density of 3×10^4 cells/cm^2 on tissue culture plates (TCPS), random and aligned poly(L-lactic acid)-*co*-poly(ε-caprolactone) (P(LLA-CL)) nanofiber meshes (NFMs). HCAECs were stained with antibody directed against platelet endothelial cell adhesion molecule-1 (PECAM-1) (green) and nuclei counterstained with propidium iodide (red) on fluorescent microscopy pictures. (**B**) Laser scanning confocal microscopy images of fibronectin and collagen type IV expression from HCAECs on tissue culture plates, random NFM (RNF), and aligned NFM (ANF). (**C**) Reverse transcriptase polymerase chain reaction analysis of expression of PECAM-1, fibronectin, and collagen type IV in HCAECs cultured on tissue culture plates, random NFM, and aligned NFM. Color images available online at www.liebertpub.com/ten.

Phenotype studies of endothelial cells were carried out from 2 main aspects: 1) phenotypic maintenance of endothelial cells and 2) the ECM remolding potential of endothelial cells. For the first step, immunostaining of PECAM-1, CD31, a universal endothelial cell marker, shows the differentiation status and phenotypic maintenance of endothelial cells (Fig. 6A, top) on both tissue culture plates and random and aligned P(LLA-CL) NFMs. For the second step, Fig. 6B shows immunostaining of fibronectin and collagen type IV from HCAECs on the tissue culture plates

and random and aligned P(LLA-CL) NFMs. HCAECs cultured on the NFMs possessed the phenotypic expression of endothelial cell–characteristic ECM protein, indicating the potential capability of HCAECs to remold ECM when cultured on NFMs *in vitro*. Fig. 6C further reveals the expression of these 3 molecules (PECAM-1, fibronectin, and collagen type IV) at the gene level by RT-PCR analysis.

cDNA microarray analysis of HCAECs

To analyze functional maintenance of HCAECs cultured on the synthetic NFMs, a cDNA microarray was applied to study gene expression profiles of HCAECs cultured on the tissue culture plates and random and aligned NFMs in a high-throughput fashion. Fig. 7A shows the expression profile of 112 genes, printed onto nylon membranes in the form of an 8×14 grid, which are associated with 4 major functions of endothelial cells: permissibility and tone, angiogenesis, endothelial cell activation, and endothelial cell injury. Fig. 7B shows 3 comparison groups by scatter plots: random NFM vs. tissue culture plates (Fig. 7B1); aligned NFM vs. tissue culture plates (Fig. 7B2); aligned NFM vs. random NFM (Fig. 7B3). Quantitative analysis of the scatter plot reveals similarities of 87.5%, 89.3%, and 94.6%, respectively. This means, for example, that 87.5% of the genes from HCAECs cultured on random NFM have an expression level similar to that on tissue culture plates. The results are further summarized in Table 3. This table shows the functional maintenance of HCAECs on tissue culture plates and random and aligned NFMs. RT-PCR analysis (Fig. 7C) was performed to verify gene expression profile from the microarray. Three continuous spotted genes from the integrin family—integrin $\alpha5$, integrin αV, and integrin $\beta1$—were picked up, highlighted by a red quadrangle in Fig. 7A. The microarray results show a clear pattern of higher expression levels of integrin $\alpha5$ and integrin $\beta1$ than with integrin αV. RT-PCR results (Fig. 7C) displayed the highest level of expression of integrin αV among the 3 integrins. However, integrin $\beta1$ and integrin αV seem to have the same expression level.

DISCUSSION

In this study, collagen-coated electrospun random and aligned P(LLA-CL) NFMs were successfully fabricated. The NFMs have several favorable characteristics, such as ECM-like architecture, high porosity, adjustable mechanical properties, suitable surface chemistry, and controllable fiber alignment. The potential application of the NFMs as tissue-engineered vascular grafts was primarily studied with regard to phenotypic and functional maintenance of endothelial cells.

The ECM-like architecture of the NFMs may provide cells with a friendly environment. As the specific ECM around endothelial cells, basement membrane was reported to possess a nano to submicron-scale topography of ECM macromolecules, including fiber mesh, pores, ridges, grooves, and peak valleys,[12] which are also features of the NFM. Thus, it is reasonable to expect that ECM-mimicking NFMs may play a role in promoting tissue regeneration *in vitro* similar to that of the native ECM *in vivo*.[6]

Porosity is an important measure for tissue engineering scaffolds. Vascular grafts should be porous, and the porosity should both allow cell infiltration from the adventitial side and maintain hemostasis, as well as allow sufficient mass transfer of gases and nutrients.[21] It is generally accepted that a higher-porosity vascular graft exhibits high patency.[22] Longer fibril expanded polytetrafluoroethylene (60 and 90 μm) provided a much higher degree of endothelialization and collagen production than the shorter fibril groups (20 and 40 μm).[23] Previous studies suggest that effective pore diameters of vascular grafts for cell ingrowth are 20–60 μm,[24] which is larger than the diameter we obtained with the P(LLA-CL) NFMs (Fig. 3B). The phenomena of dynamic interactions between cells and nanofibers may explain possible cell ingrowth into pores of nanofibers, which are smaller than the size of the cell. Researchers have hypothesized that cells might push fibers aside to force ingrowth since the loose and small fibers offer little resistance to cell movement.[25]

Mechanical properties affect long-term patency of vascular grafts.[26,27] One of the main failure modes of synthetic vascular grafts, intimal hyperplasia, is associated with shear stress disturbances due to compliance mismatch of natural arteries and vascular grafts.[26] Compliance is a mechanical property of a tube, and it depends on the tube dimension and modulus.[27] We studied the tensile modulus, tensile strength, and ultimate strain of the NFMs (Fig. 5, Table 2) and could use these findings to fabricate, evaluate, and optimize compliant tube-like structure for tissue-engineered vascular grafts.

Surface chemistry of materials mediates protein adsorption, which regulates cell adhesion, proliferation, and migration[25] and affects the tissue regeneration rate. As an adhesion protein that facilitates cell attachment and proliferation,[28] collagen is commonly used to modify the surface of vascular grafts. The first complete tissue-engineered vascular graft was fabricated with collagen gel.[29] However, pure collagen scaffolds always encountered mechanical limitations.[30] Electrospinning of collagen nanofibers and modification of nanofibers with collagen are new approaches that may improve scaffold strength.[31] The collagen-coated P(LLA-CL) NFMs showed improved attachment, spreading, and proliferation of HCAECs compared with the unmodified P(LLA-CL) NFMs (data not shown). However, collagen is not cell-specific; thus, its use causes adhesion of any type of cells, such as platelets, which may result in a thrombogenic surface. Thus, it is critical to establish confluence and stable endothelial cells on a collagen-modified vascular surface.[21]

Ability of the aligned NFMs to control cell orientation is meaningful for tissue-engineered vascular grafts.[32] Shear

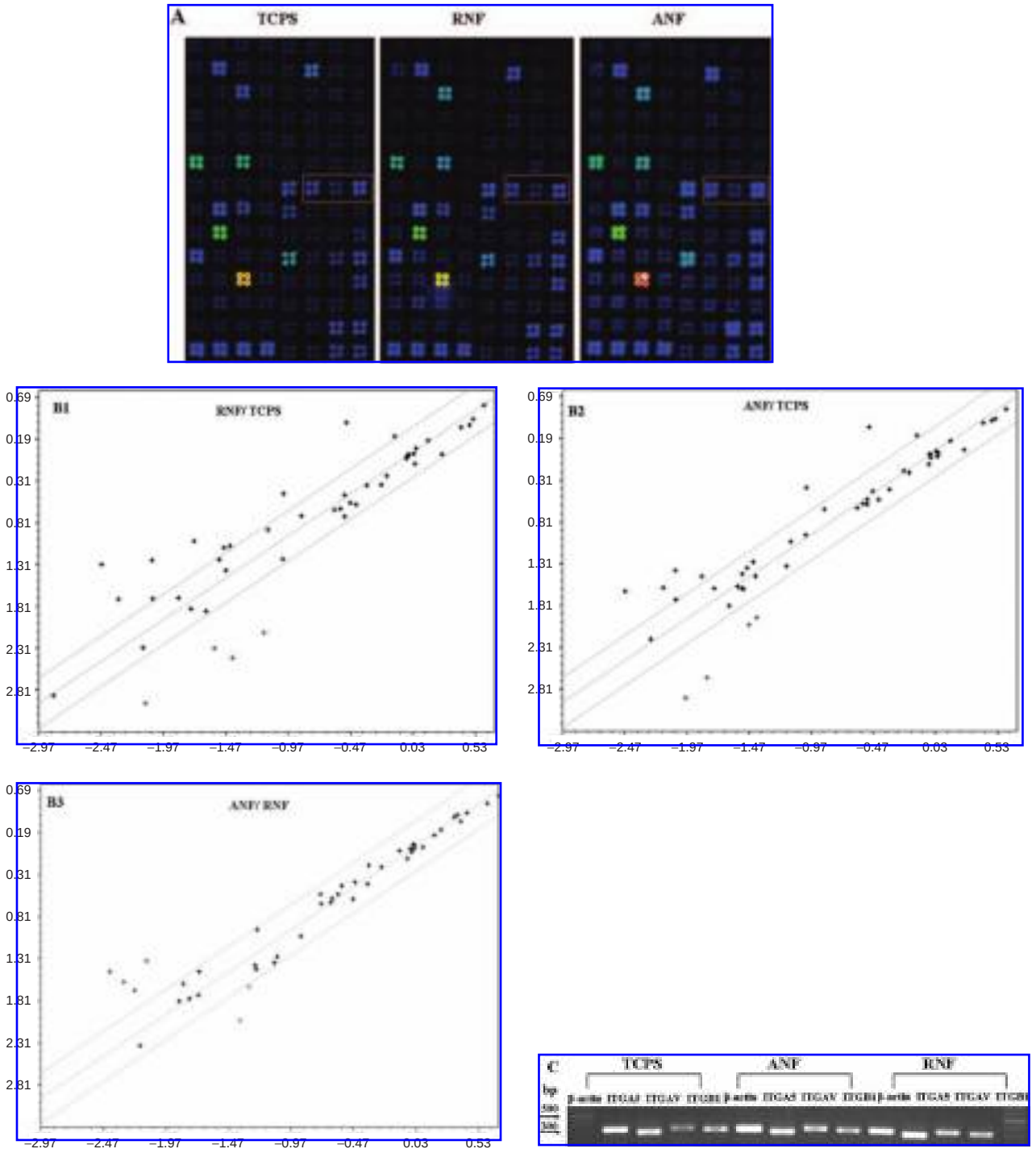

FIG. 7. (**A**) Gene expression profiles of human coronary artery endothelial cells (HCAECs) on tissue culture plates (TCPS), random (RNF) and aligned (ANF) poly(L-lactic acid)-*co*-poly(ε-caprolactone) nanofiber meshes (NFMs) by microarray analysis. Expression of each gene is represented by the fluorescence of the tetraspot. (**B**) Scatter plot showing the relative gene expression of random NFM versus tissue culture plates, aligned NFM versus tissue culture plates, and random versus aligned NFMs. (**C**) Reverse transcriptase polymerase chain reaction analysis of integrin α5, integrin αV, and integrin β1 expression from HCAECs cultured on tissue culture plates, random NFM, and aligned NFM, which correlate to the genes in a red frame in part A. Color images available online at www.liebertpub.com/ten.

Table 3. Percentage of Genes with Overexpressed, Similar, and Less Expressed Levels between HCAECs Grown on Tissue Culture Plates, Random Nanofiber Meshes, and Aligned Nanofiber Meshes

Comparison groups	*Over-expressed genes*	*Genes with similar expression level*	*Less-expressed genes*
RNF/TCPS	8.9	87.5	3.6
ANF/TCPS	7.1	89.3	3.6
ANF/RNF	3.6	94.6	1.8

stress caused by blood flow *in vivo* orientates endothelial cell growth along the direction of the blood flow,[33] which may increase the ability of endothelial cells to resist shear stress and decrease desquamation of these cells from vascular grafts. Thus, it is important to mimic the orientation of endothelial cells *in vitro* on vascular grafts. One way to orientate cells is through dynamic cell culture in a bioreactor. Jeong *et al.* reported that smooth muscle cells cultured in a perfusion bioreactor showed contractile phenotype, significant cell alignment, and increased collagen production.[34] Similarly, Lee *et al.* found that human ligament fibroblast cultured on the aligned polyurethane nanofibers were oriented along the fiber direction and secreted more collagen than on the randomly orientated nanofibers.[35] Thus, aligned NFMs might be used as substitute for a bioreactor, which necessitates a complicated fluid systems, in this specific application where cell alignment is important.

Phenotype and gene expression studies of cells on biomaterials can characterize the biological state and functional development of cells. Phenotype studies of PECAM-1, fibronectin, and collagen type IV expression in protein levels indicate that HCAECs remained differentiated and may be able to remold ECM when cultured on NFMs *in vitro* (Fig. 6). Functional study of HCAECs through screening 112 genes with cDNA microarray shows the similar gene expression pattern of HCAECs (Fig. 7), indicating the functional maintenance of HCAECs cultured on the P(LLA-CL) NFMs and tissue culture plates. These findings suggest effective and fast endothelialization on the NFMs.

We fabricated collagen-coated random and aligned P(LLA-CL) NFMs that featured ECM-like architecture, high porosity, adjustable mechanical properties, suitable surface chemistry, and controllable fiber alignment. Collagen was evenly coated throughout the NFMs. The aligned P(LLA-CL) NFMs have higher mechanical strength and modulus than the random NFMs. HCAECs grew along the direction of nanofiber alignment and showed elongated morphology. Both random and aligned NFMs can support phenotypic and functional maintenance of HCAECs. These findings suggest that effective and quick endothelialization onto the NFMs can be established.

ACKNOWLEDGMENTS

We thank Mr. Yanzhong Zhang and Dr. Yang Fang for their help in mechanical testing and scanning electron microscopy, respectively. This study was supported by the Academic Research Fund from the National University of Singapore.

REFERENCES

1. Seal, B.L., Otero, T.C., and Panitch, A. Polymeric biomaterials for tissue and organ regeneration. Mater. Sci. Engin. R. **34**, 147, 2001.
2. Sayers, R.D., Raptis, S., Berce, M., and Miller, J.H. Long-term results of femorotibial bypass with vein or polytetrafluoroethylene. Br. J. Surg. **85**, 934, 1998.
3. Nerem, R.M., and Seliktar, D. Vascular tissue engineering. Annu. Rev. Biomed. Eng. **3**, 225, 2001.
4. Xue, L., and Greisler, H.P. Blood vessels. In: Lanza, R.P., ed. Principle of Tissue Engineering. San Diego, CA: Academic Press, 2000, pp. 427–446.
5. Shin, H., Jo, S., and Mikos, A.G. Biomimetic materials for tissue engineering. Biomaterials **24**, 4353, 2003.
6. Ma, Z.W., Kotaki, M., Inai, R., and Ramakrishna, S. Potential of nanofiber matrix as tissue engineering scaffolds. Tissue Eng. **11**, 101, 2005.
7. Xu, C.Y., Inai, R., Kotaki, M., and Ramakrishna, S. Aligned biodegradable nanofibrous structure: a potential scaffold for blood vessel engineering. Biomaterials **25**, 877, 2004.
8. Mo, X.M., Xu, C.Y., Kotaki, M., and Ramakrishna, S. Electrospun P(LLA-CL) nanofiber: a biomimetic extracellular matrix for smooth muscle cell and endothelial cell proliferation. Biomaterials **25**, 1883, 2004.
9. Xu, C.Y., Inai, R., Kotaki, M., and Ramakrishna, S. Electrospun nanofiber fabrication as synthetic extracellular matrix and its potential for vascular tissue engineering. Tissue Eng. **10**, 1160, 2004.
10. Ma, Z.W., Kotaki, M., Yong, T., He, W., and Ramakrishna, S. Surface engineering of electrospun polyethylene terephthalate (PET) nanofibers towards development of a new material for blood vessel engineering. Biomaterials **26**, 2527, 2005.
11. Ma, Z.W., He, W., Yong, T., and Ramakrishna, S. Grafting of gelatin on electrospun poly(caprolactone) (PCL) nanofibers to improve endothelial cell's spreading and proliferation and to control cell orientation. Tissue Eng. **11**, 1149, 2005.
12. Keun, K.I., Kidoaki, S., and Matsuda, T. Electrospun nano- to microfiber fabrics made of biodegradable copolyesters: structural characteristics, mechanical properties and cell adhesion potential. Biomaterials **26**, 3929, 2005.
13. Kenawy, E.R., Bowlin, G.L., Mansfield, K., Layman, J., Simpson, D.G., Sanders, E.H., and Wnek, G.E. Release of tetracycline hydrochloride from electrospun poly(ethylene-co-vinylacetate), poly(lactic acid), and a blend. J. Control. Release **81**, 57, 2002.
14. Luu, Y.K., Kim, K., Hsiao, B.S., Chu, B., and Hadjiargyrou, M. Development of a nanostructured DNA delivery scaffold via electrospinning of PLGA and PLA–PEG block copolymers. J. Control. Release **89**, 341, 2003.

15. Lee, H.B., Khang, G., and Lee, J.H. Polymeric biomaterials. In: Park, J.B., and Bronzino, J.D., eds. Biomaterials: Principles and Applications. Boca Raton, FL: CRC Press, 2002, pp. 55–77.
16. Wan, Y., Qu, X., Lu, J., Zhu, C., Wan, L., Yang, J., Bei, J., and Wang, S. Characterization of surface property of poly (lactide-co-glycolide) after oxygen plasma treatment. Biomaterials **25**, 4777, 2004.
17. Chan, C.M., Ko, T.M., and Hiraoka, H. Polymer surface modification by plasmas and photons. Sur. Sci. Rep. **24**, 1, 1996.
18. He, W., Yong, T., Teo, W.E., Ma, Z.W., and Ramakrishna, S. Fabrication and endothelialization of collagen-blended biodegradable polymer nanofiber: potential vascular grafts for the blood vessel tissue engineering. Tissue Eng. **11**, 1575, 2005.
19. Yang, F., Murugan, R., Wang, S., and Ramakrishna, S. Electrospinning of nano/micro scale poly(L-lactic acid) aligned fibers and their potential in neural tissue engineering. Biomaterials **26**, 2603, 2005.
20. Matthews, J.A., Wnek, G.E., Simpson, D.G., and Bowlin, G.L. Electrospinning of collagen nanofibers. Biomacromolecules **3**, 232, 2002.
21. Sullivan, S.J., and Brockbank, K.G.M. Small-diameter vascular grafts. In: Lanza, R.P., ed. Principle of Tissue Engineering. San Diego, CA: Academic Press, 2002, pp. 447 – 454.
22. Niklason, L.E., and Seruya, M. Small-diameter vascular grafts. In: Atala, A., and Lanza, R.P., eds. Methods of Tissue Engineering. San Diego, CA: Academic Press, 2002, pp. 905–913.
23. Hirabayashi, K., Saitoh, E., Ijima, H., Takenawa, T., Kodama, M., and Hori, M. Influence of fibril length upon ePTFE graft healing and host modification of the implant. J. Biomed. Mater. Res. **26**, 1433, 1992.
24. von Recum, A.F., Shannon, C.E., Cannon, C.E., Long, K.J., and van Kooten, T.G. Surface roughness, porosity, and texture as modifiers of cellular adhesion. Tissue Eng. **2**, 241, 1996.
25. Li, W.J., Laurencin, C.T., Caterson, E.J., Tuan, R.S., and Ko, F.K. Electrospun nanofibrous structure: a novel scaffold for tissue engineering. J. Biomed. Mater. Res. **60**, 613, 2002.
26. Greenwald, S.E., and Berry, C.L. Improving vascular grafts: the importance of mechanical and haemodynamic properties. J. Pathol. **190**, 292, 2000.
27. Salacinski, H.J., Goldner, S., Giudiceandrea, A., Hamilton, G., Seifalian, A.M., Edwards, A., and Carson, R.J. The mechanical behavior of vascular grafts: a review. J. Biomater. Appl. **15**, 241, 2001.
28. Ruoslahti, E., and Pierschbacher, M.D. New perspectives in cell adhesion: RGD and integrin. Science **238**, 491, 1987.
29. Weinberg, C.B., and Bell, E. A blood vessel model constructed from collagen and cultured vascular cells. Science **231**, 397, 1986.
30. L'Heureux, N., Germain, L., Labbe, R., and Auger, F.A. In vitro construction of a human blood vessel from cultured vascular cells: amorphologic study. J. Vasc. Surg. **17**, 499, 1993.
31. Matthews, J.A., Stitzel, J.D., Wnek, G.E., Simpson, D.G., and Bowlin, G.L. Smooth muscle cell migration in electrospun poly(lactic acid) and collagen/elastin. Cardiovasc. Pathol. **11**, 13, 2002.
32. Nerem, R.M., and Seliktar, D. Vascular tissue engineering. Annu. Rev. Biomed. Eng. **3**, 225, 2001.
33. Dewey, C.F., Jr., Bussolari, S.R., Gimbrone, M.A., Jr., and Davies, P.F. The dynamic response of vascular endothelial cells to fluid shear stress. J. Biomech. Eng. **103**, 177, 1981.
34. Jeong, S.I., Kwon, J.H., Lim, J.I., Cho, S.W., Jung, Y., Sung, W.J., Kim, S.H., Kim, Y.H., Lee, Y.M., Kim, B.S., Choi, C.Y., and Kim, S.J. Mechano-active tissue engineering of vascular smooth muscle using pulsatile perfusion bioreactors and elastic PLCL scaffolds. Biomaterials **26**, 1405, 2005.
35. Lee, C.H., Shin, H.J., Cho, I.H., Kang, Y.M., Kim, I.A., Park, K.D., and Shin, J.W. Nanofiber alignment and direction of mechanical strain affect the ECM production of human ACL fibroblast. Biomaterials **26**, 1261, 2005.

Address reprint requests to:
Wei He, M.Sc.
Nanobioengineering Labs
National University of Singapore
Singapore

E-mail: hewei@nus.edu.sg

This article has been cited by:

1. Dong Yixiang , Thomas Yong , Susan Liao , Casey K. Chan , S. Ramakrishna . 2008. Degradation of Electrospun Nanofiber Scaffold by Short Wave Length Ultraviolet Radiation Treatment and Its Potential Applications in Tissue Engineering. *Tissue Engineering Part A* **14**:8, 1321-1329. [Abstract] [PDF] [PDF Plus] [Supplementary material]
2. Megan E. Francis , Shiri Uriel , Eric M. Brey . 2008. Endothelial Cell–Matrix Interactions in Neovascularization. *Tissue Engineering Part B: Reviews* **14**:1, 19-32. [Abstract] [PDF] [PDF Plus]
3. Megan E. Francis , Shiri Uriel , Eric M. Brey . Endothelial Cell–Matrix Interactions in Neovascularization. *Tissue Engineering*, ahead of print. [Abstract] [PDF] [PDF Plus]
4. Ramalingam Murugan , Seeram Ramakrishna . 2007. Design Strategies of Tissue Engineering Scaffolds with Controlled Fiber Orientation. *Tissue Engineering* **13**:8, 1845-1866. [Abstract] [PDF] [PDF Plus]

Available online at www.sciencedirect.com
SCIENCE DIRECT®
Biomaterials 26 (2005) 7606–7615
Biomaterials
www.elsevier.com/locate/biomaterials

Fabrication of collagen-coated biodegradable polymer nanofiber mesh and its potential for endothelial cells growth

Wei He[a,*], ZuWei Ma[b], Thomas Yong[a], Wee Eong Teo[c], Seeram Ramakrishna[a,b,c]

[a]*Division of Bioengineering, National University of Singapore, 9 Engineering Drive 1, Singapore 117576, Singapore*
[b]*Nanoscience and Nanotechnology Initiative, National University of Singapore, 9 Engineering Drive 1, Singapore 117576, Singapore*
[c]*Department of Mechanical Engineering, National University of Singapore, 9 Engineering Drive 1, Singapore 117576, Singapore*

Received 21 January 2005; accepted 16 May 2005
Available online 5 July 2005

Abstract

Endothelialization of biomaterials is a promising way to prevent intimal hyperplasia of small-diameter vascular grafts. The aim of this study was to design a nanofiber mesh (NFM) that facilitates viability, attachment and phenotypic maintenance of human coronary artery endothelial cells (HCAECs). Collagen-coated poly(L-lactic acid)-*co*-poly(ε-caprolactone) P(LLA-CL 70:30) NFM with a porosity of 64–67% and a fiber diameter of 470 ± 130 nm was fabricated using electrospinning followed by plasma treatment and collagen coating. The structure of the NFM was observed by SEM and TEM, and mechanical property was studied by tensile test. The presence of collagen on the P(LLA-CL) NFM surface was verified by X-ray photoelectron spectroscopy (XPS) and quantified by colorimetric method. Spatial distribution of the collagen in the NFM was visualized by labelling with fluorescent probe. The collagen-coated P(LLA-CL) NFM enhanced the spreading, viability and attachment of HCAECs, and moreover, preserve HCAEC's phenotype. The P(LLA-CL) NFM is a potential material for tissue engineered vascular graft.

Keywords: Nanofiber; PLLA; PCL; Collagen; Coating; Endothelial cells; Tissue engineering; Vascular grafts

1. Introduction

The main reason for the long-term failure of small-diameter (<6 mm) vascular grafts is due to the occlusion (thrombus formation) in the early phase followed by a continuous and excessive tissue ingrowth (intimal hyperplasia) in the chronic phase, both of which are caused by the immunoreactions towards the implanted materials [1]. Tissue engineered vascular grafts fabricated with biodegradable materials provide an approach to obtain vascular substitute with long-term patency. Upon complete degradation, the scaffold will not leave prosthetic materials to keep stimulating foreign body reactions. However, methods still need to be taken to prevent the intimal hyperplasia during the early days after the implantation of the scaffold. One of the effective approaches to prevent thrombus and enhance graft survival includes endothelial cells (ECs) seeding onto synthetic materials to render the surface anti-thrombogenic [2] because endothelial cells can release factors to control thrombogenesis or fibrinolysis, and platelet activation or inhibition [3]. However endothelialization has always been limited because attached ECs often detach from the surface upon exposure to blood circulation [4]. Thus natural extracellular matrix (ECM) proteins have been used to modify the surface of vascular graft to introduce cell recognition sites to induce cell–material interactions [2].

Polymeric nanofibers fabricated by electrospinning technology has received great interest in recent years due to the nanostructured morphology of the nanofibers

*Corresponding author. Tel.: 65 6874 8929; fax: 65 6874 3346.
E-mail addresses: hewei@nus.edu.sg (W. He), nnimzw@nus.edu.sg (Z. Ma), engyongt@nus.edu.sg (T. Yong), engtwe@nus.edu.sg (W.E. Teo), seeram@nus.edu.sg (S. Ramakrishna).

0142-9612/$ - see front matter © 2005 Elsevier Ltd. All rights reserved.
doi:10.1016/j.biomaterials.2005.05.049

mimicking the natural extracellular matrix, which is composed of three-dimensional networks of nanoscaled fibrous proteins embedded in a glycosaminoglycan (GAG) hydrogel [5]. Studies have already been made in the application of polymer nanofibers for tissue engineering of bone [6], blood vessel [7–10], cartilage [11–12], cardiac tissue [13], peripheral nerve system (PNS) [14], ligament [15], liver [16] and skin [17]. More importantly, the non-woven polymer nanofiber mesh (NFM) has a similar structure with natural basement membrane, which lies under the monolayer of endothelial cells in blood vessel [18]. Also the basement membrane shows a nano- to submicron-scale topography of ECM macromolecules, including fiber mesh, pores, ridges, grooves and peak valleys [19], which are also the features of the NFM.

The objective of this study was to fabricate collagen-coated biodegradable NFM, and evaluate the EC behaviors on it. We chose the copolymer from the biodegradable aliphatic polyesters family, random poly(L-lactic acid)-*co*-poly(ε-caprolactone) P(LLA-CL 70:30), because the degradation rate of the copolymer can be controlled readily by adjusting the ratio of two components. The collagen-coated P(LLA-CL) NFM was fabricated through plasma treatment of the electrospun P(LLA-CL) NFM followed by the collagen coating. The behavior of human coronary artery endothelial cells (HCAECs) on the collagen-coated polymer NFM was analyzed with respect to cell morphology, viability and attachment and phenotypic studies.

2. Materials and methods

2.1. Materials

The random poly(L-lactic acid)-*co*-poly(ε-caprolactone) P(LLA-CL 70:30) was bought from Boehringer Ingelheim (Germany) with a molecular weight of 150 kDa. Dichloromethane (DCM), *N*, *N*-dimethylformamide (DMF) and hydrochloric acid (HCl) were bought from Merck (USA). Collagen Type I (calf skin) and 1, 1, 1, 3, 3, 3-hexafluoro-2-propanol (HFP) were purchased from Sigma (Sigma-Aldrich, MO, USA). HCAECs were obtained from Biowhittaker (New Jersey, USA). The endothelial cell basal medium (Clonetics™ EBM®-2) and the growth factors were purchased from Cambrex (New Jersey, USA). CMFDA fluorescent CellTracker probe was purchased from Molecular Probe (Eugene, OR, USA).

2.2. Methods

2.2.1. Fabrication of the P(LLA-CL) NFM

For electrospinning of the P(LLA-CL) NFM, the P(LLA-CL 70:30) (10 wt %) solution in DCM and DMF (70:30 wt:wt) was added into a plastic syringe with a needle (inner diameter, 0.21 mm). With the aid of a syringe pump, the solution was injected out at a feed-rate of 0.5 ml/h. Electrospinning voltage was applied to the needle at 10 kV using a high-voltage power supply (Gamma High Voltage Research, USA). The resultant nanofibers were collected on an aluminum collector [7]. For the cell culture in the 24-well plate, coverslips (15 mm in diameter) were put onto the aluminum to collect the NFM.

The thickness of the P(LLA-CL) NFM was measured by a micrometer (Mitutoyo, Japan) and its apparent density and porosity were calculated using the following equations [10]:

$$\text{NFM apparent density (g/cm}^3\text{)} = \frac{\text{NFM mass (g)}}{\text{NFM thickness (cm)} \times \text{NFM area (cm}^2\text{)}},$$

$$\text{NFM porosity} = \left(1 - \frac{\text{NFM apparent density (g/cm}^3\text{)}}{\text{bulk density of P(LLA-CL) (g/cm}^3\text{)}}\right) \times 100\%.$$

2.2.2. Collagen coating on the P(LLA-CL) NFM

The complete surface modification scheme for P(LLA-CL) NFM is shown in Fig. 1. Briefly, air plasma treatment of the P(LLA-CL) NFM was carried out in an inductive coupled radio frequency glow discharge plasma cleaner (Harrick, PDC-001, USA). The air plasma treatment lasted for 5 min with the radio frequency power set as 30 W. Plasma treatment can increase the surface hydrophilicity of materials [20,21], which make the NFM wettable by collagen solution. The plasma-treated NFM was immersed into the collagen solution in 0.01 M HCl with a concentration of 290 μg/ml at 4 °C overnight, and then was dried under room temperature.

2.2.3. Characterization of the NFM

SEM micrographs of the NFM were obtained on a JSM-5800LV scanning electron microscope (JEOL, Japan). TEM micrographs of the NFM were obtained from a JEM-2010F FasTEM field emission electron microscope (JEOL, Japan) operated at 100 keV. Tensile tests were carried out using a 5848 microtester (Instrom, Canton, MA) at a stroke rate of 10 mm/min with a 40 mm gauge length. The NFM was prepared in a rectangular (10 × 60 mm) shape with a thickness around 20 μm for the test.

Wettabilities of the P(LLA-CL) NFM and film before and after plasma treatment were measured by sessile drop contact angle measurement using a VCA Optima Surface Analysis System (AST products, Billerica, MA). To get water contact angle on plane P(LLA-CL) surface, P(LLA-CL) films were prepared by a solvent casting (SC) method described in [7] in detail.

XPS spectra of the NFM were obtained on a VG Escalab 2201-XL Base System (Thermo VG Scientific, England) with a take-off angle of 90°.To get pure collagen NFM's spectrum, collagen nanofibers were fabricated by dissolving collagen in 1, 1, 1, 3, 3, 3-hexafluoro-2-propanol (HFP) and then electrospinning into nanofibers.

The amount of collagen coated onto the P(LLA-CL) NFM was measured by the BCA Protein Assay Kit (Pierce, USA) according to the RT (room temperature) Test Tube Protocol provided by the manufacturer. Briefly, the collagen-coated P(LLA-CL) NFM was immersed in 0.1 ml PBS together with

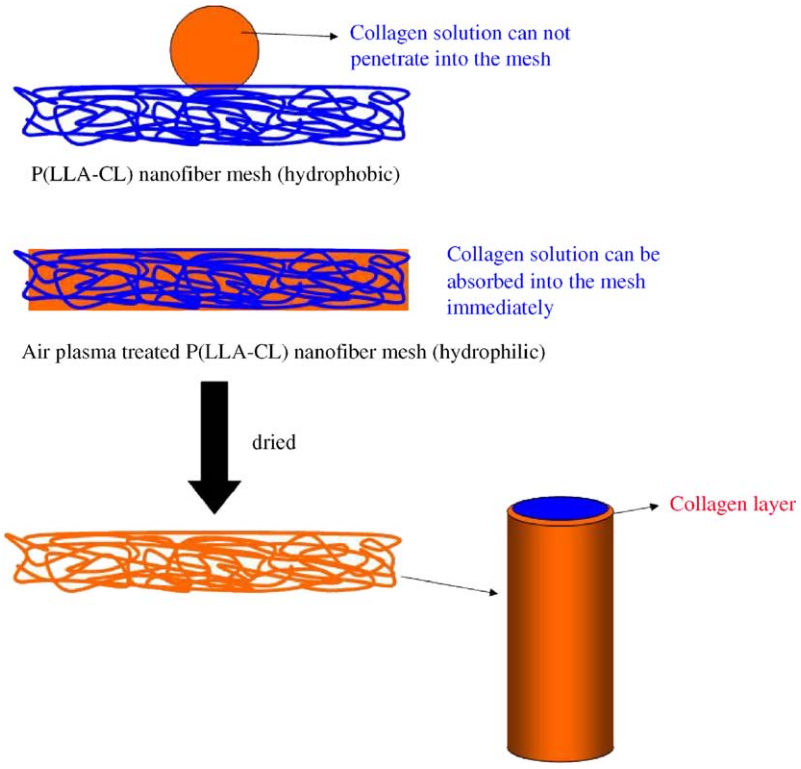

Fig. 1. Schematic representation of the plasma treatment and collagen coating of the electrospun P(LLA-CL) NFM.

2 ml working reagent at room temperature for 2 h, and then the absorbance at 562 nm was measured. The collagen concentration was calculated from the collagen standard curve.

To visualize the collagen distribution, P(LLA-CL) NFM coated with rhodamine B isothiocyanate (RBITC, Sigma, USA) labeled collagen was observed on a laser scanning confocal microscope (LSCM, Leica, Germany). The RBITC-labeled collagen was prepared as follows: collagen ($M_w = 285$k) solution (1 mg/ml) in 0.01 M HCl was mixed with the RBITC ($M_w = 536.1$) at the molar ratio of rhodamine to collagen 50:1. The mixed solution was incubated in darkness at RT for 3 h and then added into a dialysis tubing cellulose membrane (molecular weight cutoff, MWCO = 12,400) and dialysed in 0.01 M HCl solution until no more RBITC can be released into the HCl solution.

2.2.4. *In vitro culture of HCAECs*

HCAECs were bought at passage 3. The cells were cultured in Clonetics™ EBM®-2 complete medium supplemented with 5% fetal bovine serum, penicillin (100 units/ml) and streptomycin (100 μg/ml). The medium was replaced every 4 days and cultures were maintained in a humidified incubator at 37 °C with 5% CO_2. When the cells reached 80–90% confluence (5×10^4 cells/cm^2), they were trypsinized and subcultured at 1:3 ratios.

2.2.5. *HCAECs morphology, viability and attachment study*

Cell morphology was studied using LSCM and SEM. HCAECs were seeded at a density of 3×10^4 cells/cm^2 and observed 3 days later. For LSCM observation, live cells were stained with green fluorescent probe 5-chloromethyl fluorescein diacetate (CMFDA) and observed under LCSM (excitation 492 nm, emission 517 nm). Cells viability and attachment were determined by the colorimetric MTS assay (CellTiter 96® AQ_{ueous} One Solution Cell Proliferation Assay, Promega, USA).

2.2.6. *HCAECs phenotype study*

After 3 days' culturing at a seeding density of 3×10^4 cells/cm^2, HCAECs were washed with PBS, fixed with 2.5% paraformaldehyde and blocked by 2% BSA. HCAECs were then incubated for 2 h at 37 °C with primary antibody (mouse anti-human platelet endothelial cell adhesion molecule-1 (PECAM-1, CD 31)) (Cymbus Biotechnology, UK) diluted at 1:50. After washing, fluorescein isothiocyanate (FITC) labeled rabbit anti-mouse IgG (Chemicon, USA) diluted at 1:50 was added and incubated for 2 h at 37 °C, followed by washing and counterstaining with PI (2.5 μg/ml) for 1 min at 37 °C. The immunostained cellular construct samples were then mounted on glass slides with FluorSave™ reagent (CALBIOCHEM, Germany), and viewed under LSCM.

2.2.7. *Statistical analysis*

Data were made at least in triplicate and expressed as mean ± standard deviation (SD). Each experiment was repeated two or three times. Statistical analysis was carried out for HCAECs viability and attachment studies using one-way ANOVA testing by SPSS for Windows (SPSS Inc., Copyright

1989–2002) version 11.5.0. Significant difference between data groups was determined by the Student–Newman–Keuls (SNK) post hoc test ($p<0.05$).

3. Results and discussion

3.1. Morphology of the P(LLA-CL) NFM

Morphology of the P(LLA-CL) NFM, plasma-treated (5 min) P(LLA-CL) NFM and collagen-coated P(LLA-CL) NFM is shown in Fig. 2, which shows the randomly interconnected structure and smooth morphology of the NFM. TEM analysis of a single P(LLA-CL) nanofiber with a diameter of 390 nm verified the nanometer scale of the NFM. The diameter of the nanofiber was in the range of 200–600 nm (90% nanofibers) with a mean diameter of 470 ± 130 nm by image analysis software (ImageJ, National Institutes of Health, USA). NFM with a thickness of around 26 μm was obtained through 2 h electrospinning. With the known bulk density of the P(LLA-CL) (1.2–1.3 g/cm^3), the porosity of the P(LLA-CL) NFM can be calculated by measuring its apparent density, the results of which are summarized in Table 1.

Porosity is an important parameter for tissue engineering scaffolds. Vascular grafts should be porous, the porosity of which should allow cell infiltration from the adventitial side while maintaining hemostasis, as well as sufficient mass transfer of gases and nutrients [22]. It is generally accepted that a higher-porosity vascular graft exhibits high patency [23]. Longer fibril ePTFE (60 and 90 μm) provided a much higher degree of endothelialization and collagen production than the shorter fibril groups (20 and 40 μm) [24].

The porosity of the electrospun P(LLA-CL) NFM with diameter 470 ± 130 nm is around 60–70%, which is comparable to the porosity of scaffolds made from phase separation and solid free-form fabrication, which is between 60% and 90% [25]. Pores of the NFM are formed by nanofibers lying loosely upon each other which are different from "real" isotropic pores made by using particles or bubbles when the scaffold is solidified. It is also not easy to create pores by electrospinning with well-defined shape as the solid free-form fabrication made. However, the overall nanofiber-network architecture of NFM could better mimic the natural ECM such as basement membrane which shows a nano- to submicron-scale topography of macromolecules, including fiber mesh, pores, ridges, grooves and peak valleys [19]. This bio-mimicry property of nanofibers may possess unique advantage in application for tissue engineering scaffolds.

3.2. Mechanical properties of the P(LLA-CL) NFM

Fig. 3 shows the typical stress–strain curve of the P(LLA-CL) NFM under tensile loading. Tensile properties obtained from two independent experiments, together with that for Dacron and coronary artery, were summarized in Table 2. For P(LLA-CL) NFM, the average tensile modulus is 44 ± 4 MPa and tensile strength is 6.3 ± 1.4 MPa with the ultimate strain of $175\pm49\%$. The desirable distension property of the P(LLA-CL) NFM quantified in ultimate strain may result from randomly orientated fibers rearranging

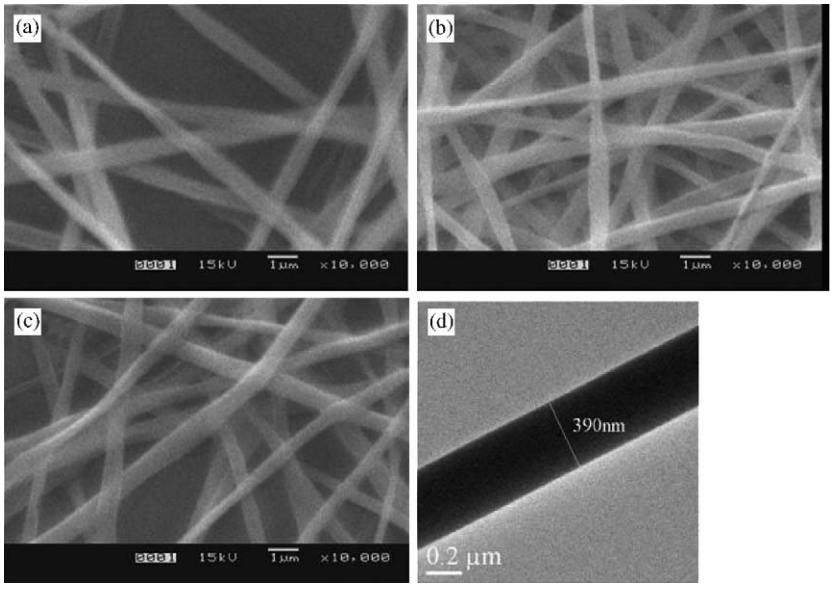

Fig. 2. SEM (a, b, c) and TEM (d) micrographs of the (a, d) P(LLA-CL) NFM, (b) plasma-treated P(LLA-CL) NFM and (c) collagen-coated P(LLA-CL) NFM.

Table 1
Diameter, thickness, apparent density and porosity of the P(LLA-CL) NFM

Diameter (nm)	Thickness (μm)	Mass per unit area (mg/cm^2)	Apparent density (g/cm^3)	Porosity (%)
470 ± 130	26 ± 5	1.13 ± 0.20	0.43 ± 0.08	64–67

Data are representative of three independent experiments and represented as mean ± SD ($n = 6$).

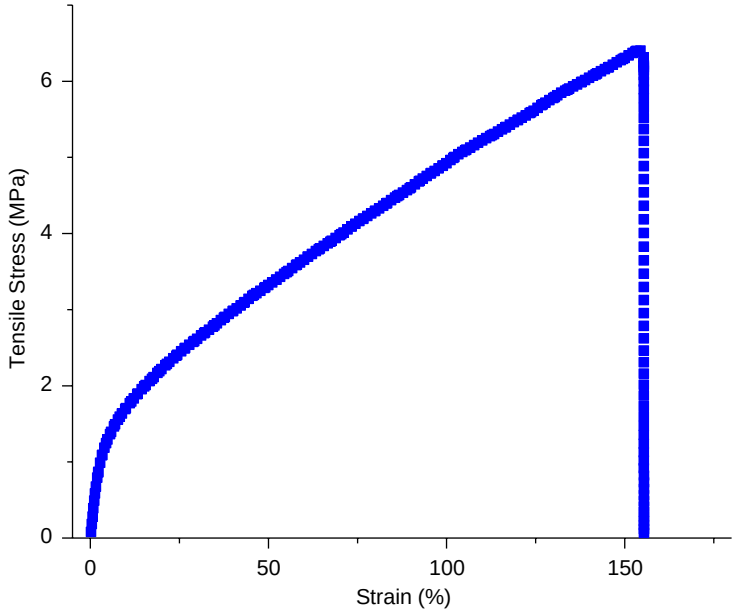

Fig. 3. Stress–strain curve for the electrospun P(LLA-CL) NFM under tensile loading.

Table 2
Tensile properties of the electrospun P(LLA-CL) NFM, Dacron (PET) and coronary artery

	P(LLA-CL) NFM	Dacron (PET)[a]	Coronary artery[b]
Tensile modulus (MPa)	44 ± 4	14,000	—
Tensile strength (MPa)	6.3 ± 1.4	170–180	1.40–11.14
Ultimate strain (%)	175 ± 49	—	45–99

Data are representative of two independent experiments and represented as mean ± SD ($n = 3$) for P(LLA-CL) NFM group.
[a]See Ref. [27].
[b]See Ref. [9].

themselves in the direction of stress [26]. In theory, the random NFM would become gradually aligned during uniaxial tensile test; thus the tensile modulus of it would increase accordingly. Such a phenomenon was not found from the stress–strain curve where the slope was maintained initially and then began to decrease. Similar results were also reported by other researchers [19,26]. One of the possible reasons may be due to the fracture of fibers simultaneously during fiber rearrangement.

The P(LLA-CL) NFM shows much smaller stiffness compared to the Dacron (PET), the commonly used large-diameter vascular grafts, which has a tensile strength of 170–180 MPa in orientated form and a tensile modulus of about 14,000 MPa [27]. The tensile properties of the NFM are closer to that of the natural coronary artery than Dacron (Table 2). Ideally less stiff (more compliant) and biodegradable scaffolds like P(LLA-CL) NFM are better choices for constructing a completely biological and fully functional neo-artery [27].

3.3. Plasma treatment of the P(LLA-CL) NFM

To make the collagen solution easily go into the porous NFM, the hydrophobic P(LLA-CL) NFM was treated by air plasma to make it highly wettable. The

effectiveness of the plasma treatment to increase NFM's wettability was checked by water contact angle measurement, the results of which were summarized in Table 3. P(LLA-CL) NFM exhibited different water contact angles from the film due to different surface structure. The P(LLA-CL) NFM and film were both hydrophobic in nature before plasma treatment and the NFM showed higher contact angle than the film. Although the original P(LLA-CL) NFM showed high water contact angle, after plasma treatment, it became highly wettable. The water drop, upon contact with the plasma treated P(LLA-CL) NFM, was immediately absorbed into the NFM, giving a zero apparent water contact angle. Although the film also tended to be more hydrophilic after plasma treatment, the contact angle difference is not so big compared with the NFM. It was also shown in Table 3 that plasma treatment of 5 min is enough to increase the NFM's wettability. The big difference of electrospun polymer NFM's wettability before and after plasma treatment was explained in [10] in detail.

Table 3
Water contact angles of the P(LLA-CL) NFM and P(LLA-CL) film before (0 min) and after plasma treatment for different times (5, 15, 30 min)

Plasma treatment time (min)	P(LLA-CL) NFM (deg)	P(LLA-CL) film (deg)
0	129±1	96±6
5	0±0	60±1
15	0±0	57±3
30	0±0	55±3

Data are representative of three independent experiments and represented as mean±SD ($n = 6$).

3.4. Characterization of the collagen-coated P(LLA-CL) NFM

The presence of collagen on the nanofiber's surface was confirmed by the appearance of the N1S peak (indicated in N atomic ratio) in the XPS spectrum of the collagen-coated P(LLA-CL) NFM (Table 4), while no nitrogen peak was found in the pure P(LLA-CL) NFM's spectrum. Compared with the pure electrospun collagen NFM (15.1%), much less nitrogen was found on the collagen-coated P(LLA-CL) NFM (5.2%).

To visualize spatial distribution of the collagen coated in the P(LLA-CL) NFM, rhodamine-labeled collagen was coated onto the NFM and observed under LSCM. It is shown in the 2D image of NFM (Fig. 4a) that collagen was uniformly coated on the surface of every nanofiber. Depth projection images for 3D micrographs (Fig. 4b), constructed from 20 horizontal slices of step size 1 μm, also exhibit the uniform collagen coating.

Table 4
Atomic ratio of C, N and O on the surface of the P(LLA-CL) NFM, the collagen-coated P(LLA-CL) NFM and the pure electrospun collagen NFM determined by XPS

NFM	C atomic ratio (%)	N atomic ratio (%)	O atomic ratio (%)
P(LLA-CL)	65.9	0	34.1
Collagen-coated P(LLA-CL)	61.5	5.2	33.3
Collagen	61.6	15.1	23.3

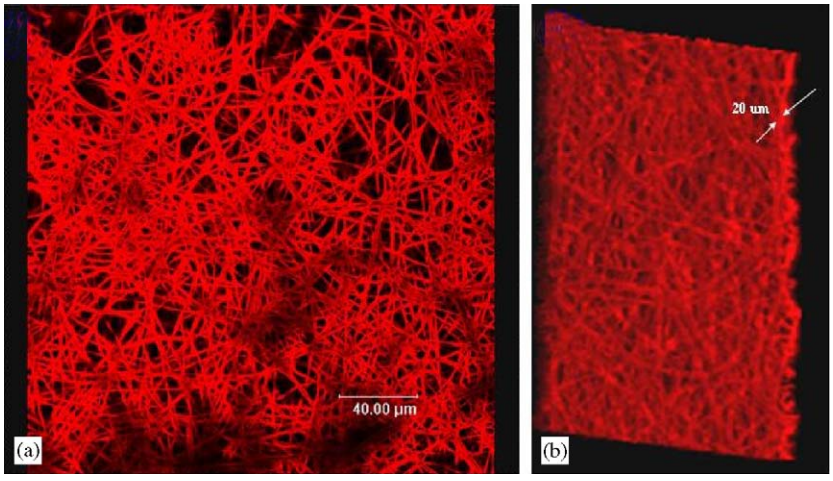

Fig. 4. 2-D (a) and 3-D (b) LSCM micrographs of the collagen-coated P(LLA-CL) NFM. The collagen was labeled with RBITC. Depth projection images for 3D micrographs were constructed from 20 horizontal slices of step size 1 μm.

By BCA protein assay analysis, the amount of collagen in the P(LLA-CL) NFM was measured and normalized by NFM's weight. It was found that $15 \pm 5\,\mu g$ collagen was coated per 1 mg NFM.

3.5. Morphology of HCAECs

Fig. 5 shows the fluorescent and SEM micrographs of HCAECs on TCPS (a, d), P(LLA-CL) NFM (b, e) and the collagen-coated P(LLA-CL) NFM (c, f). HCAECs cultured on the P(LLA-CL) NFM were rounded in shape instead of a spreading morphology, whereas on the collagen-coated P(LLA-CL) NFM HCAECs adopted a spreading polygonal shape which is typical of the normal cell morphology on TCPS. These characteristics are prerequisites for an effective endothelialization of vascular graft materials.

3.6. HCAECs viability and attachment studies

Viability of HCAECs at day 1, 3, 5, 7 cultured on the TCPS, collagen-coated P(LLA-CL) NFM and unmodified P(LLA-CL) NFM after cell seeding is shown in Fig. 6. HCAECs viability on the collagen-coated P(LLA-CL) NFM was obviously increased compared with the unmodified NFM from day 3 onwards ($p < 0.05$).

The attachment of HCAECs to TCPS, collagen-coated P(LLA-CL) NFM and unmodified P(LLA-CL) NFM is shown in Fig. 7. More cells attached on the collagen-coated P(LLA-CL) NFM than the unmodified P(LLA-CL) NFM. HCAECs were found to attach on the collagen-coated P(LLA-CL) NFM at very similar rate as on the TPCS. This is because collagen is the most abundant ECM protein with both structural and adhesive functions, facilitating cell adhesion through the integrin receptors [28].

3.7. HCAECs phenotype analysis

The surface adhesion protein characteristically expressed by ECs was studied using immunofluorescent microscopy. Platelet endothelial cell adhesion molecule-1 (PECAM-1, CD31) is an universal EC marker, expression of which can represent the differentiation status of endothelial cells. Fig. 8 shows the LSCM images of immuno-stained HCAECs cultured on TCPS and the collagen-coated P(LLA-CL) NFM. The P(LLA-CL) NFM was red in color because rhodamine-labeled collagen was coated on the nanofiber's surface. The white arrows indicate that PECAM-1 staining occurs mainly at cell–cell interfaces. HCAECs cultured on the collagen-coated P(LLA-CL) NFM have a similar pattern of PECAM-1 staining (Fig. 8b) as compared to the cells on TCPS (Fig. 8a). The results indicated preservation of EC's characteristic phenotype on both TCPS and the collagen-coated P(LLA-CL) NFM.

4. Conclusions

After the electrospun P(LLA-CL 70:30) NFM was treated with air plasma, collagen was effectively

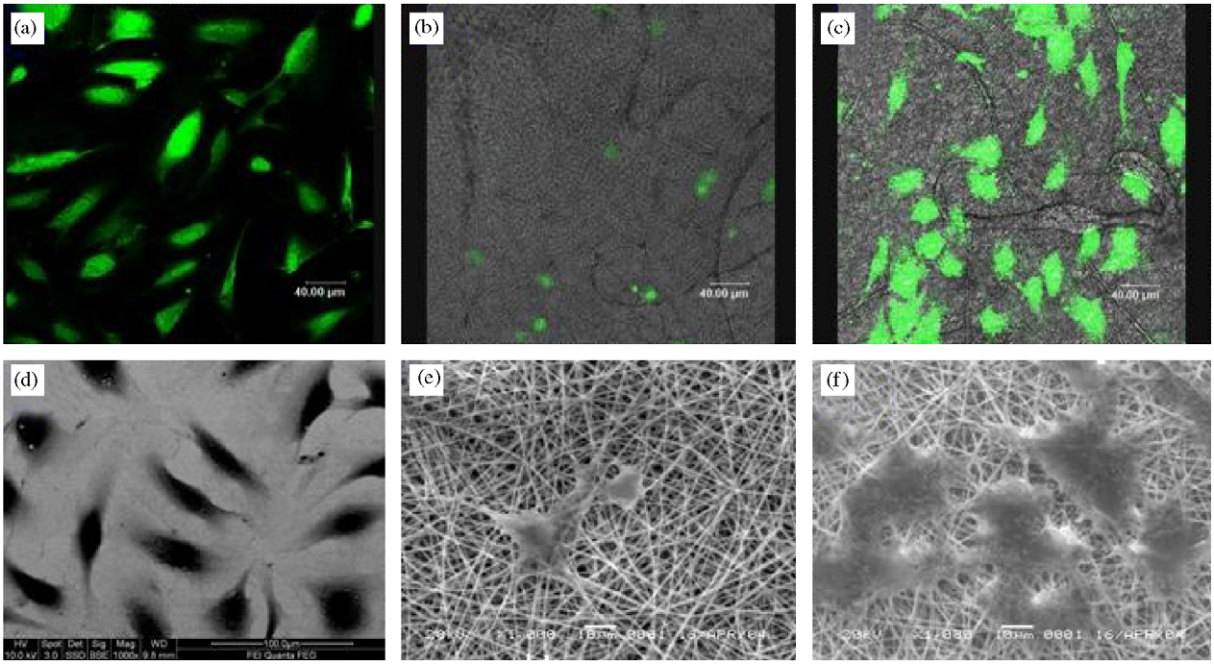

Fig. 5. LSCM and SEM images of HCAECs cultured on (a, d) TCPS, (b, e) P(LLA-CL) NFM and (c, f) collagen-coated P(LLA-CL) NFM. HCAECs were seeded at a density of 3×10^4 cells/cm^2 and stained with CMFDA for fluorescent observation or fixed for SEM study 3 days later.

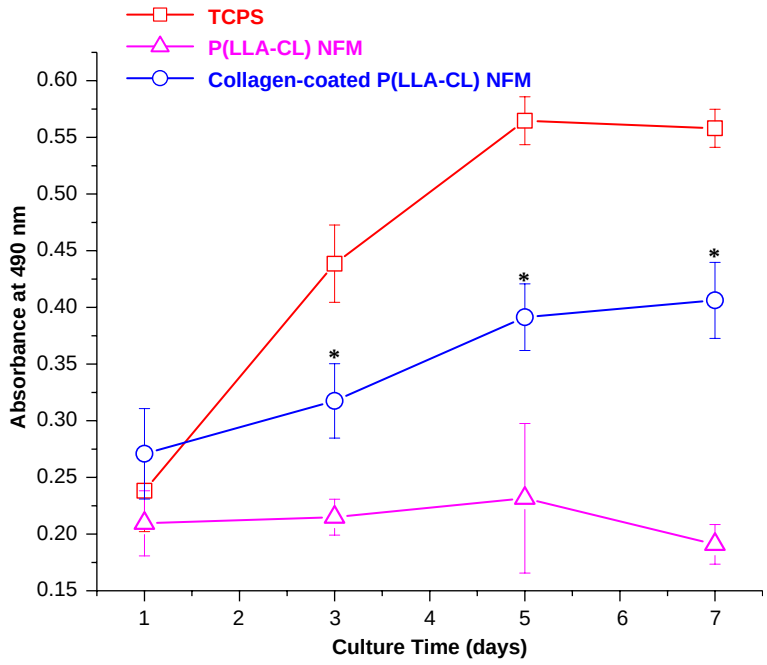

Fig. 6. Viability of HCAECs on the TCPS, P(LLA-CL) NFM and collagen-coated P(LLA-CL) NFM. Cells were seeded at a density of 1.5×10^4 cells/cm^2 and cultured for a period of 7 days. Data are representative of three independent experiment and all data points plotted as mean $\pm$ SD ($n = 3$) (*$p < 0.05$ compared to the P(LLA-CL) NFM group).

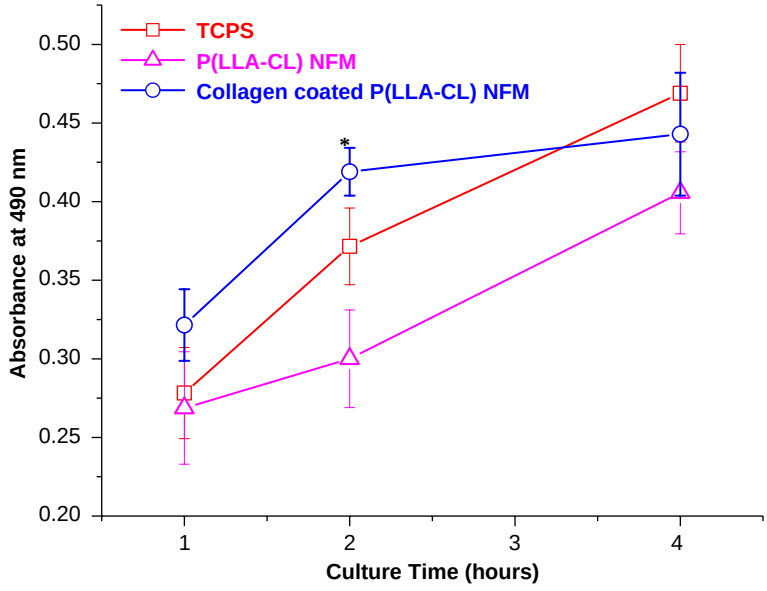

Fig. 7. Attachment of HCAECs on the TCPS, P(LLA-CL) NFM and collagen-coated P(LLA-CL) NFM. Cells were seeded at a density of 3×10^4 cells/cm^2. Data are representative of three independent experiment and all data points plotted as mean $\pm$ SD ($n = 3$) (*$p < 0.05$ compared to the P(LLA-CL) NFM group).

coated onto nanofiber's surface. The collagen was found to be evenly coated throughout the NFM. The amount of collagen was quantified to be 15 ± 5 μg per mg of NFM. The collagen-coated P(LLA-CL) NFM enhanced endothelialization, as observed in a spreading cell morphology, increased cell viability and attachment, and phenotypic maintenance of the cells. The collagen-coated P(LLA-CL) NFM also showed mechanical properties suitable for vascular graft.

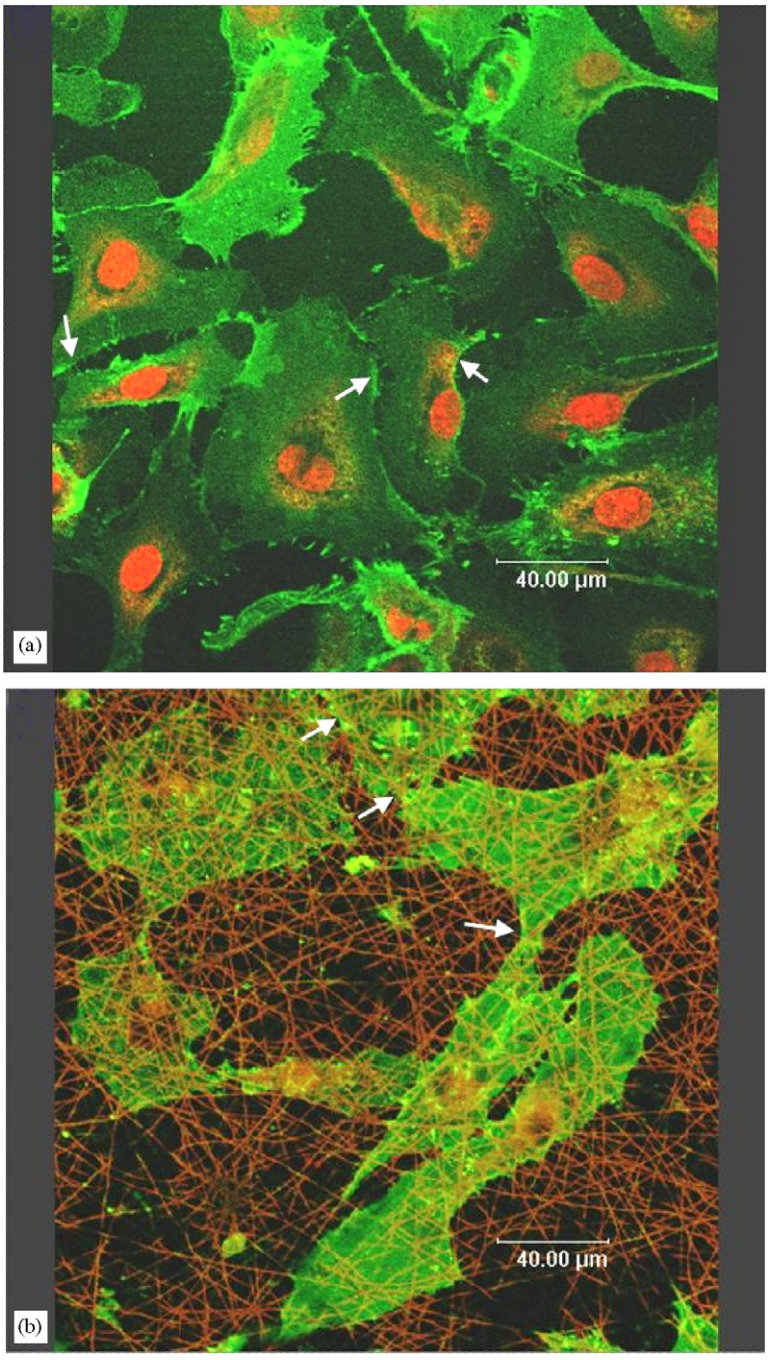

Fig. 8. Immunofluorescent staining of PECAM-1(CD31) on HCAECs cultured for 3 days on TCPS (a) and the collagen-coated P(LLA-CL) NFM. HCAECs were seeded at a density of 3×10^4 cells/cm^2. The RBITC-labeled collagen-coated NFM was red color. White arrows indicate strong PECAM-1 expression at cell–cell interfaces.

Acknowledgements

We thank Dr. Jun Li, Dr. Xiaojing Xu and Mr. Yanzhong Zhang for their help in the XPS, TEM and mechanical test experiments, respectively. This study was supported by the Academic Research Fund from the National University of Singapore.

References

[1] Matsuda T. Recent progress of vascular graft engineering in Japan. Artif Organs 2004;28:64–71.
[2] Shin H, Jo S, Mikos AG. Biomimetic materials for tissue engineering. Biomaterials 2003;24:4353–64.
[3] Luscher TF, Barton M. Biology of the endothelium. Clin Cardiol 1997;20(suppl. II):3–10.

[4] Xue L, Greisler HP. Blood vessels. In: Lanza RP, editor. Principle of tissue engineering. San Diego: Academic Press; 2000. p. 427–46.
[5] Ma ZW, Kotaki M, Inai R, Ramakrishna S. Potential of nanofiber matrix as tissue engineering scaffolds. Tissue Eng 2005; 11:101–9.
[6] Yoshimoto H, Shin YM, Terai H, Vacanti JP. A biodegradable nanofiber scaffold by electrospinning and its potential for bone tissue engineering. Biomaterials 2003;24:2077–82.
[7] Xu CY, Inai R, Kotaki M, Ramakrishna S. Aligned biodegradable nanofibrous structure: a potential scaffold for blood vessel engineering. Biomaterials 2004;25:877–86.
[8] Mo XM, Xu CY, Kotaki M, Ramakrishna S. Electrospun P(LLA-CL) nanofiber: a biomimetic extracellular matrix for smooth muscle cell and endothelial cell proliferation. Biomaterials 2004;25:1883–90.
[9] Xu CY, Inai R, Kotaki M, Ramakrishna S. Electrospun nanofiber fabrication as synthetic extracellular matrix and its potential for vascular tissue engineering. Tissue Eng 2004;10: 1160–8.
[10] Ma ZW, Kotaki M, Yong T, He W, Ramakrishna S. Surface engineering of electrospun polyethylene terephthalate (PET) nanofibers towards development of a new material for blood vessel engineering. Biomaterials 2005;26:2527–36.
[11] Li WJ, Tuli R, Okafor C, Derfoul A, Danielson KG, Hall DJ, Tuan RS. A three-dimensional nanofibrous scaffold for cartilage tissue engineering using human mesenchymal stem cells. Biomaterials 2005;26:599–609.
[12] Li WJ, Danielson KG, Alexander PG, Tuan RS. Biological response of chondrocytes cultured in three-dimensional nanofibrous poly(epsilon-caprolactone) scaffolds. J Biomed Mater Res 2003;67:1105–14.
[13] Shin M, Ishii O, Sueda T, Vacanti JP. Contractile cardiac grafts using a novel nanofibrous mesh. Biomaterials 2004;25:3717–23.
[14] Bini TB, Shujun Gao, Ter Chyan Tan, Shu Wang, Aymeric Lim, Lim Ben Hai, Ramakrishna S. Electrospun poly(L-lactide-co-glycolide) biodegradable polymer nanofiber tubes for peripheral nerve regeneration. Nanotechnology 2004;15:1459–64.
[15] Lee CH, Shin HJ, Cho IH, Kang YM, Kim IA, Park KD, Shin JW. Nanofiber alignment and direction of mechanical strain affect the ECM production of human ACL fibroblast. Biomaterials 2005;26:1261–70.
[16] Chua KN, Lim WS, Zhang PC, Lu HF, Wen J, Ramakrishna S, Leong KW, Mao HQ. Stable immobilization of rat hepatocyte spheroids on galactosylated nanofiber scaffold. Biomaterials 2005; 26:2537–47.
[17] Li WJ, Laurencin CT, Caterson EJ, Tuan RS, Ko FK. Electrospun nanofibrous structure: a novel scaffold for tissue engineering. J Biomed Mater Res 2002;60:613–21.
[18] Albert B, Johnson A, Lewis J, Raff M, Roberts K, Peters, Walter P, editors. Molecular biology of the cell, 4th ed. New York: Garland Science; 2002. p. 1106–9.
[19] Keun Kwon I, Kidoaki S, Matsuda T. Electrospun nano- to microfiber fabrics made of biodegradable copolyesters: structural characteristics, mechanical properties and cell adhesion potential. Biomaterials 2005;26:3929–39.
[20] Chen M, Zamora PO, Som P, Pena LA, Osaki S. Cell attachment and biocompatibility of olytetrafluoroethylene (PTFE) treated with glow-discharge plasma of mixed ammonia and oxygen. J Biomater Sci-Polym Ed 2003;14:917–35.
[21] Wan YQ, Yang J, Yang JL, Bei JZ, Wang SG. Cell adhesion on gaseous plasma modified poly (L-lactide) surface under shear stress field. Biomaterials 2003;24:3757–64.
[22] Sullivan SJ, Brockbank KGM. Small-diameter vascular grafts. In: Lanza RP, editor. Principle of tissue engineering. San Diego: Academic Press; 2000. p. 447–54.
[23] Niklason LE, Seruya M. Small-diameter vascular grafts. In: Atala A, Lanza RP, editors. Methods of tissue engineering. San Diego: Academic Press; 2002. p. 905–13.
[24] Hirabayashi K, Saitoh E, Ijima H, Takenawa T, Kodama M, Hori M. Influence of fibril length upon ePTFE graft healing and host modification of the implant. J Biomed Mater Res 1992;26: 1433–47.
[25] Hutmacher DW. Scaffolds in tissue engineering bone and cartilage. Biomaterials 2000;21:2529–54.
[26] Stankus JJ, Guan J, Wagner WR. Fabrication of biodegradable elastomeric scaffolds with sub-micron morphologies. J Biomed Mater Res 2004;70:603–14.
[27] Salacinski HJ, Goldner S, Giudiceandrea A, Hamilton G, Seifalian AM, Edwards A, Carson RJ. The mechanical behavior of vascular grafts: a review. J Biomater Appl 2001;15:241–78.
[28] Ruoslahti E, Pierschbacher MD. New perspectives in cell adhesion: RGD and integrin. Science 1987;238:491–7.

TISSUE ENGINEERING
Volume 11, Number 9/10, 2005

Fabrication and Endothelialization of Collagen-Blended Biodegradable Polymer Nanofibers: Potential Vascular Graft for Blood Vessel Tissue Engineering

WEI HE, M.Sc.,[1] THOMAS YONG, Ph.D.,[1] WEE EONG TEO, B.Sc.,[2] ZUWEI MA, Ph.D.,[3] and SEERAM RAMAKRISHNA, Ph.D.[1–3]

ABSTRACT

Electrospun collagen-blended poly(L-lactic acid)-*co*-poly(ε-caprolactone) [P(LLA-CL), 70:30] nanofiber may have great potential application in tissue engineering because it mimicks the extracellular matrix (ECM) both morphologically and chemically. Blended nanofibers with various weight ratios of polymer to collagen were fabricated by electrospinning. The appearance of the blended nanofibers was investigated by scanning electron microscopy and transmission electron microscopy. The nanofibers exhibited a smooth surface and a narrow diameter distribution, with 60% of the nanofibers having diameters between 100 and 200 nm. Attenuated total reflectance-Fourier transform infrared spectra and X-ray photoelectron spectroscopy verified the existence of collagen molecules on the surface of nanofibers. Human coronary artery endothelial cells (HCAECs) were seeded onto the blended nanofibers for viability, morphogenesis, attachment, and phenotypic studies. Five characteristic endothelial cell (EC) markers, including four types of cell adhesion molecule and one EC-preferential gene (von Willebrand factor), were studied by reverse transcription-polymerase chain reaction. Results showed that the collagen-blended polymer nanofibers could enhance the viability, spreading, and attachment of HCAECs and, moreover, preserve the EC phenotype. The blending electrospinning technique shows potential in refining the composition of polymer nanofibers by adding various ingredients (e.g., growth factors) according to cell types to fabricate tissue-engineering scaffold, particularly blood vessel-engineering scaffold.

INTRODUCTION

ELECTROSPUN POLYMER NANOFIBERS have elicited great interest in tissue engineering because the nanostructured morphology of the nanofibers mimicks the natural extracellular matrix (ECM), which is composed of a three-dimensional network of nanoscaled fibrous proteins embedded in a glycosaminoglycan (GAG) hydrogel.[1] In addition to their morphology, which is similar to natural ECM, polymer nanofibers have additional desirable features as a tissue-engineering scaffold, such as their high porosity and high surface area-to-volume ratio.[2] Many studies have been carried out in the application of polymer nanofibers in the tissue engineering of bone,[3] blood vessels,[4–7] cartilage,[8,9] cardiac tissue,[10] peripheral nervous system (PNS),[11] ligament,[12] liver,[13] and skin.[14] In most of these studies, biodegradable polymer materials such as poly(caprolactone) (PCL), poly(L-lactide) (PLA), and poly(glycolide) (PGA) were used.

In addition to synthetic materials, naturally occurred materials such as collagen,[15,16] elastin,[17] silk protein,[18] fibrinogen,[19] chitosan,[20] dextran,[21] hyaluronic acid,[22] ca-

[1]Division of Bioengineering, [2]Department of Mechanical Engineering, and [3]Nanoscience and Nanotechnology Initiative, National University of Singapore, Singapore.

sein and lipase enzyme,[23] and even DNA[24] and virus[25] have also been electrospun into nanofibers, but far fewer works using these nanofibers as tissue-engineering scaffolds have been reported, perhaps because of the poor mechanical properties of natural materials on contacting water. For synthetic materials, the biggest disadvantage, however, is the lack of cell recognition signals.[26] These problems can be overcome by surface immobilization of natural materials on synthetic materials or simply by physically blending the two materials, which may improve the biocompatibility of the synthetic nanofibers while preserving the mechanical strength, thus combining the advantages of two types of materials.

The objective of our present study was to fabricate collagen-blended biodegradable polymer nanofibers, and to evaluate the behavior of cells on it. We chose a random copolymer from the biodegradable aliphatic polyester family, poly(L-lactic acid)-*co*-poly(ϵ-caprolactone) [P(LLA-CL), 70:30], because the degradation rate of this copolymer can be controlled readily by adjusting the ratio of the two components. The collagen-blended polymer [P(LLA-CL), 70:30] nanofibers were fabricated by electrospinning the collagen–polymer mixture solution with 1,1,1,3,3,3-hexafluoro-2-propanol (HFP) as solvent. The blended nanofibers, as a new type of a composite material, could be a biomimetic synthetic ECM both in fiber diameter and constituent components. The biocompatibility study was focused on the behaviors of human coronary artery endothelial cells (HCAECs) with respect to cell viability, morphology, attachment, and gene expression.

MATERIALS AND METHODS

Materials

Poly(L-lactic acid)-*co*-poly(ϵ-caprolactone) [P(LLA-CL), 70:30] copolymer was bought from Boehringer Ingelheim (Ingelheim, Germany), at a molecular mass of 150 kDa. 1,1,1,3,3,3-Hexafluoro-2-propanol (HFP) and collagen type I from calf skin were purchased from Sigma-Aldrich (St. Louis, MO). Human coronary artery endothelial cells (HCAECs) were obtained from Cambrex Bio Science Walkersville (Walkersville, NJ). Endothelial cell basal medium (Clonetics EBM-2) and growth factors were purchased from Cambrex Bio Science Walkersville. CMFDA fluorescent CellTracker probe was purchased from Molecular Probes (Eugene, OR). CellTiter 96 AQ_{ueous} One Solution assay was purchased from Promega (Madison, WI).

Fabrication of collagen-blended P(LLA-CL) nanofibers

P(LLA-CL) and collagen solutions (5 wt%) were prepared by mixing the components for 2 h at room temperature in 1,1,1,3,3,3-hexafluoro-2-propanol (HFP). The mixture was then placed in a plastic syringe with a needle tip diameter of 0.21 mm. With the aid of a syringe pump, the solution was dispersed at a feed rate of 1.2 mL/h. Electrospinning voltage was applied to the needle at 12-kV DC voltage, using a high-voltage power supply (Gamma High Voltage Research, Ormond Beach, FL). The electric field generated by the surface charge caused the solution drop at the tip of the needle to distort into a Taylor cone. Once the electric potential at the surface charge exceeded a critical value, the electrostatic forces would overcome the solution surface tension and a thin jet of solution would erupt from the surface of the cone. The schematic setup and the optimized parameters for fabrication of collagen-blended P(LLA-CL) nanofibers are shown in Fig. 1. The resultant nanofibers were collected on an aluminum collector located 12 cm from the needle tip. For cells cultured in a 24-well plate, coverslips (Assistent, 15 mm in diameter; Karl Hecht, Sondheim, Germany) were placed on top of the aluminum to collect the nanofiber sheet directly. The thickness of the nanofiber sheet was determined by the collection time. The thickness of the collagen-blended P(LLA-CL) nanofiber mesh (NFM) was measured with a micrometer (Mitutoyo, Kawasaki, Japan) and its apparent density and porosity were calculated according to the following equations:

$$\text{NFM apparent density (g/cm}^3\text{)} = \frac{\text{NFM mass (mg)} = 10}{\text{NFM thickness } (\mu\text{m}) \times \text{NFM area (cm}^2\text{)}}$$

$$\text{NFM porosity (\%)} = \left(1 - \frac{\text{NFM apparent density (g/cm}^3\text{)}}{\text{bulk density of PET (g/cm}^3\text{)}}\right) \times 100$$

where PET is polyethylene terephthalate (see Ma *et al.*[7]).

Fabrication of P(LLA-CL)–collagen films by solvent casting

Uniform smooth films of P(LLA-CL)–collagen (1:1, w/w) were generated by a solvent-casting (SC) method. Briefly, P(LLA-CL) and collagen were first dissolved at a concentration of 5 wt% in HFP. The resulting solution was then cast onto tissue culture polystyrene (TCPS). After solvent evaporation, the P(LLA-CL)–collagen-coated TCPS [hereafter referred to as P(LLA-CL)–collagen film] was placed in a vacuum dryer overnight to remove any remaining solvent.

Characterization of collagen-blended P(LLA-CL) nanofibers

Scanning electron microscopy (SEM) micrographs of collagen-blended P(LLA-CL) nanofibers were obtained

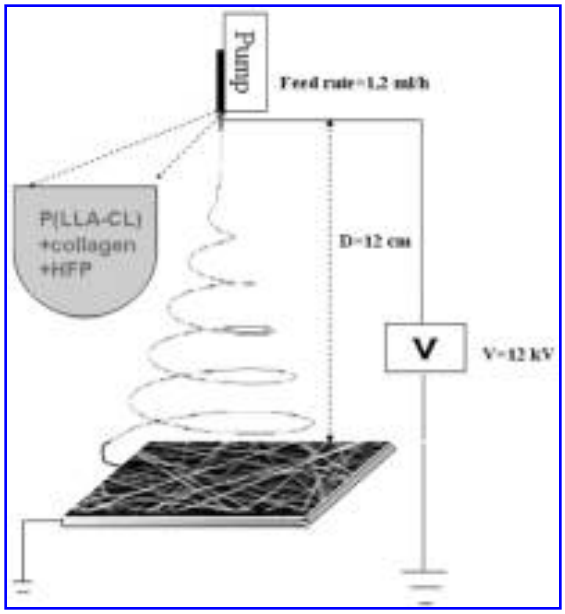

FIG. 1. Schematic setup and optimized operation parameters such as the voltage, feed rate, and collector distance for fabrication of the random collagen-blended P(LLA-CL) nanofibers by electrospinning. HFP, 1,1,1,3,3,3-hexafluoro-2-propanol.

with a JSM-5800LV scanning electron microscope (JEOL, Tokyo, Japan). Transmission electron microscopy (TEM) micrographs of the nanofibers were obtained with a JEM-2010F FasTEM field emission electron microscope (JEOL) operated at 100 keV. Electrospun nanofibers for the TEM observation were prepared by directly depositing the as-spun nanofibers onto copper grids that had been coated with a supportive Formvar film (Structure Probe, SPI Supplies Division, West Chester, PA).

Diameter range of the fabricated nanofibers was measured on the basis of SEM images, using image analysis software (ImageJ; National Institutes of Health, Bethesda, MD). Attenuated total reflectance Fourier transform infrared (ATR-FTIR) spectra were obtained with an AVATAR 380 FTIR machine (Thermo Electron, Waltham, MA). Surface chemistry analysis of the nanofibers was performed by X-ray photoelectron spectroscopy (XPS) (VG Escalab 2201-XL; Thermo VG Scientific/Thermo Electron, East Grinstead, UK) with a takeoff angle of 90°. The binding energy was referenced to the C1s of saturated hydrocarbon at 285.0 eV.

Tensile tests were carried out with a 5848 microtester (Instron, Norwood, MA) at a stroke rate of 10 mm/min and with a 40-mm gauge length. Nanofibers were rectangular (10 × 60 mm) in shape. This tensile test was performed in the same manner as standard mechanical tests for fabric materials.

In vitro *culture of human coronary artery endothelial cells*

Human coronary artery endothelial cells (HCAECs) were bought at passage 3. The cells were cultured in endothelial cell basal medium supplemented with EC growth supplements (vascular endothelial growth factor [VEGF], human epidermal growth factor [hEGF], human fibroblast growth factor-B [hFGF-B], insulin-like growth factor type I [IGF-I], hydrocortisone, and ascorbic acid), 5% fetal bovine serum, penicillin (100 units/mL), and streptomycin (100 μg/mL). The medium was replaced every 4 days and cultures were maintained in a humidified incubator at 37°C with 5% CO_2. When the cells reached 80–90% confluence (confluence density, 5×10^4 cells/cm^2), they were trypsinized and subcultured at 1:3 ratios.

Collagen-blended P(LLA-CL) nanofiber mesh was deposited on round 15 mm-diameter coverslips, which were placed into the wells of a 24-well tissue culture plate to exactly cover the well bottom. A small amount of implant-grade silicone adhesive (Silbione, MED ADH 4300 RTV; Rhodia, Boulogne-Billancourt, France) was applied along the edge of the nanofiber sheet to immobilize it on the glass surface. Experiments had been conducted in our laboratory to show that the highly inert silicone adhesive has no toxic effects on the cells. Ethanol solution (75%) was used to sterilize the samples and was removed by exchanging with phosphate-buffered saline (PBS).

HCAEC morphology study

Cell morphology was studied by laser scanning confocal microscopy (LSCM; Leica Microsystems, Wetzlar, Germany) and SEM (JSM-5800LV; JEOL). For fluorescence microscopic observation, live cells were stained with green fluorescent probe CMFDA (5-chloromethyl fluorescein diacetate) without fixation. A stock solution of CMFDA (25 μM in dimethyl sulfoxide [DMSO]) was diluted with serum-free cell culture medium to obtain a 2.5 μM working solution (concentration range for short-term staining of cells, 0.5 to 5 μM). Prewarmed CMFDA working solution (200 μL) was added to cover the bottom of the wells of the 24-well plate for 45 min. Cells were washed three times with 1 × PBS and incubated with 200 μL of EC culture medium for another 30 min. Subsequently, the culture medium was replaced with another 1 mL of culture medium, in which the cells were cultured further. Cells were observed by LCSM (excitation, 492 nm; emission, 517 nm).

SEM micrographs were taken for detailed cell morphology studies on different substrates. Cells cultured on coverslips were washed with 1 × PBS to remove nonadherent cells and then fixed with 2.5% glutaraldehyde for 45 min at 4°C. Thereafter, the samples were dehydrated

in 75% alcohol solutions and dried under vacuum. The samples were sputter coated with gold (JFC-1200 fine coater; JEOL) and observed with an SEM at an accelerating voltage of 15 or 20 kV.

MTS assay for HCAEC viability and attachment studies

Cell viability and attachment on the nanofibers were determined by colorimetric MTS assay (CellTiter 96 AQ_{ueous} One Solution cell proliferation assay; Promega). Briefly, the cell–nanofiber complex was incubated with 20% 3-(4,5-dimethylthiazol-2-yl)-5-(3-carboxymethoxyphenyl)-2-(4-sulfophenyl)-2*H*-tetrazolium) (MTS) reagent in complete medium for 4 h. Thereafter aliquots were pipetted into the wells of a 96-well plate and placed into a spectrophotometric plate reader (FLUOstar OPTIMA; BMG Labtech, Offenburg, Germany), and the absorbance at 490 nm for each well was measured.

For the cell viability test, cells were seeded onto nanofiber substrate at a density of 1.5×10^4 cells/cm^2 (30% confluence). On days 1, 3, 5, and 7 after cell seeding, unattached cells were washed out and the attached cells were quantified by MTS assay. For the cell attachment study, cells were seeded at a density of 3×10^4 cell/cm^2 (60% confluence). One, 2, 4, 6, and 8 h after cell seeding, unattached cells were washed out and the attached cells were quantified by MTS assay. A lower seeding density was used for viability studies as compared with attachment studies. The reason was that there would be more available area for cells to proliferate so as to avoid their reaching confluence prematurely.

Analysis of HCAEC gene expression

Four typical cell adhesion molecules (CAMs) characteristic of endothelial cells (platelet endothelial cell adhesion molecule-1 [PECAM-1 or CD31], intercellular adhesion molecule-1 [ICAM-1 or CD54], vascular cell adhesion molecule-1 [VCAM-1 or CD106], and E-selectin [or CD62E]) and the endothelial cell universal marker von Willebrand factor (vWF) were studied by reverse transcription-polymerase chain reaction (RT-PCR) for gene expression analysis. Total RNA was extracted from 2.5×10^6 subconfluent HCAECs cultured in a 75-cm^2 flask or from nanofiber mesh deposited on a petri dish (86 mm in diameter; 58 cm^2 in area), using an RNeasy mini kit (Qiagen, Hilden, Germany). Cells were lysed and homogenized in guanidine isothiocyanate (GITC)-containing buffer and then applied to a column in which total RNA bound to the silica gel-based membrane and contaminants were efficiently washed away. Last, high-quality RNA was eluted in 30 μL of RNase-free water and RNA yields were measured on the basis of absorbance at 260 nm.

For RT-PCR, cDNA was reverse transcribed from 1 μg of total RNA and then stored at -20°C. Briefly, a 10.5-μL reaction mixture containing 1 μg of total RNA, 0.5 μg of oligodeoxythymidine [oligo(dT)$_{18}$; 1st BASE, Singapore], and distilled water was heated at 75°C for 5 min and then put on ice for 5 min. Next, dNTPs (dATP, dTTP, dGTP, and dCTP; 2 mM each), 20 units of recombinant ribonuclease inhibitor (RNasin; Promega), and 200 units of Moloney murine leukemia virus (M-MLV) reverse transcriptase (Promega) were added in a final 20-μl reaction mixture. This mixture was incubated for 1 h at 37°C followed by heating for 5 min at 95°C, and then put on ice for 5 min.

A 1-μL aliquot of the reaction mixture was subjected to PCR amplification in a final 20-μl reaction mixture that contained 20 pmol of each forward and reverse primer (Table 1), 1.5 mM $MgCl_2$, a 0.3 mM concentration of each of the four deoxynucleotides, and 1 unit of

Table 1. Polymerase Chain Reaction Primers for Reverse Transcription-Polymerase Chain Reaction Analysis

Gene	*GenBank no.*	*Size (bp)*	*Primer pair sequences*
β-Actin	BC002409	318	5′-GAG TCC TGT GGC ATC CAC G-3′ 5′-GAA GCA TTT GCG GTG GAC G-3′
PECAM-1 (CD31)	BC051822	367	5′-TCA TCG GAG TGA TCA TTG CTC-3′ 5′-CTA GAG TAT CTG CTT TCC ACG-3′
von Willebrand factor (vWF)	BC022258	274	5′-TGA GGC TGG GTA CTA CAA GC-3′ 5′-GGA GAT GTT GCA TGA GCT GC-3′
ICAM-1 (CD54)	J03132	352	5′-GCT TCG TGT CCT GTA TGG C-3′ 5′-CTG GCG GTT ATA GAG GTA CG-3′
VCAM-1 (CD106)	X53051	297	5′-TTC TGA GAG TGT CAA AGA AGG-3′ 5′-AAG GAG GAT GCA AAA TAG AGC-3′
E-selectin (E-SEL, CD62E)	NM_000450	280	5′-GCA CTG TGT GCA AGT TCG C-3′ 5′-GGC TTT TGG TAG CTT CCG TC-3′

Abbreviations: ICAM, intercellular adhesion molecule; PECAM, platelet endothelial cell adhesion molecule; VCAM, vascular cell adhesion molecule.

Taq polymerase (Promega). Amplification of endothelial cells specific genes by PCR was carried out in a PTC-100 Peltier thermal cycler (MJ Research, Waltham, MA) for 30 cycles. In each cycle, an initial denaturation at 94°C for 1 min was carried out, followed with primer annealing at 55°C for 1 min and polymerization at 72°C for 1 min. This was followed by a final extension step at 72°C for 10 min and storage at 4°C. The PCR products were analyzed by electrophoresis of 10 μL of each sample in a 1% agarose gel, with the bands visualized under ultraviolet light by ethidium bromide staining, using the Gel Doc 2000 gel documentation system (Bio-Rad, Hercules, CA).

Statistical analysis

Values (at least triplicate) were averaged and expressed as means ± standard deviation (SD). Each experiment was repeated two or three times. Statistical differences were determined by Student two-tailed *t* test. Differences were considered statistically significant at $p < 0.05$.

RESULTS

Morphology and diameter range of collagen-blended P(LLA-CL) nanofibers with various weight ratios of P(LLA-CL) to collagen

SEM and TEM micrographs of collagen-blended P(LLA-CL) nanofibers with various weight ratios of P(LLA-CL) to collagen are shown in Fig. 2, revealing the nonwoven and interconnected structure of the nanofibers. Similar morphology of the blended nanofibers was also observed, suggesting that the ratios of the two compositions did not affect nanofiber morphology. TEM analysis of blended nanofibers with a diameter of 114 nm and of collagen nanofibers with a diameter of 100 nm verified the nanometer scale and smooth morphology of the blended nanofibers.

The diameter range of the blended nanofibers was further determined by directly measuring nanofiber diameters from Fig. 2; the result is shown in Fig. 3. It shows the well-controlled diameter distribution of blended nanofibers with various weight ratios of P(LLA-CL) to collagen. Basically, more than 60% of the blended

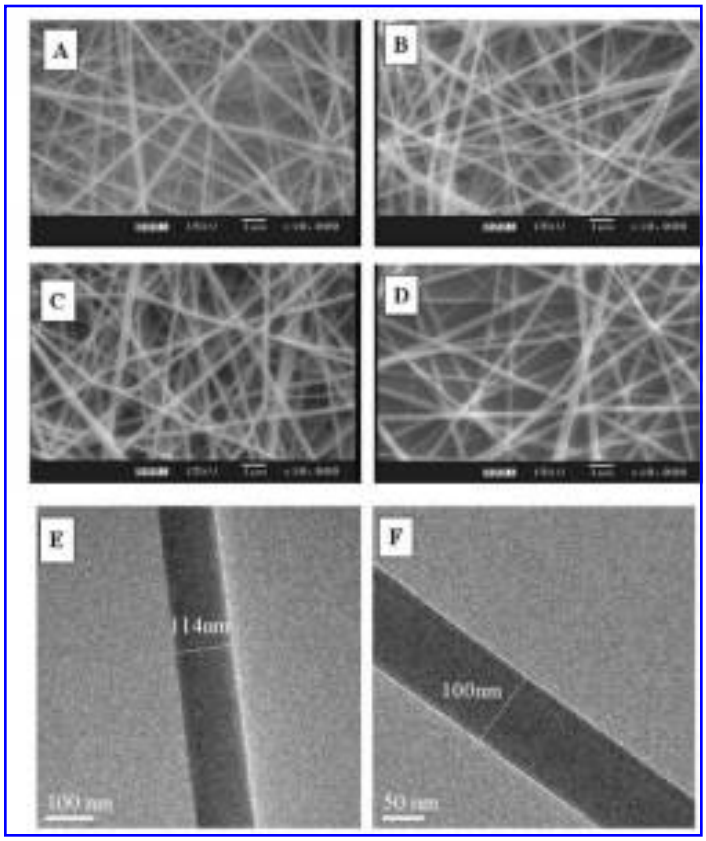

FIG. 2. SEM (**A**–**D**; original magnification, ×10,000) and TEM (**E** and **F**) micrographs of collagen-blended P(LLA-CL) nanofibers with various weight ratios of P(LLA-CL) to collagen. Ratios of P(LLA-CL) to collagen: (**A**) 4:1; (**B**) 2:1; (**C** and **E**) 1:1; (**D** and **F**) 0:1 (pure collagen nanofiber).

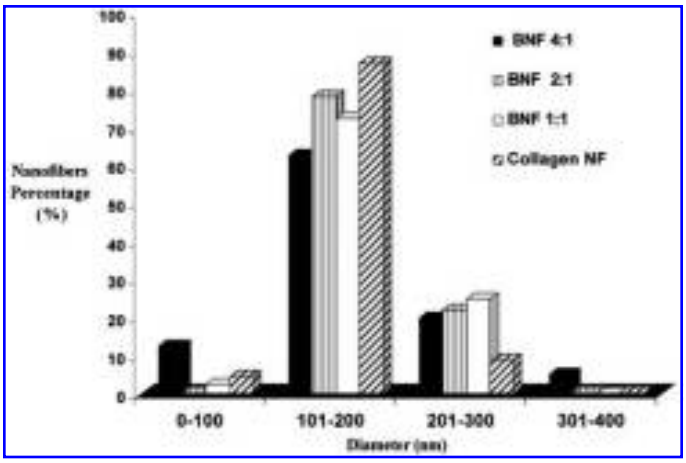

FIG. 3. Diameter ranges of collagen-blended P(LLA-CL) nanofibers (BNF) with various weight ratios of P(LLA-CL) to collagen.

nanofibers ranged from 100 to 200 nm in diameter, with about 20% of nanofibers ranging from 200 to 300 nm. The diameter range of the blended nanofibers was affected by the concentration of the mixture solution of P(LLA-CL) and collagen (data not shown) rather than by the ratio of P(LLA-CL) to collagen.

Diameter, thickness, and apparent density of blended nanofibers with various weight ratios of P(LLA-CL) to collagen are summarized in Table 2. The thickness of blended nanofibers was controlled by the deposition time if electrospinning operation parameters such as voltage, feed rate, and collector distance were fixed. Table 2 shows that blended nanofiber [P(LLA-CL):collagen, 1:1] deposited for 1 h was thicker than others deposited for 30 min. The apparent density of all the blended nanofibers was in the range of 0.30–0.40 g/cm^3. No obvious relationship existed between the apparent density and weight ratio of P(LLA-CL) to collagen. As the electrospun collagen-blended P(LLA-CL) nanofibers are highly porous materials, with the known bulk density of P(LLA-CL)–collagen blends, the porosity of the blended nanofibers can be calculated on the basis of apparent density. However, it is not easy to accurately measure the bulk density of the P(LLA-CL)–collagen blend because it contains a mixture of different compositions, so the bulk density was estimated to be in the range of 1.2–1.3 g/cm^3 on the basis of the bulk density range of P(LLA-CL) copolymer, and the porosity of the blended nanofibers was calculated to be in the range of 68–76%.

In this work the electrospun nanofibers were in the shape of a sheet. The thickness of nanofiber mesh could be further increased by extruding solution through additional orifices during electrospinning, with electrospinning speed proportional to the number of orifices. This method, called mixing or multiple-jet electrospinning, may be used to quickly produce three-dimensional (3-D) nanofibrous scaffolds in future.

Mechanical properties of collagen-blended P(LLA-CL) nanofibers

One of the main failure modes of synthetic vascular grafts is intimal hyperplasia (IH), which is caused by the shear stress disturbances caused by compliance mismatch

TABLE 2. DIAMETER, THICKNESS, APPARENT DENSITY, AND POROSITY OF COLLAGEN-BLENDED POLY(L-LACTIC ACID)-*CO*-POLY(ε-CAPROLACTONE) [P(LLA-CL)] NANOFIBERS WITH VARIOUS WEIGHT RATIOS OF P(LLA-CL) TO COLLAGEN[a]

P(LLA-CL): collagen (wt:wt)	*Diameter (nm)*	*Thickness (mm)*	*Apparent density (g/cm^3)*	*Porosity (%)*
4:1	160 ± 68	9 ± 2	0.31 ± 0.01	74–76
2:1	168 ± 40	6 ± 1	0.39 ± 0.05	68–70
1:1[b]	181 ± 47	15 ± 3	0.38 ± 0.08	68–71
1:2	191 ± 63	9 ± 0	0.33 ± 0.06	73–75

[a]Data are representative of two independent experiments and represent means ± SD ($n = 5$).
[b]Electrospinning deposition time is 60 min. For other blended nanofibers, deposition time is 30 min.

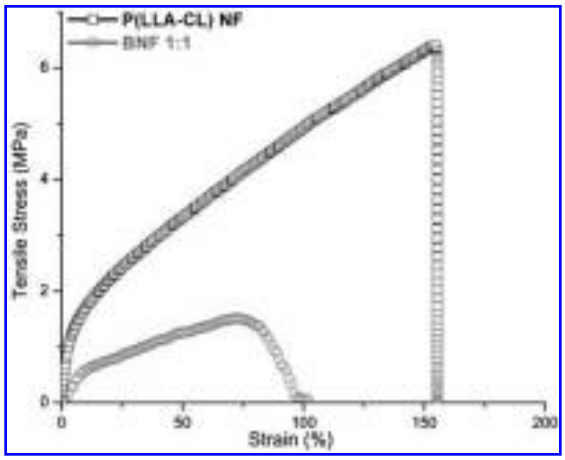

FIG. 4. Typical stress–strain curve for the electrospun P(LLA-PCL) nanofibers (NF) and collagen-blended P(LLA-CL) (BNF) with the weight ratio of the P(LLA-CL) to collagen 1:1 under tensile loading.

at the end-to-end anastomosis between artery and rigid graft.[27] Thus the mechanical properties of nanofibers are critical for their successful application in tissue-engineered vascular grafts. The compliance of a tube is a mechanical property, the value of which depends on the tube dimensions and modulus. In this work we studied mainly the elastic modulus, tensile strength, and tensile modulus of nanofibers, from which we intend to fabricate elastic tubelike structures, to predict the compliance value. Figure 4 shows the typical stress–strain curve of collagen-blended P(LLA-CL) nanofibers (NF) and P(LLA-CL) NF under tensile loading. Mechanical evaluation of both nanofibers revealed the typical nonlinear stress–strain behavior of biological tissue. Incorporation of collagen at a P(LLA-CL)-to-collagen weight ratio of 1:1 led to a significant decrease in tensile strength and ultimate strain ($p < 0.05$) of nanofibers. No significant difference in tensile modulus was observed ($p > 0.05$). Tensile properties of the nanofibers obtained from two independent experiments are summarized in Table 3. Tensile properties of the nanofibers were comparable to those of human coronary artery. Compared with P(LLA-CL) NF, blended NF has a more desirable ultimate strain value, one closer to the value of coronary artery. Also, both nanofibers showed much less stiffness compared with Dacron (PET; commonly used in large-diameter vascular grafts), which has a tensile strength of 170–180 MPa in oriented form and a tensile modulus of about 14,000 MPa.[27] Ideally, less stiff (compliant) and biodegradable scaffolds such as P(LLA-CL) nanofibers are a better choice for constructing a completely biological and fully functional neoartery.

It is perhaps not feasible to increase the mechanical strength of blended nanofibers only by cross-linking (although it is easy to cross-link pure collagen nanofibers with a fixative such as glutaraldehyde vapor), because polymer molecules in blended nanofibers are difficult to cross-link. Other methods, such as adjusting the orientation and diameter of the nanofibers, could be used to further tailor the mechanical strength of nanofibers more readily.[15] Thus the mechanical properties of blended nanofibers may be adjusted according to the requirements of tissue-engineered vascular grafts.

Characterization of collagen-blended P(LLA-CL) nanofibers

The chemical composition of collagen-blended P(LLA-CL) nanofibers was verified by attenuated total reflectance-Fourier transform infrared (ATR-FTIR) spectrometry. Figure 5 shows the infrared spectra of pure P(LLA-CL) nanofiber (Fig. 5A), pure collagen nanofiber (Fig. 5B), and collagen-blended P(LLA-CL) nanofiber (Fig. 5C). Spectra of blended nanofibers revealed peaks characteristic of type I collagen at wavenumbers of 1651 cm^{-1} (amide I band) and 1537 cm^{-1} (amide II band), and a P(LLA-CL) peak at 1747 cm^{-1}, together with a peak at 3310 cm^{-1} (N–H stretch), demonstrating that blended nanofibers are a mixture of P(LLA-CL) and collagen. ATR-FTIR cannot analyze the surface chemistry of nanofibers accurately because it probes 100 nm into the surface of materials. For nanofibers with a diameter range from 100 to 200 nm, ATR-FTIR may show the composition inside the nanofibers. Therefore XPS was

TABLE 3. TENSILE PROPERTIES OF ELECTROSPUN P(LLA-CL) NANOFIBERS, COLLAGEN-BLENDED P(LLA-CL) NANOFIBERS WITH P(LLA-CL):COLLAGEN WEIGHT RATIO OF 1:1, AND CORONARY ARTERY[a,b]

	BNF 1:1	*P(LLA-CL)*	*Coronary artery*[b]
Tensile modulus (MPa)	26.33 ± 6.66	43.99 ± 4.04	—
Tensile strength (MPa)	1.54 ± 0.32	6.27 ± 1.38	1.40–11.14
Ultimate strain (%)	66 ± 22	176 ± 49	45–99

Abbreviations: BNF, collagen-blended P(LLA-CL) nanofiber.

[a]Data are representative of two independent experiments and represent means ± SD ($n = 3$).

[b]See Ref. 6.

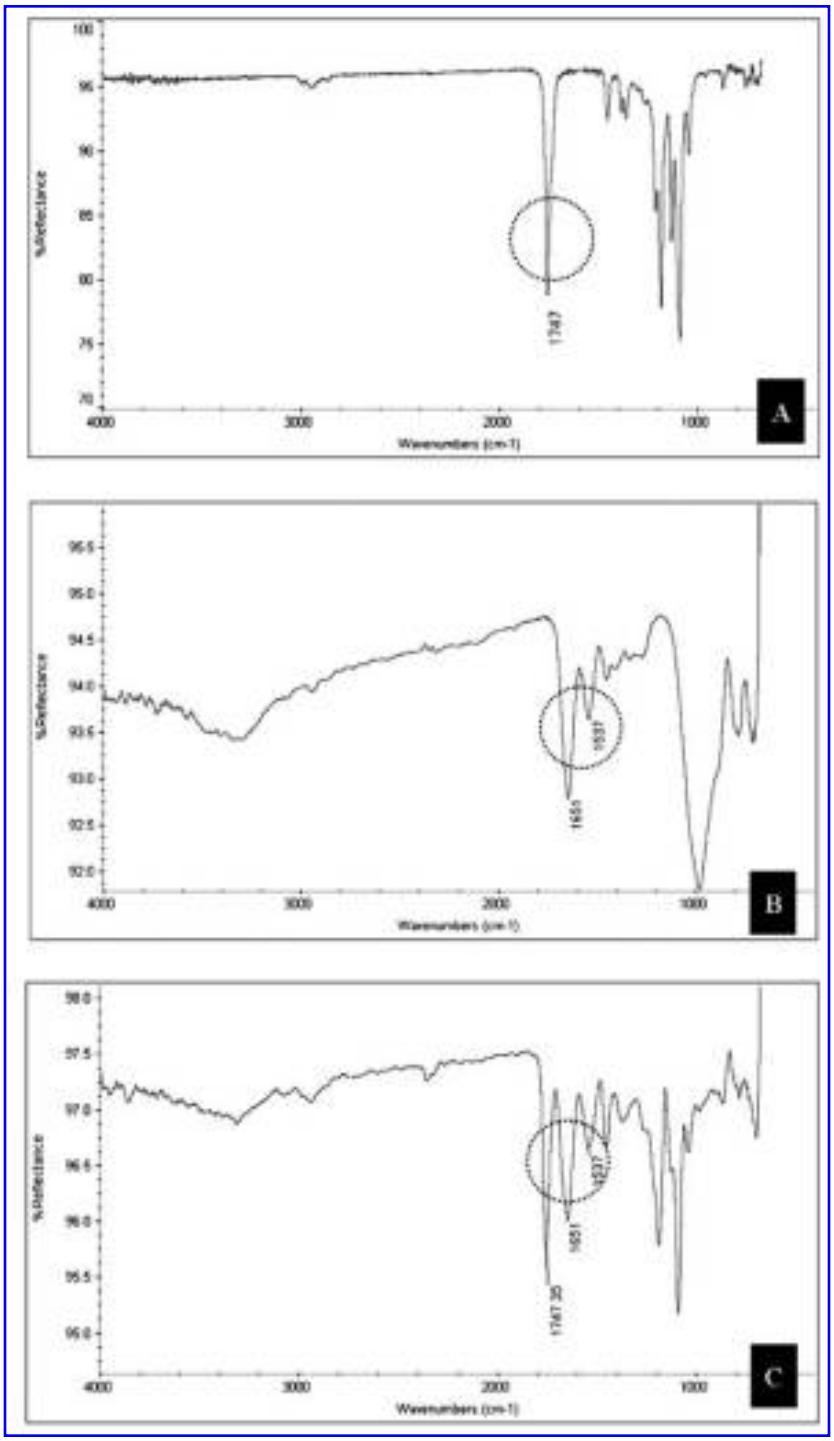

FIG. 5. ATR-FTIR spectra of (**A**) P(LLA-CL) nanofibers, (**B**) collagen nanofibers, and (**C**) collagen-blended P(LLA-CL) nanofibers with a 1:1 weight ratio of P(LLA-CL) to collagen.

required to check whether collagen was present on the surface of nanofibers.

The surface chemistry of blended nanofibers was further verified by XPS spectroscopy. Table 4 shows the atomic ratios of carbon, nitrogen, and oxygen on blended nanofibers with various weight ratios of P(LLA-CL) to collagen, together with those of pure P(LLA-CL) nanofibers and pure collagen nanofibers. Concerning blended nanofibers, more collagen was found to be present on the surface of nanofibers with increased collagen weight ratios. Pure collagen nanofibers showed the highest amount of surface collagen compared with other, blended nanofibers.

Table 4. Atomic Ratios of Carbon, Nitrogen, and Oxygen on the Surface of P(LLA-CL) Nanofibers, Collagen-Blended P(LLA-CL) Nanofibers with Various Weight Ratios of P(LLA-CL) to Collagen, and Collagen Nanofibers as Determined by X-Ray Photoelectron Spectroscopy

Nanofibers	*C atomic ratio (%)*	*N atomic ratio (%)*	*O atomic ratio (%)*
P(LLA-CL)	65.9	0	34.1
P(LLA-CL):collagen, 4:1	67	Not detectable	33
P(LLA-CL):collagen, 2:1	56.2	9.2	34.6
P(LLA-CL):collagen, 1:1	59	11.7	29.3
P(LLA-CL):collagen, 1:2	63.3	13.3	23.4
Collagen	61.6	15.1	23.3

Viability of HCAECs on collagen-blended P(LLA-CL) nanofibers

The viability of HCAECs on days 1, 3, 5, and 7 after seeding on collagen-blended P(LLA-CL) nanofibers with various weight ratios of P(LLA-CL) to collagen is shown in Fig. 6. The viability of HCAECs cultured on blended nanofibers was compared with that of cells cultured on tissue culture polystyrene (TCPS), pure collagen nanofibers, pure P(LLA-CL) nanofibers, and P(LLA-CL)–collagen film (blended film). It was revealed that HCAEC viability increased with increased collagen weight ratio in the blended nanofibers, which was consistent with previous results showing that more collagen was present on the surface of nanofibers with increased collagen weight ratios. It is crucial to adjust the weight ratios of P(LLA-CL) to collagen for optimal cell growth. From this study, we found that at a P(LLA-CL)-to-collagen weight ratio of 1:1, blended nanofibers have normal morphology, a well-controlled diameter, and good cell viability. The following studies therefore focused on blended nanofibers at this ratio. Although pure collagen nanofibers showed the best cell viability among all the samples, it was not chosen because collagen nanofibers swollen into hydrogels in cell culture medium showed poor mechanical strength (data not shown).

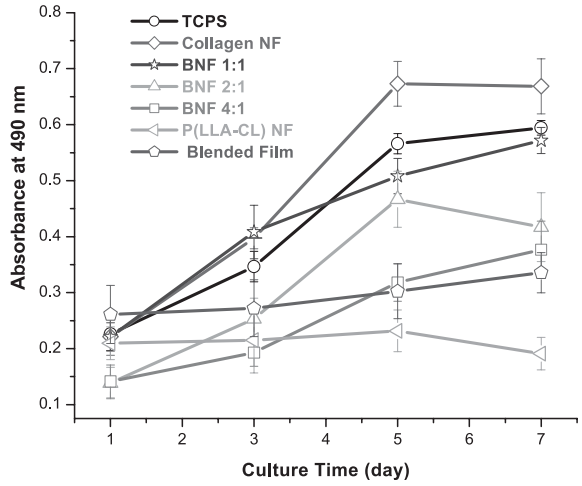

FIG. 6. Viability of HCAECs cultured on TCPS, collagen nanofibers (NF), collagen-blended P(LLA-CL) nanofibers (BNF) with various weight ratios of P(LLA-CL) to collagen (BNF 1:1, BNF 2:1, and BNF 4:1), P(LLA-CL) NF, and collagen-blended P(LLA-CL) film (Blended Film). HCAECs cultured on TCPS and collagen NF acted as positive controls. P(LLA-CL) NF acted as a negative control. Collagen-blended P(LLA-CL) film served as a control specifically for BNF 1:1. HCAECs were seeded at a density of 1.5×10^4 cells/cm^2 and were cultured for 7 days. Results showed that HCAEC viability increased with increased collagen weight ratio in blended nanofibers. Data are representative of three independent experiments and all data points are plotted as means ± SD ($n = 3$).

To show the specific effect of collagen in blended nanofibers on HCAEC growth, HCAECs were culture on three substrates [TCPS, blended nanofibers, and P(LLA-CL) nanofibers] in three kinds of medium: (1) serum-containing medium (SCM), that is, EC culture medium with 5% FBS and growth supplements, including four growth factors (VEGF, hEGF, hFGF-B, and IGF-I); (2) serum-free medium (SFM), that is, EC culture medium without FBS but with growth factors; and (3) blank medium (BM), that is, EC culture medium without FBS and without growth factors. HCAECs were seeded at a density of 3×10^4 cells/cm^2 and were stained with CMFDA 1 and 3 days later for fluorescence observation. It can be seen in Fig. 7 that fewer HCAECs attached to pure P(LLA-CL) nanofibers and cells had a round morphology compared with those on collagen-blended P(LLA-CL) nanofibers. The results also revealed that blended nanofibers could enhance HCAEC adhesion and spreading in culture medium without serum and growth factors. This may reflects the direct effect of collagen on HCAEC growth. Figure 7 shows the morphology of HCAECs after 3 days of culture. Similar results were also observed for day 1 (data not shown). More interestingly, HCAECs organized into longer shapes when cultured in

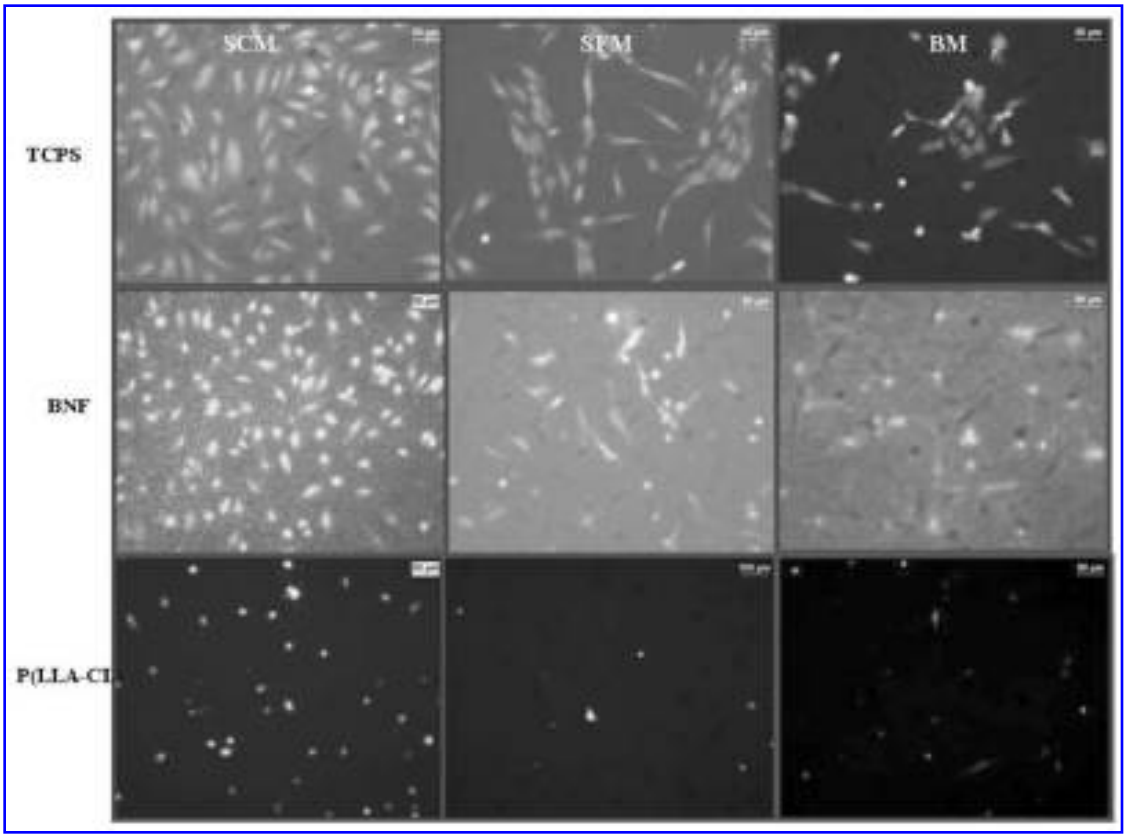

FIG. 7. Morphology of HCAECs (original magnification, ×200) cultured for 3 days on TCPS, collagen-blended P(LLA-CL) nanofibers (BNF), and pure P(LLA-CL) nanofibers. HCAECs were seeded at a density of 3×10^4 cells/cm^2 and stained with CMFDA for fluorescence observation. HCAECs were cultured in three kinds of medium: (1) serum-containing medium (SCM), that is, culture medium with serum and all growth factors (VEGF, hEGF, hFGF-B, and IGF-I); (2) serum-free medium (SFM), that is, medium without serum but with growth factors; and (3) bland medium (BM), that is, culture medium without serum and without growth factors. Similar results were also observed for HCAECs cultured for 1 day (data not shown).

serum-free medium, compared with the normal cobblestone morphology of HCAECs in serum-contained medium. A similar phenomenon was also observed for cells on blended nanofibers. In summary, several conclusions can be drawn from the above-described study. First, HCAECs require serum and growth factors for normal phenotypic morphology. Second, collagen could improve HCAEC growth directly, even without serum or growth factors, compared with cells on pure polymer nanofibers.

Morphology of HCAECs on nanofibers

Figure 8 shows fluorescence and SEM micrographs of HCAECs on TCPS (Fig. 8a and d), P(LLA-CL) nanofibers (Fig. 8b and e), and collagen-blended P(LLA-CL) nanofibers (Fig. 8c and f). HCAECs were seeded at a density of 3×10^4 cells/cm^2 and observed 5 days later for fluorescence microscopic observation or were fixed for SEM study. It was observed that HCAECs cultured on P(LLA-CL) nanofibers were rounded in shape instead of spreading (Fig. 8b and e), whereas on collagen-blended P(LLA-CL) nanofibers HCAECs adopted a spreading polygonal shape that is typical of normal cell morphology on TCPS (Fig. 8a and d). On day 5, HCAECs reached subconfluence on blended nanofibers (Fig. 8c and f), whereas few HCAECs remained on P(LLA-CL) nanofibers.

Figure 9 shows higher magnification SEM micrographs of the interactions between HCAECs and nanofibers. Compared with HCAECs on P(LLA-CL) nanofibers, on which cells adopted a rounded shape possibly indicating apoptosis (Fig. 9a), HCAECs on blended nanofibers showed better phenotypic spreading. It was also observed that HCAECs interconnected well with the nanofibers and that pseudopods of the cells were oriented along the blended nanofibers (Fig. 9b). Thus cells maintained a typical motility shape: broad, flat lamella extending in the direction of migration and terminating in a narrow ruffling lamellipodium.[28] Thus blended nanofibers clearly increased cytocompatibility compared with P(LLA-CL) nanofibers.

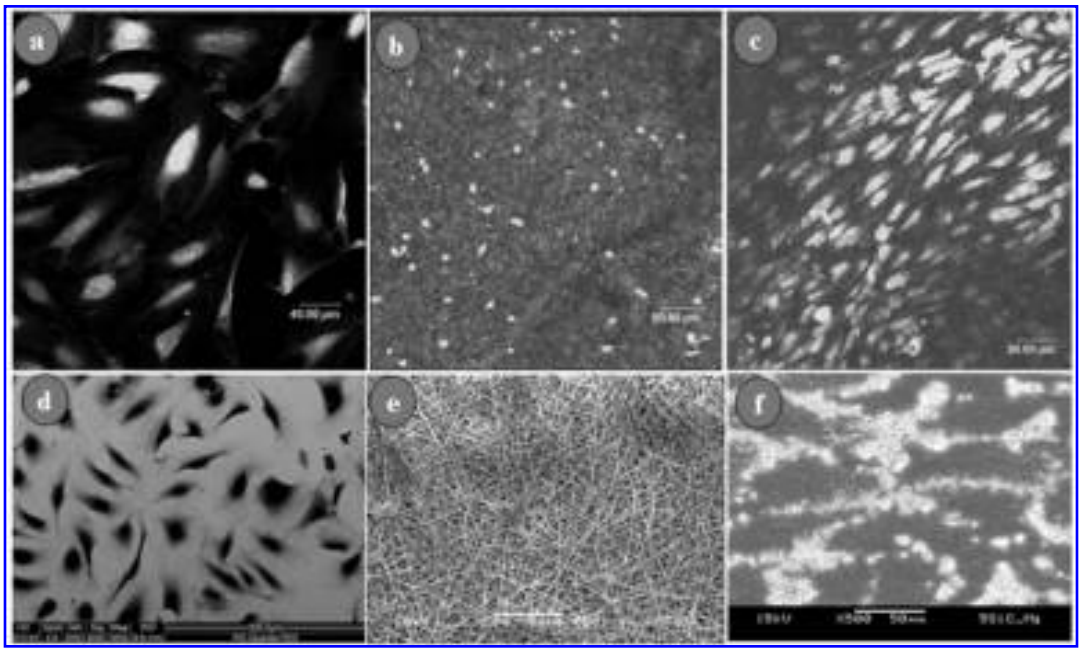

FIG. 8. LSCM [original magnification: (**a**) ×400; (**b** and **c**) ×200] and SEM [original magnification: (**d–f**) ×500] images of HCAECs cultured on (**a** and **d**) TCPS, (**b** and **e**) P(LLA-CL) nanofibers, and (**c** and **f**) collagen-blended P(LLA-CL) nanofibers. HCAECs were seeded at a density of 3×10^4 cells/cm^2 and stained with CMFDA for fluorescence observation or were fixed for SEM study 5 days later. HCAECs on collagen-blended P(LLA-CL) nanofibers exhibited a morphology similar to that of cells on TCPS. Compared with collagen-blended P(LLA-CL) nanofibers (**c** and **f**), fewer HCAECs attached to uncoated P(LLA-CL) nanofibers (**b** and **e**) and cells had a rounded-up morphology.

Attachment of HCAECs on nanofibers

The attachment of HCAECs to TCPS, P(LLA-CL) nanofibers, and collagen-blended P(LLA-CL) nanofibers is shown in Fig. 10. Significantly more HCAECs attached to collagen-blended P(LLA-CL) nanofibers than to pure P(LLA-CL) nanofibers in the first 4 h ($p < 0.05$). Collagen is the most abundant ECM protein having both structural and adhesive functions facilitating cell adhesion through integrin receptors.[29] HCAECs were shown to attach to blended nanofibers at a rate similar to that at which they attached to TPCS. Similar results were also observed with collagen-coated P(LLA-CL) nanofibers (data not shown).

EC-characteristic gene expression

Platelet endothelial cell adhesion molecule-1 (PECAM-1, CD31), intercellular adhesion molecule-1 (ICAM-1, CD54), vascular cell adhesion molecule-1 (VCAM-1, CD106), and endothelial leukocyte adhesion molecule-1 (E-selectin, ELAM-1, CD62E) are important homotypic or heterotypic adhesion molecules. PECAM-1 is involved mainly in homotypic cell–cell adhesion, which favors maintenance of endothelium integrity, and can be used to indicate reduced adhesion to materials.[30] It is also a universal EC marker, together with von Willebrand factor, which can represent the differentiation status of endothelial cells. Upregulated expression of ICAM-1, VCAM-1, and E-selectin indicates the onset of the inflammatory response.[30] Figure 11 shows the gene expression of HCAECs cultured on blended nanofibers for 10 days. The expression of all these genes indicates preservation of the characteristic phenotype of ECs. The expression of PECAM-1 and vWF revealed that the endothelial cells maintained their differentiated status after 10 days of culture on blended nanofibers. The similar expression level of PECAM-1 further represented the normal attachment of cells on blended nanofibers compared with cells on TCPS, which is important especially for endothelial cells to function well under shear force in a natural environment. The upregulated expression of ICAM-1, VCAM-1, and E-selectin perhaps indicates a higher degree of undesirable preinflammatory reactions.

DISCUSSION

In this study, we fabricated collagen-blended biodegradable P(LLA-CL) biohybrid nanofibers for endothelial cell growth because the naturally occurring collagen may improve the bioactivity of the P(LLA-CL) nanofibers. Although previous studies in our laboratory

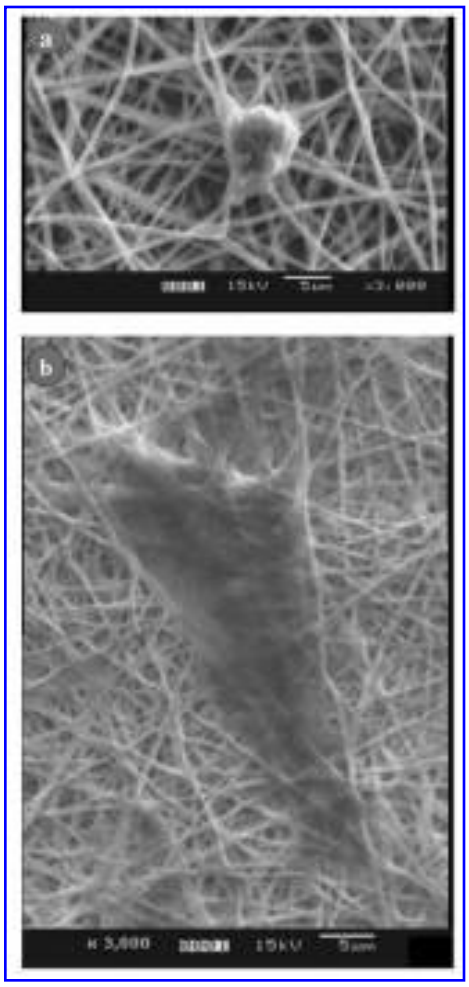

FIG. 9. Higher magnification SEM micrographs (original magnification, ×3000) showing the detailed interaction between HCAECs and (**a**) P(LLA-CL) nanofibers and (**b**) collagen-blended P(LLA-CL) nanofibers after 5 days of culture at a seeding density of 3×10^4 cells/cm^2.

have demonstrated that human coronary artery smooth muscle cells cultured on synthetic polymer P(LLA-CL) nanofibrous scaffolds showed normal morphology and good proliferation, human coronary artery endothelial cells were found not to be able to grow well on unmodified nanofibers,[6] which may be due to the lack of endothelial cell recognition sites on P(LLA-CL) nanofibers. Collagen is the native ECM component serving as adhesion proteins that enhance cell attachment and proliferation through specific interactions between domains, such as RGD in collagen molecules and integrins in cell membranes.[29] Their specific bindings result in focal contact of cells on the substratum, which benefit cell attachment and movement. Therefore, it is probable that the inclusion of collagen in P(LLA-CL) nanofiber would increase its biocompatibility. Herein we fabricated collagen-blended biodegradable P(LLA-CL) (70:30) nanofibers by electrospinning a mixed solution of collagen and P(LLA-CL).

Some of the methods used to introduce proteins onto a substrate surface include physical coating[31] and chemical grafting.[7] However, one of the problems these surface modification techniques face is the slow mass transfer of proteins into the three-dimensional porous materials. For example, it took more than 3 days to effectively graft gelatin molecules onto poly(ethylene terephthalate) (PET) nanofiber surfaces.[7] Compared with the surface modification of polymer nanofibers, direct electrospinning of a blended collagen–polymer mixture is much simpler because it avoids the slow mass transfer process and also uses lesser amounts of chemical reagents during protein immobilization. The blending method has additional potential to readily refine the composition of nanofibers by adding new components such as growth factors, proteoglycan, and glycoproteins to the nanofibers according to cell type. Moreover, the existence of collagen molecules on the surface and inside the nanofibers provides sustained cell recognition signals with polymer degradation, which is important for cell function development. Also, blended nanofibers may have improved mechanical strength compared with pure non-cross-linked collagen nanofibers, which would combine the advantages of both synthetic and natural materials.

There are some important parameters for blended nanofibers that might affect the nanofiber diameter distribution and cell response. In this study, blended

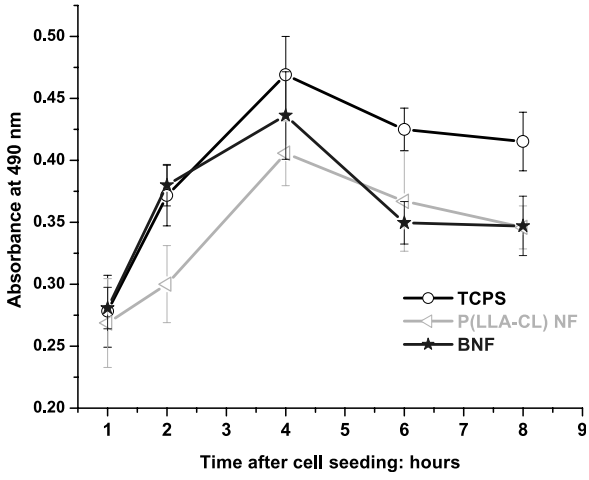

FIG. 10. Attachment of HCAECs to TCPS, P(LLA-CL) nanofibers (NF), and collagen-blended P(LLA-CL) nanofibers (BNF). HCAECs were seeded at a density of 3×10^4 cells/cm^2. Significantly more HCAECs attached to collagen-blended P(LLA-CL) nanofibers than to P(LLA-CL) nanofibers in the first 4 h ($p < 0.05$). Data are representative of three independent experiments and all data points are plotted as means ± SD ($n = 3$).

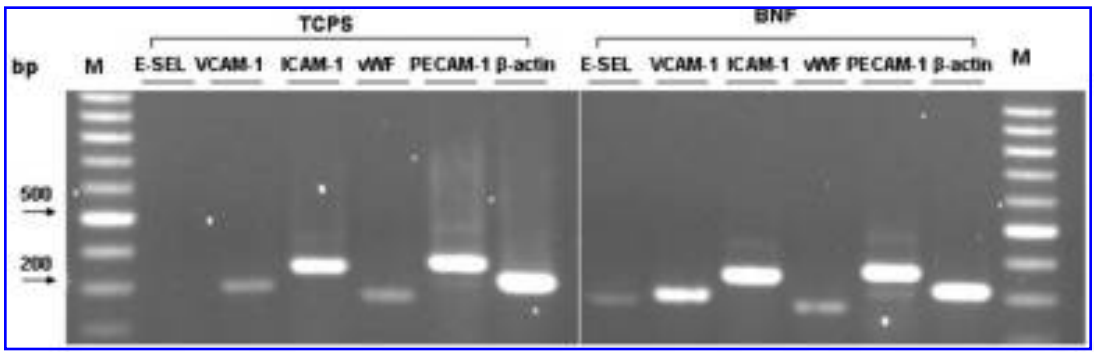

FIG. 11. RT-PCR analysis of expression of endothelial cell-characteristic genes in HCAECs seeded onto TCPS and collagen-blended P(LLA-CL) nanofibers (BNF) for 10 days of culture. On day 10, total RNA was extracted and RT-PCR was performed with the gene-specific primer pairs shown in Table 1, including E-selectin (E-SEL), VCAM-1, ICAM-1, von Willebrand factor (vWF), PECAM-1, and β-actin as a housekeeping gene. The expression of all these genes of HCAECs on TCPS or BNF indicates preservation of the characteristic phenotype of ECs. The upregulated expression of ICAM-1, VCAM-1, and E-selectin of HCAECs on BNF perhaps indicate a higher degree of undesirable preinflammatory reactions.

nanofibers with diameter ranging from 100 to 200 nm (60% of nanofibers) were obtained by electrospinning mixtures of collagen and polymer at a concentration of 5 wt%. The diameter range of the blended nanofibers was affected by the concentration of the mixture of polymer and collagen (data not shown). Other parameter such as the weight ratio of polymer to collagen did not affect the diameter distribution of nanofibers (Fig. 3), but did influence HCAEC viability (Fig. 6). With a higher content of collagen in the blended nanofibers, cells accordingly showed enhanced viability.

In addition to biocompatibility, biodegradation is a critical issue for tissue-engineering application of nanofibers. Although the speed of degradation of collagen-blended P(LLA-CL) nanofibers may be difficult to predict precisely, it is possible that the nanoscaled material will degrade faster than large bulk materials because the high surface area-to-volume ratio of the nanofibers provides a large contact area between the materials and the water or enzymes involved in the degradative process. Although the effect of material size on the degradation rate is still a controversial subject, some authors believe that a nanoscaled object, consisting of only a few polymer chains, should degrade fast.[32] Other authors have also predicted that because nanofibers possess a specific surface area between that of films and nano- or microparticles, among which nanoparticles degrade most quickly, intermediate biodegradation rates are expected.[33] P(LLA-CL) and collagen may also affect each other's degradation processes. The degradation products, lactic acid and hydroxyhexanoic acid for P(LLA-CL) and amino acid for collagen, will all affect the pH value, thus further affecting the degradation speed of P(LLA-CL) and collagen. Generally speaking, the biodegradative behavior of nanofibers with different compositions has been little studied.[34] The degradation behavior of these materials needs to be studied systematically in future in terms of molecular weight decrease, mass loss, and mechanical strength loss.

Another critical issue for the tissue-engineering application of nanofiber scaffolds is mechanical strength, which depends both on the physical properties of nanofibers such as orientation, diameter, pore size, and porosity and on chemical properties such as the composition of the nanofibers. Nanofiber scaffolds should not only act as a residence for cells but also provide sufficient mechanical support during tissue regeneration and structure degradation. As highly porous materials, the mechanical properties of nanofibers under cell culture conditions may change with the biodegradation of nanofibers and cell migration, which will exert force on the nanofibers. The dynamic cell–nanofiber interaction observed in some studies indicated that cells could adjust the pore size for ingrowth into a nanofiber mesh.[9] This kind of cellular ingrowth may further change the mechanical properties of the loosened nanofiber mesh. As for blended nanofibers described here, the diameter range was from 100 to 200 nm (60% of nanofibers), which is much smaller and better distributed than that of most nanofibers we have reported previously.[4–7] The pore size (the length of the diagonals of the pore square) of the blended nanofibers was about 2–5 μm, which is much smaller compared with the size of HCAECs (average, 25×50 μm). The ingrowth of cells into the nanofibers was not obvious on the basis of the SEM study (Fig. 9). Thus the cell–nanofiber interaction may not be the dominant factor affecting the mechanical properties of nanofibers. However, because of the collagen in the nanofibers, the biodegradation by collagenase secreted by the cells may degrade the nanofibers faster and weaken

their mechanical strength. Thus to systematically study the mechanical strength changes of nanofibers, two aspects will need further study: *in vitro* biodegradation of nanofibers, and ECM secretion and remolding of blended nanofibers by HCAECs.

HCAECs cultured on collagen-blended P(LLA-CL) nanofibers showed spreading and subconfluent morphology similar to that of cells cultured on TCPS. In contrast, HCAECs cultured on pure P(LLA-CL) nanofibers were rounded in shape (Figs. 7–9). In addition, cell viability and attachment on blended nanofibers were obviously increased compared with that on pure polymer nanofibers (Figs. 6 and 10). These results are the basis for endothelialization of vascular grafts, which can prevent the thrombogenicity and intimal hyperplasia (excess tissue ingrowth) that are the most common causes of graft failure.[35] However, tissue-engineered vascular grafts should not only possess good phenotypic properties such as spreading morphology, cell viability, and cell attachment but also encourage endothelial cell functions, which can be assessed through expression of cell adhesion molecules.[36] This is more important because, for suitable vascular prosthesis, the material should not hamper the adhesion of endothelial cells or favor inflammation phenomena.[30] Thus for proper prediction of material efficacy and the endothelialization process, study of endothelial cell adhesion to the substratum and of endothelial cell involvement in the inflammatory response is required.[24] In this study, endothelial cell functions were assessed mainly through gene expression analysis for cell adhesion molecules and endothelial cell universal markers. The functions of cell adhesion molecules are to mediate cell–cell or cell–matrix interactions; ICAM-1, VCAM-1, and E-selectin are important mediators of the adhesion and migration of leukocytes or lymphocytes from the blood to tissues during the immune response, whereas PECAM-1 is involved mainly in homotypic cell–cell adhesion. von Willebrand factor, the universal EC marker, is an adhesive glycoprotein synthesized exclusively in endothelial cells and megakaryocytes. It plays a central role in hemostasis by mediating the adhesion of an initial platelet plug to the subendothelium of injured blood vessels and serves as the carrier for factor VIII in plasma.[37] We found that day 10 gene expression levels of the cell adhesion molecules and vWF from endothelial cells cultured on blended nanofibers were comparable to those of endothelial cells cultured on TCPS, demonstrating that normal cell function is preserved during *in vitro* culture.

From this work, we have shown that collagen-blended P(LLA-CL) nanofibers show great potential as tissue-engineered vascular grafts because they can promote good endothelial cell viability, attachment, and phenotypic morphology and preserve the functions of endothelial cells. The ease of fabricating blended nanofibers provides more possibilities for adding particular ingredients to nanofibers according to cell type. Furthermore, blended nanofibers will most likely possess the advantages of both natural and synthetic materials. Hence blended nanofibers could be a practical and effective material for tissue-engineered vascular grafts.

CONCLUSION

The electrospinning technique was employed to fabricate collagen-blended P(LLA-CL) (70:30) nanofibers with smooth surface morphology and a well-controlled diameter distribution ranging from 100 to 200 nm. The existence of collagen on the surface of blended nanofibers was verified by ATR-FTIR and XPS. Blended nanofibers supported endothelialization observed as good cell-spreading morphology, cell attachment and viability, and phenotypic maintenance of cells. Blended nanofibers can improve bioactivity relative to pure polymer nanofibers and possess the potential to refine the composition of nanofibers readily by adjusting ingredients according to cell type. All these data strongly suggest the potential application of blended nanofibers as vascular engineering scaffolds with good endothelialization.

ACKNOWLEDGMENTS

The authors thank Dr. Jun Li, Dr. Xiaojing Xu, and Mr. Yanzhong Zhang for help in XPS, TEM, and mechanical test experiments, respectively. This study was supported by the Academic Research Fund of the National University of Singapore.

REFERENCES

1. Ma, Z.W., Kotaki, M., Inai, R., and Ramakrishna, S. Potential of nanofiber matrix as tissue engineering scaffolds. Tissue. Eng. **11,** 101, 2005.
2. Li, D., and Xia, Y. Electrospinning of nanofibers: Reinventing the wheel? Adv. Mater. **16,** 1151, 2004.
3. Yoshimoto, H., Shin, Y.M., Terai, H., and Vacanti, J.P. A biodegradable nanofiber scaffold by electrospinning and its potential for bone tissue engineering. Biomaterials **24,** 2077, 2003.
4. Xu, C.Y., Inai, R., Kotaki, M., and Ramakrishna, S. Aligned biodegradable nanofibrous structure: A potential scaffold for blood vessel engineering. Biomaterials **25,** 877, 2004.
5. Mo, X.M., Xu, C.Y., Kotaki, M., and Ramakrishna, S. Electrospun P(LLA-CL) nanofiber: A biomimetic extracellular matrix for smooth muscle cell and endothelial cell proliferation. Biomaterials **25,** 1883, 2004.
6. Xu, C.Y., Inai, R., Kotaki, M., and Ramakrishna, S. Electrospun nanofiber fabrication as synthetic extracellular matrix and its potential for vascular tissue engineering. Tissue Eng. **10,** 1160, 2004.

7. Ma, Z.W., Kotaki, M., Yong, T., He, W., and Ramakrishna, S. Surface engineering of electrospun polyethylene terephthalate (PET) nanofibers towards development of a new material for blood vessel engineering. Biomaterials **26,** 2527, 2005.
8. Li, W.J., Tuli, R., Okafor, C., Derfoul, A., Danielson, K.G., Hall, D.J., and Tuan, R.S. A three-dimensional nanofibrous scaffold for cartilage tissue engineering using human mesenchymal stem cells. Biomaterials **26,** 599, 2005.
9. Li, W.J., Laurencin, C.T., Caterson, E.J., Tuan, R.S., and Ko, F.K. Electrospun nanofibrous structure: A novel scaffold for tissue engineering. J. Biomed. Mater. Res. **60,** 613, 2002.
10. Shin, M., Ishii, O., Sueda, T., and Vacanti, J.P. Contractile cardiac grafts using a novel nanofibrous mesh. Biomaterials **25,** 3717, 2004.
11. Bini, T.B., Gao, S., Tan, T.C., Wang, S., Lim, A., Hai, L.B., and Ramakrishna, S. Electrospun poly(L-lactide-*co*-glycolide) biodegradable polymer nanofibre tubes for peripheral nerve regeneration. Nanotechnology **15,** 1459, 2004.
12. Lee, C.H., Shin, H.J., Cho, I.H., Kang, Y.M., Kim, I.A., Park, K.D., and Shin, J.W. Nanofiber alignment and direction of mechanical strain affect the ECM production of human ACL fibroblast. Biomaterials **26,** 1261, 2005.
13. Chua, K.N., Lim, W.S., Zhang, P.C., Lu, H.F., Wen, J., Ramakrishna, S., Leong, K.W., and Mao, H.Q. Stable immobilization of rat hepatocyte spheroids on galactosylated nanofiber scaffold. Biomaterials **26,** 2537, 2005.
14. Li, W.J., Laurencin, C.T., Caterson, E.J., Tuan, R.S., and Ko, F.K. Electrospun nanofibrous structure: A novel scaffold for tissue engineering. J. Biomed. Mater. Res. **60,** 613, 2002.
15. Matthews, J.A., Wnek, G.E., Simpson, D.G., and Bowlin, G.L. Electrospinning of collagen nanofibers. Biomacromolecules **3,** 232, 2002.
16. Matthews, J.A., and Boland, E.D. Electrospinning of collagen type II: A feasibility study. J. Bioact. Compat. Polym. **18,** 125, 2003.
17. Boland, E.D., Matthews, J.A., Pawlowski, K.J., Simpson, D.G., Wnek, G.E., and Bowlin, G.L. Electrospinning collagen and elastin: Preliminary vascular tissue engineering. Front. Biosci. **9,** 1422, 2004.
18. Kim, S.H., Nam, Y.S., Lee, T.S., and Park, W.H. Silk fibroin nanofiber: Electrospinning, properties, and structure. Polym. J. **35,** 185, 2003.
19. Wnek, G.E., Carr, M.E., Simpson, D.G., and Bowlin, G.L. Electrospinning of nanofiber fibrinogen structures. Nano Lett. **3,** 216, 2003.
20. Ohkawa, K., Cha, D., Kim, H., Nishida, A., and Yamamoto, H. Electrospinning of chitosan. Macromol. Rapid Commun. **25,** 1600, 2004.
21. Jiang, H., Fang, D., Hsiao, B.S., Chu, B., and Chen, W. Optimization and characterization of dextran membranes prepared by electrospinning. Biomacromolecules **5,** 326, 2004.
22. Um, I.C., Fang, D., Hsiao, B.S., Okamoto, A., and Chu, B. Electro-spinning and electro-blowing of hyaluronic acid. Biomacromolecules **5,** 1428, 2004.
23. Xie, J.B., and Hsieh, Y.L. Ultra-high surface fibrous membranes from electrospinning of natural proteins: Casein and lipase enzyme. J. Mater. Sci. **38,** 2125, 2003.
24. Fang, X., and Reneker, D.H. DNA fibers by electrospinning. J. Macromol. Sci. Phys. B **36,** 169, 1997.
25. Lee, S.W., and Belcher, A.M. Virus-based fabrication of micro- and nanofibers using electrospinning. Nano Lett. **4,** 387, 2004.
26. Kim, B.S., and Mooney, D.J. Development of biocompatible synthetic extracellular matrices for tissue engineering. Trends Biotechnol. **16,** 224, 1998.
27. Salacinski, H.J., Goldner, S., Giudiceandrea, A., Hamilton, G., Seifalian, A.M., Edwards, A., and Carson, R.J. The mechanical behavior of vascular grafts: A review. J. Biomater. Appl. **15,** 241, 2001.
28. Wittmann, T., and Waterman-Storer, C.M. Cell motility: Can rho GTPase and microtubules point the way? J. Cell Sci. **114,** 3795, 2001.
29. Ruoslahti, E., and Pierschbacher, M.D. New perspectives in cell adhesion: RGD and integrin. Science **238,** 491, 1987.
30. Cenni, E., Granchi, D., Arciola, C.R., Ciapetti, G., Savarino, L., Stea, S., Cavedagna, D., Di Leo, A., and Pizzoferrato, A. Adhesive protein expression on endothelial cells after contact *in vitro* with polyethylene terephthalate coated with pyrolytic carbon. Biomaterials **16,** 1223, 1995.
31. van den Dolder, J., Bancroft, G.N., Sikavitsas, V.I., Spauwen, P.H., Mikos, A.G., and Jansen, J.A. Effect of fibronectin- and collagen I-coated titanium fiber mesh on proliferation and differentiation of osteogenic cells. Tissue Eng. **9,** 505, 2003.
32. Zong, X., Ran, S., Kim, K.S., Fang, D., Hsiao, B.S., and Chu, B. Structure and morphology changes during *in vitro* degradation of electrospun poly(glycolide-*co*-lactide) nanofiber membrane. Biomacromolecules **416,** 4, 2003.
33. Zeng, J., Chen, X., Liang, Q., Xu, X., and Jing, X. Enzymatic degradation of poly(L-lactide) and poly(ϵ-caprolactone) electrospun fibers. Macromol. Biosci. **4,** 1118, 2004.
34. You, Y., Min, B.M., Lee, S.J., Lee, T.S. and Park, W.H. *In vitro* degradation behavior of electrospun polyglycolide, poly lactide, and poly(lactide-*co*-glydolide). J. Appl. Polym. Sci. **193,** 95, 2005.
35. Ogle, B.M., and Mooradian, D.L. Manipulation of remodeling pathways to enhance the mechanical properties of a tissue engineered blood vessel. J. Biomech. Eng. **124,** 72, 2002.
36. Kooten, T.G., Klein, C.L., Kohler, H., Kirkpatrick, C.J., Williams, D.F., and Eloy, R. From cytotoxicity to biocompatibility testing *in vitro*: Cell adhesion molecule expression defines a new set of parameters. J. Mater. Sci. Mater. Med. **8,** 835, 1997.
37. Mohlke, K.L., Nichols, W.C., Westrick, R.J., Novak, E.K., Cooney, K.A., Swank, R.T., and Ginsburg, D. A novel modifier gene for plasma von Willebrand factor level maps to distal mouse chromosome 11. Proc. Natl. Acad. Sci. U.S.A. **93,** 15352, 1996.

Address reprint requests to:
Wei He, M.Sc.
Nanoscience and Nanotechnology Initiative
BLK E3, #05-14
National University of Singapore
9 Engineering Drive 1
Singapore 117576

E-mail: g0305833@nus.edu.sg

This article has been cited by:

1. Dong Yixiang , Thomas Yong , Susan Liao , Casey K. Chan , S. Ramakrishna . 2008. Degradation of Electrospun Nanofiber Scaffold by Short Wave Length Ultraviolet Radiation Treatment and Its Potential Applications in Tissue Engineering. *Tissue Engineering Part A* **14**:8, 1321-1329. [Abstract] [PDF] [PDF Plus] [Supplementary material]
2. Nureddin Ashammakhi, A Ndreu, L Nikkola, I Wimpenny, Y Yang. 2008. Advancing tissue engineering by using electrospun nanofibers. *Regenerative Medicine* **3**:4, 547-574. [CrossRef]
3. N. Ashammakhi, A. Ndreu, Y. Yang, H. Ylikauppila, L. Nikkola. 2008. Nanofiber-based scaffolds for tissue engineering. *European Journal of Plastic Surgery* . [CrossRef]
4. Scott A. Sell, Gary L. Bowlin. 2008. Creating small diameter bioresorbable vascular grafts through electrospinning. *Journal of Materials Chemistry* **18**:3, 260. [CrossRef]
5. Li Liu, Shengrong Guo, Jiang Chang, Congqin Ning, Changming Dong, Deyue Yan. 2008. Surface modification of polycaprolactone membrane via layer-by-layer deposition for promoting blood compatibility. *Journal of Biomedical Materials Research Part B: Applied Biomaterials* . [CrossRef]
6. J. Venugopal, Sharon Low, Aw Tar Choon, S. Ramakrishna. 2008. Interaction of cells and nanofiber scaffolds in tissue engineering. *Journal of Biomedical Materials Research Part B Applied Biomaterials* **84b**:1, 34. [CrossRef]
7. Ming Chen , Prabir K. Patra , Steven B. Warner , Sankha Bhowmick . 2007. Role of Fiber Diameter in Adhesion and Proliferation of NIH 3T3 Fibroblast on Electrospun Polycaprolactone Scaffolds. *Tissue Engineering* **13**:3, 579-587. [Abstract] [PDF] [PDF Plus]
8. B.P. Chan , T.Y. Hui , O.C.M. Chan , K.-F. So , W. Lu , K.M.C. Cheung , E. Salomatina , A. Yaroslavsky . 2007. Photochemical Cross-Linking for Collagen-Based Scaffolds: A Study on Optical Properties, Mechanical Properties, Stability, and Hematocompatibility. *Tissue Engineering* **13**:1, 73-85. [Abstract] [PDF] [PDF Plus]
9. Vinoy Thomas, Xing Zhang, Shane A Catledge, Yogesh K Vohra. 2007. Functionally graded electrospun scaffolds with tunable mechanical properties for vascular tissue regeneration. *Biomedical Materials* **2**:4, 224. [CrossRef]
10. B. V. Stanzel, M. Englander, D. J. Strick, S. S. Sanislo, P. Huie, M. S. Blumenkranz, S. Binder, M. F. Marmor. 2007. Perspektive: Tissue engineering bei RPE-Transplantation in AMD. *Spektrum der Augenheilkunde* **21**:4, 212. [CrossRef]
11. Andreas Greiner, Joachim H. Wendorff. 2007. Electrospinning: A Fascinating Method for the Preparation of Ultrathin Fibers. *Angewandte Chemie International Edition* **46**:30, 5670. [CrossRef]
12. Nureddin Ashammakhi, Albana Ndreu, Ying Yang, Hanna Ylikauppila, Lila Nikkola, V. Hasirci. 2007. Tissue Engineering. *Journal of Craniofacial Surgery* **18**:1, 3. [CrossRef]
13. Chou Chai, Kam W Leong. 2007. Biomaterials Approach to Expand and Direct Differentiation of Stem Cells. *Molecular Therapy* **15**:3, 467. [CrossRef]
14. Andreas Greiner, Joachim H. Wendorff. 2007. Elektrospinnen: eine faszinierende Methode zur Präparation ultradünner Fasern. *Angewandte Chemie* **119**:30, 5770. [CrossRef]
15. Wei He , Thomas Yong , Zu Wei Ma , Ryuji Inai , Wee Eong Teo , Seeram Ramakrishna . 2006. Biodegradable Polymer Nanofiber Mesh to Maintain Functions of Endothelial Cells. *Tissue Engineering* **12**:9, 2457-2466. [Abstract] [PDF] [PDF Plus]
16. Joseph Jagur-Grodzinski. 2006. Polymers for tissue engineering, medical devices, and regenerative medicine. Concise general review of recent studies. *Polymers for Advanced Technologies* **17**:6, 395. [CrossRef]
17. Wee-Eong Teo, Wei He, Seeram Ramakrishna. 2006. Electrospun scaffold tailored for tissue-specific extracellular matrix. *Biotechnology Journal* **1**:9, 918. [CrossRef]
18. Tanida Srisuwan, Daniel J. Tilkorn, Jeremy L. Wilson, Wayne A. Morrison, Harold M. Messer, Erik W. Thompson, Keren M. Abberton. 2006. Molecular aspects of tissue engineering in the dental field. *Periodontology 2000* **41**:1, 88. [CrossRef]
19. Yanping Karen Wang, Thomas Yong, Seeram Ramakrishna. 2005. Nanofibres and their Influence on Cells for Tissue Regeneration. *Australian Journal of Chemistry* **58**:10, 704. [CrossRef]

DOI 10.1002/biot.200600044 Biotechnol. J. 2006, 1, 918–929

Review

Electrospun scaffold tailored for tissue-specific extracellular matrix

Wee-Eong Teo[1], Wei He[2] and Seeram Ramakrishna[1,3,4]

[1]Nanoscience and Nanotechnology Initiative, National University of Singapore, Singapore
[2]Graduate Program in Bioengineering, National University of Singapore, Singapore
[3]Department of Mechanical Engineering, National University of Singapore, Singapore
[4]Division of Bioengineering, National University of Singapore, Singapore

The natural extracellular matrix (ECM) is a complex structure that is built to meet the specific requirements of the tissue and organ. Primarily consisting of nanometer diameter fibrils, ECM may contain other vital substances such as proteoglycans, glycosaminoglycan and various minerals. Current research in tissue engineering involves trying to replicate the ECM such that it provides the environment for tissue regeneration. Electrospinning is a versatile process that results in nanofibers by applying a high voltage to electrically charge a liquid. A variety of polymers and other substances have been incorporated into the artificial nanofibrous scaffold. Surface modification and cross-linking of the nanofibers are some ways to improve the biocompatibility and stability of the scaffold. Electrospun scaffolds with oriented nanofibers and other assemblies can be constructed by modifying the electrospinning setup. Using electrospinning, researchers are able to specifically tailor the electrospun scaffold to meet the requirements of the tissue that they seek to regenerate. *In vitro* and *in vivo* experiments demonstrate that electrospun scaffolds hold great potential for tissue engineering applications.

Received 2 April 2006
Revised 14 June 2006
Accepted 17 July 2006

Keywords: Nanofibers · Extracellular matrix · Electrospinning

1 Introduction

Decades of studies have given researchers a greater understanding of the complex interaction between cells and their environment. Typically in the range of 10–100 μm in diameter, cells respond to stimuli from the macro environment down to the molecular level. Interaction between a typical cell and its environment is achieved through an array of receptor systems that are found on its outer membrane, which responds to adjacent cells, ligands in the surrounding extracellular matrix (ECM) and secreted signaling molecules.

The ECM in particular is able to influence the cells by both chemical cues and the physical arrangement of fibers. The physical structure, composition and arrangement of the ECM are often tissue specific. Fibrils that make up the ECM of tendon are parallel and aligned, while those found on the skin are mesh-like. Thus, it is a daunting task for researchers trying to mimic the natural ECM. Recently, with the development of new processing methods, it is possible to synthesize scaffolds that match some characteristics of tissue-specific ECMs.

The ECM consists mainly of two classes of macromolecules, polysaccharide chains known as glycosaminoglycans (GAG) and fibrous proteins. Recently, researchers have used a process known as electrospinning to fabricate nanofibrous scaffolds to mimic the fibrous structure of ECM. Perhaps the main advantage is its ability to fab-

Correspondence: Professor Seeram Ramakrishna, Nanoscience and Nanotechnology Initiative, National University of Singapore, 9 Engineering Drive 1, Singapore 117576, Singapore
E-mail: seeram@nus.edu.sg
Fax: +61-6872-3638,

Abbreviations: **AMEP**, acrylate modified elastomeric protein; **ECM**, extracellular matrix; **GAG**, glycosaminoglycans; **HA**, hydroxyapatite; **MSC**, mesenchymal stem cell; **PCL**, polycaprolactone; **PEO**, polyethylene oxide; **PLGA**, polylactic-co-glycolic acid; **PLCL**, poly(L-lactide-co-ε-caprolactone); **PLLA**, poly(L-lactic acid)

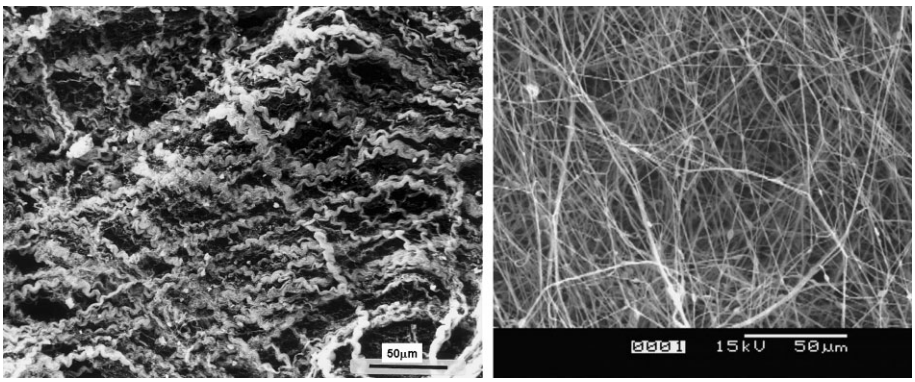

Figure 1. Structural comparison between the nonwoven collagen bundles of the connective stroma of the small intestine [1] and the electrospun nonwoven collagen mesh.

ricate nanometer diameter fibers, while another key advantage is the range of materials that can electrospun. Synthetic non-biodegradable polymers, biodegradable polymers, natural polymers, composites and even ceramic precursors can be electrospun to form nanofibers. Figure 1 shows the structural similarity between electrospun nonwoven collagen mesh and the connective stroma ECM of the small intestine, which is made out of nonwoven collagen bundles [1]. Various other fibrous assemblies can also be constructed using electrospinning. Although typical electrospun fiber scaffolds are in the form of a 2-D non-woven fiber mesh, scaffolds consist of aligned fibers and tubular scaffold can be made through simple modification of the setup.

A schematic for a typical electrospinning setup is shown in Fig. 2. The material to be electrospun is first dissolved in a suitable solvent to obtain a viscous solution. Although, polymer melt can also be electrospun, the resultant fiber is generally above 1 μm in diameter [2–5], while for electrospun polymer solution, average fiber diameter of 19 nm has been obtained [6]. The solution is first passed through a spinneret and a high voltage supply is use to charge the solution. At a critical voltage, typically above 200 V/m [7], the repulsive forces of the charged solution particles result in a jet of solution erupting from the tip of the spinneret. As the jet accelerates toward a ground target, the solvent evaporates and the semi-dry fiber is collected as a non-woven mat. Through the use of high-speed camera and mathematical modeling, Reneker *et al*. [8] have shown that the acceleration of the electrospinning jet from the tip of the spinneret to the collector proceeds in a spiraling path when it enters the bending instability state.

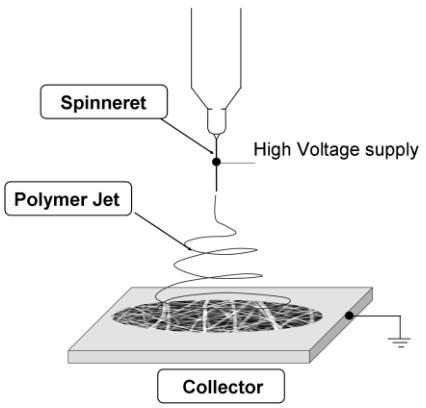

Figure 2. Schematic of the electrospinning setup.

In this review, we discuss several important issues when tailoring a scaffold to resemble tissue-specific ECM. Factors such as material selection, modification of scaffold and its structure, and how electrospun fibers can be used to address these issues are discussed. Current research on using electrospun scaffold tailored to mimic specific tissues such as cartilage and bone grafts, skin grafts, vascular grafts, nerve grafts and cardiac grafts are also reviewed.

2 Material selection

One of the most important factors when tailoring the artificial graft for the specific tissue is the material to be used. The variety of biocompatible materials that can be used in the construction of tissue scaffolds is huge. Several factors such as mechanical properties, degradation rate and cell proliferation, and adhesion on the material must be considered when selecting one for specific tissue or organ scaffold [9]. Polymers, ceramics, metals and composites have all been used as scaffold [10] to meet the various demands and requirements.

As seen in Fig. 3, biodegradable polymer made up the majority of the materials used by researchers in the study of electrospun tissue scaffolds followed by natural polymers. Generally, biodegradable polymers are preferred over their non-biodegradable counterpart for tissue implants, as they can be resorbed into the body over a period of time, and hence long-term complications of a foreign body may be avoided [11]. Table 1 shows a list of polymers that had been electrospun and the corresponding mechanical properties of their non-woven fibrous scaffold.

Biotechnol. J. 2006, 1, 918–929

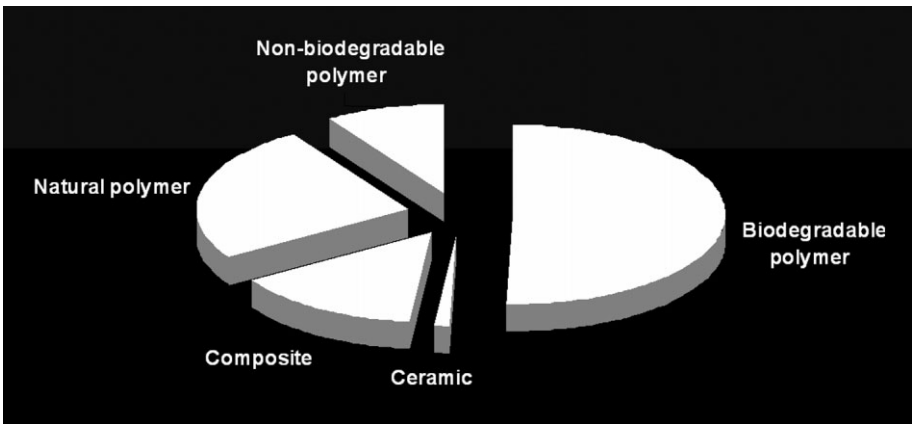

Figure 3. Analysis of published literature based on the biomaterials used from 2001 to mid-2006.

Several studies have been carried out on the biocompatibility and the degradation rate of various biodegradable polymers [12–14]. A study by Li *et al*. [15] showed that cell-matrix interaction and cell proliferation are highly dependent on the stability of the fibrous scaffold thus poly(L-lactic acid) (PLLA) and polycaprolactone (PCL) with its slower degradation rate may be more suitable candidate as tissue scaffold than poly(DL-lactic acid) (PDLLA), polyglycolic acid (PGA) and its copolymers. In cases where mechanical strength is important, synthetic polymers generally have an edge over natural polymers. Figure 4 shows a bundle of electrospun PCL fibers which can be used as tendon scaffold. A similar electrospun collagen fiber bundle will probably have a lower mechanical strength.

Although synthetic materials have superior mechanical strength, its lack of cell-recognition signal [25] has prompted many researchers to use natural polymers instead. The ECM is not merely an inert supporting material on which cells resides. The matrix has an active and complex role in regulating cell behavior, influencing their survival, migration, proliferation, shape and function [26, 27]. Natural polymers, such as collagen, have been widely used as tissue scaffolds [28] since they may retain the necessary cell stimuli [29]. Nevertheless, it is vital that the processed natural polymer retains most of its original characteristics. Matthews *et al.* [30] reported that their electrospun type I collagen had an average diameter of 250 nm and was found to exhibit 67-nm banding typical of native collagen [31]. Other types of ECM components such as hyaluronic acid [31] and collagen type II have also been electrospun [32, 33].

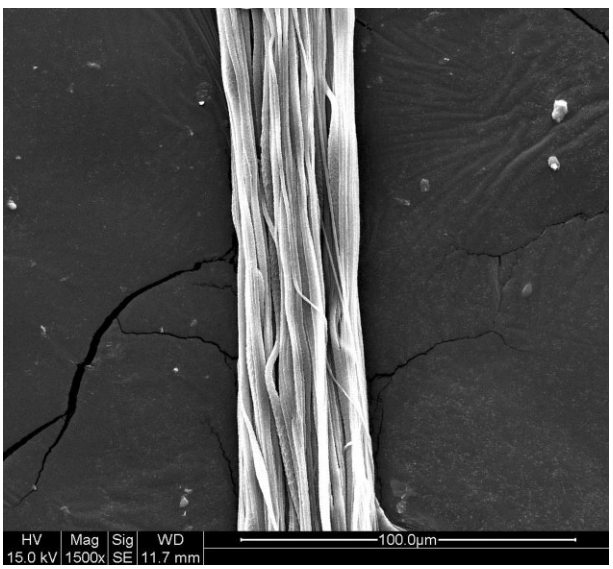

Figure 4. Electrospun PCL fiber bundle that has the potential to be used as a tendon scaffold.

Depending on the application, synthetic, natural or a mixture of the materials can be used. In most cases, the

Table 1. Mechanical properties of some polymer used in tissue engineering

Material	Fiber diameter (nm)	Stress (MPa)	Tensile modulus (MPa)
Poly(glycolic acid) [16]	630	–	~19
Poly(DL-lactide-co-glycolide), (85:15) [17]	500–800	22.67	323.15
Poly(DL-lactide-co-glycolide), (75:25) [18]	550	4.67	110.78
Poly(L-lactide-co-ε-caprolactone), (70:30) [19]	470	6.3	44
Polycaprolactone [20] 950 2.84 - Fibrinogen [21]	700	2	80
Acrylate modified elastomeric protein [22]	300–500	16.2	700
50% Collagen type I:50% polyethylene oxide [23]	100–150	0.37	12
Gelatin [24]	200	5.77	499

scaffold constructed from natural occurring proteins in the ECM such as collagen allows much better infiltration of cells into the scaffold. A study by Telemeco *et al.* [34] comparing the cellular response on implanted electrospun collagen, gelatin, PGA, polylactic acid (PLA) and polylactic-co-glycolic acid (PLGA) scaffold into the belly of the *vastus lateralis* of the rat showed that electrospun collagen scaffolds were densely infiltrated by interstitial and endothelial cells with evidence of functional blood vessels, while the other scaffolds were not infiltrated and induced fibrosis after 7 days. However, mechanical strength of the electrospun collagen scaffold is weak, thus for most applications, modification of the scaffold is required.

3 Modification of electrospun fibers

Although electrospinning is able to produce fibers made of selected material, this is often not enough to meet the complex demands of the tissue scaffold. Modification of the scaffolds is often necessary to enhance some of its properties, which just by electrospinning and material selection alone are inadequate. A material that favors the proliferation and attachment of the specific cell may be lacking in mechanical strength. Thus, the nanofibrous scaffold would have to be modified to enhance its stability and mechanical strength. Cross-linking is a widely adopted method of improving the mechanical properties of the nanofibrous scaffold. Nagapudi *et al.* [22] introduced an acrylate moiety to an elastin-mimetic protein polymer, poly[(Val-Pro-Gly-Val-Gly)$_4$(Val-Pro-Gly-Lys-Gly)]. The acrylate modified elastomeric protein (AMEP) was electrospun to produce a non-woven mesh of nanofibers subsequently cross-linked by visible-light-mediated photo-irradiation. Tensile strength and the Young's modulus of the uncross-linked AMEP was 16.2 ± 6.3 MPa and 0.7 ± 0.15 GPa, respectively, while cross-linked AMEP was 43.3 ± 5.2 MPa and 1.8 ± 0.4 GPa, respectively. However, the strain to failure decreased from 3.9 ± 0.2% to 2.3 ± 0.35%. Nevertheless, upon hydration, the cross-linked AMEP showed a substantial increase in the strain to failure to 105 ± 8%, although the Young's modulus dropped to 0.45 ± 0.08 MPa. These values are comparable to published mechanical properties of native elastin, which has a strain of about 120% and Young's modulus of 0.17 MPa [35]. There are also other means of cross-linking of electrospun fibers. *N*-(3-Dimethylaminopropyl)-*N*′-carbodiimide can be used to couple carboxyl group to primary amines, or used with *N*-hydroxysuccinimide [36], while glutaraldehyde can be used either as a diluted solution [37] or as saturated vapor [38] for cross-linking.

As mentioned earlier, the ECM has an active role in several cell functions [26, 27], and since unmodified polymer does not contain any cell surface receptors, several surface modification methods have been used by various researchers to introduce proteins and ligands onto the surface of the scaffold. Fertala *et al.* [39] electrospun a mixture of PLLA and poly(ε-CBZ-L-lysine), which have free NH_2 groups for the attachment of recombinant collagen II. The carbobenzoxy (CBZ) protected ε-amino groups of the L-lysine were activated by submerging the electrospun fiber mesh in acid solution, which detached the CBZ from the amino group. Sodium carbonate was subsequently added to neutralize the sample. The activated amino groups were able to bind 20 times more collagen onto the surface of the nanofibers than non-activated nanofibers. Chua *et al.* [40] used a photo-polymerization method to graft polyacrylic acid on the surface of the electrospun poly(ε-caprolactone-co-ethyl ethylene phosphate) and 1-O-(6'-aminohexyl)-D-galactopyranoside was subsequently conjugated onto the scaffold. He *et al.* [19] used a simpler method of surface modification to coat collagen on the surface of poly(L-lactide-co-ε-caprolactone) (PLCL) (70:30). The electrospun polymer scaffold was air plasma treated for 5 min with a radio frequency set at 30 W. This increased the surface hydrophilicity of the material, which made it wettable by collagen solution. The polymer scaffold was immersed in collagen solution overnight before being dried at room temperature. Cells cultured on the collagen-coated fibrous scaffold were well spread out with good integration between the cell and the fibers compared to non-treated fibrous scaffold, which exhibited rounded morphology as shown in Fig. 5. Since natural ECM contains a multitude of other materials vital for cell growth and maintaining the structural integrity of the ECM, other biological substances such as GAG [31] have been added to the collagen solution before electrospinning [38].

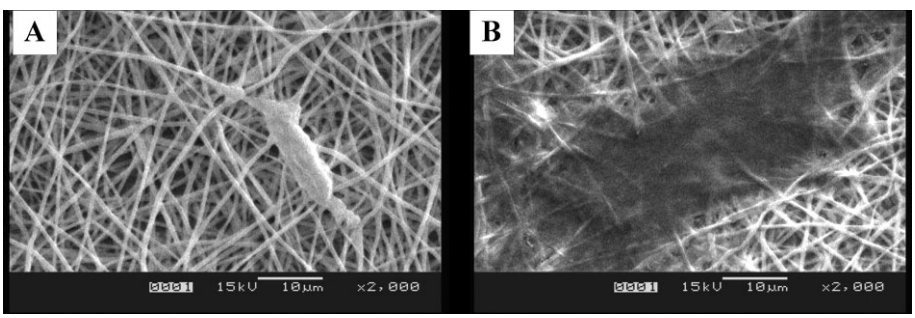

Figure 5. The effect of surface modification of fibrous scaffold on endothelial cells. (A) Untreated PLCL electrospun fibers. (B) Collagen-coated PLCL electrospun fibers.

In some applications where mechanical strength is required, the use of natural polymers alone may not be sufficient. A common practice for incorporating the properties of two materials is by blending the two together. Collagen has been blended with biodegradable synthetic polymers and electrospun to give a scaffold that promotes good cell adhesion and proliferation and exhibits superior mechanical strength [41]. Conductive polymers such as polyaniline have also been blended with gelatin and electrospun for use as a tissue scaffold [24]. This was based on the hypothesis that a multitude of cell functions such as cell proliferation, migration and differentiation can be modulated by electrical stimulation [42]. For bone grafts, Kim *et al.* [43] electrospun nanofibrous composite made out of hydroxyapatite (HA) nanocrystals and gelatin. The composite demonstrated improved bone-derived cellular activity as compared to pure gelatin nanofibers.

4 Electrospun assemblies

The ability to electrospin a variety of nanofibrous assemblies has allowed researchers to mimic the structure and composition of natural ECM. Natural ECM can be considered as a composite consisting of a complex mixture of structural and functional proteins, glycoproteins and proteoglycans. To mimic natural ECM, Min *et al.* [44] fabricated a composite scaffold for dermal reconstruction consisting of electrospun PLGA and electrosprayed chitin nanoparticles. The electrospinning and electrospraying were carried out simultaneously such that both the PLGA fibers and chitin nanoparticles were evenly distributed throughout the scaffold. Due to the dense mat of deposited nanofibers, cells have difficulty in migrating into the interior of the fibrous scaffold. Stankus *et al.* [45] overcame this problem by simultaneously electrospinning poly(ester urethane)urea and electrospraying vascular smooth muscle cells. High cell density integration with the electrospun fibers were observed after perfusion culture. Despite the application of a high voltage, a study by Jayasinghe *et al.* [46] suggested no sign of cellular damage after the cells have been electrosprayed. The rate of cell division after electrospraying continued as normal.

For more than a decade, researchers have shown that the topography of a substrate has an effect on the cells, such as cell orientation and rate of movement [47]. By using various electrospinning setups, such as using a rotating collector [30, 48] as shown in Fig. 6, scaffold with aligned nanofibers can be fabricated [49]. Several studies have demonstrated the migration and proliferation of cells in the direction of the electrospun fibers alignment [50, 51] as shown in Fig. 7. This will be suitable for region of specific tissue regeneration such as the tunica media of the artery, where the smooth muscle cells are circumferentially aligned.

In the construction of a small diameter tubular scaffold, a rotating tube or rod of appropriate diameter can be used to collect the electrospun nanofibers. When a sufficient thickness of nanofibers is accumulated on the collector, a tubular fibrous scaffold can be obtained by extracting the collector. Matsuda *et al.* [52] was able to fabricate a tubular scaffold with the inner fibrous layer being circumferentially aligned and the other fibrous layer randomly distributed. This is achieved by rotating a 3-mm di-

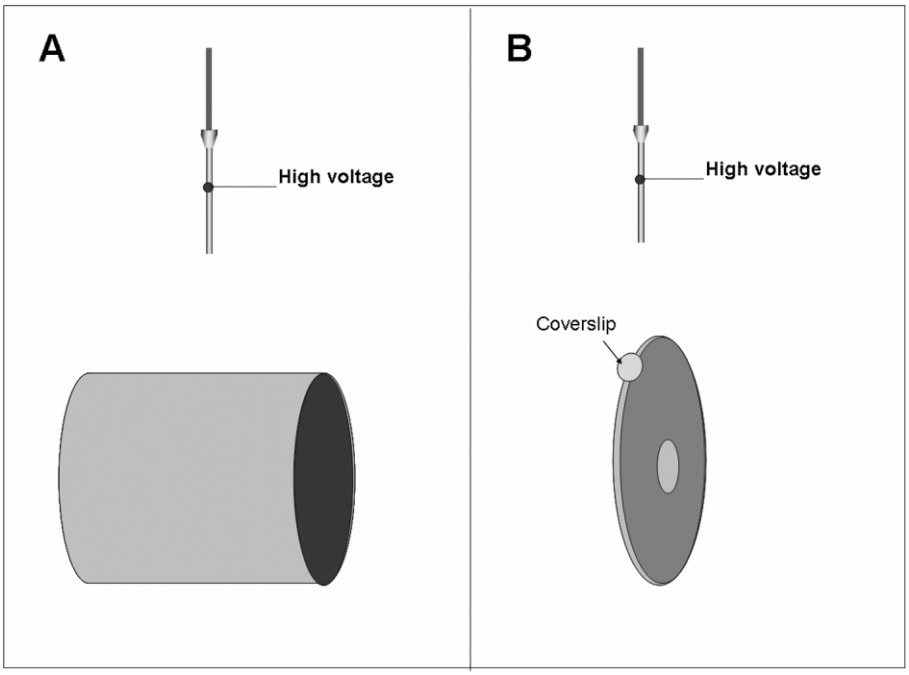

Figure 6. Schematic of rotating collector to deposit aligned fibers. (A) Rotating drum to collect large area of aligned fibers [30]. (B) Knife-edge rotating disk to collect better aligned fibers on the coverslip [48].

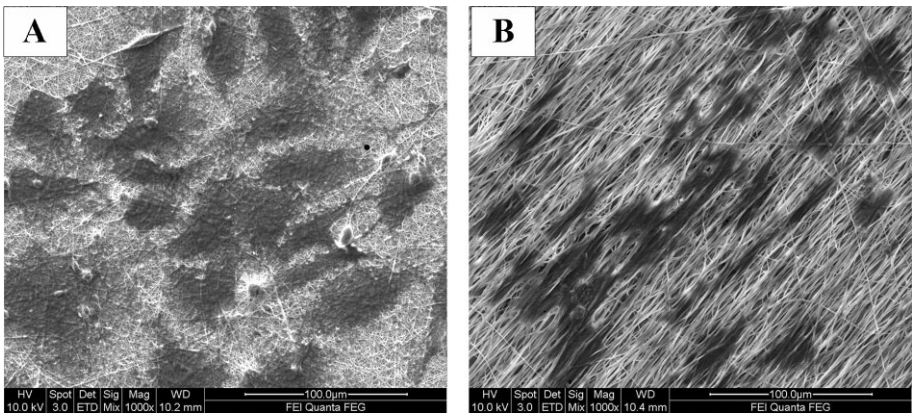

Figure 7. Comparing the effects of fiber surface topography on endothelial cells. (A) Randomly oriented collagen-coated PLCL copolymer fibers. (B) Aligned collagen-coated PLCL copolymer fibers.

ameter metallic tube at a speed of 3400 rpm. Other tubular scaffold consisting of multi-layers of electrospun fibers have also been fabricated [53, 54]. This way, various desirable properties of the material can be incorporated into the resultant scaffold.

5 Cartilage and bone grafts

In a cartilage graft, the nanotopography of electrospun nanofibers has been shown to provide a favorable condition for the growth of chondrocytes. Comparing electrospun fibrous scaffold consisting of 75:25 PLGA and PLGA solvent-cast film in terms of chondrocytes proliferation and ECM formation, DNA and GAG content in the electrospun scaffold was higher than in the film from day 7 of culture onwards [18]. Since cartilage is composed mainly of type II collagen, electrospinning of type II collagen has been carried out to form a non-woven mesh of nanofibers [55]. Chondrocytes seeded on the scaffold were evenly distributed across the scaffold thickness after 1 week of culture [33].

Li *et al.* [56] demonstrated that cell proliferation and differentiation on a PCL electrospun scaffold were differently affected by serum-containing media or serum-free media. In the presence of serum-containing medium, fetal bovine chondrocytes (FBC) seeded on electrospun fibers showed greater proliferation but less differentiation than in serum-free medium. The chondrocytes were able to efficiently maintain their differentiated phenotype in contrast to those kept as a monolayer on tissue culture polystyrene (TCPS), which dedifferentiate and lose their chondrocytic phenotype. Thus, the unique structural feature of electrospun nanofibrous scaffold combined with the composition of culture medium has a strong influence on the biological response of FBCs.

Cell maturation and differentiation are affected by regulatory molecules. However, it has been suggested that various mechanical stimuli may play a part in the development of articular cartilage [57] and it has been demonstrated that chondrocytes respond to mechanical stimuli [58]. Using an electrospun PLGA (75:25) scaffold, Shin *et al.* [18] demonstrated that by applying an intermittent hydrostatic pressure of 0.2 MPa using a bioreactor on the scaffold seeded with chondrocytes, cell proliferation and ECM formation was significantly increased.

In bone tissue engineering, Yoshimoto *et al.* [59] seeded mesenchymal stem cells (MSC) on an electrospun PCL scaffold in osteogenic differentiation medium. These MSCs differentiated into osteoblasts in the rotational bioreactor system and migrated into the scaffold. The cells produced ECM of collagen throughout the scaffold. The electrospun PCL scaffold was able to support mineralized tissue formation without compromising its structural stability, thus making it an attractive candidate for treatment of bone defects.

Since natural bone is a composite structure made out of fibrous collagen and other vital minerals, Fujihara *et al.* [60] fabricated an electrospun fibrous scaffold consisting of a blend of PCL nanofibers and calcium carbonate ($CaCO_3$). Although osteoblast proliferation was greater in the scaffold with a lower calcium carbonate content, more granules, indicating mineralization, were observed on the scaffold with a greater $CaCO_3$ content. Supaphol and colleagues [20] have embedded HA nanoparticles in PCL nanofibers. Osteoblasts were shown to grow slightly better in PCL/HA nanofibrous composite than in a PCL/$CaCO_3$ nanofibrous composite scaffold. Kaplan and colleagues [61] made a detail comparison study of the effect of electrospun polyethylene oxide (PEO) scaffold with the addition of silk, bone morphogenetic protein 2 (BMP-2), and HA nanoparticles on bone formation from human bone marrow-derived MSCs (hMSCs). Their tests showed that silk/PEO scaffolds showed the lowest calcium content but the highest level of DNA, whereas higher calcium deposits were found on silk/PEO with HA and/or BMP-2 added. The highest level of calcium deposition was found on silk/PEO/HA/BMP-2 scaffold.

In an animal study on guided bone regeneration, Kim *et al.* [62] used electrospun silk fibroin to facilitate bone

wound healing. Two 8-mm diameter calvarial defects were first created in New Zealand White rabbits. In the rabbits in which an electrospun silk fibroin membrane was used for guided bone regeneration, the defects completely healed, and were replaced with new bone after 12 weeks with no evidence of any inflammatory reaction. In contrast, the control group with no membrane did not show complete healing of the bone. Shin *et al.* [63] used an electrospun PCL scaffold, which was first seeded with MSCs and cultured with osteogenic supplements in a rotating bioreactor for 4 weeks before implanting in the omenta of rats for another 4 weeks. Following removal of the scaffold from the bioreactor, cells and ECM formation were observed throughout the scaffold with mineralization and type I collagen detected.

6 Skin grafts

To develop a stable and biocompatible scaffold for skin grafting, several researchers have used fiber scaffolds made out of different polymer blends. Pan *et al.* [64] electrospun a blend of dextran and PLGA solution, and the resultant fibers were subsequently stabilized by photo-cross-linking of the dextran component. Dermal fibroblasts seeded onto the scaffold were able to migrate into the highly porous 3-D matrix of the scaffold and organized into dense multi-layered structures that resembled dermal structure. Min *et al.* [44] used a mixture of PLGA fibers, chitin nanoparticles and adsorption of type I collagen or laminin onto the fibrous composite to mimic natural dermal ECM. Human keratinocytes showed improved attachment on PLGA-chitin electrospun composites compared to pure PLGA fibers. While type I collagen coated on the fibrous scaffolds promoted the adhesion and proliferation of normal human keratinocytes and fibroblast, only human fibroblast responded to laminin coating on the scaffold with results similar to that of collagen coating.

Since type I collagen is known to promote the adhesion and proliferation of normal human keratinocytes, Rho *et al.* [65] used pure type I collagen to electrospin a nanofibrous scaffold. The nanofibers were then vapor cross-linked using glutaraldehyde to improve its stability of the scaffold in water. However, when normal human keratinocytes were seeded onto the scaffold, unexpectedly low level of cell adhesion was observed. A possible reason could be the denaturation of the collagen conformation caused by electrospinning or cross-linking. The use of solvent and chemicals for the electrospinning and cross-linking process, respectively, may denature the collagen. Stretching of the viscous collagen solution during the electrospinning process may destroy the triple-helix structure of the collagen. To the our knowledge, only Matthews *et al.* [30] have reported electrospun collagen fibers exhibiting 67-nm banding typical of native collagen [31]. Thus, a more detailed study should be carried out on the effect of electrospinning and cross-linking on the structure and properties of electrospun collagen fibers. Rho *et al.* [65] reported that the adhesion of type I collagen or laminin onto the surface of collagen scaffold would significantly increase the adhesion of proliferating human keratinocytes compared with pure collagen-only nanofiber scaffold. In another attempt to incorporate collagen into the nanofibrous scaffold to promote cell adhesion and proliferation, Venugopal *et al.* [66] used a blend of type I collagen and PCL for electrospinning. The growth rate of human dermal fibroblasts cultured on the nanofibrous scaffold was shown to be the same as those cultured on TCPS.

7 Vascular grafts

In the selection of materials to be electrospun for arterial blood vessels, the energy and shape recovery are critical parameters to be considered. Energy stored during the expansion of the blood vessel should be recoverable and used in the contraction of the vessel without any distortion to the vessel. Natural polymers such as elastin have been used for electrospinning. Huang *et al.* [67] used recombinant protein based on repeating elastomeric peptide sequence of elastin $(Val\text{-}Pro\text{-}Gly\text{-}Val\text{-}Gly)_4(Val\text{-}Pro\text{-}Gly\text{-}Lys\text{-}Gly)$ to electrospin a non-woven mesh of fibers. The ultimate tensile strength of the nonwoven fabrics was 35 MPa and the material modulus was 1.8 GPa.

Besides selection of material according to its mechanical properties, another important factor is the cell adhesion and proliferation on it. Constructed vascular graft should express anti-coagulant activity until the endothelial cell lining is fully achieved. To meet these two characteristics, Kwon and Matsuda [68] electrospun two different solution blends. The first blend consisted of PLCL and collagen fibers, and the second blend consisted of PLCL and a tri-*n*-butylamine salt of heparin (heparin-TBA). Human umbilical vein endothelial cells cultured on electrospun fibrous scaffold containing 5 and 10 wt% collagen in the blend were highly elongated and well spread on the fibrous surface but cells on the scaffold containing 30–50 wt% collagen in the blend showed round or restricted-spread morphology. This observation runs contrary to reports by other research groups where endothelial cells cultured on collagen and polymer blended (ratio 1: 1) fibers showed spreading with a polygonal shape [41]. With the scaffold containing a blend of heparin and PLCL, a burst release was observed in the first 12 h when it was soaked in PBS at 37°C, after which relatively sustained release rate was observed for 4 weeks. This was probably due to the degradation of the copolymer. By electrospinning both blends simultaneously on the same collector, it may be possible to fabricate a scaffold that is able to encourage cell adhesion and proliferation and exhibit antithrombogenic properties [68].

Stitzel *et al.* [69] made a comparison between a vascular graft made out of purely electrospun PLA fibers and a composite consisting of collagen microfibers (~10 μm) and electrospun PLA fibers. The winding of the collagen microfibers exerted an outward force on the matrix, which the outer layers of electrospun PLA fibers must take up, and this mimics the stressed state of a native artery. When smooth muscle cells (SMC) were cultured on the two vascular grafts, SMCs on the pure PLA electrospun fibers were randomly distributed, while those cultured on the composite showed general orientation along the principal stress lines. Therefore, it is possible to impose a residual stress on the electrospun scaffold, which in turn would affect the proliferation and orientation of the SMCs.

An attractive option of using electrospinning to fabricate vascular graft is its ability to electrospin small diameter tubes of different sizes with uniform thickness and fiber distribution throughout the scaffold as shown in Fig. 8. Stitzel *et al.* [37] fabricated a tubular scaffold of 4.75-mm inner diameter consist of randomly oriented PLGA, type I collagen and elastin electrospun fibers. Axial and circumferential testing of the scaffolds demonstrated no significant difference in the mechanical properties. The burst pressure of the cross-linked fibers was found to be 12 times systolic pressure and the compliance test was 12–14% compared to 9% of the native vessel. The tubular scaffold was found to support both smooth muscle cells and endothelial cells. Matsuda and colleagues [70] used PLCL as the base material in the construction of a smaller diameter vascular graft. A series of tests carried out on the electrospun PLCL tubular scaffold showed that the smaller the wall thickness, the greater the compliance of the tube. Using a simulated circulatory system, it was found that at higher flow condition, the strain of the graft matches well with that of rabbit aorta.

There are various ways to alter the structure, topography and material composition of the electrospun tubular scaffold. Vaz *et al.* [53] electrospun a bi-layered tubular scaffold with a stiff oriented PLA outer fibrous layer and a compliant randomly oriented PCL inner fibrous layer. The oriented outer layer was achieved by rotating the collector at high speed. Culturing of human myofibroblasts after 30 days showed that the cells were mostly concentrated on the outer layer. This is probably due to the inadequate pore size between the fibers. Matsuda and coworkers [54] also fabricated bilayered tubular scaffold with a thin inner layer of collagen and a thick outer layer of segmented polyurethane.

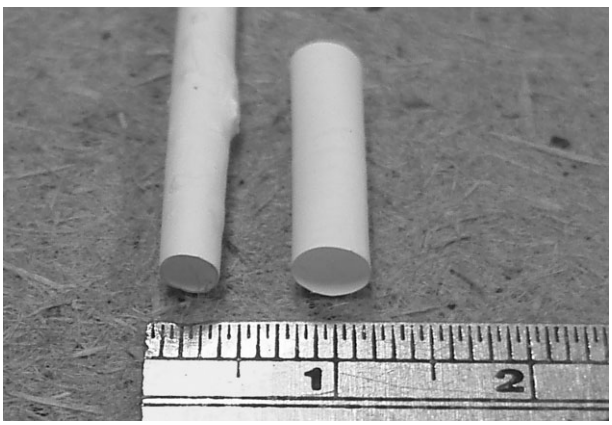

Figure 8. Electrospun tubular scaffolds of different diameter made of PCL-PLA copolymers.

8 Nerve grafts

In the development of bioresorbable nerve conduits, Ramakrishna and colleagues [71] used electrospun biodegradable fibers to fabricate the conduit. Neural stem cells (NSC) seeded on the PLA nanofibrous scaffold were found to interact favorably with the environment with good cell attachment and differentiation, as shown by the neurite outgrowth. When the NSCs were cultured on aligned nanofiber scaffolds, the cells elongated along the direction of the fiber alignment and the neurite outgrowth was also along the same direction as shown in Fig. 9. Compared to the microfibers, the differentiation rate of the NSCs on the nanofibers was higher [72]. In an animal study, PLGA (10:90) fibers were collected over a Teflon tube of 1.27-mm diameter to form a nerve conduit after the Teflon tube was removed. The conduit was implanted into the right sciatic nerve of a rat. The porous nanofibrous scaffold allowed the entry of nutrients into the lumen to promote nerve regeneration but at the same time

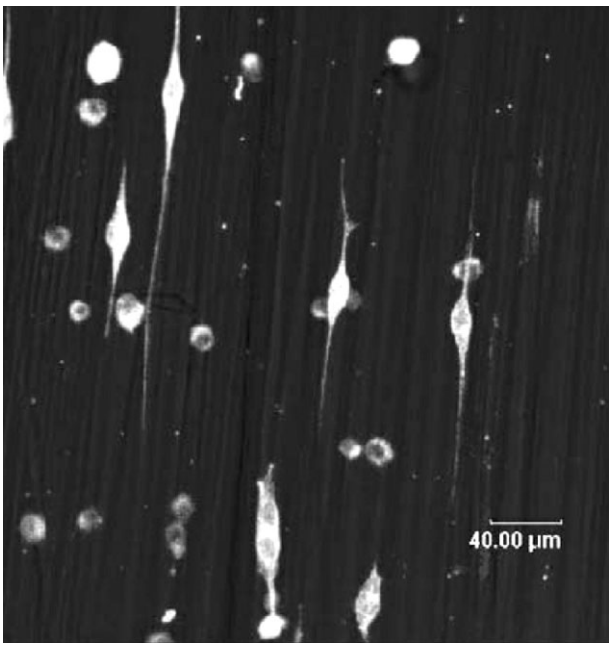

Figure 9. Neural stem cells elongate along the direction of the aligned electrospun fibers and the neurite outgrowth also occurs along the same direction [72].

Table 2. Electrospun materials used in tissue grafts

Graft	Material
Skin graft	
Fibroblast	Dextran and poly(lactide-co-glycolide) [64] Poly(lactide-co-glycolide) [44] Poly(lactide-co-glycolide) and chitin nanoparticles composite [44]
Normal human keratinocytes	Collagen type I coated with collagen type I and laminin [65] Poly(lactide-co-glycolide) and chitin nanoparticles composite [44]
Vascular graft	
Arterial Smooth Muscle Cell	40% Poly(DL-lactide-co-glycolide), 45% collagen type I and 15% elastin [23]
Myofibroblasts	Polylactic acid [53]
Human coronary artery endothelial cells	50% Poly(L-lactide acid-co-ε-caprolactone) (70:30), 50% Type I collagen [41]
Cartilage graft	
Chondrocytes	Collagen Type II [33, 55] Polycaprolactone [56]
Bone graft	
Mesenchymal stem cells	Polycaprolactone [59] Silk/polyethylene oxide/hydroxyapatite / bone morphogenetic protein 2 [61]
Osteoblast	Polycaprolactone/calcium carbonate [60] Polycaprolactone/hydroxyapatite [20]
Nerve graft	
Neural stem cells	Poly(L-lactic acid) [71]
Cardiac graft	
Cardiomyocytes	Polycaprolactone coated with collagen Type I [74] Polylactide [76]
Cardiac myoblast	Polyaniline and gelatin [24]
Others	
Normal rat kidney cells	Polyamide [77, 78]
Rabbit conjunctiva fibroblasts	Type I collagen and chondroitin sulfate [38]
Rat hepatocytes	Galactosylated poly(ε-caprolactone-co-ethyl ethylene phosphate) [40]
Breast epithelial cells	Polyamide [78]
Human ligament fibroblast	Polyurethane [51]

acted as a barrier to unwanted tissues infiltration. Positive reflex responses were observed in 45% of the rats 1 month after implantation and 8out of 11 rats had regenerated cable inside the conduits [73].

9 Cardiac grafts

In the fabrication of a scaffold as a cardiac graft, Shin *et al.* [74] electrospun PCL onto a wire ring of 15-mm diameter. The scaffolds were coated with purified type I collagen solution to promote cell attachment. Neonatal rat cardiomyocytes were cultured on the electrospun PCL scaffolds. The cardiomyocytes attached well to the scaffold and contraction of the cardiomyocytes was observed on the 10-μm thick scaffold 3 days after seeding. Tight arrangement and intercellular contacts of the cardiomyocytes were formed throughout the entire mesh, although more cells were found on the surface. The electrospun scaffold was sufficiently soft such that contractions of the cardiomyocytes were not impeded and stable enough for handling. By suspending the mesh across a ring, the cardiomyocytes are allowed to contract at their natural frequency.

The use of electrical stimulations has been shown to increase adsorption of serum proteins onto electrically conducting polymer, which leads to significantly enhanced neurite extension [75]. Thus, in developing "smart" nano-fibrous scaffolds to modulate various cell functions such as proliferation, differentiation and migration through electrical simulation, Li *et al.* [24] electrospun a blend of polyaniline and gelatin. The resultant scaffold was found to be biocompatible, supporting attachment, migration and proliferation of H9c2 rat cardiac myoblasts.

10 Concluding remarks

With the advances in the tissue engineering field, researchers are looking at ways to mimic natural ECM to reduce the incidence of rejection by the body when it is implanted. The use of electrospinning meant that structurally, the fabricated scaffolds can be made to resemble the ECM. Progress in elecrospinning will bring the artificial scaffold closer to that of the fiber arrangement in specific tissue. Table 2 is a summary of the cells that have been cultured on electrospun fibers. In the future, ECM scaffolds needs to be both biomimetic and bioactive. For this, the fibers will have to be modified to incorporate chemical cues where electrospinning offers its greatest flexibility. Through the incorporation of proteins such as collagen, improved cell proliferation and differentiation has been achieved on electrospun scaffolds. Selected *in vivo* tests such as guided bone regeneration using electrospun scaffold has yielded positive results.

In this review, we have concentrated on the potential of electrospun scaffold for use in tissue engineering by mimicking tissue-specific ECM. However, electrospun fibers have also shown potential in other areas such as drug delivery and cell encapsulation, which, in some cases, have been mentioned in this paper for tissue engineering purposes. Given the advantages of electrospinning in terms of material flexibility, scaffold assembly, numerous modification possibilities and relative ease of incorporation into other processes, electrospininng is one of the most promising tissue fabrication techniques so far this century.

11 References

[1] Ottani, V., Raspanti, M., Ruggeri, A., Collagen structure and functional implications. *Micron* 2001, *32*, 251–260.

[2] Larrondo, L., Manley, R. St. J., Electrostatic fiber spinning from polymer melts. I. Experimental observations on fiber formation and properties. *J. Polym. Sci. Pol. Phys.* 1981, *19*, 909–920.

[3] Larrondo, L., Manley, R. St. J., Electrostatic fiber spinning from polymer melts. II. Examination of the flow field in an electrically driven jet. *J. Polym. Sci. Pol. Phys.* 1981, *19*, 921–932.

[4] Larrondo, L., Manley, R. St. J., Electrostatic fiber spinning from polymer melts. III. Electrostatic deformation of a pendant drop of polymer melt. *J. Polym. Sci. Pol. Phys.* 1981, *19*, 933–940.

[5] Lyons, J., Li, C., Ko, F., Melt-electrospinning part I: processing parameters and geometric properties. *Polymer* 2004, *45*, 7597–7603.

[6] Tan, S. H., Inai, R., Kotaki, M., Ramakrishna, S., Systematic parameter study for ultra-fine fiber fabrication via electrospinning process. *Polymer* 2005, *46*, 6128–6134.

[7] Doshi, J., Reneker, D. H., Electrospinning process and applications of electrospun fibers. *J. Electrostat.* 1995, *35*, 151–160.

[8] Reneker, D. H., Yarin, A. L., Fong, H., Koombhongse. Bending instability of electrically charged liquid jets of polymer solutions in electrospinning. *J. Appl. Phys.* 2000, *87*, 4531–4547.

[9] Seal, B. L., Otero, T. C., Panitch, A., Polymeric biomaterials for tissue and organ regeneration. *Mater. Sci. Eng. R* 2001, *34*, 147–230.

[10] Shi, D. (Ed.), *Introduction to Biomaterials*, World Scientific, Singapore 2006.

[11] Hasırcı, V., Lewandrowski K., Gresser, J. D., Wise, D. L., Trantolo, D. J., Versatility of biodegradable biopolymers: degradability and an *in vivo* application. *J. Biotechnol.* 2001, *86*, 135–150.

[12] You, Y., Min, B. M., Lee, S. J., Lee, T. S., Park W. H., *In vitro* degradation behavior of electrospun polyglycolide, polylactide, and poly(lactide-co-glycolide). *J. Appl. Polym. Sci.* 2005, *95*, 193–200.

[13] Zeng, J., Chen, X., Liang, Q., Xu, X., Jing, X., Enzymatic degradation of poly(L-lactide) and poly(ε-caprolactone) electrospun fibers. *Macromol. Biosci.* 2004, *4*, 1118–1125.

[14] Bolgen, N., Menceloglu, Y. Z., Acatay, K., Vargel, I., Piskin, E., *In vitro* and *in vivo* degradation of non-woven materials made of poly(ε-caprolactone) nanofibers prepared by electrospinning under different conditions. *J. Biomater. Sci. Polymer Ed.* 2005, *16*, 1537–1555.

[15] Li, W. J., Cooper, J. A. Jr., Mauck, R. L., Tuan, R. S., Fabrication and characterization of six electrospun poly(α-hydroxyester)-based fibrous scaffolds for tissue engineering applications. *Acta Biomater.* 2006, *2*, 377–385.

[16] Boland, E. D., Wnek, G. E., Simpson, D. G., Pawlowski, K. J. *et al.,* Tailoring tissue engineering scaffolds using electrostatic processing techniques : A study of poly(glycolic acid) electrospinning. *J. Macromol. Sci. Pure Appl. Chem.* 2001, *A38*, 1231–1243.

[17] Li, W. J., Laurencin, C. T., Caterson, E. J., Tuan, R. S., Ko, F. K. Electrospun nanofibrous structure: A novel scaffold for tissue engineering. *J. Biomed. Mater. Res.* 2002, *60*, 613–621.

[18] Shin, H. J., Lee, C. H., Cho, I. H., Kim, Y. J. *et al.,* Electrospun PLGA nanofiber scaffolds for articular cartilage reconstruction: mechanical stability, degradation and cellular responses under mechanical stimulation *in vitro*. *J. Biomater. Sci. Polym. Ed.* 2006, *17*, 103–119.

[19] He, W., Ma, Z. W., Yong, T., Teo, W. E., Ramakrishna, S., Fabrication of collagen-coated biodegradable polymer nanofiber mesh and its potential for endothelial cells growth. *Biomaterials* 2005, *26*, 7606–7615.

[20] Wutticharoenmongkol, P., Sanchavanakit, N., Pavasant, P., Supaphol, P., Preparation and characterization of novel bone scaffolds based on electrospun polycaprolactone fibers filled with nanoparticles. *Macromol. Biosci.* 2006, *6*, 70–77.

[21] Wnek, G. E., Carr., M. E., Simpson, D. G., Bowlin, G. L., Electrospinning of nanofiber fibrinogen structures. *Nano Lett.* 2003, *3*, 213–216.

[22] Nagapudi, K., Brinkman, W. T., Leisen, J. E., Huang, L. *et al.,* Photomediated solid-state cross-linking of an elastin-mimetic recombinant protein polymer. *Macromolecules* 2002, *35*, 1730–1737.

[23] Huang, L., Nagapudi, K., Apkarian, R. P., Chaikof, E. L., Engineered collagen – PEO nanofibers and fabrics. *J. Biomater. Sci. Polymer Ed.* 2001, *12*, 979–993.

[24] Li, M., Guo, Y., Wei, Y., MacDiarmid, A. G., Lelkes, P. I., Electrospinning polyaniline-contained gelatin nanofibers for tissue engineering applications. *Biomaterials* 2006, *27*, 2705–2715.

[25] Kim, B. S, Mooney, D. J., Development of biocompatible synthetic extracellular matrices for tissue engineering. *Trends Biotechnol.* 1998, *16*, 224–230.
[26] Nathan, C., Sporn, M., Cytokines in context. *J. Cell. Biol.* 1991, *113*, 981–986.
[27] Perris, R., Perissinotto, D., Role of the extracellular matrix during neural crest cell migration. *Mech. Dev.* 2000, *95*, 3–21.
[28] Lee, C. H., Singla, A., Lee, Y., Biomedical applications of collagen. *Int. J. Pharm.* 2001, *221*, 1–22.
[29] Bokel, C., Brown, N. H., Integrins in development: Moving on, responding to, and sticking to the extracellular matrix. *Dev. Cell* 2002, *3*, 311–321.
[30] Matthews, J. A., Wnek, G. E., Simpson, D. G., Bowlin, G. L., Electrospinning of collagen nanofibers. *Biomacromolecules* 2002, *3*, 232–238.
[31] Alberts, B., Johnson, A., Lewis, J., Raff, M. et al, *Molecular Biology of the Cell*, Garland Science, Singapore 2002, pp. 1099.
[32] Um, I. C., Fang, D., Hsiao, B. S., Okamoto, A., Chu, B., Electro-spinning and electro-blowing of hyaluronic acid. *Biomacromolecules* 2004, *5*, 1428–1436.
[33] Matthews, J. A., Boland, E. D., Wnek, G. E., Simpson, D. G., Bowlin, G. L., Electrospinning of collagen type II: A feasibility study. J. Bioact. Compat. Pol. 2003, 18, 125–134.
[34] Telemeco, T. A., Ayres, C., Bowlin, G. L., Wnek, G. E. *et al.,* Regulation of cellular infiltration into tissue engineering scaffolds composed of submicron diameter fibrils produced by electrospinning. *Acta Biomater.* 2005, *1*, 377–385.
[35] Lillie, M. A., Gosline, J. M., The viscoelastic basis for the tensile strength of elastin. *Int. J. Biol. Macromol.* 2002, *30*, 119–127.
[36] Buttafoco, L., Kolkman, N. G., Engbers-Buijtenhuijs, P., Poot, A. A. *et al.,* Electrospinning of collagen and elastin for tissue engineering applications. *Biomaterials* 2006, *27*, 724–734.
[37] Stitzel, J., Liu, J., Lee, S. J., Komura, M. *et al.,* Controlled fabrication of a biological vascular substitute. *Biomaterials* 2006, *27*, 1088–1094.
[38] Zhong, S., Teo, W. E., Zhu, X., Beuerman, R. *et al.,* Formation of collagen-glycosaminoglycan blended nanofibrous scaffolds and their biological properties. *Biomacromolecules* 2005, *6*, 2998–3001.
[39] Fertala, A., Han, W. B., Ko, F. K., Mapping critical sites in collagen II for rational design of gene-engineered proteins for cell-supporting materials. *J. Biomed. Mater. Res.* 2001, *57*, 48–58.
[40] Chua, K. N., Lim, W. S., Zhang, P., Lu, H. *et al.,* Stable immobilization of rat hepatocyte spheroids on galactosylated nanofiber scaffold. *Biomaterials* 2004, *26*, 2537–2547.
[41] He, W., Yong, T., Teo, W. E., Ma, Z., Ramakrishna, S., Fabrication and endothelialization of collagen-blended biodegradable polymer nanofibers: Potential vascular graft for blood vessel tissue engineering. *Tissue Eng.* 2005, *11*, 1574–1588.
[42] Pedrotty, D. M., Koh, J., Davis, B. H., Taylor D. A. *et al.,* Engineering skeletal myoblasts: roles of three-dimensional culture and electrical stimulation. *Am. J. Physiol. Heart Circ. Physiol.* 2005, *288*, 1620–1626.
[43] Kim, H. W., Song, J. H., Kim, H. E., Nanofiber generation of gelatin-hydroxyapatite biomimetics for guided tissue regeneration. *Adv. Func. Mater.* 2005, *15*, 1988–1994.
[44] Min, B. M., You, Y., Kim, J. M., Lee, S. J., Park, W. H., Formation of nanostructured poly(lactic-co-glycolic acid)/chitin matrix and its cellular response to normal human keratinocytes and fibroblasts. *Carbohyd. Polym.* 2004, *57*, 285–292.
[45] Stankus, J. J., Guan, J., Fujimoto, K., Wagner, W. R., Microintegrating smooth muscle cells into a biodegradable, elastomeric fiber matrix. *Biomaterials* 2006, *27*, 735–744.
[46] Jayasinghe, S. N., Qureshi, A. N., Eagles, P. A. M., Electrohydrodynamic jet processing: An advanced electric-field-driven jetting phenomenon for processing living cells. *Small* 2006, *2*, 216–219.

Prof. Seeram Ramakrishna completed his postgraduate studies in Materials Science and Engineering, at the University of Cambridge, UK, in 1992. In 1996, he was offered the prestigious Lee Kuan Yew fellowship and joined the Institute of Materials Research and Engineering in the same year. He became a Senior Lecturer in the Department of Mechanical Engineering at the National University of Singapore in 1997, was promoted to Associate Professor in 1999, and was conferred full Professorship in 2003. In 2001, he was appointed as Co-Director of the NUS Nanoscience and Nanotechnology Initiative (NUSNNI) to promote Nanotechnology education, research and development efforts across NUS. In 2003, Prof. Ramakrishna was appointed Dean of the NUS Faculty of Engineering, one of the largest research-intensive engineering schools around the world. His research interests are manufacturing technology and design aspects of electrospun nanofibers, to realize their full potential in healthcare, energy and environment. He serves on the editorial boards of ten international journals and has published extensively across a broad range of areas, including biocomposites, tissue engineering, electrospinning, nanofibers, and membranes, and authored two books.

[47] Curtis, A., Wilkinson, C., Topographical control of cells. *Biomaterials* 1997, *18*, 1573–1583.
[48] Theron, A., Zussman, E., Yarin, A. L., Electrostatic field-assisted alignment of electrospun nanofibres. *Nanotechnology* 2001, *12*, 384–390.
[49] Teo, W. E., Ramakrishna, S., A review on electrospinning design and nanofibre assemblies. *Nanotechnology* 2006, *17*, R89–R106.
[50] Xu, C. Y., Inai, R., Kotaki, M., Ramakrishna, S., Aligned biodegradable nanofibrous structure: a potential scaffold for blood vessel engineering. *Biomaterials* 2004, *25*, 877–886.
[51] Lee, C. H., Shin, H. J., Cho, I. H., Kang, Y. M., Nanofiber alignment and direction of mechanical strain affect the ECM production of human ACL fibroblast. *Biomaterials* 2005, *26*, 1261–1270.
[52] Matsuda, T., Ihara, M., Inoguchi, H., Kwon, I. K., Takamizawa, K., Kidoaki, S., Mechano-active scaffold design of small-diameter artificial graft made of electrospun segmented polyurethane fabrics. *J. Biomed. Mater. Res.* 2005, *73A*, 125–131.
[53] Vaz, C. M., Tuijl, S., Bouten, C. V. C., Baaijens, F. P. T., Design of scaffolds for blood vessel tissue engineering using a multi-layering electrospinning technique. *Acta Biomater.* 2005, *1*, 575–582.
[54] Kidoaki, S., Kwon, I. K., Matsuda, T., Mesoscopic spatial designs of nano- and microfiber meshes for tissue-engineering matrix and scaffold based on newly devised multilayering and mix electrospinning techniques. *Biomaterials* 2005, *26*, 37–46.
[55] Shields, K. J., Beckman, M. J., Bowlin, G. L., Wayne, J. S., Mechanical properties and cellular proliferation of electrospun collagen type II. *Tissue Eng.* 2004, *10*, 1510–1517.
[56] Li, W. J., Danielson, K. G., Alexander, P. G., Tuan, R. S., Biological response of chondrocytes cultured in three-dimensional nanofibrous poly(e-caprolactone) scaffolds. *J. Biomed. Mater. Res.* 2003, *67A*, 1105–1114.
[57] Wong, M., Carter, D. R., Articular cartilage functional histomorphology and mechanobiology: a research perspective. *Bone* 2003, *33*, 1–13.

[58] Wong, M., Siegrist, M., Goodwin, K., Cyclic tensile strain and cyclic hydrostatic pressure differentially regulate expression of hypertrophic markers in primary chondrocytes. *Bone* 2003, *33*, 685–693.

[59] Yoshimoto, H., Shin, Y. M., Terai, H. Vacanti, J. P., A biodegradable nanofiber scaffold by electrospinning and its potential for bone tissue engineering. *Biomaterials* 2003, *24*, 2077–2082.

[60] Fujihara, K., Kotaki, M., Ramakrishna, S., Guided bone regeneration membrane made of polycaprolactone/calcium carbonate composite nano-fibers. *Biomaterials* 2004, *26*, 4139–4147.

[61] Li, C., Vepari, C., Jin, H. J., Kim, H., J., Kaplan, D. Electrospun silk-BMP-2 scaffolds for bone tissue engineering. *Biomaterials* 2006, *27*, 3115–3124.

[62] Kim, K. H., Jeong, L., Park, H. N., Shin, S. Y. *et al.,* Biological efficacy of silk fibroin nanofiber membranes for guided bone regeneration. *J. Biotechnol.* 2005, *120*, 327–339.

[63] Shin, M., Yoshimoto, H., Vacanti, J. P., *In vivo* bone tissue engineering using mesenchymal stem cells on a novel electrospun nanofibrous scaffold. *Tissue Eng*. 2004, *10*, 33–34.

[64] Pan, H., Jiang, H., Chen, W., Interaction of dermal fibroblasts with electrospun composite polymer scaffolds prepared from dextran and poly lactide-co-glycolide. *Biomaterials* 2006, *27*, 3209–3220.

[65] Rho, K. S., Jeong, L., Lee, G., Seo, B. M. *et al.,* Electrospinning of collagen nanofibers: Effects on the behavior of normal human keratinocytes and early-stage wound healing. *Biomaterials* 2006, *27*, 1452–1461.

[66] Venugopal, J., Ma, L. L., Ramakrishna, S., Biocompatible nanofiber matrices for the engineering of a dermal subsititute for skin regeneration. *Tissue Eng.* 2005, *11*, 847–854.

[67] Huang, AL., McMillan, R. A., Apkarian, R. P., Pourdeyhimi, B. *et al.,* Generation of synthetic elastin-mimetic small diameter fibers and fiber networks. *Macromolecules* 2000, *33*, 2989–2997.

[68] Kwon, I. K., Matsuda, T., Co-electrospun nanofiber fabrics of poly(L-lactide- co-ε-caprolactone) with type I collagen or heparin. *Biomacromolecules* 2005, *6*, 2096–2105.

[69] Stitzel, J. D., Pawlowski, K. J., Wnek, G. E., Simpson, D. G., Bowlin, G. L., Arterial smooth muscle cell proliferation on a novel biomimicking, biodegradable vascular graft scaffold. *J. Biomater. Appl.* 2001, *16*, 22–33.

[70] Inoguchi, H., Kwon, I. K., Inoue, E., Takamizawa, K., Mechanical responses of a compliant electrospun poly(L-lactide-co-ε-caprolactone) small-diameter vascular graft. *Biomaterials* 2006, *27*, 1470–1478.

[71] Yang, F., Xu, C. Y., Kotaki, M., Wang, S., Ramakrishna, S., Characterization of neural stem cells on electrospun poly(L-lactic acid) nanofibrous scaffold. *J. Biomater. Sci. Polymer Ed.* 2004, *15*, 1483–1497.

[72] Yang, F., Murugan, R., Wang, S., Ramakrishna, S. Electrospinning of nano/micro scale poly(L-lactic acid) aligned fibers and their potential in neural tissue engineering. *Biomaterials* 2004, *26*, 2603–2610.

[73] Bini, T. B., Gao, S., Tan, T. C., Wang, S., Electrospun poly(L-lactide-co-glycolide) biodegradable polymer nanofibre tubes for peripheral nerve regeneration. *Nanotechnology* 2004, *15*, 1459–1464.

[74] Shin, M., Ishii, O., Sueda, T., Vacanti, J. P., Contractile cardiac grafts using a novel nanofibrous mesh. *Biomaterials* 2004, *25*, 3717–3723.

[75] Kotwal, A., Schmidtm C. E., Electrical stimulation alters protein adsorption and nerve cell interactions with electrically conducting biomaterials. *Biomaterials* 2001, *22*, 1055–1064.

[76] Zong, X., Bien, H., Chung, C. Y., Yin, L. *et al.*, Electrospun fine-textured scaffolds for heart tissue constructs. *Biomaterials* 2005, *26*, 5330–5338.

[77] Nur-E-Kamal, A., Ahmed, I., Kamal, J., Schindler, M., Meiners, S., Three dimensional nanofibrillar surfaces induce activation of Rac. *Biochem. Bioph. Res. Co.* 2005, *331*, 428–434.

[78] Schindler, M., Ahmed, I., Kamal, J., Nur-E-Kamal, A., A synthetic nanofibrillar matrix promotes *in vivo*-like organization and morphogenesis for cells in culture. *Biomaterials* 2005, *26*, 5624–5631.

INSTITUTE OF PHYSICS PUBLISHING BIOMEDICAL MATERIALS

Biomed. Mater. **1** (2006) R45–R53 doi:10.1088/1748-6041/1/3/R01

TOPICAL REVIEW

Biomimetic electrospun nanofibers for tissue regeneration

Susan Liao, Bojun Li, Zuwei Ma, He Wei, Casey Chan and Seeram Ramakrishna

Nanoscience and Nanotechnology Initiative (NUSNNI), Faculty of Engineering, National University of Singapore, 117576 Singapore

E-mail: bieliaos@nus.edu.sg

Received 20 June 2006
Accepted for publication 7 July 2006
Published 28 July 2006
Online at stacks.iop.org/BMM/1/R45

Abstract

Nanofibers exist widely in human tissue with different patterns. Electrospinning nanotechnology has recently gained a new impetus due to the introduction of the concept of biomimetic nanofibers for tissue regeneration. The advanced electrospinning technique is a promising method to fabricate a controllable continuous nanofiber scaffold similar to the natural extracellular matrix. Thus, the biomedical field has become a significant possible application field of electrospun fibers. Although electrospinning has developed rapidly over the past few years, electrospun nanofibers are still at a premature research stage. Further comprehensive and deep studies on electrospun nanofibers are essential for promoting their biomedical applications. Current electrospun fiber materials include natural polymers, synthetic polymers and inorganic substances. This review briefly describes several typically electrospun nanofiber materials or composites that have great potential for tissue regeneration, and describes their fabrication, advantages, drawbacks and future prospects.

1. Introduction

From a component perspective, the extracellular matrix (ECM) is composed of three major classes of biomolecules: (1) structural proteins: collagen and elastin; (2) specialized proteins: e.g., fibrillin, fibronectin and laminin; (3) proteoglycans: these are composed of a protein core to which are attached long chains of repeating disaccharide units termed glycosaminoglycans (GAGs), forming extremely complex high molecular weight components of the ECM. The ECM also contains many other components: minerals such as hydroxyapatite, or fluids such as the blood plasma or serum with secreted free-flowing antigens. From a structural perspective, natural ECMs consisted of various protein fibrils and fibers interwoven within a hydrated network of GAG chains, which provides an important model for the design of biomaterials [1]. The nanoscale structure of the ECM offers a natural network of intricate nanofibers to support cells and present an instructive background to guide their behavior [3, 4]. Each fiber contains clues that pave the way for cells to form tissues as complex as bone, liver, heart and kidney. Typically, cells respond to environmental features at all length scales from the macro down to the molecular. The outer membrane of a typical cell is covered by specific carbohydrate structures and a forest of at least six different receptor systems that can be activated by interactions with adjacent cells, ligands in the surrounding ECM and secreted signaling molecules. Collectively, these extrinsic factors make up a highly defined and specialized cell microenvironment, which is essential for correct tissue development and continued function.

Materials composed of naturally occurring (biologically derived) building blocks, including extracellular matrix components, are being studied for applications such as direct tissue replacement and tissue engineering. For example, collagen has been used for many years in biomedical applications, and it is now possible to create artificial analogs of ECM proteins using recombinant DNA technology [2]. However, current artificial biomaterial scaffolds designed to

support cell and tissue growth have traditionally been aimed at a macroscopic level to match the properties of the organs they are to replace, such as hard scaffolds for bone and elastic for bladder, veins and arteries—without the complexity and nanoscale detail observed in real organs at the level of the cell matrix interaction.

The use of nanoscale material structuring to control cell behavior has important implications when designing new biomaterials for tissue regeneration. To regenerate tissue, engineered scaffolds act as hosts to cells harvested from natural tissue. Since the ability to engineer materials aided by modern nanotechnology to a similar level of complexity is becoming a reality, in this review we will discuss this nanotechnology—electrospinning—for the fabrication of nanofibers, which could create biomimetic cellular environments. Electrospinning is a process to make nanofibers from polymer solution through electrostatic force. The electrospinning process, in its simplest form, consists of a pipette to hold polymer solution, two electrodes and a dc voltage supply in the kilovolt range. The polymer solution drop from the tip of the pipette is drawn into a fiber due to the high voltage. These fibers, for example as shown in figure 1(*a*), have a large surface area per unit mass so that fabrics of these nanofibers collected on a screen can be used in biomedical applications, which include tissue regeneration, drug and gene delivery, artificial organs and medical facemasks [5, 6]. Here, we focus on several potential types of electrospun nanofibers for tissue regeneration.

2. Electrospinning nanotechnology

In 1934, the experimental setup of a process patented by Formhals [7] was outlined for the production of polymer microfibers using electrostatic force. When used to spin fibers in this way, the process is termed electrospinning. Modern electrospinning technology, developed by a number of researchers, is able to make continuous fibers with diameters in the range of nanometers to a few micrometers. Electrospinning has the unique ability to produce nanofibers of different materials in various fibrous assemblies. The relatively high production rate and simplicity of the setup make electrospinning highly attractive to both academia and industry [8]. In the basic process of electrospinning, we need to consider two types of factors: (1) system parameters—molecular weight, molecular weight distribution and architecture (branched, linear etc) of the polymer and solution properties (viscosity, conductivity and surface tension); (2) process parameters—electric potential, flow rate and concentration, distance between the capillary and collector, ambient parameters (temperature, humidity and air velocity in the chamber) and motion of the collector. By varying the above parameters, it is possible to get some variation in the morphology of the nanofibers. Nanofibers in the range 10–2000 nm in diameter can be achieved by choosing an appropriate polymer solvent system. The diameter and parameters of electrospun fibers of select artificial and biodegradable polymers, as examples, are listed in table 1. Usually, we can decrease the concentration of polymer in the solution, and decrease the humidity in the chamber as well to fabricate relatively smaller fibers.

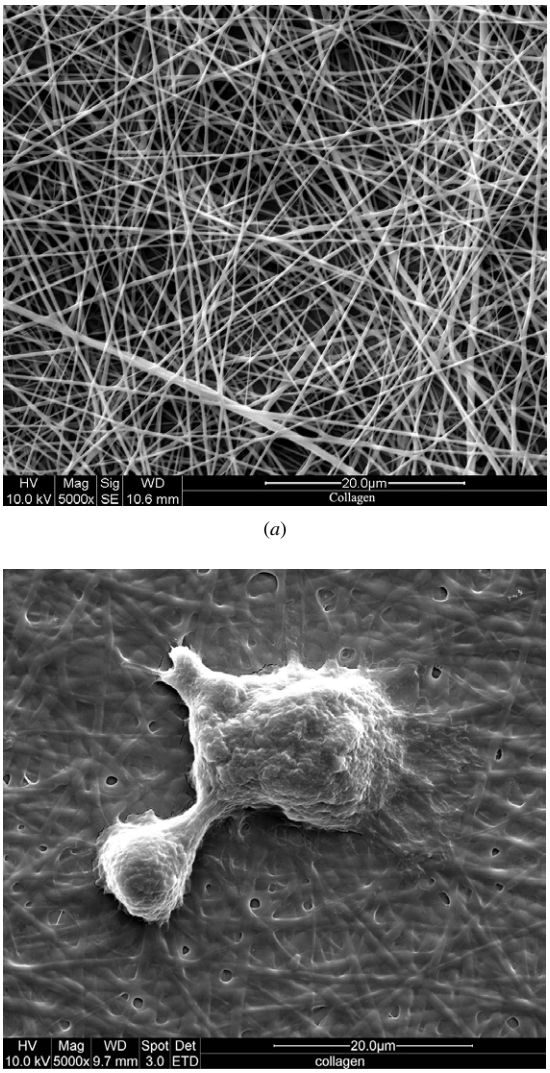

Figure 1. Electrospun collagen I nanofibers (*a*), and seeding MSCs on collagen nanofibers (*b*).

The versatility of electrospinning also means that fibers of different morphology and different materials can be made directly or indirectly from electrospinning. Therefore, different polymers, blends, mixtures or precursors can be made into fibers to suit a specific application. Basic electrospinning can only yield random nanofibers, but using a rotating mandrel as a collector, aligned nanofibers can be successfully obtained, such as aligned PGA fibers at 1000 rpm rotating speed [17] and aligned type I collagen fibers at 4500 rpm rotating speed [18]. If using the knife-edge disc as a collector, the alignment degree of the fibers will increase [19]. To alter the electric field such that more electric field lines converge toward the auxiliary electrode, parallel knife-edged bars can be used instead of strips. These were also found to improve on the degree of alignment [20]. Tubular scaffolds or yarns, made of

Table 1. Various electrospun nanofibers of synthetic and biodegradable polymers.

Polymer	Solvent	Concentration	Diameter (nm)	Reference
Poly(ε-caprolactone) (PCL) Mn = 80 000	7:3 Dichloromethane (DCM):methanol	8 wt%	810 ± 150	[9]
PCL Mn = 80 000	1:1 Tetrahydrofuran (THF): *N*, *N*-dimethylformamide (DMF)	0.14 g ml^{-1}	700 ± 200	[10–12]
Poly(L-lactic acid) (PLA) Mw = 300 000	Dichloromethane (DCM)/*n*,*n*-dimethylformamide (DMF) (70:30)	2 wt% 5 wt%	150–500 800–3000	[13]
PLA Mw = 450 000	Hexafluoropropanol (HFIP) or chloroform	5 wt%	290 (100–600)	[14]
Poly(glycolic acid) PGA Mw = 14 000–20 000	HFIP or chloroform	15 wt%	310 (50–650)	[14]
PLGA (l-lactide/glycolide = 50/50) Mw = 108 000	Chloroform	8 wt%	760 (200–1800)	[14]
PLGA 85/15	1:1 THF and DMF	0.05 g ml^{-1}	500–800	[15]
PLGA 10/90	HFIP	5–7%	3900	[16]

Table 2. Electrospun collagen fibers.

Material	Solvent and concentration	Parameter	Diameter (nm)	Reference
Collagen type I	HFIP 0.083 g ml^{-1}	Voltage = 25 kV, distance = 125 mm, feed rate = 5 ml h^{-1}, target mandrel rotating = 4500 rpm	100 ± 40 (calfskin) 100–730 (human placenta)	[18]
Collagen type I	HFIP 8%	Voltage = 15–20 kV, distance = 80 mm, feed rate = 0.02 ml min^{-1}	460 (100–1200)	[22]
Collagen type I	HFIP 6.7%	Voltage = 12 kV, distance = 120 mm, feed rate = 1.2 ml h^{-1}	350 ± 250	Our lab
Collagen type II	HFIP 40 mg ml^{-1}	Voltage = 22 kV, feed rate = 2 ml h^{-1}	496 (110 ± 30)	[24, 25]
Collagen type III	HFIP 0.04 g ml^{-1}	Voltage = 25 kV, distance = 125 mm, feed rate = 5 ml h^{-1}, target mandrel rotating = 4500 rpm	250 ± 150	[18]
50% collagen type I: 50% collagen type III	HFIP 0.06 g ml^{-1}	Voltage = 25 kV, distance = 125 mm, feed rate = 5 ml h^{-1}, target mandrel rotating = 4500 rpm	390 ± 290	[18]

both aligned and random fibers, can be produced currently by using specific parameters and setups [5].

3. Current electrospun nanofiber biomaterials

Mainly biomedical applications of nanofibers are used as scaffolds for tissue engineering, which are aimed at tissue regeneration. The detailed applied forms will be discussed in section 4. Here, we described several representative biomaterials, including natural and artificial polymers, bioceramic-calcium phosphate and carbon. We hope that this review will serve as a timely basis for further research on developing biomedical applications of nanofibers.

3.1. Polymers

3.1.1. Natural polymers. Natural polymers that have been electrospun are proteins and polysaccharides. One of the most commonly used is collagen, naturally found in connective tissue where it provides mechanical support as ECMs. It is possible for electrospun collagen fibers to mimic the extracellular matrix in the body. *In vitro* and *in vivo* studies have shown that cells respond positively to scaffolds made of electrospun collagen fibers [21–23]. Table 2 lists electrospun collagen fibers obtained by different research groups. Collagen I nanofibers before and after mesenchymal stem cell (MSC) seeding are shown in figures 1(*a*) and (*b*) respectively. Generally, collagen can be relatively strong and form stable fibers after cross-linking or blending with other polymers such as PEO for higher mechanical properties [24, 26]. A cheaper alternative to collagen would be gelatin, which also can be electrospun [27]. Another protein that is electrospun for use in tissue engineering is fibrinogen [28].

The other typical naturally occurring polysaccharide is hyaluronic acid (HYA) commonly found in specialized tissues

Table 3. Electrospun hyaluronic acid fibers.

Material	Solvent and concentration	Parameter	Diameter (nm)	Reference
HYA	HCl solution (pH = 1.5) 2.0–3.0%	Voltage = 25–40 kV, distance = 90 mm, feed rate = 20–60 μl min^{-1}, air-blowing rate = 35–150 ft^3 h^{-1}	50–90	[29]
HYA	HCl solution (pH = 1.5) 1.3–1.5%	Voltage = 40 kV, distance = 95 mm, feed rate = 40 μl min^{-1}, air-blowing rate = 70 ft^3 h^{-1} (57 °C)	74	[30]
HYA	Water 1.3%, 1.5% DMF: water = 2,1.5,1,0.5, 1.5%	Voltage = 22 kV, distance = 150 mm, feed rate = 60 μl min^{-1}	120–250	[31]
HYA-DTPH (3,3′-dithiobis (propanoic dihydrazide))	PEO/DMEM solution 2.0% (w/v)	Voltage = 18 kV, distance = 100 mm, feed rate = 20 μl min^{-1}	60–120 0–400 (PEO extraction)	[32]
HYA-gelatin	DMF:water = 1.5, 1.5% HYA 1.5–7.5% gelatin	Voltage = 22 kV, distance = 150 mm, feed rate = 60 μl min^{-1}	190–500	[33]

such as synovial fluid, dermis and cartilage. Electrospun pure HYA fibers and those blended with other polymers are listed in table 3. Due to extremely high biocompatibility, both collagen and HYA have been used extensively in many biomedical applications. Thus the optimal application of these electrospun nanofibers could be achieved in the near future.

3.1.2. Synthetic polymers. Because there are several limitations encountered in the use of naturally derived polymers, including batch-to-batch (or source-to-source) variation in materials isolated from tissues, restricted flexibility in the range of accessible material properties, and concerns about disease transmission associated with materials isolated from mammalian sources, artificial polymers were synthesized as alternative materials for biomedical applications [2]. Current synthetic biodegradable polymers for tissue regeneration include PLA, PGA, PLGA, PCL etc. The electrospun fibers of these polymers are listed in table 1. The other important advantages of these biodegradable polymers are their relatively strong mechanical properties and the fact that they are inexpensive. So the relatively low biocompatibility of these polymers can be accepted for practical applications.

3.2. Hydroxyapatite

As a major mineral component of human hard tissues, hydroxyapatite (HA) possesses excellent biocompatibility with bones, teeth, skin and muscles, both *in vitro* and *in vivo*. Because of its bioactivity and osteoconductivity, HA has found extensive applications in orthopedics and dentistry [33]. Kim *et al* [34] describe an effective method for HA nanofiber fabrication by combining the electrospinning technique and sol–gel reaction. They used 10% polyvinyl butyral (PVB)/ethanol as a precursor for electrospun nanofibers, subsequently heated to 700 °C in order to remove the polymeric precursor and to bring about the crystallization of HA. The parameters are as follows: feed rate = 0.2 ml h^{-1}, electrostatic voltage = 12 kV, distance = 8 cm. The diameter of the resultant fibers was exploited in the range of 240 nm to 1.55 μm by means of adjusting the concentration of the sols. By the same process and with NH_4F added into the sol solution, fluorhydroxyapatite (FHA) can also be fabricated successfully.

3.3. Carbon

Carbon nanomaterials are arguably the most celebrated products of nanotechnology to date, encompassing fullerenes, nanotubes, nanofibers and a wide variety of related forms [35]. Although there are no consistent opinions on the biocompatibility of carbon nanomaterials, pilot studies showed positive results on subcutaneous implantation and osteoblast co-culture experiments [36–38]. Fabrication of carbon nanofibers comprises electrospinning of polyacrylonitrile (PAN) and carbonization of deposited nanofibers. Dzenis [39] for the first time used this idea to fabricate carbon nanofiber materials. Wang *et al* [40] prepared PAN/dimethylformamide (DMF) solution by adding 600 mg PAN in 10 ml DMF at room temperature, then electrospinning on 15 kV, 15 cm distance, following carbonization at 560–1200 °C. The resultant graphite domain size in carbon fibers was enlarged from 1.5 to 2.6 nm with higher carbonization temperature. As potential scaffolds, the carbon nanofibers needed to be investigated on more aspects. The advantage of using a carbon nanofiber is its high electroconductive property: it can conduct electricity stimulus into the tissue healing process, whereas other polymer or ceramic materials cannot achieve this.

3.4. Electrospun nanofiber composites

The concept of nanocomposites exploited more optimal choices for nanofibers with high mechanical properties and high biocompatibility simultaneously. Regarding the

electrospun nanofiber materials, we can not only electrospin the blended polymer with nanoparticles, but also use coating or immobilization technologies to functionalize the electrospun nanofibers. For example, PCL/$CaCO_3$ composite nanofibers are fabricated under 20 kV voltages, 1.0 ml h^{-3} feeding rate and 130 mm distance [41]. A nanocomposite with different ratios of PCL and $CaCO_3$ can be attained by the above parameters, such as 75:25, 50:50 and 25:75. Two kinds of PLLA-CL/collagen nanocomposites, the blended PLLA-CL and collagen solution that can be electrospun at 0.5 ml h^{-1} feeding rate and 10 kV voltages and coated electrospun PLLA-CL nanofibers by collagen, were designed for tissue engineered vascular graft [42, 43]. The PCL nanofibers grafted with gelatin are treated by air plasma to yield carboxyl groups after electrospinning [44]. Apart from our lab's work, Patcharaporn Wutticharoenmongkol *et al* [45] also prepared electrospun PCL/$CaCO_3$ and PCL/HA composites by using PCL solution containing nanoparticles of calcium carbonate or hydroxyapatite. Cytotoxicity evaluation of the electrospun PCL/$CaCO_3$ and PCL/HA fibers based on human osteoblasts (SaOS2) and mouse fibroblasts (L929) revealed that these composite nanofibers posed no negative effect to the cells, which corresponded to our results.

4. Potential tissue regeneration applications

From the structural viewpoint, almost all of the human tissues consist of nanofibers, such as blood vessels, skin, cartilage and bones. Enhanced cell growth on nanofibrous scaffolds has been expected. But most fibrous materials used in tissue engineering have no pertinence to a specific tissue/organ; in fact different tissue regenerations have quite different mechanisms, although their matrices are all fibrous scaffolds. In this section, we summarize the nanofiber studies on tissue-specific regeneration. Along these lines, electrospun nanofiber biomaterials for tissue regeneration will be explored deeply for biomimetic repairs in the form of natural tissue regeneration.

4.1. Blood vessel

Attempts have been made for many years to develop small blood vessels, but all have encountered high failure rates for one reason or another. In particular, it was found that graft patency rates were greatly reduced when synthetic grafts were used for small diameter arteries, such as coronary and infragenicular vessels. Three-dimensional nanomatrix scaffolds made of collagen or other cell-secreting natural substances can be used to seed the smooth muscle cells (SMCs) to mimic natural, small diameter vessels. Studies suggested that muscle cells, once implanted in the scaffold, could partly develop the function, shape, morphology and cellular architecture of the normal vessel [46]. Poly(glycolide-co-ε-caprolactone) scaffolds possess elastic mechanical properties and promote the SMC adhesion and subsequent tissue formation [47]. Typical materials currently used as vascular grafts include poly(ethylene terephthalate) (PET) and poly(tetrafluoroethylene) (PTFE) etc. Surface modification of electrospun PET fibers improved the spreading and proliferation of endothelial cells (ECs) [48]. Furthermore, not only the surface roughness of the nanofibers, but the fiber alignment of the scaffold is also important [49, 50]. The aligned nanofiber scaffolds showed special favorable interactions between SMCs and the scaffold as the orientation of the fibers encouraged cell proliferation in that direction. In natural blood vessels, the SMCs in the middle layer are arranged in a concentric manner. If SMCs are cultured on the electrospun nanofibers that are oriented in a concentric manner to form a tubular scaffold, the cells are expected to grow in a concentric manner resembling that of a natural blood vessel.

The alternative approach is to form tubular scaffolds made of the electrospun nanofibers. By using a rotating collector and controlling the electric field, it is possible to align the electrospun nanofibers on the circumference of the small diameter tube which can be extracted to give a tubular scaffold [51]. Moreover, tubular scaffolds made of different materials have also been made by multilayering and other mixing electrospinning techniques [52]. In the near future, human endothelial cells, smooth muscle cells and fibroblasts will be used in the inner, middle and outer layers, respectively, of the vascular constructs to achieve the 'real' synthetic blood vessel. This is the greatest challenge in blood vessel regeneration.

4.2. Skin

As the outermost tissue of the human body, the passive and active functions of skin are carried out by specialized cells and structures located in the two main layers of skin: the epidermis and dermis. The epidermis, composed primarily of keratinocytes, is formed into a stratified squamous epithelium. Proliferating cells in the basal layer of the epidermis anchor the epidermis to the dermis and replenish the terminally differentiated epithelial cells lost through normal sloughing from the surface of the skin [53].

Collagen is a leading candidate for skin regeneration. Experiments of open wound healing in rats showed that collagen nanofibrous matrices were very effective as wound-healing accelerators in early-stage wound healing. Alternatively, coating type I collagen is also a good candidate for wound dressing [21, 26]. This system has been demonstrated by our group using electrospun PCL nanofibers coating collagen I for fibroblast growth, proliferation and migration inside the matrices [54]. Then this biodegradable PCL/collagen composite nanofiber supported the attachment and proliferation of human dermal fibroblasts and has potential in tissue engineering as a dermal substitute for skin regeneration.

Other non-biodegradable polymer nanofibers, such as polystyrene and polyurethane, were also fabricated for wound dressing by electrospinning [55, 56]. Although it does not seem optimal material for tissue regeneration, its unique results of cell co-culture are worth considering. In the absence of serum, keratinocytes, fibroblasts and endothelial cells did not grow when cultured alone. However, when fibroblasts were co-cultured with keratinocytes and endothelial cells, expansion of keratinocytes and endothelial cells occurred even in the absence of serum, which was

not consistent with the fibroblasts and keratinocytes cultured on the electrospun silk fibroin (SF) nanofiber non-woven membrane [57]. We hypothesized that when all three cell types were introduced at random to the proper nanofiber scaffold, the cells displayed native spatial three-dimensional organization. As evidence, Huang [58] demonstrated that co-culturing with fibroblasts enables keratinocytes and endothelial cells to proliferate without serum, but also to self-organize according to the native epidermal–dermal structure given the symmetry-breaking field of an air–liquid interface. Moreover, the electrospun nanofibrous polyurethane membrane shows controlled evaporative water loss, excellent oxygen permeability, promotes fluid drainage ability, and inhibits exogenous microorganism invasion because its pores are ultra-fine. Based upon the above properties, the electrospun polyurethane membrane still has potential applications for wound dressing [56].

The development of the electrospinning technique itself certainly enhanced the potential applications. With a modified coaxial electrospinning technique, a pencil-like, core-shell composite nanofiber can be obtained. The drugs resveratrol and gentamycin sulfate were encapsulated respectively into the cores of biodegradable PCL ultra-fine fibers with diameters down to a few hundred nanometers. Such composite nanofibers will be useful in controlled drug release and in the development of new medical devices as wound-dressing materials [58]. As the most direct biomedical application of electrospun nanofiber membranes, it is hoped that skin regeneration will be realized by incorporating the drugs into the nanofibers.

4.3. Cartilage

Cartilage is a dense connective tissue that is to a certain extent pliable, making it resilient. These characteristics are due to the nature of its matrix, which is rich in proteoglycans consisting of a core protein attached by the repeating units of disaccharides termed glycosaminoglycans (GAGs) mainly consisting of HYA, chondroitin sulfate, collagen II and keratin sulfate. Articular cartilages are important in load-bearing and reducing friction of the articular surfaces. Due to the limited capacity of articular cartilage to repair itself, and cartilage defects resulting from aging, joint injury and developmental disorders cause joint pain and loss of mobility [11]. As promising candidates, the electrospun HYA or HYA-based composite nanofibers have been fabricated successfully, but the chondrocyte response on these fibers is still unknown, which has a bearing on the efficiency of cartilage repair [29–32].

Other nature-derived materials, the electrospinning of collagen type II and subsequent seeding chondrocyte, were investigated for potential use in cartilage tissue engineering. The electrospinning parameters of this material were described in section 3.1.1 (table 2) [24, 25]. Individual scaffold specimens were evaluated as uncross-linked, cross-linked or cross-linked/seeded in the study of Shields [24]. Scanning electron microscopy of cross-linked scaffolds cultured with chondrocytes demonstrated the ability of the cells to infiltrate the scaffold surface and interior. Electrospun collagen type II scaffolds produce a suitable environment for chondrocyte growth, which establishes the foundation for the development of articular cartilage repair.

As well as random nanofibers, oriented chitosan fibers were studied for their biocompatibility with chondrocytes by Subramanian *et al* [59]. As expected, the oriented electrospun chitosan provides better chondrocyte biocompatibility than the cast chitosan film. This electrospun membrane also has a significantly higher elastic modulus (2.25 MPa) than that of the cast film (1.19 MPa). Following this, the electrospun chitosan still needs to be further processed into three-dimensional scaffolds for cartilage tissue repair.

Synthetic biodegradable polymers are also studied for chondrocyte scaffolds. Shin and colleagues [60] investigated the potential of four different nanofiber-based types of PLGA scaffolds (lactic acid/glycolic acid content ratio = 75:25, 50:50, or a blend of 75:25 and 50:50) to be used for cartilage reconstruction. The mechanical properties of the nanofiber scaffold were slightly lower than those of human cartilage, which suggested that the nanofiber scaffold was mechanically stable to withstand implantation and to support regenerated cartilage. Proliferation of chondrocytes from porcine articular cartilage and ECM formation in nanofiber scaffolds were superior to those in the conventional cast membrane, because of the intermittent hydrostatic pressure applied to the cell-seeded nanofiber [60]. Nanofibrous PCL was evaluated for its ability to maintain chondrocytes in a functional state using fetal bovine chondrocytes (FBCs) [12]. Gene expression analysis by a reverse transcription-polymerase chain reaction showed that chondrocytes seeded on the PCL nanofibrous scaffold continuously maintained their chondrocytic phenotype by expressing cartilage-specific extracellular matrix genes, including collagen types II and IX, aggrecan, and cartilage oligomeric matrix protein. Expression of the collagen type II splice variant transcript, which is indicative of the mature chondrocyte phenotype, was significantly up-regulated. The FBCs exhibited either a spindle or round shape on the nanofibrous scaffolds, in contrast to the flat, well-spread morphology seen in monolayer cultures on TCP. In addition to promoting phenotypic differentiation, the nanofibrous scaffold also supported cellular proliferation as evidenced by a 21-fold increase in cell growth over 21 days when the cultures were maintained in a serum-containing medium. Thus, PCL nanofibers may be a suitable candidate scaffold for cartilage tissue engineering.

4.4. Bone

As a connective tissue distinguished by the fact that its matrix is mineralized by calcium phosphate, bone is both hard and resilient, mainly consisting of collagen I and carbonated hydroxyapatite. Ideally, scientists want to mimic the natural process—collagen induces calcium, phosphate and hydroxide to form hydroxyapatite crystallites within bone, which are necessary for its structural rigidity [3]. Three strategies were carried out: adding calcium phosphate into the scaffold, seeding bone marrow stromal cells (BMSC) into the scaffold

and combining with growth factors, which is described as follows.

For bone tissue regeneration, biodegradable polymers are commonly combined with bioceramics either before or after the electrospinning process. Fujihara *et al* [41] prepared the PCL/$CaCO_3$ composite electrospun fibers as expected to encourage osteoblast attachment from the *in vitro* experiments. Alternatively, the electrospun nanofibrous film was soaked in the simulated body fluid, as in the study of Ito [61]. The formed HA changed the hydrophobic of the poly(3-hydroxybutyrate-co-3-hydroxyvalerate) (PHBV) film to hydrophilic, as a result increasing the degradation rate. However, the HA composition did not significantly affect the cell adhesion. On replacing the PHBV with silk/polyethylene oxide (PEO) containing poly(L-aspartate) (poly-Asp), and changing SBF to $CaCl_2$ and Na_2HPO_4 solution, the apatite growth occurred preferentially along the longitudinal direction of the fibers [62]. It is highly possible to develop mineralized nanofibers, but it is still necessary to investigate the osteoblast reactions on mineralized nanofibers.

Mesenchymal stem cells (MSCs), derived from the bone marrow of neonatal rats, were used for seeding on electrospun PCL scaffolds by Yoshimoto *et al* [63]. The cell–polymer constructs were cultured with osteogenic supplements under dynamic culture. Ordinarily, the cell–polymer constructs should maintain the size and shape of the original scaffolds as it is necessary for space support *in vivo* implantation. At 4 weeks, the surfaces of the cell–polymer constructs were covered with cell multilayers. In addition, type I collagen secretion and cell mineralization both can be detected at that time. Developed from PCL nanofiber material, gelatin/PCL composite electrospun nanofibers were fabricated by mixing the solution of 50% gelatin solution and 50% PCL solution, in which gelatin concentration was ranging from 2.5% w/v to 12.5% w/v [64]. Contact-angle measurement and tensile tests indicated that the gelatin/PCL complex fibrous membrane exhibited improved mechanical properties as well as more favorable wettability than that obtained from either gelatin or PCL alone. BMSCs could not only favorably attach and grow well on the surface of these scaffolds, but were also able to migrate inside the scaffold up to 114 μm within 1 week of culture, which shows better biocompatibility than PCL nanofibrous material. The positive reactions of MSC on the nanofibers matrix also showed up on PLA and silk electrospun nanofibers [10, 65].

Bone growth factors such as BMP-2, OP-1 etc gradually became attractive clinical drugs for bone defect repair. The previous mineralized collagen/PLA 3-D scaffold with BMP-2 had already shown some exciting healing effects *in vivo* [66]. In principle, the nanofiber materials will more easily absorb growth factors for a high surface area, and then possibly result in more optimal healing effect. The silk fibroin nanofiber scaffolds containing BMP-2 and/or nanoparticles of hydroxyapatite (nHA) prepared via electrospinning were selected as a matrix for *in vitro* bone formation from human bone marrow derived mesenchymal stem cells (hMSCs) [67]. The scaffolds with the coprocessed BMP-2 supported higher calcium deposition, higher crystallinity apatite and enhanced transcript levels of bone-specific markers than in the controls (without BMP-2), indicating that these nanofibrous electrospun silk scaffolds were an efficient delivery system for BMP-2. The coexistence of BMP-2 and nHA in the electrospun silk fibroin fibers resulted in the highest calcium deposition and up-regulation of BMP-2 transcript levels when compared with other systems. Fortunately, the mild aqueous process required to electrospin the fibers offers an important option for delivery of labile cytokines and other biomolecules into the system.

5. Improvement of electrospun nanofibers

With a greater understanding of electrospinning, we may be able to have greater control over its resultant fibers with the desired morphology and structure. Although there have been many breakthroughs in electrospinning technology, as previous sections mentioned, the fundamental experimental and theoretical analysis of the process needs to develop the flexibility and reliability of its assemblies and nanocomposites [68]. We discuss the developing directions of electrospun nanofibers related to tissue regeneration application in this section.

5.1. Functionalization of nanofibers

After fabrication of nanofibers by electrospinning, we may consider the possible functionalization of these nanofibers. The polymeric nanofiber matrix has a similar structure to nanoscaled non-woven fibrous extracellular matrix proteins, and surface modification of nanofibers improved the biocompatibility. Collagen-coated PLA-CL has demonstrated higher cell attachment, spreading and viability than the unmodified nanofibers by endothelial cell culture [43]. This gives rise to the possibility of composites with the advantages of both artificial polymer and natural protein, maintaining the nanofiber form at the same time.

In addition to coating or blending for composite nanofiber fabrication, the covalently grafted protein on the nanofiber surface is another choice for functionalization, which has long been used for surface modification for conventional biomaterials. However, not all surface modification methods developed have been appropriate for functionalizing nanofibers, because only moderate methods can possibly be useful for modification of nanofibers, otherwise the nanofibers will be themselves destroyed. Moreover, we do not know whether this functionalization will have effect on *in vivo* tissue repair or not; the study of *in vivo* implantation is too limited. A specific and systemic functionalizing technique with electrospinning needs to be established through further investigations.

5.2. Three-dimensional extension

Electrospinning technology enables the production of continuous nanofibers. Then most people will think about yarns and textiles, where it is possible to fabricate three-dimensional (3D) textile fabrics for bridging the gap from

the nano- to microscales. Previous studies of non-nanofibrous polymer scaffolds showed that the 3D form reacted differently from the 2D materials based on *in vitro* and *in vivo* experiments. If we want to extend the biomimetic nanofibers as optimal scaffolds for tissue regeneration, 3D extension of nanofibers has to be done as soon as possible. Up to now, electrospinning technology has enhanced continuous fibers to continuous yarns. Then the definite pattern structure of the nanofibers will become the second attraction of nanofiber technology.

In an attempt to obtain a continuous yarn made of aligned fibers, fiber bundles were fabricated by collecting the electrospun fibers on a rotating drum. The collected nanofibers were linked and twisted into yarns [69]. Moreover, Khil *et al* [70] designed a particular setup for yarn collection: they used a water bath for deposition of the electrospun fibers, then the deposited fibers were drawn out of the water as a bundle from one side of the bath using a filament guide bar and collected onto a roller in the form of a yarn. If we replace the parallel electrodes of straight bars with rings, with one of the rings rotated, twisting of the aligned fiber bundle is achieved [71]. Although by using the above methods it is possible to get a twisted fiber bundle, a significant drawback is that the length of the twisted fiber bundle is limited to the space between the fibers, and the distance outside the range would result in a poor profile of the fibers on the rings with fibers either depositing mainly at the top of the ring or at the bottom of it.

5.3. Mechanical strength

From the material science viewpoint, the effect of size on the properties of a single fiber should be an interesting topic. There are as yet few scientific papers discussing the mechanical properties of electrospun single nanofibers. At present, three testing apparatuses are available to measure tensile and bending properties of a single nanofiber: the cantilever technique, the AFM-based nanoindentation system and the nanotensile tester [71–75]. Using the AFM-based nanoindentation system, a bending test of a PLLA single fiber was conducted by suspending a fiber over the etched groove in a silicon wafer of 4 μm width and 2.5 μm depth [73]. The crosshead speed of the cantilever tip was 1.8 μm s^{-1} and the applied maximum load to a single PLLA nanofiber was 15 nN. We have described only this method in detail because it can measure the mechanical properties of cultured cells, and therefore make it possible for us to co-consider mechanical properties of an electrospun nanofiber to the natural ECM fibers *in situ*. The stress stimulus effect to cell and tissue growth is still to be understood; this nanotechnique possibly gives us a new tool to investigate this aspect. Research on the relationship between cell behavior and stress provided by nanofibers is still in its infancy when the electrospun nanofibers are selected as a matrix for cell culture.

On the macroscale, as a basic property for practical biomedical application, the traditional tensile testing method has been applied to test the nanofibrous membrane and nanoyarns. However, even for the most widely used PLGA polymer, systemic research is limited. Zong *et al* [76] obtained 6 MPa and 4.9 MPa of tensile stress from 400 nm and 1000 nm PLGA (LA:GA = 10:90) fibers, and from the study of Li *et al* [77], it is 22.67 MPa of 500–800 nm PLGA (LA:GA = 85:15) nanofibers. For aligned nanofiber membranes, the tensile property in each drum rotating direction and transverse direction should be considered. Actually, even if nanofibers are collected with a rotating drum, there is no certainty that their alignment can be unidirectionally oriented. In order to get more precise fiber alignment, the current fiber collection system using a rotating drum still needs further improvement.

6. Future prospects

Polymeric nanofibers can be processed by a number of techniques such as drawing, templated synthesis, phase separation, self-assembly and electrospinning. The significant advantage of electrospinning is that long and continuous nanofibers can be produced in a cost-effective way, which makes it a potential application for industrial processing. But the disadvantage it shares with other nanotechniques is its low productivity. In order for electrospinning to be commercially viable, it is necessary to increase the production rate of the nanofibers. To do so, we try to use a multiple-spinning setup to increase the product yield, such as using eight needles at one syringe pump and a 24 ml h^{-1} feed rate for PCL nanofiber fabrication [5]. Even now, we still need to investigate the corresponding parameters of electrospun nanofibers with optimal and stable properties.

In addition to single-electrospinning technology for obtaining nanofibers, other variations of electrospinning exist in order to absorb both advantages of other modern nanotechniques, such as the combined electrospinning process [78, 79]. Further assembly of nanofibers will be possible with a combination of self-assemblies, which generally occurs throughout nature.

Most current nanofibrous scaffold research is at the experimental stage. The trend is heading to animal study with or without seeded cells, aimed at achieving biomedical applications. Potential therapies include stem cell implantation with nanofibers. In this respect, it can be said that the biomedical application of nanofibers has a bright future, and can certainly progress rapidly by collaboration between biomaterials researchers and clinicians.

References

[1] Lutolf M P and Hubbell J A 2005 *Nat. Biotechnol.* **23** 47
[2] Stevens M M and George J H 2005 *Science* **310** 1135
[3] Griffith L G and Naughton G 2002 *Science* **295** 1009
[4] Langer R and Tirrell D A 2004 *Nature* **428** 487
[5] Ramakrishna S, Fujihara K, Teo W E, Lim T C and Ma Z 2005 *An Introduction to Electrospinning and Nanofibers* (Singapore: World Scientific)
[6] Huang Z M, Zhang Y Z, Kotaki M and Ramakrishna S 2003 *Compos. Sci. Technol.* **63** 2223
[7] Formhals A 1934 *US Patent* 1,975,504
[8] Ramakrishna S, Fujihara K, Teo W E, Yong T, Ma Z and Ramaseshan R 2006 *Mater. Today* **9** 40
[9] Van E L, Grøndahl L, Chua K N, Leong K W, Nurcombe V and Cool S M 2006 *Biomaterials* **27** 2042
[10] Li W J, Tuli R, Huang X, Laquerriere P and Tuan R S 2005 *Biomaterials* **26** 5158

[11] Li W J, Tuli R, Okafor C, Derfoul A, Danielson K G, Hall D J and Tuan R S 2005 *Biomaterials* **26** 599
[12] Li W J, Danielson K G, Alexander P G and Tuan R S 2003 *J. Biomed. Mater. Res.* A **67** 1105
[13] Yang F, Murugan R, Wang S and Ramakrishna S 2005 *Biomaterials* **26** 2603
[14] You Y, Min B M, Lee J S, Lee T S and Park W H 2005 *J. Appl. Polym. Sci.* **95** 193
[15] Li W J, Laurencin C T, Caterson E J, Tuan R S and Ko F K 2002 *J. Biomed. Mater. Res.* **60** 613
[16] Bini T B, Gao S J, Tan T C, Wang S, Lim A, Hai L B and Ramakrishna S 2004 *Nanotechnology* **15** 1459
[17] Boland E D, Wnek G E, Simpson D G, Palowski K J and Bowlin G L 2001 *J. Macromol. Sci. Pure Appl. Chem.* A **38** 1232
[18] Matthews J A, Wnek G E, Simpson D G and Bowlin G L 2002 *Biomacromolecules* **3** 232
[19] Theron S A 2001 *Nanotechnology* **12** 384
[20] Teo W E, Kotaki M, Mo X M and Ramakrishna S 2005 *Nanotechnology* **16** 918
[21] Rho K S, Jeong L, Lee G, Seo B M, Park Y J, Hong S D, Roh S, Cho J J, Park W H and Min B M 2006 *Biomaterials* **27** 1452
[22] Venugopal J, Ma L L, Yong T and Ramakrishna S 2005 *Cell Biol. Int.* **29** 861
[23] Telemeco T A, Ayres C, Bowlin G L, Wnek G E, Boland E D, Cohen N, Baumgarten C M, Mathews J and Simpson D G 2005 *Acta Biomater.* **1** 377
[24] Shields K J, Beckman M J, Bowlin G L and Wayne J S 2004 *Tissue Eng.* **10** 1510
[25] Matthews J A, Boland E D, Wnek G E, Simpson D G and Bowlin G L 2003 *J. Bioact. Compat. Polym.* **18** 125
[26] Huang L, Nagapudi K, Apkarian R P and Chaikof E L 2001 Engineered collagen-PEO nanofibers and fabrics *J. Biomater. Sci. Polym. Ed.* **12** 979
[27] Huang Z M, Zhang Y Z, Kotaki M and Ramakrishna S 2004 *Polymer* **45** 5361
[28] Wnek G E, Carr M E, Simpson D G and Bowlin G L 2003 *Nano Lett.* **3** 213
[29] Wang X, Um I C, Fang D, Okamoto A, Hsiao B S and Chu B 2005 *Polymer* **46** 4853
[30] Um I C, Fang D, Hsiao B S, Okamoto A and Chu B 2004 *Biomacromolecules* **5** 1428
[31] Li J, He A, Han C C, Fang D, Hsiao B S and Chu B 2006 *Macromol. Rapid Commun.* **27** 114
[32] Ji Y, Ghosh K, Shu X Z, Li B, Sokolov J C, Prestwich G D, Clark R A F and Rafailovich M H 2006 *Biomaterials* **27** 3782
[33] Hench L L 1998 *J. Am. Ceram. Soc.* **81** 1785
[34] Kim H W and Kim H E 2006 *J. Biomed. Mater. Res.* B **77** 323
[35] Hurt R H, Monthioux M and Kane A 2006 *Carbon* **44** 1028
[36] Yokoyama A *et al* 2005 *Nano Lett.* **5** 157
[37] Elias K L, Price R L and Webster T J 2002 *Biomaterials* **23** 3279
[38] Price R L, Waid M C, Haberstroh K M and Webster T J 2003 *Biomaterials* **24** 1877
[39] Dzenis Y A and Wen Y K *Mater. Res. Soc. Symp. Proc.* **702** U5.4.1
[40] Wang Y, Serrano S and Santiago-Avile J J 2003 *Synth. Met.* **138** 423
[41] Fujihara K, Kotaki M and Ramakrishn S 2005 *Biomaterials* **26** 4139
[42] He W, Yong T, Teo W E, Ma Z W and Ramakrishna S 2005 *Tissue Eng.* **11** 1574
[43] He W, Ma Z W, Yong T, Teo W E and Ramakrishna S 2005 *Biomaterials* **26** 7606
[44] Ma Z W, He W, Yong T and Ramakrishna S 2005 *Tissue Eng.* **11** 1149
[45] Wutticharoenmongkol P, Sanchavanakit N, Pavasant P and Supaphol P 2006 *Macromol. Biosci.* **6** 70
[46] Bowlin G L 2003 http://www.futurepundit.com
[47] Lee S H, Mooney D J and Kim Y H 2003 *J. Biomed. Mater. Res.* A **66** 29
[48] Ma Z, Kotaki M, Yong T, He W and Ramakrishna S 2005 *Biomaterials* **26** 2527
[49] Xu C Y, Inai R, Kotaki M and Ramakrishna S 2004 *Biomaterials* **25** 877
[50] Xu C Y, Inai R, Wang S and Ramakrishna S 2004 *J. Biomed. Mater. Res.* A **71** 154
[51] Bornat A 1987 *US Patent* 4,689,186
[52] Kidoaki S, Kwon I K and Matsuda T 2005 *Biomaterials* **26** 37
[53] Mason C 2005 *Medical Device Technology* **16** 22 (www.medicaldeviceonline.com)
[54] Venugopal J and Ramakrishna S 2005 *Tissue Eng.* **11** 847
[55] Sun T, Mai S M, Norton D, Haycock J W, Ryan A J and MacNeil S 2005 *Tissue Eng.* **11** 1023
[56] Khil M S, Cha D I, Kim H Y, Kim I S and Bhattarai N 2003 *J. Biomed. Mater. Res.* B **67** 675
[57] Min B M, Lee G, Kim S H, Nam Y S, Lee T S and Park W H 2004 *Biomaterials* **25** 1289
[58] Huang Z M and Yang A H 2006 *Acta Polym. Sin.* **1** 48
[59] Subramanian A, Vu D, Larsen G F and Lin H Y 2005 *J. Biomater. Sci. Polym. Ed.* **16** 861
[60] Shin H J, Lee C H, Cho I H, Kim Y J, Lee Y J, Kim I A, Park K D, Yui N and Shin J W 2006 *J. Biomater. Sci. Polym. Ed.* **17** 103
[61] Ito Y, Hasuda H, Kamitakahara M, Ohtsuki C, Tanihara M, Kang I K and Kwon O H 2005 *J. Biosci. Bioeng.* **100** 43
[62] Li C M, Jin H J, Botsaris G D and Kaplan D L 2005 *J. Mater. Res.* **20** 3374
[63] Yoshimoto H, Shin Y M, Terai H and Vacanti J P 2003 *Biomaterials* **24** 2077
[64] Zhang Y Z, Ouyang H W, Lim C T, Ramakrishna S and Huang Z M *J. Biomed. Mater. Res.* B **72** 156
[65] Boudriot U, Goetz B, Dersch R, Greiner A and Wendorff J H 2005 *Macromol. Symp.* **225** 9
[66] Liao S S, Cui F Z, Zhang W and Feng Q L 2004 *J. Biomed. Mater. Res.* B **69** 158
[67] Li C, Vepari C, Jina H J, Kim H J and Kaplan D L 2006 *Biomaterials* **27** 3115
[68] Dzenis Y 2004 *Science* **304** 1917
[69] Fennessey S F and Farris R J 2004 *Polymer* **45** 4217
[70] Khil M S, Bhattarai S R, Kim H Y, Kim S Z and Lee K H 2005 *J. Biomed. Mater. Res.* B **72** 117
[71] Dalton P D, Klee D and Moller M 2005 *Polym. Commun.* **46** 611
[72] Buer A, Ugbolue S C and Warner S B 2001 *Tex. Res. J.* **71** 323
[73] Tan E P S and Lim C T 2004 *Appl. Phys. Lett.* **84** 1603
[74] Tan E P S, Ng S Y and Lim C T 2005 *Biomaterials* **26** 1453
[75] Inai R, Kotaki M and Ramakrishna S 2005 *Nanotechnology* **16** 208
[76] Zong X, Ran S, Fang D, Hsiao B S and Chu B 2003 *Polymer* **44** 4959
[77] Li W J, Laurencin C T, Caterson E J, Tuan R S and Ko F K 2002 *J. Biomed. Mater. Res.* **60** 613
[78] Choi S S, Lee S G, Im S S, Kim S H and Joo Y L 2003 *J. Mater. Sci. Lett.* **22** 891
[79] Lyons J, Li C and Ko F K 2004 *Polymer* **45** 7597

TISSUE ENGINEERING
Volume 11, Number 7/8, 2005

Grafting of Gelatin on Electrospun Poly(caprolactone) Nanofibers to Improve Endothelial Cell Spreading and Proliferation and to Control Cell Orientation

ZUWEI MA, Ph.D.,[1,2] WEI HE,[2] THOMAS YONG, Ph.D.,[1,2] and S. RAMAKRISHNA, Ph.D.[1–3]

ABSTRACT

We modified the surface of electrospun poly(caprolactone) (PCL) nanofibers to improve their compatibility with endothelial cells (ECs) and to show the potential application of PCL nanofibers as a blood vessel tissue-engineering scaffold. Nonwoven PCL nanofibers (PCL NF) and aligned PCL nanofibers (APCL NF) were fabricated by electrospinning technology. To graft gelatin on the nanofiber surface, PCL nanofibers were first treated with air plasma to introduce –COOH groups on the surface, followed by covalent grafting of gelatin molecules, using water-soluble carbodiimide as the coupling agent. The chemical change in the material surface during surface modification was confirmed by X-ray photoelectron spectroscopy and quantified by colorimetric methods. ECs were cultured to evaluate the cytocompatibility of surface-modified PCL NF and APCL NF. Gelatin grafting can obviously enhance EC spreading and proliferation compared with the original material. Moreover, gelatin-grafted APCL NF readily orients ECs along the fibers whereas unmodified APCL NF does not. Immunostaining micrographs showed that ECs cultured on gelatin-grafted PCL NF were able to maintain the expression of three characteristic markers: platelet–endothelial cell adhesion molecule 1 (PECAM-1), intercellular adhesion molecule 1 (ICAM-1), and vascular cell adhesion molecule 1 (VCAM-1). The surface-modified PCL nanofibrous material is a potential candidate material in blood vessel tissue engineering.

INTRODUCTION

THE MOST IMPORTANT REASON for the long-term failure of small-diameter (<6-mm) vascular grafts is intimal hyperplasia, which is characterized by a cascade of immunoreactions caused by contact between the blood and foreign materials.[1–3] These immunoreactions, including formation of thrombus; infiltration of macrophages, neutrophils, and monocytes; secretion of cytokines; ingrowth and proliferation of smooth muscle cells (SMCs) and production of extracellular matrix (ECM); and so on, lead to abnormal tissue growth inside the vascular grafts, thereby blocking blood flow and finally causing the failure of the grafts.

A blood vessel tissue-engineering scaffold fabricated with biodegradable materials provides an excellent approach to obtain a vascular substitute with long-term patency. However, methods still need to be taken to prevent intimal hyperplasia during the early phase after implantation of the scaffold. An effective approach is endothelialization of the blood-facing surface of the scaffold, would prevent thrombosis and enhance graft sur-

[1]Nanoscience and Nanotechnology Initiative, National University of Singapore, Singapore.
[2]Division of Bioengineering, National University of Singapore, Singapore.
[3]Department of Mechanical Engineering, National University of Singapore, Singapore.

vival.[4–6] Therefore, an ideal blood vessel tissue-engineering scaffold should have a confluent endothelial cell lining and the cells should be able to resist the shear stress of the blood flow and possess desirable physiologic functions such as anticoagulation abilities.

Polymeric nanofibers produced by electrospinning technology have been of interest because the nanoscaled morphology of the nanofibers is analogous to the structure of protein fibrils/fibers in natural ECM. Studies on the use of electrospun nanofibers as tissue-engineering scaffolds for the regeneration of bone,[7] cartilage,[8] blood vessels,[9–11] and cardiac tissue[12] have been reported. In particular, a two-dimensional polymer nanofiber mat is similar in structure to the natural basal lamina, which lies under the endothelial cells in blood vessels and consists of collagen IV and laminin-1 fibrils/fibers with nanoscaled diameters.[13,14] It therefore makes sense to use the two-dimensional polymer nanofiber mat as a basal lamina-mimicking material to construct the inner surface of tissue-engineering scaffolds.

In this work, electrospun poly(caprolactone) (PCL) nanofiber mats were fabricated and surface modified to create an artificial basal lamina with both ECM-mimicking structures and cell-compatible surfaces. Both nonwoven PCL nanofiber mats (PCL NF) and aligned PCL nanofiber mats (APCL NF) were prepared and surface modified. PCL NF can be prepared much more easily than APCL NF. Therefore this article describes how PCL NF was used for surface modification, and then how the same surface modification method was employed to modify APCL NF. Endothelial cell behavior on both materials was studied in terms of cell morphology, proliferation, and phenotype. The ability of APCL NF to control cell orientation is described.

EXPERIMENTS

Materials and reagents

Poly(caprolactone) (PCL, M_n = 80,000; Sigma-Aldrich, St. Louis, MO), 2-(*N*-morpholino)ethanesulfonic acid (MES; Sigma, St. Louis, MO), 1-ethyl-3-(3-dimethylaminopropyl)carbodiimide hydrochloride (EDAC; Sigma), *N*-hydroxysuccinimide (NHS; Sigma), and gelatin (Sigma-Aldrich) were all used as received.

Preparation of PCL nanofiber

PCL nanofiber mats were produced by an electrospinning method, using the instruments schematically shown in Fig. 1 and described in detail in Xu *et al.*[9] and Mo *et al.*[11]. Briefly, 2 mL of PCL solution (10 w%) in a mixture of chloroform and *N*,*N*-dimethylformamide (DMF) (70:30, w/w) was placed in a 20-mL syringe. A syringe pump was used to squeeze out the polymer solution at 0.5 mL/h through a needle with an inner diameter of 0.21 mm. Directly below the needle an aluminum plate was placed at a distance of 15 cm from the needle. Voltage (15 kV) was loaded between the needle and the aluminum plate. The polymer solution was drawn into the fibers by

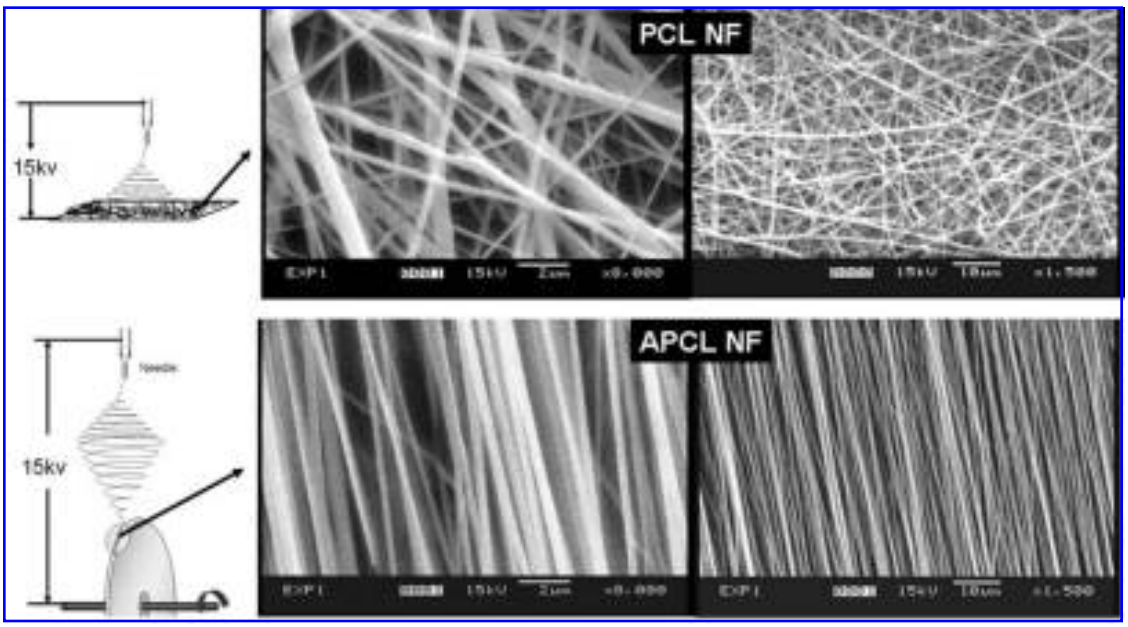

FIG. 1. Schematic representations of the fabrication process for nonwoven PCL nanofiber mat (PCL NF) and aligned PCL nanofiber mat (APCL NF). SEM images of PCL NF and APCL NF are also shown.

the high voltage and deposited on the aluminum plate to give a nonwoven PCL nanofiber mat (PCL NF).

To make aligned PCL nanofibers (APCL NF), fiber was collected with a rotating aluminum wheel (1000 rpm) instead of the static aluminum plate (Fig. 1). The wheel has a sharpened edge that is capable of strengthening the electric field near the collector. The distance between the needle and the wheel edge is 15 cm and a round glass coverslip (diameter, 15 mm) was fixed to the wheel edge with its surface normal to the wheel. The fibers collected on the coverslips were aligned along the direction of the wheel edge to form APCL NF mats. Other conditions were the same as used to prepare PCL NF, as described above.

Surface modification

The surface modification reaction scheme is shown in Fig. 2. Air plasma treatment of PCL nanofiber was carried out in an electrodeless, inductively coupled radio-frequency glow discharge (RFGD) plasma cleaner (PDC-001; Harrick Plasma, Ithaca, NY). The air plasma treatment lasted for 5 min with the radio-frequency power set at 30 W. Air plasma-treated PCL nanofiber mats were immersed into MES buffer solution (0.1 M, pH 5.0) containing EDAC (5 mg/mL) and NHS (5 mg/mL) at 4°C for 2 h. The material was then rinsed with MES buffer, immersed into gelatin solution (4 mg/mL in MES buffer), and reacted for 24 h at 4°C. The gelatin-grafted material was finally rinsed with deionized water for 24 h to remove the physically adsorbed gelatin, and dried under vacuum.

Surface characterization

Scanning electron microscopy (SEM) images of PCL NF and APCL NF were taken with a JSM-5800LV scanning electron microscope (JEOL, Tokyo, Japan). X-ray photoelectron spectra of control and modified PCL NF were taken on a VG ESCALAB 2201-XL base system (Thermo VG Scientific, East Grinstead, UK) with a take-off angle of 90°. The binding energy was referenced to the C1S of saturated hydrocarbon at 285.0 eV. The C1s: O1s: N1s intensity ratio of the equipment is 1:2.85:1.7.

COOH groups on air plasma-treated PCL NF was measured by the toluidine blue O (TBO) method described in detail by Ying *et al.*[15] and Gupta *et al.*[16] The measurement is based on the formation of complexes between carboxyl groups and TBO molecules. The amount of gelation on the gelatin-grafted PCL NF surface was measured by the Coomassie Brilliant Blue G (CBBG; Sigma) staining method,[17,18] which is based on the combination between protein molecules and the CBBG molecule.

Wettability of original and modified PCL NF was studied by sessile drop water contact angle measurement, using a surface contact angle tester (VCA Optima, AST Products, Billerica, MA). Water (7.5 μL) was dropped on the material surface and the water drop shape was recorded over 30 s. The sessile drop water contact angle was calculated with software provided by the manufacturer.

Endothelial cell culture

For endothelial cell (EC) culturing, PCL NF and APCL NF were deposited on round coverslips (diameter, 15 mm) Assistent; Glaswarenfabrik Karl Hecht, Sondheim, Germany), which exactly covered the well bottoms of 24-well tissue culture plates. Fiber collecting time was controlled at 40 min. ECs were seeded onto original and modified PCL NF or APCL NF with tissue culture polystyrene

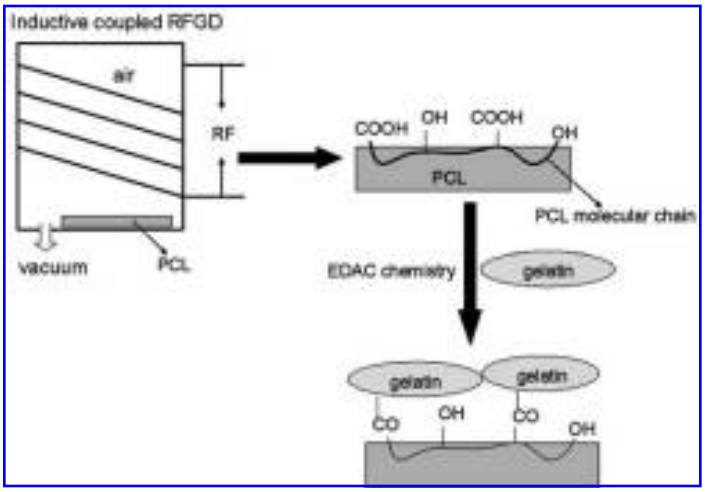

FIG. 2. Reaction scheme of the surface modification process for PCL nanofiber. Air plasma treatment was used to introduce carboxyl groups onto the PCL nanofiber surface, followed by the covalent attachment of gelatin molecules, using EDAC as the coupling agent. RFGD, Radio-frequency glow discharge.

(TCPS) set as a control. Ethanol solution (75%, v/v) was used to sterilize the samples.

Human coronary artery endothelial cells (HCAECs; Cambrex Bio Science, Walkersville, MD) were purchased at passage 3. The cells were cultured in endothelial cell basal medium 2 containing growth factors (EGM-2; Cambrex Bio Science) supplemented with penicillin (100 U/mL) and streptomycin (100 U/mL). During cell culture, the culture medium was changed every 4 days. ECs at passage 9 were used in this work.

Cell morphology

Cell morphology was studied by fluorescence microscopy (Leica Microsystems, Bensheim, Germany) and SEM (JSM-5800LV; JEOL). Living cells were stained with chloromethyl fluorescein diacetate (CMFDA; Molecular Probes, Eugene, OR) and observed directly by fluorescence microscopy without fixation.[19] A stock solution of CMFDA (25 μM/mL in dimethyl sulfoxide [DMSO]) was diluted with cell culture medium to obtain a 2.5 μM/mL working solution. Working solution (200 μL) was added to every well and cells were observed 4 h later. For SEM, cells were fixed with 2.5% (v/v) glutaraldehyde solution for 30 min and dried under vacuum. To observe the cytoskeleton, cells were fixed with 2.5% (v/v) glutaraldehyde solution for 30 min, extracted with 0.1% Triton X-100 in phosphate-buffered saline (PBS), incubated in phalloidin–tetramethylrhodamine B isothiocyanate (5 μg/mL in PBS) for 1 h at 37°C, rinsed with PBS repeatedly, and observed under a laser scanning confocal microscope (LSCM) (TCS SP2; Leica Microsystems).

Cell proliferation

Cell proliferation on original and surface-modified PCL NF was studied by 3-(4,5-dimethylthiazol-2-yl)-5-(3-carboxymethoxyphenyl)-2-(4-sulfophenyl)-2*H*-tetrazolium (MTS) colorimetric assay. The kit (CellTiter 96 AQ_{ueous} One Solution cell proliferation assay; Promega, Madison, WI) was used according to the manufacturer's directions. Before MTS testing, old culture medium was pipetted from the 24-well tissue culture plate and 500 μL of fresh culture medium was added to every well. CellTiter 96 AQ_{ueous} One Solution reagent (100 μL) was then added to every well. After culturing for 4 h, the deeply colored culture medium was pipetted out and added to a 96-well plate (100 μL/well), and the absorbance at 490 nm was recorded using an enzyme-linked immunosorbent assay (ELISA) plate reader. Samples with culture medium but without cells were set as the control, to determine background absorbance to be subtracted.

Cell phenotypic study

Three typical cell surface markers of ECs (platelet–endothelial cell adhesion molecule 1 [PECAM-1 or CD31], vascular cell adhesion molecule 1 [VCAM-1 or CD106], and intercellular adhesion molecule 1 [ICAM-1 or CD54]) were studied. After fixation with 2.5% paraformaldehyde and blocking with 2% bovine serum albumin (BSA), cells were incubated for 2 h at 37°C with a 200-μL/well concentration of primary antibody (mouse anti-human PECAM-1, mouse anti-human VCAM-1, or mouse anti-human ICAM-1; BD Biosciences Pharmingen, San Diego, CA) diluted 1:60 with PBS–2% BSA. After washing, fluorescein isothiocyanate (FITC)-labeled rabbit anti-mouse IgG (BD Biosciences Pharmingen) diluted 1:60 with PBS–2% BSA was added (200 μL/well) and incubated for 2 h at 37°C, followed by washing and counterstaining with propidium iodide (PI, 2 μg/mL, 100 μL/well) for 10 min. The immunostained ECs were then viewed under a laser scanning confocal microscope (Leica TCS SP2). Control experiments showed that secondary antibody alone cannot specifically stain cells.

RESULTS AND DISCUSSION

PCL nanofiber

SEM images of PCL NF and APCL NF are shown in Fig. 1. PCL NF is a highly porous nonwoven fabric material. From the higher magnification image in Fig. 1 it can be seen that the fiber diameter has a wide distribution, mainly between 200 nm and 1 μm. The thickness of PCL NF mats can be controlled by adjusting the electrospinning time. In this work PCL NF with a thickness of 25 $\pm$ 3 and 100 $\pm$ 10 μm was obtained after electrospinning for 40 min or 3 h, respectively.

APCL NF was obtained by depositing the nanofiber on the edge of a rotating plate (1000 rpm) instead of a static collector. As shown in Fig. 1, the fiber diameter of APCL NF is about 200–500 nm, which is smaller than that of PCL NF. The smaller fiber diameter for APCL NF may be attributed to the stretching force loaded on the fiber, produced by the rotating plate during electrospinning. After electrospinning for 40 min, APCL NF mat with a width of $\sim$5 mm was obtained on the coverslip (Fig. 1).

Plasma treatment of PCL NF

Radio-frequency glow discharge (RFGD) treatment using air or oxygen as reactive gas is a traditional method to introduce oxygen-containing groups (such as carboxyl and hydroxyl groups) onto polymer surfaces. This simple method was used in this work to introduce carboxyl groups on PCL nanofiber surfaces. The air plasma used here was produced by an electrodeless, inductively coupled RFGD instrument (PDC-001; Harrick Plasma), which is different from the more commonly used captive coupled RFGD instruments employing two planar elec-

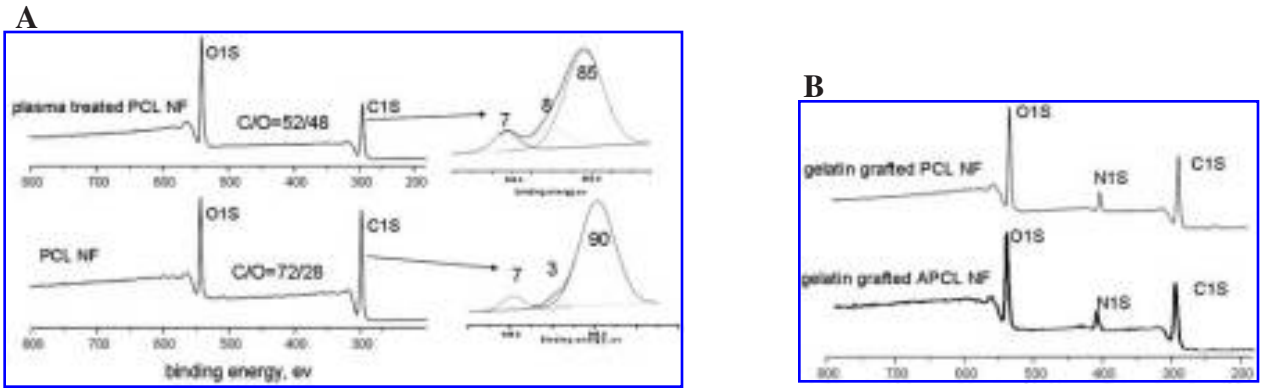

FIG. 3. (**a**) Survey scan XPS and C1s core level scan spectra of original and plasma-treated PCL NF. Atomic ratio of carbon to oxygen (C:O) are shown. (**b**) Survey scan XPS of gelatin-grafted PCL NF and APCL NF. N1s peaks directly verified the existence of gelatin on the nanofiber surface.

trodes. The plasma produced by the inductively coupled RFGD is more uniform, and therefore more appropriate for the surface modification of three-dimensional polymer scaffolds. The surface chemical composition of PCL NF before and after air plasma treatment was studied by X-ray photoelectron spectroscopy (XPS). Figure 3a shows the survey scan spectra of original PCL NF and air plasma-treated PCL NF. The atomic ratio of C to O (shown in the Fig. 3a) on the material surface can be calculated from the peak area ratio of C1s to O1s and the corresponding intensity factors. After air plasma treatment, the proportion of oxygen is increased, due obviously to the introduction of oxygen atoms. From the C1s core level scan spectra of the original and air plasma-treated PCL NF shown in Fig. 3a, it can be seen that the percentage of the saturated hydrocarbon C1s peak at 285.0 eV decreased after the plasma treatment because of the introduction of oxygen atoms.

The oxygen-containing groups introduced by the air plasma treatment are not specific and have great variety. Therefore, TBO, a dye that can specifically combine with carboxyl groups,[15,16] was used to verify the existence of the –COOH group and to quantitatively measure its amount on air plasma-treated PCL NF. Figure 4 shows the COOH density as a function of plasma treatment time and fiber mat thickness. The number of COOH groups clearly increased with treatment time. Increasing thickness of PCL NF produced greater amounts of COOH, indicating that the surface modification occurred not only on the outer surface, but deeper in the whole three-dimensional mat.

Gelatin grafting on PCL NF

For gelatin grafting, the air plasma treatment time was set at 5 min to yield enough COOH groups. Water-soluble carbodiimide was used to activate the COOH groups, which were subsequently reacted with gelatin molecules. The existence of gelatin can be confirmed by the appearance of the N1s peak in the XPS of gelatin-grafted PCL NF (Fig. 3b). Using the CBBR staining method,[17,18] the amount of gelatin grafted on PCL NF with thicknesses of 25 and 100 μm was measured as 0.22 and 0.72 mg/cm^2, respectively.

Wettability

The wettability of original and modified PCL NF mat was studied by water contact angle test (Table 1). Plain PCL film with a smooth surface was used as a control. Original PCL NF has a much higher water contact angle than original plain PCL film because of high surface roughness. Air plasma treatment effectively increased the hydrophilicity of the PCL film surface, whereas for air plasma-treated PCL NF, the water drop was suddenly sucked into the nanofiber mat, giving a contact angle of 0°. Here the notable difference between the wettability

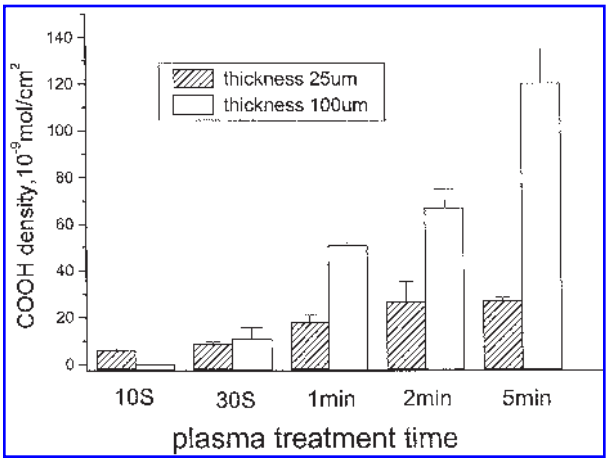

FIG. 4. Density of COOH groups yielded by air plasma treatment of PCL NF, plotted against treatment time.

Table 1. Water Contact Angle of Original and Surface-Modified Poly(caprolactone) Nanofiber

Sample	*Water contact angle (degrees)*
Original PCL film	85 ± 3
Original PCL NF	131 ± 2
Air plasma-treated PCL film[a]	43 ± 1
Air plasma-treated PCL NF[a]	0
Gelatin-grafted PCL NF[a]	0

[a]Air plasma treatment time, 5 min.

of plain PCL film and PCL NF is in agreement with common experience[20], that is, the water contact angle increases with surface roughness for a hydrophobic material, and decreases with surface roughness for a hydrophilic material. PCL NF has much higher surface roughness than does PCL film, so it has a higher water contact angle before air plasma treatment and a lower contact angle (0°) after air plasma treatment. Gelatin-grafted PCL NF also showed a water contact angle of 0°.

EC morphology on PCL NF

Figure 5 shows a set of fluorescence and SEM micrographs of ECs on original and gelatin-grafted PCL NF taken after various times in culture. In the fluorescence micrographs the ECs were stained with CMFDA, which stains only living cells.[19] ECs cultured on unmodified PCL NF always kept a rounded shape from the beginning of cell seeding and never spread with increasing culture time, whereas on gelatin-grafted PCL NF the ECs adopted a rounded shape at an early stage after cell seeding (6 h), but become fully spread by days 2 and 4. The SEM images of single ECs (Fig. 5d and h) show that the pseudopods of ECs can be formed along gelatin-grafted nanofiber, but not along unmodified nanofiber. Cell morphology is an important parameter to be considered when tissue engineering blood vessel scaffolds. A confluent EC monolayer covering the foreign material surfaces may prevent the development of intimal hyperblasia by preventing the thrombosis and immunoreactions caused by direct contact between the blood and the foreign material.

EC proliferation on PCL NF

Cell growth behavior on original and gelatin-modified PCL NF was measured by MTS cell proliferation analysis. EC growth curves are shown in Fig. 6, with TCPS set as control. The grafting of gelatin on PCL NF clearly improves cell proliferation, compared with the poor cell growth on unmodified PCL NF. However, the difference in cell growth rate between gelatin-modified PCL NF and TCPS implies that there is still room for improvement for the material.

APCL NF and its ability to control EC orientation

Aligned PCL nanofiber was also prepared in this work to obtain a controllable orientation of ECs, because former studies[9,21] have shown that aligned electrospun nanofiber is capable of controlling the orientation of

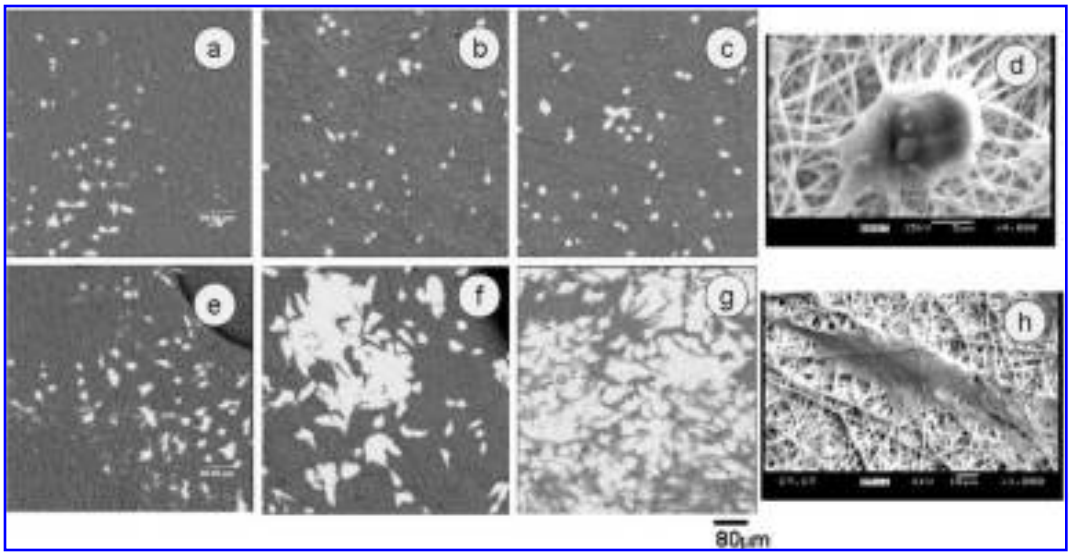

FIG. 5. Fluorescence and SEM micrographs of ECs cultured on original PCL NF (**a**–**d**) and gelatin-grafted PCL NF (**e**–**h**) for various cell-culturing times. Cell-culturing times: (**a** and **e**) 6 h; (**b** and **f**) 2 days; (**c, d, g,** and **h**) 4 days. Cell-seeding density, 30,000 per well.

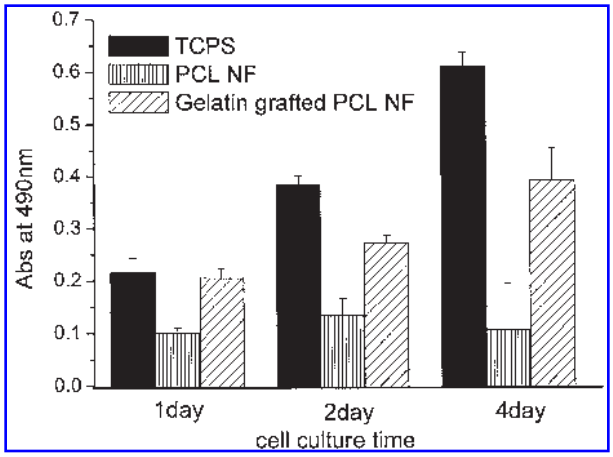

FIG. 6. EC proliferation, determined by MTS assay, on TCPS, original PCL NF, and gelatin-grafted PCL NF. Cell-seeding density, 30,000 per well.

smooth muscle cells and neurons by a mechanism called "contact guidance." Large APCL NF meshes with uniform thickness were not available because of limitations of the technique (Fig. 1), making some quantitative surface chemistry analysis and cell compatibility study of the APCL NF impossible. However, the ability of APCL NF to control cell orientation could be verified, as is described below.

The same surface modification strategy for PCL NF was used to covalently immobilize gelatin molecules on APCL NF, which was confirmed by the N1s peak appearing in the XPS of gelatin-grafted APCL NF (Fig. 3b). Figure 7 shows the appearance of ECs on original and gelatin-grafted APCL NF after various times in culture. As on PCL NF, ECs cultured on unmodified APCL NF always kept a rounded shape from the beginning of cell seeding. On gelatin-grafted APCL NF, however, ECs adopted spread shapes shortly (6h) after cell seeding, with the cells oriented along the nanofibers. The orientation of the cells parallel to the nanofibers became more obvious with increasing culturing time (2 and 4 days). Instead of the polygonal shape observed on gelatin-grafted PCL NF (Fig. 5), the ECs adopted a spindle shape, with the long axes parallel to each other on gelatin-grafted APCL NF. The orientation of ECs on APCL NF was more obviously demonstrated after cell skeletons were visualized by staining with rhodamine-labeled phalloidin. Figure 7i and j show that cell skeletons were organized parallel to the fibers on gelatin-grafted APCL NF, but were randomly oriented on gelatin-grafted PCL NF.

In the human body, shear stress caused by blood flow *in vivo* can orient endothelial cells in the direction of

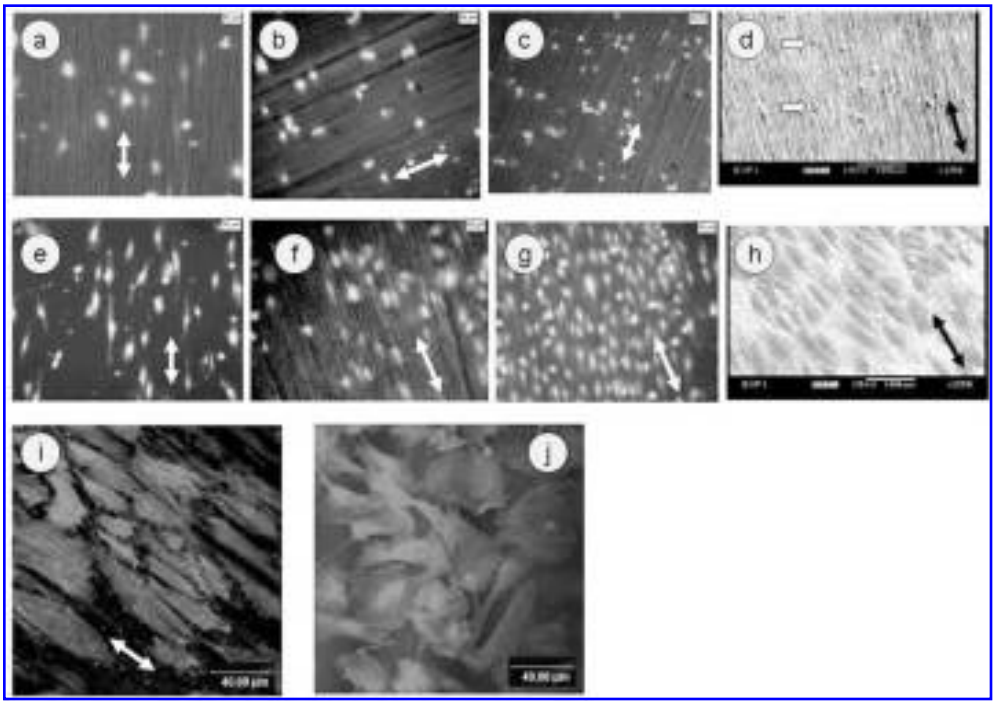

FIG. 7. Fluorescence and SEM micrographs of ECs cultured on original APCL NF (**a–d**) and gelatin-grafted APCL NF (**e–h**) for various cell-culturing times. (**i** and **j**) LSCM images of rhodamine–phalloidin-stained ECs on gelatin-grafted APCL NF and gelatin-grafted PCL NF, respectively. Cells were stained with rhodamine-labeled phalloidin to visualize actin in the cytoskeletons. Cell-culturing times: (**a** and **e**) 6 h; (**b** and **f**) 2 days; (**c,d,** and **g–j**) 4 days. Cell-seeding density, 30,000 per well. Double-headed arrows point out the direction of the aligned nanofibers.

blood flow.[22–24] The elongated endothelial cell shape is speculated to be important in preventing the atherosclerotic process because atherosclerosis develops preferentially in regions where ECs are round shaped, whereas arterial regions largely resistant to atherosclerosis are characterized by elongated ECs.[25] It is therefore important to control EC orientation in blood vessel scaffolds to mimic the natural situation. Moreover, the orientation of ECs in the direction of flow may be able to increase the ability of ECs to resist shear stress and to decrease the desquamation of ECs from material surfaces.

Surface-modified APCL NF provides a convenient strategy to obtain cells with controlled orientation by static cell culturing instead of dynamic culturing, which necessitates a complicated fluid system. Although other approaches to control EC orientation without a fluid field have been developed, such as grooved surfaces produced via lithography[26] or physical grinding[27] or micropatterned surfaces produced via self-assembly monolayer,[28,29] these techniques are relatively more complicated and, above all, are not practical to apply to tissue-engineering scaffolds.

Phenotypic study of ECs on PCL NF and APCL NF

Three important surface markers expressed by ECs cultured on gelatin-grafted PCL NF and APCL NF were studied by immunostaining, using TCPS as control. The surface markers studied, PECAM-1 (CD31), VCAM-1 (CD106), and ICAM-1 (CD54), are all adhesion proteins characteristically expressed on cell membranes of blood vessel endothelial cells. Figure 8 shows LCSM images of immunostained ECs cultured on TCPS, gelatin-grafted PCL NF, and APCL NF. ECs on TCPS strongly expressed three surface markers. ECs cultured on gelatin-grafted PCL NF and APCL NF also expressed all three markers.

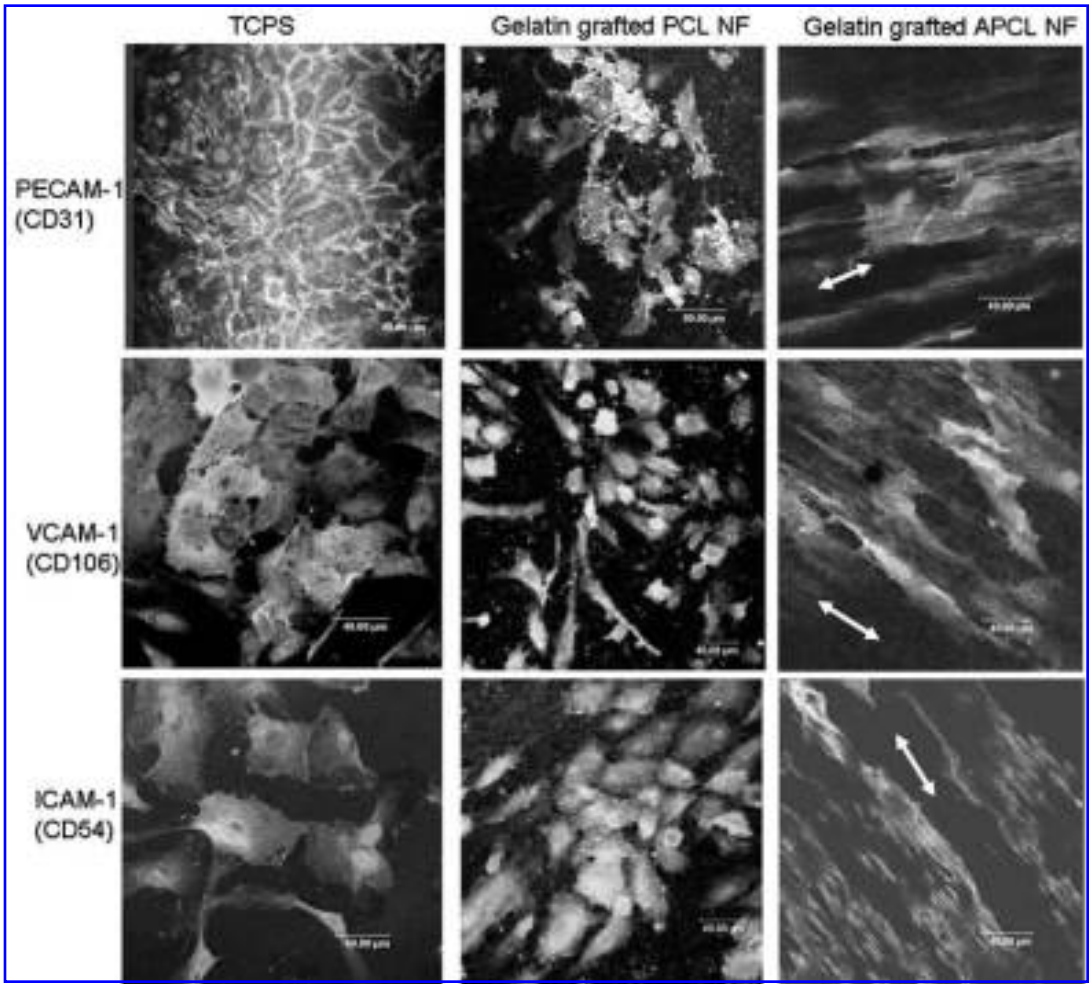

FIG. 8. Expression of PECAM-1 (CD31), VCAM-1 (CD106), and ICAM-1 (CD54) on membranes of ECs cultured on TCPS, gelatin-grafted PCL NF, and gelatin-grafted APCL NF. Cells were first immunostained with the appropriate primary antibody and then with FITC-labeled secondary antibody, and finally counterstained with PI to visualize cell nuclei. Representative LSCM micrographs are shown. Double-headed arrows point out the direction of the aligned nanofibers.

CD31 occurs on the EC membrane close to intercellular junctions and regulates EC–EC adhesion and EC–leukocyte adhesion. It is usually believed that increased expression of CD31 favors endothelialization,[30] whereas decreased expression of CD31 by ECs is an implication of cell damages.[31] CD106 and CD56 belong to EC surface markers that are up-regulated in the case of inflammation. CD106 and CD56 can mediate the adhesion of leukocytes on endothelial cells, and the migration of leukocytes out of the endothelial cell layer and into the surrounding tissue to kill invading bacteria or viruses.[30,32–34] Expression of the three surface markers on gelatin-modified PCL NF and APCL NF indicated that the novel nanofibrous biomaterials can successfully maintain the phenotype of ECs and therefore the corresponding important cell functions described above.

CONCLUSION

Electrospun PCL nanofiber was surface modified with gelatin to improve cell compatibility. Inductively coupled radio-frequency glow discharge plasma treatment with air as the reaction gas can effectively introduce –COOH groups on PCL nanofiber surfaces. The COOH groups were further utilized to covalently graft gelatin molecules, using water-soluble carbodiimide as the coupling agent. Gelatin grafting can significantly improve EC spreading and growth on PCL nanofiber. Moreover, aligned gelatin grafted PCL nanofiber showed a strong ability to control the orientation of ECs in the direction of the fibers, thus providing an effective way to control EC orientation without using a fluid field. ECs cultured on gelatin-grafted PCL nanofiber can maintain their phenotypic character.

REFERENCES

1. Xue, L., and Greisler, H.P. Biomaterials in the development and future of vascular grafts. J. Vasc. Surg. **37,** 472, 2003.
2. Xue, L., and Greisler, H.P. Blood vessels. In: Principles of Tissue Engineering, 2nd ed. San Diego, CA: Academic Press, 1997, p. 427.
3. Ratcliffe, A. Tissue engineering of vascular grafts. Matrix Biol. **19,** 353, 2000.
4. Jarrell, B.E., and Stockes, S.K. Use of freshly isolated capillary endothelial cells for the immediate establishment of a monolayer on a vascular graft at surgery. Surgery **100,** 392, 1986.
5. Jarrel, B.E., and Williams, S.K. Microvessel-derived endothelial cell isolation, adherence, and monolayer formation for vascular grafts. J. Vasc. Surg. **13,** 733, 1991.
6. Deutsch, M., Meinhart, J., Fischlein, T., Preiss, P., and Zilla, P. Clinical autologous *in vitro* endothelialization of infrainguinal ePTFE grafts in 100 patients: A 9-year experience. Surgery **126,** 847, 1999.
7. Yoshimoto, H., Shin, Y.M., Terai, H., and Vacanti, J.P. A biodegradable nanofiber scaffold by electrospinning and its potential for bone tissue engineering. Biomaterials **24,** 2077, 2003.
8. Li, W.J., Danielson, K.G., Alexander, P.G., and Tuan, R.S. Biological response of chondrocytes cultured in three-dimensional nanofibrous poly(caprolactone) scaffolds. J. Biomed. Mater. Res. **67A,** 1105,2003
9. Xu, C.Y., Inai, R., Kotaki, M., and Ramakrishna, S. Aligned biodegradable nanofibrous structure: A potential scaffold for blood vessel engineering. Biomaterials **25,** 877, 2004
10. Xu, C.Y., Inai, R., Kotaki, M., and Ramakrishna, S. Electrospun nanofiber fabrication as synthetic extracellular matrix and its potential for vascular tissue engineering. Tissue Eng. **10,** 1160, 2004.
11. Mo, X.M., Xu, C.Y., Kotaki, M., and Ramakrishna, S. Electrospun P(LLA-CL) nanofiber: A biomimetic extracellular matrix for smooth muscle cell and endothelial cell proliferation. Biomaterials **25,** 1883, 2004.
12. Shin, M., Ishii, O., Sueda, T., and Vacanti, J.P. Contractile cardiac grafts using a novel nanofibrous mesh. Biomaterials **25,** 3717, 2004.
13. Albert, B., Johnson, A., Lewis, J., Raff, M., Roberts, K., Peters, and Walter, P., eds. Molecular Biology of the Cell, 4th ed. New York: Garland Science, pp. 1106–1109, 2002.
14. Flemming, R.G., Murphy, C.J., Abrams, G.A., Goodman, S.L., and Nealey, P.F. Effects of synthetic micro- and nano-structured surfaces on cell behavior. Biomaterials **20,** 573, 1999.
15. Ying, L., Yin, C., Zhuo, R.X., Leong, K.W., Mao, H.Q., Kang, E.T., and Neoh, K.G. Immobilization of galactose ligands on acrylic acid graft-copolymerized poly(ethylene terephthalate) film and its application to hepatocyte culture. Biomacromolecules **4,** 157, 2003.
16. Gupta, B., Hilborn, J.G., Bisson, I., and Frey, P. Plasma-induced graft polymerization of acrylic acid onto poly(ethylene terephthalate) films. J. Appl. Polym. Sci. **81,** 2993, 2001.
17. Kang, I.K., Kwon, B.K., Lee, J.H., and Lee, H.B. Immobilization of proteins on polyl(methyl methacrylate) films. Biomaterials **14,** 787, 1993.
18. Gumusderelioglu, M., and Turkoglu, H. Biomodification of non-woven polyester fabrics by insulin and RGD for use in serum-free cultivation of tissue cells. Biomaterials **23,** 3927, 2002.
19. Poole, C.A., Brooks, N.H., Gilbert, R.T., Beaumont, B.W., Crowther, A., Scott, L., and Merrilees, M.J. Detection of viable and non-viable cells in connective tissue explants using the fixable fluoroprobes 5-chloromethylfluorescein diacetate and ethidium homodimer-1. Connect. Tissue Res. **33,** 233, 1996.
20. Shaw, D.J. Introduction to Colloid and Surface Chemistry. Boston: Butterworth-Heinemann, 1980, p. 134.
21. Yang, F., Murugan, R., Wang, S., and Ramakrishna, S. Electrospinning of nano/microscale poly(L-lactic acid) aligned fibers and their potential in neural tissue engineering. Biomaterials **26,** 2603, 2005.

22. Viggers, R.F., Wechezak, A.R., and Sauvage, L.R. An apparatus to study the response of cultured endothelium to shear stress. J. Biomech. Eng. **108,** 332, 1986.
23. Levesque, M.J., Liepsch, D., Moravec, S., and Nerem, R.M. Correlation of endothelial cell shape and wall shear stress in a stenosed dog aorta. Arteriosclerosis **6,** 220, 1986.
24. Sirois, E., Charara, J., Ruel, J., Dussault, J.C., Gagnon, P., and Doillon, C.J. Endothelial cells exposed to erythrocytes under shear stress: An *in vitro* study. Biomaterials **19,** 1925, 1998.
25. Gray, B.L., Lieu, D.K., Collins, S.D., Smith, R.L., and Barakat, A.I. Microchannel platform for the study of endothelial cell shape and function. Biomed. Microdevices **4,** 9, 2002.
26. Matsuzaka, K., Walboomers, X.F., de Ruijter, J.E., and Jansen, J.A. The effect of poly-L-lactic acid with parallel surface microgroove on osteoblast-like cells *in vitro*. Biomaterial **20,** 1293, 1999.
27. Manwaring, M.E., Walsh, J.F., and Trsco, P.A. Contact guidance induced organization of extracellular matrix. Biomaterials **25,** 3631, 2004.
28. Spargo, B.J., Testoff, M.A., Nielsen, T.B., Stenger, D.A., Hickman, J.J., and Rudolf, A.S. Spatially controlled adhesion, spreading, and differentiation of endothelial cells on self-assembled molecular monolayers. Proc. Natl. Acad. Sci. U.S.A. **91,** 11070, 1994.
29. Zhang, S.G., Yan, L., Altman, M., Lassle, M., Nugent, H., Frankel, F., Lauffenburger, D.A., Whitesides, G.M., and Rich, A. Biological surface engineering: A simple system for cell pattern formation. Biomaterials **20,** 1213, 1999.
30. Granchi, D., Cenni, E., Verri, E., Ciapetti, G., Gori, A., and Gamberini, S. Adhesive protein expression on human endothelial cells after *in vitro* contact with woven Dacron. Biomaterials **19,** 93, 1998.
31. Albeda, S.M., Muller, W.A., Buck, C.A., and Newmann, P.J. Molecular and cellular properties of PECAM-1 (endoCAM/CD31): A novel vascular cell–cell adhesion molecule. J. Cell Biol. **114,** 1059, 1991.
32. Lehle, K., Buttstaedt, J., and Birnbaum, D.E. Expression of adhesion molecules and cytokines *in vitro* by endothelial cells seeded on various polymer surfaces coated with titaniumcarboxonitride. J. Biomed. Mater. Res. **65A,** 393, 2003.
33. Oppenheimer-Marks, N., Davis, L.S., Bogue, D.T., Remberg, J., and Lipsky, P. Differential utilization of ICAM-1 and VCAM-1 during the adhesion and transendothelial migration of human T lymphocytes. J. Immunol. **147,** 2913, 1991.
34. Wilkinson, L.S., Edwards, J.C.W., Poston, R.N., and Haskard, D.O. Expression of vascular cell adhesion molecule-1 in normal and inflamed synovium. Lab. Invest. **68,** 82, 1993.

Address reprint requests to:
Zuwei Ma, Ph.D.
Nanoscience and Nanotechnology Initiative
BLK E3, #05-11
National University of Singapore
9 Engineering Drive 1
Singapore 117576

E-mail: nnimzw@nus.edu.sg

This article has been cited by:

1. Jian Fang, HaiTao Niu, Tong Lin, XunGai Wang. 2008. Applications of electrospun nanofibers. *Chinese Science Bulletin* **53**:15, 2265-2286. [CrossRef]
2. Jun Jia, Yuan-Yuan Duan, Jian Yu, Jian-Wei Lu. 2008. Preparation and immobilization of soluble eggshell membrane protein on the electrospun nanofibers to enhance cell adhesion and growth. *Journal of Biomedical Materials Research Part A* **86A**:2, 364-373. [CrossRef]
3. Nureddin Ashammakhi, A Ndreu, L Nikkola, I Wimpenny, Y Yang. 2008. Advancing tissue engineering by using electrospun nanofibers. *Regenerative Medicine* **3**:4, 547-574. [CrossRef]
4. Ju-Ha Song, Byung-Ho Yoon, Hyoun-Ee Kim, Hae-Won Kim. 2008. Bioactive and degradable hybridized nanofibers of gelatin–siloxane for bone regeneration. *Journal of Biomedical Materials Research Part A* **84A**:4, 875-884. [CrossRef]
5. N. Ashammakhi, A. Ndreu, Y. Yang, H. Ylikauppila, L. Nikkola. 2008. Nanofiber-based scaffolds for tissue engineering. *European Journal of Plastic Surgery* . [CrossRef]
6. Philippe Fernandez , Chantal Bourget , Reine Bareille , Richard Daculsi , Laurence Bordenave . 2007. Gene Response in Endothelial Cells Cultured on Engineered Surfaces Is Regulated by Shear Stress. *Tissue Engineering* **13**:7, 1607-1614. [Abstract] [PDF] [PDF Plus]
7. Pengcheng Zhao, Hongliang Jiang, Hui Pan, Kangjie Zhu, Weiliam Chen. 2007. Biodegradable fibrous scaffolds composed of gelatin coated poly(ε-caprolactone) prepared by coaxial electrospinning. *Journal of Biomedical Materials Research Part A* **83a**:2, 372. [CrossRef]
8. SuA Park, Koeun Park, Hyeon Yoon, JoonGon Son, Teijin Min, GeunHyung Kim. 2007. Apparatus for preparing electrospun nanofibers: designing an electrospinning process for nanofiber fabrication. *Polymer International* **56**:11, 1361. [CrossRef]
9. Aparna R. Sarasam, Afshan I. Samli, Linda Hess, Michael A. Ihnat, Sundararajan V. Madihally. 2007. Blending Chitosan with Polycaprolactone: Porous Scaffolds and Toxicity. *Macromolecular Bioscience* **7**:9–10, 1160. [CrossRef]
10. Nureddin Ashammakhi, Albana Ndreu, Ying Yang, Hanna Ylikauppila, Lila Nikkola, V. Hasirci. 2007. Tissue Engineering. *Journal of Craniofacial Surgery* **18**:1, 3. [CrossRef]
11. Andreas Greiner, Joachim H. Wendorff. 2007. Elektrospinnen: eine faszinierende Methode zur Präparation ultradünner Fasern. *Angewandte Chemie* **119**:30, 5770. [CrossRef]
12. Andreas Greiner, Joachim H. Wendorff. 2007. Electrospinning: A Fascinating Method for the Preparation of Ultrathin Fibers. *Angewandte Chemie International Edition* **46**:30, 5670. [CrossRef]
13. Sally Meiners, Ijaz Ahmed, Abdul S Ponery, Nathan Amor, Suzan L Harris, Virginia Ayres, Yuan Fan, Qian Chen, Roberto Delgado-Rivera, Ashwin N Babu. 2007. Engineering electrospun nanofibrillar surfaces for spinal cord repair: a discussion. *Polymer International* **56**:11, 1340. [CrossRef]
14. Sandip Sarkar, Thomas Schmitz-Rixen, George Hamilton, Alexander M. Seifalian. 2007. Achieving the ideal properties for vascular bypass grafts using a tissue engineered approach: a review. *Medical & Biological Engineering & Computing* **45**:4, 327. [CrossRef]
15. Vinoy Thomas, Xing Zhang, Shane A Catledge, Yogesh K Vohra. 2007. Functionally graded electrospun scaffolds with tunable mechanical properties for vascular tissue regeneration. *Biomedical Materials* **2**:4, 224. [CrossRef]
16. Wei He , Thomas Yong , Zu Wei Ma , Ryuji Inai , Wee Eong Teo , Seeram Ramakrishna . 2006. Biodegradable Polymer Nanofiber Mesh to Maintain Functions of Endothelial Cells. *Tissue Engineering* **12**:9, 2457-2466. [Abstract] [PDF] [PDF Plus]

Available online at www.sciencedirect.com
SCIENCE DIRECT®
Biomaterials 26 (2005) 2527–2536
Biomaterials
www.elsevier.com/locate/biomaterials

Surface engineering of electrospun polyethylene terephthalate (PET) nanofibers towards development of a new material for blood vessel engineering

Zuwei Ma[a,b,*], Masaya Kotaki[a,b], Thomas Yong[a,b], Wei He[b], Seeram Ramakrishna[a,b,c]

[a]*Nanoscience and Nanotechnology Initiative, National University of Singapore, 9 Engineering Drive 1, Singapore 117576, Singapore*
[b]*Division of Bioengineering, National University of Singapore, 9 Engineering Drive 1, Singapore 117576, Singapore*
[c]*Department of Mechanical Engineering, National University of Singapore, 9 Engineering Drive 1, Singapore 117576, Singapore*

Received 24 March 2004; accepted 19 July 2004
Available online 11 September 2004

Abstracts

Non-woven polyethylene terephthalate nanofiber mats (PET NFM) were prepared by electrospinning technology and were surface modified to mimic the fibrous proteins in native extracellular matrix towards constructing a biocompatible surface for endothelial cells (ECs). The electrospun PET NFM was first treated in formaldehyde to yield hydroxyl groups on the surface, followed by the grafting polymerization of methacrylic acid (MAA) initiated by Ce(IV). Finally, the PMAA-grafted PET NFM was grafted with gelatin using water-soluble carbodiimide as coupling agent. Plane PET film was also surface modified and characterized for basic understanding of the surface modification process. The grafting of PMAA and gelatin on PET surface was confirmed by XPS spectroscopy and quantitatively analyzed by colorimetric methods. ECs were cultured on the original and gelatin-modified PET NFM and the cell morphology, proliferation and viability were studied. Three characteristic surface makers expressed by ECs were studied using immuno-florescent microscopy. The gelatin grafting method can obviously improve the spreading and proliferation of the ECs on the PET NFM, and moreover, can preserve the EC's phenotype.

Keywords: Electrospinning; Nanofiber; PET; Surface modification; Vascular graft; Blood vessel; Tissue engineering

1. Introduction

Blood vessel disease such as atherosclerosis is one of the major causes of human death in modern society. The malfunctioning blood vessel can be replaced by autologous veins or arteries, but at the cost of other healthy tissues. The search for vascular graft substitute has thus been a half-century endeavor. Although PTFE and polyethylene terephthalate (PET) (Dacron^{MT}) have been used successfully in treating the pathology of large-diameter arteries (>6 mm, inner diameter), no materials have been proven to be successful in replacing small-diameter blood vessels (<6 mm). The main reason for the long-term failure of the small-diameter vascular graft is the incomplete cover of endothelial cells (ECs) on the vascular graft surfaces and the subsequent myointimal hyperplasia [1,2]. One approach to solve this problem called endothelialization [3] is to seed autologous ECs onto the luminal surface of the vascular grafts to allow the formation of a monolayer of ECs prior to implantation. This approach has been proven to be able to increase patency of the vascular grafts obviously [4].

The inner layer closest to blood flow in the blood vessel is formed by an EC monolayer attached onto a connective tissue bed of basement membrane, which is a flexible thin (40–120 nm thick) mat underlying all

*Corresponding author. Nanoscience and Nanotechnology Initiative, National University of Singapore, 9 Engineering Drive 1, Singapore 117576, Singapore. Tel.: +65-6874-6593; fax: +65-6874-2162.
E-mail address: nnimzw@nus.edu.sg (Z. Ma).

0142-9612/$ - see front matter © 2004 Elsevier Ltd. All rights reserved.
doi:10.1016/j.biomaterials.2004.07.026

epithelial or EC sheets to separate them from the underlying connective tissues. The basement membrane is mainly composed of type IV collagen and laminin fibers embedded in heparan sulfate proteoglycan hydrogels. The protein fibers in the basement membrane have nanoscaled diameters, ranging from several to several tens of nanometers [5].

A technology to fabricate polymeric nanofiber called electrospinning [6] had already been known for more than a half century, but received extensively renewed interests in recent years due to the similarity between the electrospun non-woven nanofiber and the nanoscaled protein fibers/fibrils in native extracellular matrix (ECM). The desire to build an artificial analogue of native ECM for tissue regeneration stimulated extensive studies on the possibility of applying the polymeric nanofiber as tissue engineering scaffolds [7–13].

It has been demonstrated that nanoscaled surface texture has significant influence on cell behaviors. Nanoscaled random surface roughness has been found to enhance cell adhesion and functions [14]. Cells attach and organize well around fibers with diameters smaller than the cells [15]. Recent study reported that osteoblast adhesion, proliferation, alkaline phosphatase activity and ECM secretion on carbon nanofibers increased with deceasing fiber diameter in the range of 60–200 nm [16].

In this work, a conventional polymer used in vascular graft, PET, was processed into non-woven nanofiber mat (NFM) via electrospinning. To overcome the chemical and biological inertness of the PET surface, gelatin was covalently grafted onto the PET NFM surface. The surface-modified PET NFM may be a new kind of material for blood vessel tissue engineering.

2. Experiments

2.1. Materials and reagents

PET particles ($[\eta] = 0.82 + 0.02$) were kindly donated by Mitsui Chemicals, Inc. (Japan). Methacrylic acid (MAA, Sigma-Aldrich) was purified by distillation before use. Trifluoroacetic acid (TFA, Merck), Ammonium cerium(IV) nitrate (Fluka), 1-ethyl-3-(3-dimethylaminopropyl) carbodiimide hydrochloride (EDAC, Sigma), *N*-hydroxysuccinimide (NHS, Sigma) and Gelatin (Sigma-Aldrich) were all used as received.

2.2. Preparation of PET film and PET NFM

PET films with a thickness of ~50 μm were prepared by heat-pressing of PET particles under 260 °C. Non-woven PET NFMs were prepared by electrospinning technology using equipments described in [7] in detail. Briefly, PET particles were dissolved in TFA to get a solution (0.2 g/ml). The solution was added into a 20 ml syringe and induced to flow out freely through a needle with an inner diameter of 0.21 mm. The polymer solution was deposited on an aluminum foil under a 15 kV DC voltage (Gamma High-Voltage Research) that was loaded between the needle and the aluminum foil which was at 15 cm distance from the needle. Glass pieces were put on the aluminum foil to collect the PET nanofibers. The deposition time was controlled to get PET NFMs with different thickness. The thickness of the PET NFM was measured by a micrometer and its apparent density and porosity were calculated using the following equations:

$$\text{NFM apparent density (g/cm}^3\text{)} = \frac{\text{NFM Mass (mg)} \times 10}{\text{NFM thickness (μm)} \times \text{NFM area (cm}^2\text{)}},$$

$$\text{NFM porosity} = \left(1 - \frac{\text{NFM apparent density (g/cm}^3\text{)}}{\text{bulk density of PET (g/cm}^3\text{)}}\right) 100\%,$$

where the bulk density of the PET is $1.3\,\mathrm{g\,cm^{-3}}$.

2.3. Surface modification of the PET film and PET NFM

Glue (SilbioneR, MED ADH 4300 RTV, Rhodia, USA) was used to fix the edge of the PET NFM on the glass piece to prevent it from being deformed during the surface modification. The NFM was first pre-wetted with ethanol and then immersed into deionized water to exchange the ethanol with water. For the film, there is no need for the pre-wetting process.

The whole chemical reaction scheme for PET surface modification is shown in Fig. 1.

The PET film or NFM was exposed to 18.5 vol% formaldehyde in 1 M acetic acid solution for 24 h at room temperature to yield hydroxyl groups on the PET surface [17]. The formaldehyde-treated PET film or NFM was then rinsed with deionized water for 24 h. The hydroxylated PET film/NFM was placed into a glass tube containing 10 ml MAA aqueous solution with a given concentration, 0.4 M H_2SO_4 and 0.007 M Ce(IV). The tube was sealed and purged with nitrogen, and the grafting polymerization of MMA was conducted under 80 °C. The PMAA-grafted PET film/NFM was rinsed in NaOH solution (pH = 10) for 3 h and then in deionized water for 24 h to remove the unreacted monomer and homopolymer of PMAA.

For gelatin grafting, PET film/NFM was first grafted with PMAA as described above, with the MAA concentration being 10 vol% and the grafting time being 4 h. The PMAA-grafted PET film/NFM was immersed into 10 ml 2-(*N*-Morpholino) ethanesulfonic acid (MES, Sigma) buffer solution (0.1 M, pH = 5.0) containing 5 mg/ml EDAC and 5 mg/ml NHS under 4 °C for 2 h. The material was then rinsed with deionized water,

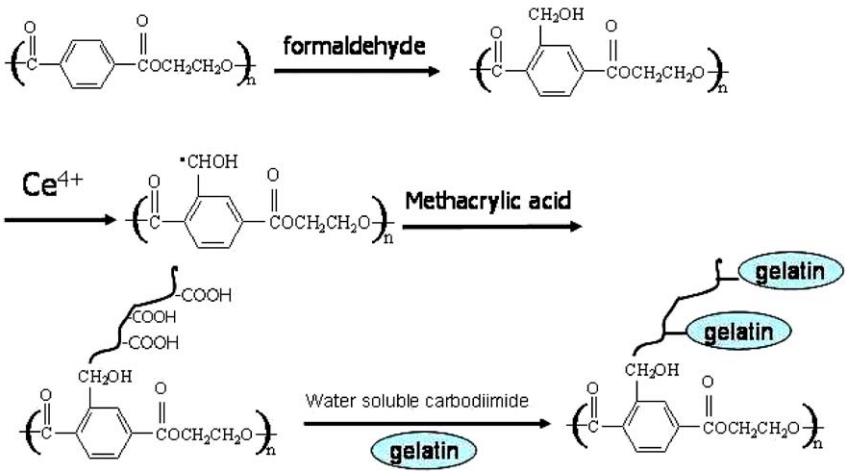

Fig. 1. Schematic representation of the PET surface modification process.

immersed into gelatin solution (4 mg/ml in MES buffer) and reacted for 24 h under 4 °C. The material was finally rinsed with deionized water for 24 h to remove the physically adsorbed gelatin, and dried under vacuum.

2.4. Surface characterization of PET NFM

SEM images of the PET NFM were obtained on a JEOL JSM-5800LV scanning electron microscope. XPS spectra of the control and modified PET surfaces were obtained on a VG ESCALAB 2201-XL Base System with a takeoff angle of 90°. The binding energy was referenced to the C1S of saturated hydrocarbon at 285.0 eV. Advancing, receding and static sessile drop water contact angle of the control and modified PET surface was measured using a VCA Optima (AST Products INC) surface contact angle tester.

COOH surface density on the PMAA-grafted PET film or NFM was measured using toluidine blue O (TBO) method [18–20] and the surface density of the gelation grafted on the PET film/NFM was measured with a modified Coomassie brilliant blue staining method [21]. For both measurements control tests with unmodified material were performed to eliminate the effects of physically adsorbed dye molecules on the material surfaces.

2.5. Endothelial cell culturing

Human coronary artery ECs at passage 3 were purchased from American Type Culture Association (ATCC; Arlington, VA). The cells were cultured in EC Basal Medium-2 (EBM-2, Clonetics™) supplemented with 100 U/ml penicillin and 100 U/ml streptomycin. During the cell culture, the culture medium was changed every 4 days. ECs at passage 9 were used in this work. The PET nanofiber was deposited on round cover slips (15 mmϕ, Assistant, Germany), which can be put into the wells of 24-well tissue culture plate and exactly covered the well bottom. A little amount of an implant grade silicon adhesive (Silbione®, MED ADH 4300 RTV, Rhodia, USA) was used along the edge of the PET nanofiber sheet to immobilize it on the glass surface. Experiments had been conducted in our lab to show that the high inert silicon adhesive has no toxic effects on the cells. Ethanol solution (75 vol%) was used to sterilize the samples and was removed by exchanging with PBS. ECs were seeded onto the original and modified PET NFM at a seeding density of 30000/well. TCPS was set as control. Cell morphology was observed on SEM (JEOL JSM-5800LV) and AFM (Dimension 3100, Digital Instruments) after 5 days' culturing and fixing with 2.5 vol% glutaraldehyde.

2.6. Cell proliferation and viability

It was found in this study that the ECs cultured on the nanofiber surfaces bonded strongly with the materials and could not be completely detached by a trypsin digestion. Therefore, cell number was measured by directly counting the cells on the material surface. The ECs were first immobilized by glutaraldehyde (2.5% in PBS). After a staining with PI (2 μg/ml, 100 μl per well), the cells were counted under a florescence microscope. The cell number per well was calculated by multiplying the measured cell surface densities with the total area of one well (1.8 cm^2) of the 24-well TCPS plate. On each sample, six different points were selected randomly and the cell numbers were averaged to calculate the cell surface density on the sample.

Cell viability was measured using the 3-(4,5-dimethylthiazol-2-yl)-5-(3-carboxymeth-oxyphenyl)-2-(4-sulfophenyl)-2H-tetrazolium (MTS) colorimetric assay. The kit (CellTiter 96® Aqueous One Solution Cell

Proliferation Assay) was purchased from Promega and the measurement was conducted according to the manufacturer's directions. Before the MTS testing, the culture medium was pipetted out from the 24-well tissue culture plate and 500 μl new fresh culture medium was added into every well. Hundred microliters of CellTiter 96® Aqueous One Solution reagent was added into every well. After culturing for 4 h, the deep colored culture medium was pipetted out and added into a 96-well plate (100 μl/well) and the absorbance at 490 nm was recorded using an ELISA plate reader. Samples with culture medium but without cells were set as control to get background absorbance to be subtracted from the absorbance of the cell-containing wells.

2.7. Cell phenotype study

After 5 days' culturing, the ECs were washed with PBS, fixed with 2.5% paraformaldehyde and blocked by BSA. The cells were then incubated for 2 h at 37 °C with 200 μl/well primary antibody (mouse anti-human platelet EC adhesion molecule (PECAM-1), mouse anti-human vascular cell adhesion molecule-1 (VCAM-1); mouse anti-human intercellular adhesion molecule-1 (ICAM-1), BD Biosciences, USA) diluted 1:60 with PBS/0.02% BSA. After washing, fluorescein isothiocyanate (FITC) labeled rabbit anti-mouse IgG (BD Biosciences, USA) diluted 1:60 with PBS/0.02% BSA was added (200 μl/well) and incubated for 2 h at 37 °C, followed by washing and counterstaining with PI (2 μg/ml, 100 μl per well) for 10 min. The immuno-stained ECs were then viewed under a laser scanning confocal microscope (Leica TCS SP2).

3. Results and discussion

3.1. Preparation of PET NFM

Morphology of the PET NFM obtained from electrospinning was shown in Fig. 2. The diameter of the nanofiber was in the range 200–600 nm. The nanoscaled fibers were randomly distributed to form a non-woven mat with good integrity. In this work, mats of different NFM thicknesses were obtained by controlling the deposition time in the electrospinning (Table 1). The electrospun PET NFM is a highly porous material. With the known bulk density of PET (1.3 g/cm^3), the porosity of the PET NFM can be calculated by measuring its apparent density, the results of which were summarized in Table 1. It can be seen that the thickness of the NFM increased with the deposition time while its porosity remained a constant value of about 82%.

3.2. Grafting polymerization of MAA

Different methods like plasma treatment [22,23], UV irradiation [24,25] and UV-induced grafting

Table 1
The thickness, apparent density and porosity of the PET NFM prepared under different deposition time

Deposition time (min)	Thickness of the nanofiber mat (μm)	Mass per unit area (mg/cm^2)	Apparent density (g/cm^3)	Porosity (%)
30	6	0.15	0.25	80.7
60	12	0.27	0.23	82.3
120	35	0.78	0.22	83.1

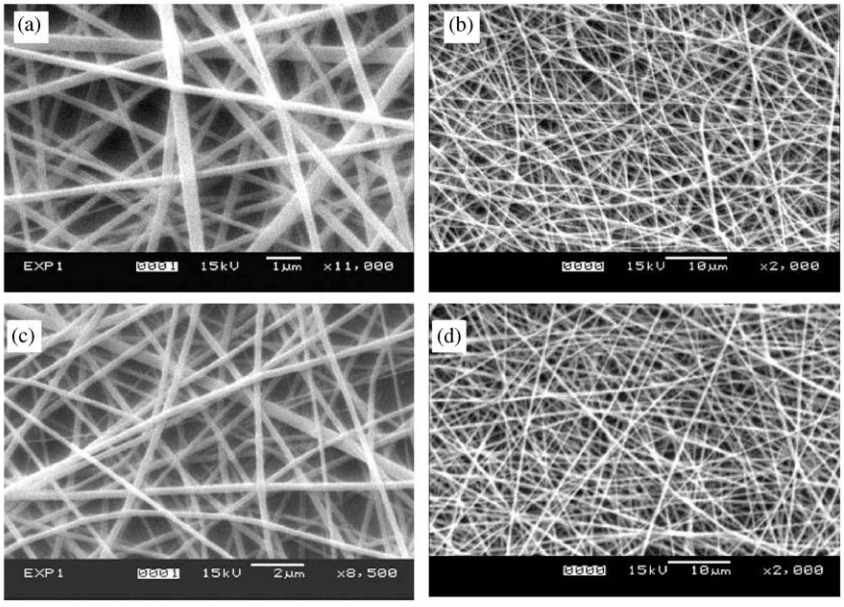

Fig. 2. SEM images of the original (a,b) and the gelatin-grafted PET NFM (c,d).

polymerization [26,27] have been employed to surface modify polymers towards improving biocompatibility for EC. However, for surface modification of polymer nanofibers, strong reaction conditions like irradiation and plasma should be avoided because the ultrafine polymeric nanofibers are not as strong as bulk materials and can be easily destroyed. For example, our recent work showed plasma treatment could destroy PET nanofibers severely. Therefore, Ce(IV) was used in this work to initiate grafting polymerization of MAA on PET surfaces. Fig. 2 showed that the morphology of the PET NFM was very well preserved after the gelatin grafting.

Although the purpose of this work is to surface modify the PET NFM; plane PET film was also surface modified to obtain a fundamental understanding of the surface modification process.

As the first step, the PET film/NFM was treated with formaldehyde to introduce hydroxyl groups [17], which can be oxidized by Ce(IV) to produce radicals to initiate the grafting polymerization (Fig. 1). The grafting of PMAA on PET surface yielded COOH groups, of which the density was quantitatively measured by TBO methods. Fig. 3 showed the COOH density on the PMAA-grafted PET film as a function of the monomer concentration. Obviously, the COOH density increased with the monomer concentration. To test the effectiveness of the formaldehyde treatment, surface grafting of non-formaldehyde-treated PET film was also conducted. It can be found that even the PET films without formaldehyde treatment have COOH groups yielded on the surface. The reason is the PET film surface can be hydrolyzed under the acidic reaction environment, producing some hydroxyl groups to be oxidized by Ce(IV) to initiate the grafting polymerization. The hydrolysis can also directly produce some COOH groups. Even so, treatment by formaldehyde can obviously increase the grafting degree and is necessary.

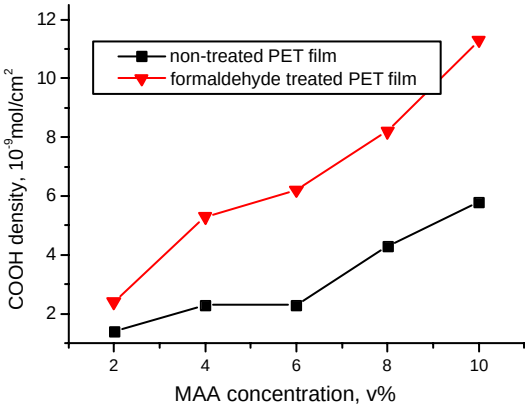

Fig. 3. COOH density on the PMAA-grafted PET film as a function of the monomer (MAA) concentration. Grafting time is 4 h.

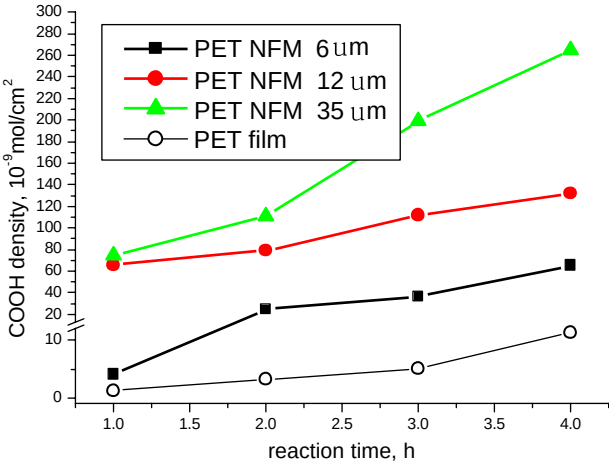

Fig. 4. COOH density on the PMAA-grafted PET film and PET NFM as a function of the grafting time. The monomer (MAA) concentration is 10 vol%. Note the change of vertical scale at 12.

For the surface modification of the PET NFM, the formaldehyde treatment was always used.

The COOH density grafted on the PET film/NFM increased with the grafting time, as shown in Fig. 4. Here the COOH density was expressed as COOH amount per unit area of the PET NFM because it is a straightforward way to show how many COOH groups exist in a piece of nanofiber sheet with a given area. The amount of the COOH groups grafted on the PET NFM was much higher than on the PET film, which can be traced to the much higher surface area of the PET NFM. It is worthy to point out that PET NFM with high thickness produced higher COOH density than the thinner PET NFM, as shown in Fig. 4, indicating that the grafting polymerization of MAA not only occurred on the outer surface, but also went deep into the NFM.

The grafting of PMAA on the PET film/NFM surface was further verified by XPS spectroscopy. Fig. 5 showed the C1S core-level scan spectra of the original and PMAA-grafted PET film/NFM. The introduction of PMAA on the PET surface increased the percentage of peak (I) at ~285 eV that corresponds to saturated hydrocarbon and decreased the percentage of peak (II) at ~286.8 eV that corresponds to the carbon atoms connected with only one oxygen atom by a single bond. Such changes are in accordance with the chemical structure of the PMAA, which has more saturated hydrocarbon atoms than PET, and contains no carbon atoms connected with only one oxygen atom by a single bond. Table 2 showed the atomic ration of C and O on the original and PMAA-grafted PET surface. It can be found that due to the similar C/O ratios in PMAA (2:1) and PET (2.5:1), there were no big changes in the atomic ratios of C and O after the PMAA grafting.

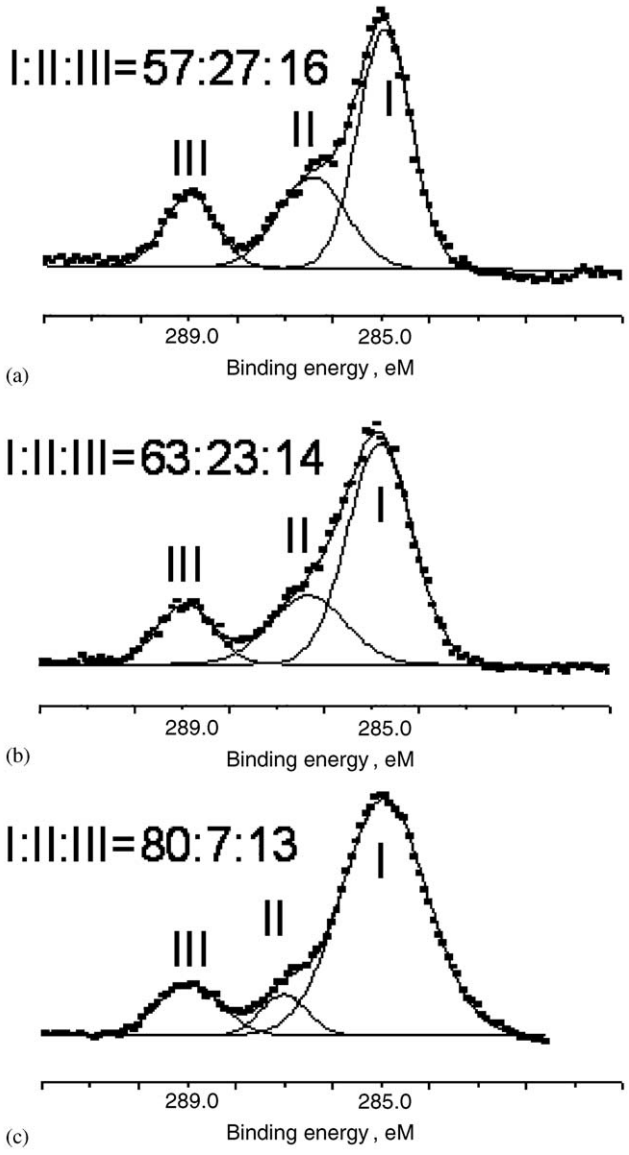

Fig. 5. C1S core level scan spectra of (a) original PET surface, (b) PMAA-grafted PET film and (c) PMAA-grafted PET NFM. The numbers in the figure indicate the percentage of the single peak area in the total C1S peak area.

Table 2
XPS data of the original and modified PET surface[a]

Sample	C atomic ratio (%)	N atomic ratio (%)	O atomic ratio (%)
PET	71.1	—	28.9
PMAA-grafted PET film	69.3	—	30.7
PMAA-grafted PET NFM	73.3	—	26.7
Gelatin-grafted PET film	69.0	10.1	20.9
Gelatin-grafted PET NFM	61.4	17.2	21.4

[a]For the grafting of PMAA in the first step, the MAA concentration is 10% and the grafting time is 4 h.

3.3. Gelatin grafting

EDAC/NHS chemistry, a commonly used approach to covalently immobilize protein molecules on –COOH-containing surfaces, was used to graft gelatin on the PET film and NFM. The gelatin grafting was directly verified by the appearance of the N1S peak in the XPS spectra of the gelatin-grafted PET film and NFM (Table 2). The amount of gelatin grafted on the PET film and NFM was quantitatively measured by CBBR-staining method (Table 3). Again, due to the higher surface area, the PET NFM had a much higher gelatin content than the PET film. The thicker the PET NFM was, the higher was the gelatin content, implying that gelatin grafting was not limited only on the outer surface of the PET NFM.

3.4. Wettability

Water contact angle of the original and modified PET film/NFM were summarized in Table 4. PET NFM showed totally different water contact angle from the PET film. The original PET NFM has a much higher advancing and sessile drop angle than the original PET film, while its receding angle is unusually much smaller. This is because the PET NFM has a highly rough surface compared with the relatively smooth PET film. The surface modification obviously increased the

Table 3
Amount of the gelatin grafted on the PET film and PET NFM with different thicknesses[a]

Sample	Amount of the gelatin grafted on the PET NFM ($\mu g/cm^2$)
Gelatin-grafted PET film	20
Gelatin-grafted PET NFM (6 μm)[b]	105
Gelatin-grafted PET NFM (12 μm)[b]	200
Gelatin-grafted PET NFM (35 μm)[b]	370

[a]Sample preparing condition is the same as in Table 2.
[b]The number in the brackets is the thickness of the PET NFM.

Table 4
Water contact angle of the original and surface-modified PET film and PET NFM[a]

Sample	Advancing (deg)	Receding (deg)	Sessile drop (deg)
Original PET film	97±3	53±4	80±2
PMAA-grafted PET film	74±2	19±1	53±2
Gelatin-grafted PET film	71±3	17±2	50±3
Original PET NFM	144±3	15±2	128±3
PMAA-grafted PET NFM	—	—	0
Gelatin-grafted PET NFM	—	—	0

[a]Sample preparing condition is the same as in Table 2.

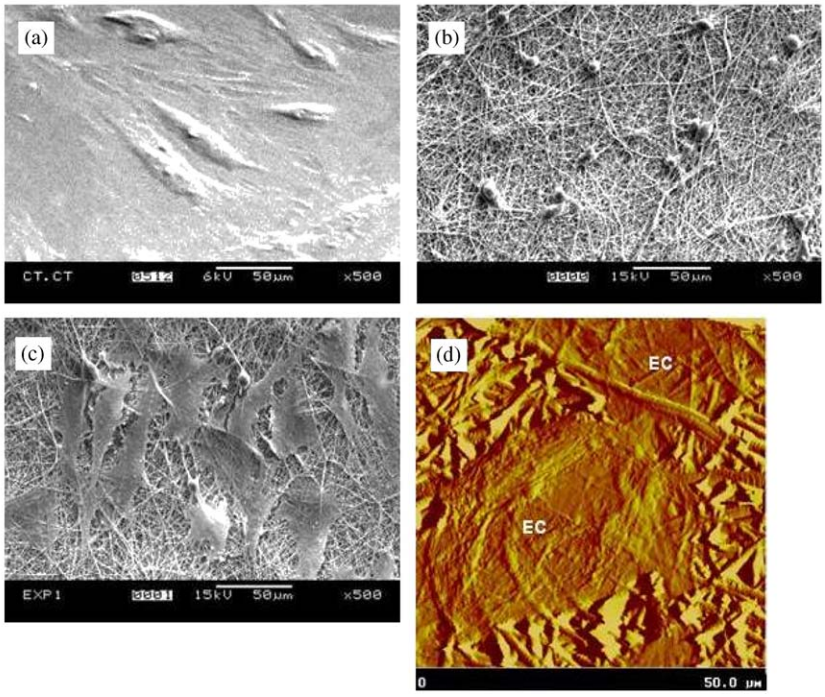

Fig. 6. SEM images of ECs cultured on (a) TCPS, (b) original PET NFM and (c) gelatin-grafted PET NFM, (d) AFM image of the ECs on the gelatin-modified PET NFM.

hydrophilicity of the PET surface. Interestingly, although the original PET NFM showed very high advancing and sessile drop water contact angle, after surface modification either by PMAA grafting or by gelatin grafting, it becomes a highly wettable material. The water drop, upon contact with the surface-modified PET NFM, was suddenly sucked into the NFM, giving a zero water contact angle.

The big difference of the PET NFM's wettability before and after the surface modification can be explained by the following experience [28]. The water contact angle of a solid surface is affected by surface roughness in such a manner: If the material is intrinsically hydrophobic, the water will not be able to penetrate into the hollows and pores on the rough surface and can be regarded as resting on a semi-solid and semi-air plane surface, which will increase the contact angle significantly. In contrast, the water will penetrate and fill up most of the hollows and pores formed by an intrinsically hydrophilic material, forming a surface which is partly solid and partly liquid and therefore leading to a low water contact angle. Having a highly rough surface, the PET NFM experienced a big improvement in wettability after it was surface modified from hydrophobic to hydrophilic.

4. EC morphology

Cell morphology is an important parameter to be considered for EC in vascular graft. A spreading shape

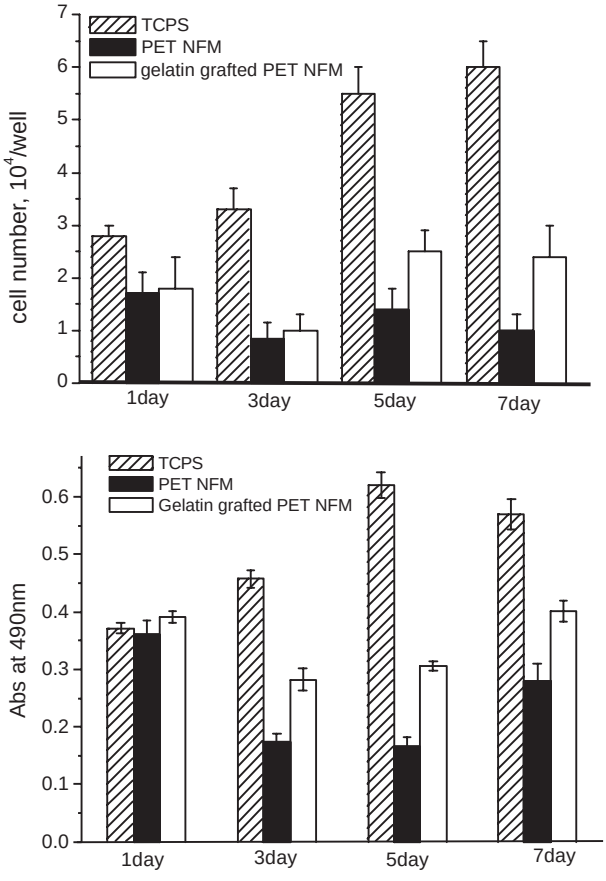

Fig. 7. EC growth curve (a) and MTT viability (b) on TCPS, the original and gelatin-modified PET NFM. Cell seeding density is 30,000/well (24-well tissue culture plate).

is of particular importance since it is needed for the neo-endothelium formation. The spreading cells can form a monolayer covering the foreign material surfaces to prevent direct contact between the blood and the foreign material; therefore, preventing immuno-reactions and thrombosis. Cell morphology on TCPS, the original and the gelatin-grafted PET NFM was checked by SEM and shown in Fig. 6. The ECs were extensively spread on TCPS. The ECs on the original PET NFM were round shaped and did not spread, while on the gelatin-grafted NFM the ECs adopted a spreading polygonal shape. From the large-magnification AFM image shown in Fig. 6(d), the profile of some nanofibers beneath the extensively spreading cells can be easily observed.

4.1. EC proliferation and viability

The cell proliferation was measured by counting the cells directly on the material surface because it was found that the ECs seeded on the nanofiber surface bonded strongly with the fiber and could not be completely detached by trypsinization. Fig. 7a showed the proliferation curves of the ECs seeded on the TCPS, original PET NFM and gelatin-grafted PET NFM. On TCPS the cell number kept increasing throughout the whole cell culture time. The ECs cultured on both the original and gelatin-grafted PET NFM decreased on the 3rd day compared with the first day, followed by an increase on the 5th day. This decrease of the cell number on the 3rd day might indicate a damage of the ECs to

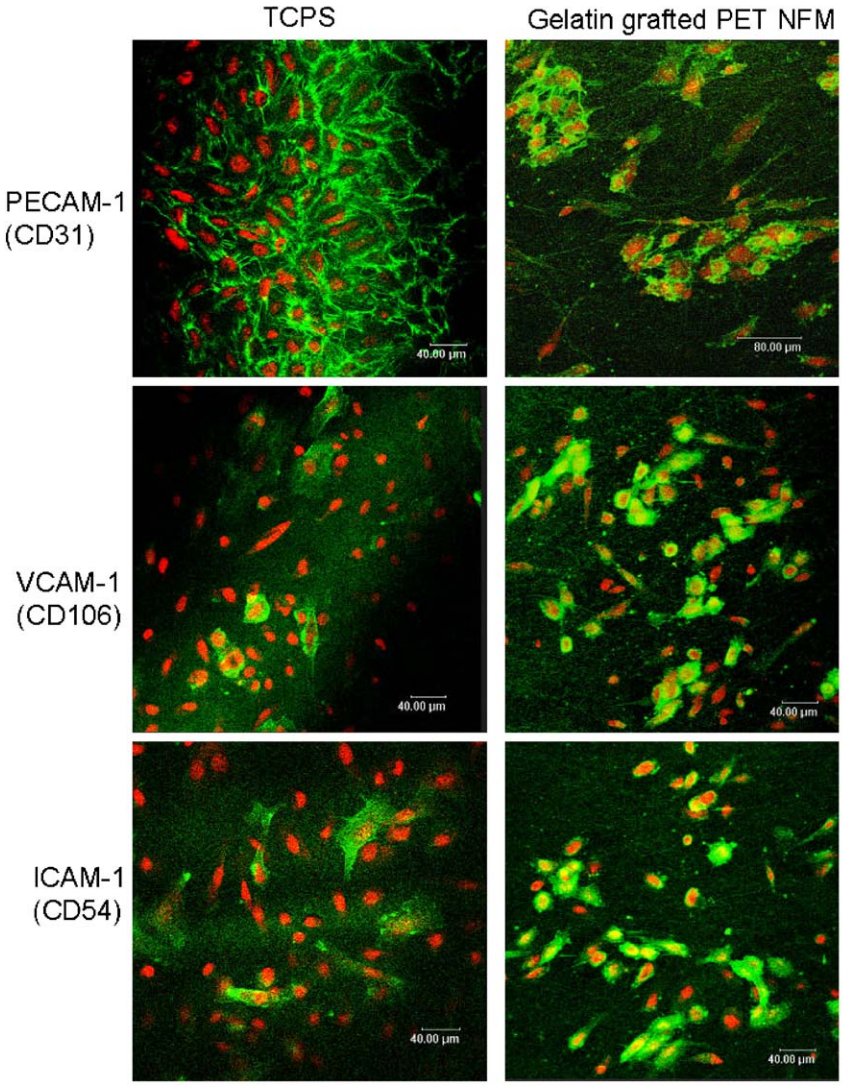

Fig. 8. Expression of PECAM-1 (CD31), VCAM-1 (CD106) and ICAM-1 (CD54) by the ECs cultured on TCPS and the gelatin-grafted PET NFM. Cells were immuno-stained with respective primary antibody and FITC labeled secondary antibody, and counterstained by PI. Representative LCSM micrographs are shown.

some extent on the original and the surface-modified PET NFM. Fig. 7b showed the cell MTT viability curves, which were roughly in accordance with the cell proliferation curves shown in Fig. 7b. It can be concluded from Fig. 7 that on the one hand, surface grafting of gelatin on the PET NFM can obviously improve the cell growth behaviors compared with the poor cell growth on the unmodified PET NFM. While on the other hand, the difference of cell number and cell viability between the gelatin-modified PET NFM and the TCPS implies a necessary further improvement of the material in the future.

4.2. EC phenotype analysis

Three typical surface adhesion proteins characteristically expressed by ECs, i.e., PECAM (or CD31), VCAM-1 (or CD106) and ICAM-1 (or CD54) were studied using immuno-florescent microscopy. Fig. 8 showed the LCSM images of the immuno-stained ECs cultured on TCPS and on the gelatin-grafted PET NFM. There were positively stained cells for all the three surface makers on both materials. The ECs on TCPS have an obviously stronger expression of CD31 than on the gelatin-grafted PET NFM. CD31 belongs to the superfamily of the immunoglobulin and occurs to regulate EC–EC adhesion and EC–leukocyte adhesion. It is usually believed that an increased expression of CD31 is in favor of endothelialization [29], while a decreased expression of CD31 by EC is a possible implication of cell damage [30]. CD106 and CD54 belong to the immunoglobulin superfamily as well, and mainly regulate EC–leukocyte adhesion [29,31–33]. The expression of all three surface makers by the ECs cultured on the gelatin-modified PET NFM indicates the preservation of EC's characteristic phenotype. However, the weaker expression of CD31 on the gelatin-modified PET NFM means a worse endothelialization than on TCPS. This result is also in agreement with the cell proliferation and viability test results shown in Fig. 7.

5. Conclusion

After the PET NFM is treated with formaldehyde, MAA can be polymerized on the PET NFM surface using Ce(IV) as initiator. The PMAA grafting degree increased with monomer concentration and grafting time. The amount of the carboxyl groups grafted on the PET NFM also increased with the mat thickness, indicating that the surface modification occurred not only on the outer layer but also throughout the whole nanofiber matrix. Using EDAC/NHS chemistry gelatin can be covalently attached to the PMAA-grafted PET NFM. The gelatin grafting method can obviously improve the spreading and proliferation of ECs on PET NFM, and the gelatin-grafted PET NFM can preserve the EC's phenotype.

References

[1] Lian X, Greisler HP. Biomaterials in the development and future of vascular grafts. J Vasc Surg 2003;37:472–80.
[2] Anthony R. Tissue engineering of vascular grafts. Matrix Biol 2000;19:353–7.
[3] Jarrell BE, Stockes SK. Use of freshly isolated capillary endothelial cells for the immediate establishment of a monolayer on a vascular graft at surgery. Surgery 1986;100:392–9.
[4] Deutsch M, Meinhart J, Fischlein T, Preiss P, Zilla P. Clinical autologous in vitro endothelialization of infrainguinal ePTFE grafts in 100 patients: a 9-year experience. Surgery 1999;126:847–55.
[5] Flemming RG, Murphy CJ, Abrams GA, Goodman SL, Nealey PF. Effects of synthetic micro- and nano-structured surfaces on cell behavior. Biomaterials 1999;20:573.
[6] Huang ZM, Zhang YZ, Kotaki M, Ramakrishna S. A review on polymer nanofibers by electrospinning and their applications in nanocomposites. Compos Sci Technol 2003;63(15):2223–53.
[7] Xu CY, Inai R, Kotaki M, Ramakrishna S. Aligned biodegradable nanofibrous structure: a potential scaffold forblood vessel engineering. Biomaterials 2004;25:877–86.
[8] Xu CY, Inai R, Kotaki M, Ramakrishna S. Electrospun, nanofiber fabrication as synthetic extra cellular matrix and its potential for vascular tissue engineering. Tissue Engineering 2004;10:1150–8.
[9] Yoshimoto H, Shin YM, Terai H, Vacanti JP. A biodegradable nanofiber scaffold by electrospinning and its potential for bone tissue engineering. Biomaterials 2003;24:2077–82.
[10] Wan-Ju LI, Dielson KG, Alexander PG, Tuan1 RS. Biological response of chondrocytes cultured in three-dimensional nanofibrous poly (caprolactone) scaffolds. J Biomed Mater Res 2003;67A:1105–14.
[11] Li WJ, Tulia R, Okafor C, Derfoul A, Danielson KG, Hall DJ, Tuan RS. A three-dimensional nanofibrous scaffold for cartilage tissue engineering using human mesenchymal stem cells. Biomaterials 2005;26:599–609.
[12] Shin M, Ishii O, Sued T, Vacanti JP. Contractile cardiac grafts using a novel nanofibrous mesh. Biomaterials 2004;25:3717.
[13] Kidoaki S, Kwon IK, Matsuda T. Mesoscopic spatial designs of nano- and microfiber meshes for tissue-engineering matrix and scaffold based on newly devised multilayering and mixing electrospinning techniques. Biomaterials 2005;26:37.
[14] Webster TJ, Siegel RW, Bizios R. Osteoblast adhesion on nanophase ceramics. Biomaterials 1999;20:1221–7.
[15] Laurencin CT, Ambrosio AMA, Borden MD, Cooper Jr. JA. Tissue engineering: orthopedic applications. Annu Rev Biomed Eng 1999;01:19.
[16] Elias KL, Price RL, Webster TJ. Enhanced functions of osteoblasts on nanometer diameter carbon fibers. Biomaterials 2002;23:3279.
[17] Peter Kingshott, Jiang Wei, Dorthe Bagge-Ravn, Nikolaj Gadegaard. Lone Gram covalent attachment of poly(ethylene glycol) to surfaces, critical for reducing bacterial adhesion. Langmuir 2003;19:6912–21.
[18] Lei Ying, Chao Yin, Zhuo RX, Leong KW, Mao HQ, Kang ET, Neoh KG. Immobilization of galactose ligands on acrylic acid graft-copolymerized poly(ethylene terephthalate) film and its application to hepatocyte culture. Biomacromolecules 2003;4:157–65.

[19] Gupta B, Hilborn JG, Bisson I, Frey P. Plasma-induced graft polymerization of acrylic acid onto poly(ethylene terephthalate) films. J Appl Polym Sci 2001;81:2993.
[20] Uchida E, Uyama Y, Ikada Y. Sorption of low-molecular-weight anions into thin polycation layers grafted onto a film. Langmuir 1993;9:1121–4.
[21] Kang IK, Kwon BK, Lee JH, Lee HB. Immobilization of proteins on polyl(methyl methacrylate) films. Biomaterials 1993;14:787.
[22] Chen M, Zamora PO, Som P, Pena LA, Osaki S. Cell attachment and biocompatibility of polytetrafluoroethylene (PTFE) treated with glow-discharge plasma of mixed ammonia and oxygen. J Biomater Sci—Polym Ed 2003;14:917.
[23] Wan YQ, Yang J, Yang JL, Bei JZ, Wang SG. Cell adhesion on gaseous plasma modified poly (L-lactide) surface under shear stress field. Biomaterials 2003;24:3757.
[24] Heitz J, Svorcik V, Bacakova L, Rockova K, Ratajova E, Gumpenberger T, Bauerle D, Dvorankova B, Kahr H, Graz I, Romanin C. Cell adhesion on polytetrafluoroethylene modified by UV-irradiation in an ammonia atmosphere. J Biomed Mater Res: Part A 2003;67A:130–7.
[25] Gumpenberger T, Heitz J, Bauerle D, Kahr H, Graz I, Romanin C, Svorcik V, Leisch F. Adhesion and proliferation of human endothelial cells on photochemically modified polytetrafluoroethylene. Biomaterials 2003;24:5139.
[26] Guan JJ, Gao GY, Feng LX, Sheng JC. Surface photo-grafting of polyurethane with 2-hydroxyethyl acrylate for promotion of human endothelial cell adhesion and growth. J Biomater Sci—Polym Ed 2000;11:523.
[27] Zhu YB, Gao CY, Guan JJ, Shen JC. Promoting the cytocompatibility of polyurethane scaffolds via surface photo-grafting polymerization of acrylamide. J Mater Sci—Mater Med 2004; 15(3):283.
[28] Shaw DJ. Introduction to colloid and surface chemistry. London: Butterworth & Co (Publishers) Ltd.; 1980. p. 134.
[29] Granchi D, Cenni E, Verri E, Ciapetti G, Gori A, Gamberini S. Adhesive protein expression on human endothelial cells after in vitro contact with woven Darcron. Biomaterials 1998;19: 93–8.
[30] Albeda SM, Muller WA, Buck CA, Newmann PJ. Molecular and cellular properties of PECAM-1 (endoCAM/CD31): a novel vascular cell-cell adhesion molecule. J Cell Biol 1991;114:1059–68.
[31] Lehle K, Buttstaedt J, Birnbaum DE. Expression of adhesion molecules and cytokines in vitro by endothelial cells seeded on various polymer surfaces coated with titaniumcarboxonitride. J Biomed Mater Res 2003;65A:393–401.
[32] Oppenheimer-Marks N, Davis LS, Tompkins Bogue D, Remberg J, Lipsky P. Differential utilization of ICAM-1and VCAM-1 during the adhesion and transendothelial migration of human T lymphocytes. J Immun 1991;147:2913–21.
[33] Wilkinson LS, Edwards JCW, Poston RN, Haskard DO. Expression of vascular cell adhesion molecule-1 in normal and infamed synovium. Lab Invest 1993;68:82–8.